Characterisation of *Mycobacterium tuberculosis* specific T cell immunity with HLA class II tetramers

One Bridget Dintwe

Thesis Presented for the Degree of

DOCTOR OF PHILOSOPHY

in the School of Child and Adolescent Health

Faculty of Health Sciences

UNIVERSITY OF CAPE TOWN

On the 17 February, 2014

Supervisors: Assoc. Prof. Thomas J Scriba

Co-supervisor: Dr. Elisa Nemes

University of Cape Town

The copyright of this thesis vests in the author. No quotation from it or information derived from it is to be published without full acknowledgement of the source. The thesis is to be used for private study or non-commercial research purposes only.

Published by the University of Cape Town (UCT) in terms of the non-exclusive license granted to UCT by the author.

University of Cape Town

Declaration

I, One Bridget Dintwe, hereby declare that the work on which this thesis is based is my original work (except where acknowledgements indicate otherwise) and that neither the whole work nor any part of it has been, is being, or is to be submitted for another degree in this or any other university.

I empower the university to reproduce, for the purpose of research, either the whole or any portion of the contents in any manner whatsoever.

Signature:

Date:

Acknowledgements

It is only by the grace of God that I have been able to achieve this.

There are so many people who have played a critical role in mentoring me and supporting me through out this journey, and at this time I do not feel that the words ‘Thank you’ can even begin to describe my gratitude.

First and foremost, I must thank my family, particularly my mother who has always been so generous and supportive. Having sacrificed so much in her life to provide for us and give us the best opportunities that she could offer. Thank you mama, ke a leboga and modimo a go segofatse.

To my partner, Pieter, who has walked this up and down road with me without ever questioning whether I would succeed, I cannot even begin to express my gratitude and appreciation of all that you have done for me.

To my family away from home, the De Gouveia’s. Thank you for taking me into your home and always making me feel like I had a family, when my own was so far away. Thank you for always supporting me and encouraging me to always want to achieve more.

To Willem Hanekom, thank you for taking me into your lab and giving me the opportunity to prove myself and to grow as a scientist.

To my friends who sat so many nights listening to me complain about experiments that didn't work even though they had no idea what I was babbling on about, you guys gave me strength (and some wine) to get through it, Thank you.

To all the people at SATVI who have always been there, and who I could always count on for advise and whom we have built so many precious memories, thank you. To the SATVI Worcester team, you guys are amazing

and thank you for always working you magic and doing your best to see my project to completion.

To the all the vaccine participants and healthy donors whom without, this project would not have been possible…..Thank you, Dankie, Enkosi.

To my co-supervisor, Dr Elisa Nemes, thank you so much for everything you have done for me and for being so willing to jump on board and provide supervision and guidance, and occasionally a shoulder to cry on. I am forever grateful.

To Thomas Scriba, my supervisor, my mentor, my shoulder to cry on and most of all, my biggest motivator on this journey, how do I even begin to say thank you. Through your guidance I have grown as a scientist and a member of society. Thank you for always helping me see that the cup was half full when all I saw was an empty and broken glass. I couldn't have asked for a better supervisor. Ke lebogile ‘serantabole’.

Finally, thank you to the funders for the financial support: Carnegie Corporation, The South African Medical Research council and The Bill and Melinda Gates Foundation

Summary:

Tuberculosis (TB) remains a global health burden, with an estimated 1.3 million people dying from the disease in 2012. Protective immunity against TB is thought to depend on specific T cells. However, exactly which T cell characteristics are required for immunological protection is unknown. To gain a better understanding of *M. tuberculosis* (*M.tb*)-specific memory T cell immunity, we studied longevity and function of *M.tb*-specific memory T cells. We reasoned that such knowledge would facilitate rational vaccine design of a TB vaccine.

We designed and developed a set of new HLA class II tetramers to perform in-depth studies of *M.tb*-specific CD4 T cell responses. We studied persons vaccinated with a novel TB vaccine, MVA85A, as well as persons naturally infected with *M.tb*. Antigen-specific CD4 T cells were detected with HLA class II tetramers and functional and phenotypic attributes of these T lymphocytes characterised by standard flow cytometric techniques. Comprehensive transcriptional analyses of *M.tb*-specific CD4 T cells, which were also sorted by FACS, were performed by microfluidic quantitative real-time PCR.

Early after intradermal vaccination with MVA85A a large proportion of Ag85A-specific CD4 T cells were highly activated, expressed skin homing markers and displayed an effector T cell phenotype. This effector response waned rapidly and gave way to antigen-specific central memory CD4 T cells with high proliferative potential, which we proposed may be desirable for protection. However, recent results from the first efficacy trial of MVA85A in infants suggested that these cells are not sufficient to enhance protection beyond that induced by BCG vaccination at birth.

Further, we characterised surface marker expression and transcriptional signatures of a newly detected and described population of *M.tb*-specific CD4 T cells, that displayed a CD45RA+CCR7+CD27+ naïve-like T cell phenotype. We hypothesised that these unique *M.tb*-specific naïve-like CD4 T cells had a transcriptional profile distinct from truly naïve, central memory and effector bulk CD4 T cells, as well as other *M.tb*-specific memory CD4 T cell subsets.

Gene expression of CFP10-specific naïve-like CD4 T cells reflected an mRNA profile that was very distinct from truly naïve bulk CD4 T cells. Rather, naïve-like CD4 T cells clustered with bulk effector CD4 T cells in unsupervised

analysis methods such as hierarchical clustering and principle component analyses. Further analyses revealed that naïve-like CFP10-specific CD4 cells expressed mRNAs coding for effector cytokines, cytotoxic molecules and chemokine receptors consistent with effector memory T cells. However, the overall transcriptional profile was more similar to CFP10-specific central memory CD4 T cells than that of the effector CD4 T cells.
We concluded that *M.tb*-specific naïve-like CD4 T cells may possess an ability to traffic to sites of infection or inflammation, where they may contribute to effector function. These hypotheses need confirmation on a protein level.

The HLA class II tetramers developed in this thesis are valuabe tools for assessing direct *ex vivo M.tb*-specific CD4 T cell responses without activation and cell perturbation. Our findings contribute to a more comprehensive understanding of T cell immunity induced by vaccines and/or natural *M.tb* infection.

List of abbreviations

Ag85A	antigen 85A
AB+	human serum from male AB plasma
Ad85A	adenovirus expressing antigen 85A
ALP	alkaline phophatase
APC	antigen presenting cell
BAL	Bronchoalveolar lavage
BCG	Bacille Calmette Guerin
CCR	chemokine (C-C motif) receptor
cDNA	complementary Deoxyribonucleic acid
CFP10	culture filtrate protein 10
CFSE	Carboxyfluorescein succinimidyl ester
CFU	colony forming units
CLA	cutaneous lymphocyte antigen
CMV	cytomegalovirus
CO_2	Carbon dioxide
cpm	cycles per minute
CT	computed tomography
Ct	Cycle threshold
CV	coefficient of variation
CXCR	CXC chemokine receptor
DC	Dendritic cell
DC SIGN	Dendritic Cell-Specific Intercellular adhesion molecule-3-Grabbing Non-integrin
DNA	Deoxyribonucleic acid
EDTA	Ethylenediamine tetra-acetic acid
ELISpot	Enzyme linked immunosorbent spot
ESAT6	6kDa early secretory antigen
Et	Threshold expression
FACS	Fluorescence activated cell sorter
FCS	Foetal calf serum
FDG	Fludeoxyglucose

FMO	fluorescence minus one
FSC	Forward scatter
HBV	Hepatitis B virus
HIV	Human Immunodeficiency virus
HLA	Human leukocyte antigen
IC_{50}	inhibitory concentration 50
ICS	intracellular cytokine assay
IEDB	Immune Epitope Database
IFN-γ	Interferon gamma
IL	interleukin
IPV	Inactivated Polio vaccine
iTreg	induced regulatory T cell
Kd	dissociation constant
LTBI	latent tuberculosis infection
M.tb	*Mycobacterium tuberculosis*
mAB	monoclonal antibody
MFI	median fluorescence intensity
MHC	Major histocompatibility complex
mL	millilitre
mM	millimolar
mRNA	messenger Ribonucleic acid
MVA85A	modified vaccinia ankara Ag85A
NHP	non-human primate
NL	naïve-like
nM	nanomolar
PAMP	pathogen associated molecular pattern
PBMC	peripheral blood mononuclear cells
PBS	Phosphate buffered saline
PCR	polymerase chain reaction
PET	Positron emission tomography
pfu	plaque forming units
PHA	Phytohaemagluttinin A
PMA	Phorbol 12-myristate 13-acetate

PMT	photomultiplier tube
PPD	Purified protein derivative of *M.tb*
PRR	pathogen recognition receptor
QFT	quantiferon
qPCR	quantitative polymerase chain reaction
rBCG	recombinant Bacille Calmette Guerin
RNA	Ribonucleic acid
ROC	receiver operator characteristics
RT	reverse transcription
R^2	coefficient of determination
SATVI	South African Tuberculosis Vaccine initiative
TB	Tuberculosis
T_{CM}	central memory T cell
TCR	T cell receptor
T_{EM}	effector memory T cell
TGF-β	Transforming growth factor β
Th	T helper
TLR	Toll like receptor
TNF-α	Tumor necrosis factor alpha
Treg	regulatory T cell
T_{SCM}	T memory stem cells
TST	Tuberculin skin test
μL	microliter
μM	micromolar
ViViD	LIVE/DEAD Fixable Violet Dead Cell Stain
WBA	whole blood assay
WHO	World Health Organisation

Table of contents

Introduction

1.1 Tuberculosis

Tuberculosis (TB) is an infectious disease, primarily of the lungs. TB is caused by the bacterium, *Mycobacterium tuberculosis* (*M.tb*). However this bacterium can spread from the lung to other sites of the body and cause pathology, this is known as TB dissemination.

1.1.1. Epidemiology

One third of the world's population is estimated to be infected with *Mycobacterium tuberculosis* (*M.tb*), the underlying cause of tuberculosis (TB) disease. South Africa ranks among the 22 countries with the highest incidence rates per capita of TB in 2013 in the world, with an estimated 1003 incident cases per 100 000 people (WHO Global Tuberculosis Report 2013) as shown in Figure 1. It is estimated that 1.3 million people died from TB in 2012 (WHO Global Tuberculosis Report 2013).

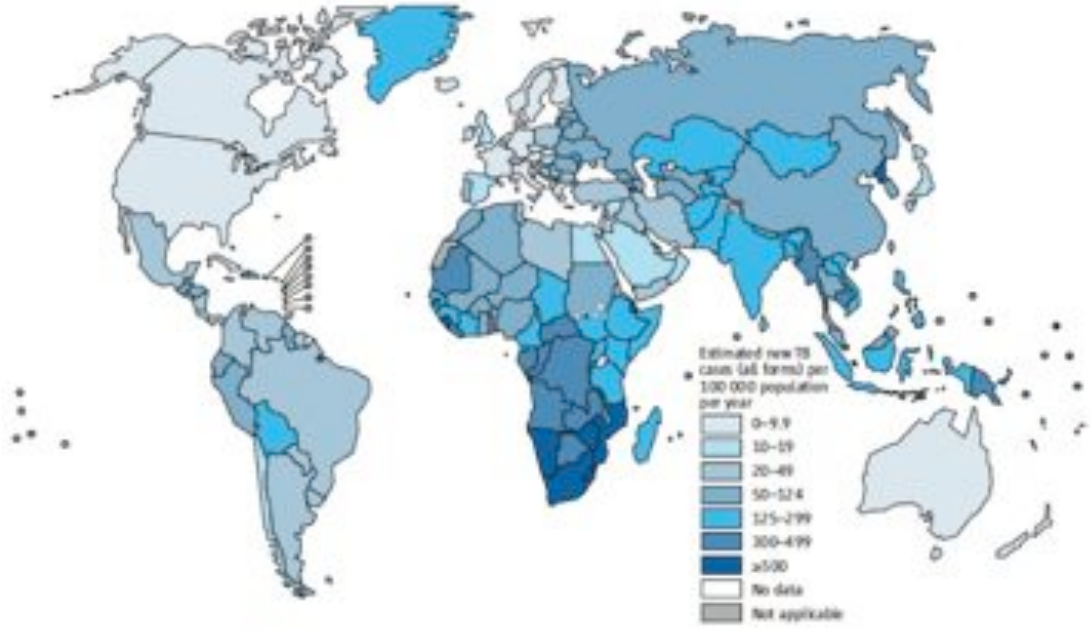

Figure 1: The global distribution of new TB cases per 100 000 population, demonstrating how developing countries are most affected. (Adapted from the WHO Global Tuberculosis Report, 2013)

An effective TB vaccine to prevent development of disease, in combination with improved diagnostic tests as well as improved drugs, would be the most cost effective and efficient intervention to control the spread of TB (Kaufmann

et al. 2010; Abu-Raddad et al. 2009). The rational development of better TB vaccines and diagnostic tests is hampered by our incomplete knowledge of immunity to mycobacterial infection and how immunological protection can be achieved by vaccination (Dye 2012).

1.1.2 Tuberculosis pathogenesis

M.tb is an intracellular pathogen, which enters the host through inhalation of aerosolised micro droplets containing the bacilli. These bacilli are deposited in the lower airways of the lung where they are recognised as foreign and are engulfed by alveolar macrophages as well as dendritic cells (DCs) (Kaufmann & McMichael 2005). Macrophages recognise bacilli via pathogen associated molecular patterns, phagocytose the bacilli and, upon activation, can kill *M.tb*. *M.tb* has developed mechanisms to manipulate the immune system to its advantage. *M.tb* has been shown to modulate the maturation of the phagosomal compartment in the macrophage, preventing it from fusing with lysosomes, and thereby creating an environment in which it can survive and multiply (Sturgill-Koszycki et al. 1994). This allows persistence and establishment of infection, which can last for decades. *M.tb* has also been shown to inhibit host cell apoptosis (J. L. Miller et al. 2010; Velmurugan et al. 2007), allowing prolonged survival in the cells. Exactly how these mechanisms are regulated remains elusive and is currently being studied in depth.

DCs that have phagocytosed *M.tb* become activated and traffic to draining lymph nodes, where *M.tb* antigens are processed and presented by Human leukocyte antigens (HLA) molecules to naïve T cells (Reiley et al. 2008). These T cells are primed as explained in depth in section 1.3.2, undergo clonal expansion, and differentiate into effector cells that traffic back to the site of infection, the lung. Here, antigen-specific T cells release pro-inflammatory cytokines, such as interferon gamma (IFN-γ) and tumor necrosis factor alpha (TNF-α) which activate macrophages, as well as releasing chemokines, which in turn recruit other cells to the site of infection. CD4 T cells and other T cells activate infected macrophages further through IFN-γ

and TNF-α production to become mycobactericidal. It has been suggested that some individuals have the capacity to completely clear the infection at this point, yet the mechanism has not yet been described and it is unknown how often this occurs. However, this is likely not the case for the majority of individuals who inhale *M.tb*. Individuals with persisting bacilli are said to have latent TB infection (LTBI) or to have asymptomatic disease. The current methods used to test for *M.tb* infection cannot distinguish between a person who may have had infection and cleared it and those truly infected. These tests are proxies for infection and test for immunological sensitisation to mycobacterial antigens (Robertson et al. 2012). Latently infected individuals are asymptomatic but have a risk of progressing to TB disease. Latency is now seen as a spectrum of infection, varying from people who may have completely cleared the infection to those with varying degrees of bacterial loads. By definition, these persons present with absence of clinical symptoms but may have subclinical active disease (Barry et al. 2009).

Infected macrophages may differentiate into several different morphotypes, including multi-nucleated giant cells and epitheloid cells. These cells aggregate, to form a structure known as a granuloma, which forms around the infected cells. The granuloma gains structure further, with macrophages containing bacilli in the center surrounded by lymphocytes, neutrophils and DCs forming a wall-like structure. This structure functions to contain the bacilli within this confined environment (Russell et al. 2009). T cells continue to produce cytokines such as TNF-α to maintain the structure of the granuloma (Russell et al. 2009).

It is postulated that the failure to form, or a breakdown in the structure of granulomas, which may be due to immune compromise either immediately or at a later stage, can lead to unsuccessful containment of the bacilli, local dissemination and subsequently, progression or reactivation of TB disease.
However, the precise role of the granuloma remains in question. Some hold the view that it is a crucial host protective structure essential to pathogen control, preventing the spread of the bacilli, while others have the view that

granulomas can also facilitate local spread of the infection (Rubin 2009). Recent studies have suggested that the granuloma may be an environment that promotes survival and spread of the bacilli. Ramakrishnan et al., have shown that intracellular mycobacteria, in the zebrafish model, recruited macrophages into the early granuloma where these macrophages become infected and then leave the granuloma again. The authors suggested that mycobacteria may use the host to facilitate spread of the bacilli (Davis & Ramakrishnan 2009; Ramakrishnan 2012).

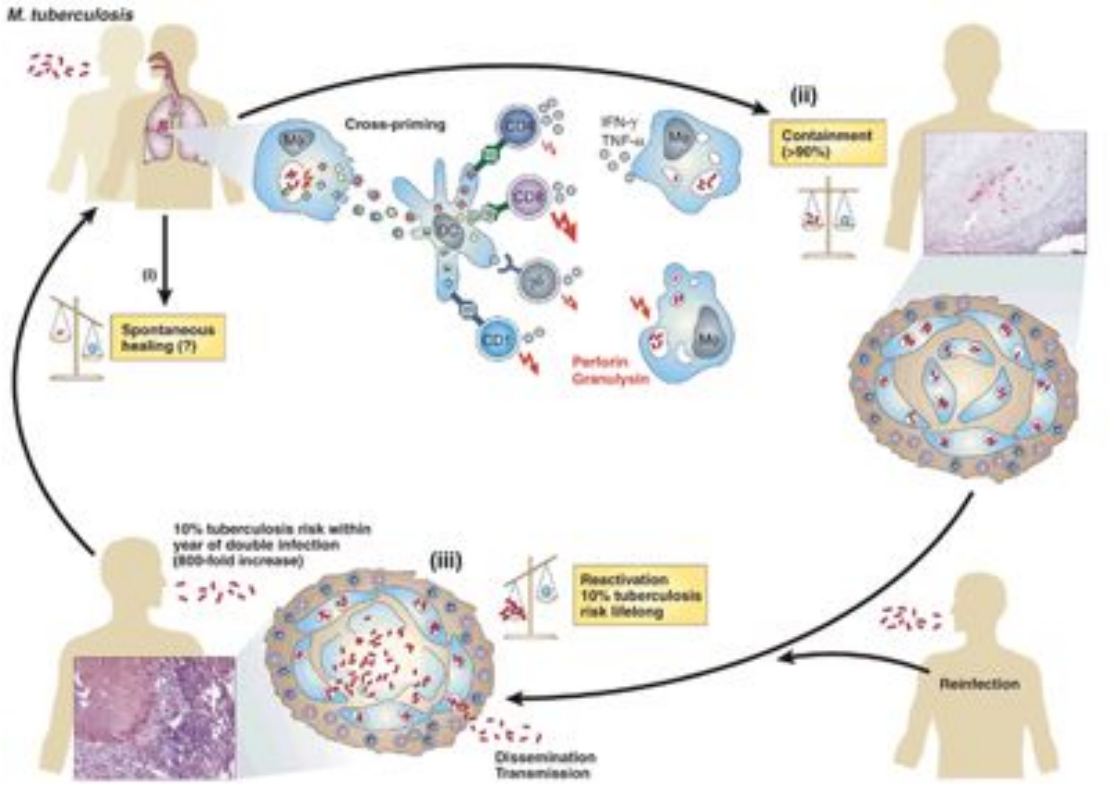

Figure 2: The possible outcomes upon inhalation of *M.tb* bacilli. (i) Upon infection it is postulated that some individuals may have the capacity to spontaneously clear the infection without developing any symptoms, (ii) Approximately 90% of individuals who become infected have the ability to contain the bacteria within a granuloma due to a well-orchestrated immune system, (iii) The other 10% of those who are infected develop disease during their lifetime, and this likelihood is increased by secondary infection. Risk of disease is highest in the first 2 years after infection and wanes, but reinfection increases the risk again. (Adapted from Kaufmann et al., Nature reviews 2005).

Studies of non-human primates (NHP) infected with *M.tb* and that go on to develop disease, have shown these NHP develop a spectrum of lung granulomas, similar to those observed in humans. Using [^{18}F]-D-deoxyglucose (FDG) positron emission tomography (PET) with computed

tomography (CT) imaging, Lin et al., were able to show that the size and metabolic activity of granulomas within an individual NHP, and even within a lung varied. At necropsy, some of the lesions within a NHP were found to be sterile, while others had viable bacilli showing the dynamic within the granulomas and the variable levels of inflammation (Lin et al. 2013).

Studies have shown heterogeneity within TB lesions in latently infected individuals at post-mortem (Vandiviere et al. 1956). Furthermore, the recovery of viable *M.tb* bacilli in these lesions is highly variable (Vandiviere et al. 1956). This heterogeneity has been suggested to reflect the immune response at different stages of infection of disease. The recent advances in imaging technology have allowed scrutiny of TB lesions in humans. High resolution CT provides structural data on the lung and lymph nodes as well as a spatial map of the granulomas within these tissues. CT scans of individuals with LTBI have shown a wide range of findings, some of which are characteristic of patients with active disease, though the individual shows no symptoms of disease (Goo et al. 2000). It is clear that this spectrum of disease or infection is hard to define, but advancements in technology have proven to be very informative in helping to begin to understand this.

Due to the complexity of host-pathogen interaction, rational designs of interventions remain a challenge.

1.2 Vaccines

Vaccines are designed to induce immunological memory that protects for prolonged periods of time.

1.2.1 Types of vaccines

It is now known that a vaccine should contain parts of or all of the pathogen it is designed to protect against, so that the host's immune system can recognise and respond to the pathogen upon challenge (Plotkin 2005). Vaccines can be categorized into 3 general groups; live attenuated vaccines, inactivated or killed vaccines or sub-unit vaccines.

Live attenuated vaccines are made from wild or disease-causing organisms, either viral or bacterial, which have been modified or attenuated to weaken or remove pathogenic factors (Plotkin 2003). Attenuated organisms used for such vaccines have the ability to grow or replicate within the human host but are unable to cause severe disease (Plotkin 2003). Live vaccines often induce mild disease-like symptoms and adverse events, however they have been shown to efficiently prime the immune response for exposure to the actual pathogen and confer protection, as seen with live attenuated measles vaccine (Sudfeld et al. 2010). Live attenuated vaccines can generate humoral (B cells) and cellular (T cells) immune responses that confer protection. Many live attenuated vaccines, such as those against measles (Sudfeld et al. 2010); poliovirus (Grassly et al. 2007) and yellow fever (Pulendran et al. 2013), are administered worldwide and are remarkably effective.

Inactivated or killed vaccines are comprised of completely inactivated pathogen, where a virus or bacterium is grown and then killed either by heat or with formalin. The organism therefore does not have the capacity to grow or replicate (Plotkin 2003). Usually these types of vaccines are not as effective as a live attenuated vaccine and may require repeated administrations. Most inactivated vaccines, such as inactivated polio vaccine (IPV), confer protection by inducing a humoral response, which may need boosting later in life due to diminishing memory responses (Murdin et al. 1996).

Sub-unit vaccines are made from parts of the pathogen, whether inactivated toxins, DNA, proteins or any component of the pathogen, but not the whole pathogen. Many novel candidate vaccines currently under development are sub-unit vaccines. Sub-unit vaccines currently licensed include those for Hepatitis B, diphtheria and tetanus toxoid (Plotkin 2005).

Vaccines that stimulate the humoral response have proven the most successful against pathogens (Plotkin 2005). It is postulated that a vaccine against TB should induce cellular immunity, as the role of T cells is likely to be crucial in the control of TB infection and disease (Kaufmann 2012; O'Garra et al. 2013; Brennan & Thole 2012). The role of B cells in immunity against TB

remains elusive and debatable (O'Garra et al. 2013; Maglione & Chan 2009). However, more recently it is thought that a vaccine that can induce both T cell and B cell responses may be better to prevent *M.tb* infection (Kaufmann 2012).

1.2.2. Vaccine strategies

Many variables need to be considered when designing vaccines. An important consideration in design of vaccines is whether the vaccine is to be given to i) prevent infection, ii) prevent progression of infection to disease or iii) to modulate disease, as shown in Figure 3 below (Kaufmann et al. 2010; Kaufmann 2010).

To have the greatest cost benefit, a vaccine should ideally be given once and protect for a lifetime. However this has not been achieved for many diseases and more than one dose of many vaccines is required. A tremendous effort has gone into studying the timing and type of vaccination requirements to optimally induce long-lived protection with multiple vaccinations. Researchers have proposed multiple strategies.

One such strategy is known as homologous boosting. Homologous boosting enhances a vaccine response after the initial vaccination, known as the prime, with the same vaccine. A second strategy is known as the heterologous prime-boost strategy in which a different vaccine is given to boost the primed immune response (McShane 2009; Kaufmann 2010). The timing between the prime and the boost vaccination should be carefully determined.

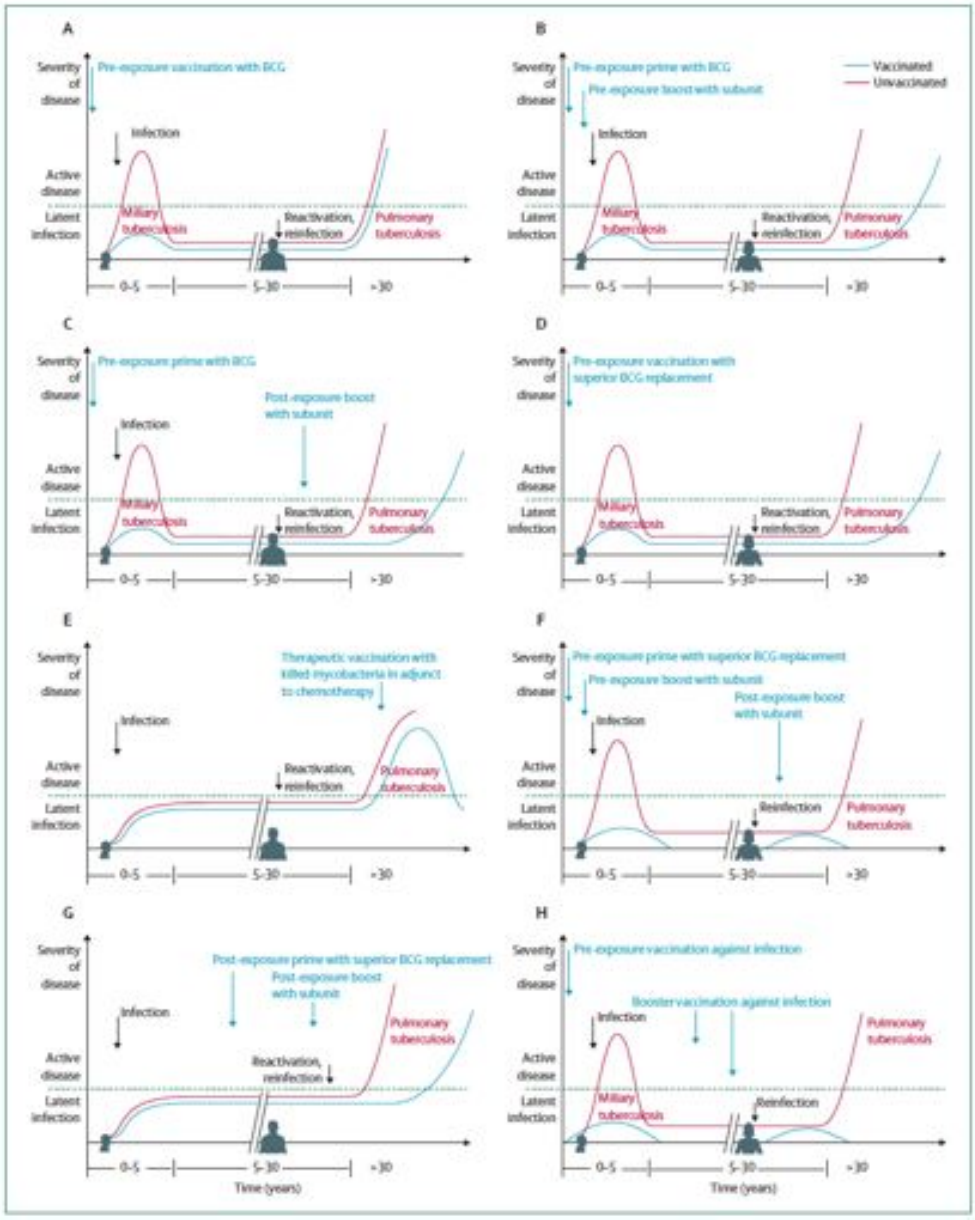

Figure 3: Vaccination strategies against TB. Graphs depict possible prime-boost strategies that have been explored, and others that may be implemented in vaccine design and clinical trials in the future. The possible predicted outcomes of disease severity or progression to disease are also shown (Kaufmann et al. 2010). The blue line represents the vaccinated population and the red line the unvaccinated population. (A) pre-exposure vaccination with BCG protects against early childhood tuberculosis but does not eradicate TB disease. This is the current vaccination strategy. (B) Priming with BCG at birth or early childhood followed by a pre-exposure boost with subunit vaccine to delay or prevent the onset of TB in adulthood; (C) Boosting of the immune response post-exposure with a subunit vaccine in adults who had been primed with BCG; (D) Priming with a superior BCG replacement to prevent TB for a lifetime; (E) vaccination of patients with active TB disease who are being treated with drugs with a therapeutic vaccine; (F) heterologous prime-boost strategy where BCG is replaced with a superior BCG and a subunit vaccine is used as a booster, which may result in sterility or complete eradication; (G) Vaccination of LTBI individuals with a superior replacement BCG prime and boosting with a subunit vaccine to prevent TB disease and (H) pre-exposure vaccination to prevent stable infection with *M.tb* (Kaufmann et al. 2010).

1.2.3. Bacillus Calmette-Guérin

The only currently available vaccine against TB is Bacillus Calmette-Guérin (BCG). BCG is widely administered and generally safe in immunocompetent individuals, however, it affords highly variable and mostly poor protection against pulmonary TB (Colditz et al. 1994) (Fine 1995). The efficacy of BCG has been reported to vary with geographical location, and this may be due to the environment and the population genetics in that region. However, BCG has been shown to protect infants against disseminated disease, such as miliary TB and TB meningitis (Rodrigues et al. 1993). The protection afforded by BCG against miliary and disseminated TB is reported to be as high as 80% (Fine 1995). Current opinions in the field include that a new TB vaccine should either boost BCG induced immunity or completely replace BCG.

The idea of not replacing BCG is to rather boost the BCG induced immunity in a heterologous prime-boost strategy. BCG is given first and then at a pre-determined interval, a different vaccine is given. This is particularly aimed at pre-exposure to *M.tb*, not only in infants but in adolescents and adults (McShane 2009).

1.2.4. Current candidate TB Vaccines

Current TB vaccine candidates are being designed to either induce an *M.tb*-specific T cell response that will be sufficient to prevent TB infection, or to prevent progression to disease, for immunotherapeutic purposes.

Live mycobacterial candidates being explored as potential TB vaccines are mostly based on improving BCG by adding or removing specific genes. One such vaccine is a recombinant BCG (rBCG) with a deletion of the gene encoding urease and integration of a gene encoding listeriolysin (Grode et al. 2005). Listeriolysin mediates lysis of the endosomal compartment within infected cells, allowing enhanced MHC-I antigen presentation, thought to result in greater induction of CD8 T cell responses. Other live attenuated vaccines are strains of *M.tb*, which have had virulence factors disrupted, such as the transcriptional regulator gene phoP disrupted (MTBVAC), which is shown in Table 1.

The majority of candidates currently in clinical trials are subunit vaccines containing antigens that are proteins secreted by *M.tb* in its active state or are expressed when *M.tb* has transformed into its latent state, where it is less metabolically active. Antigens included in these vaccines were mostly chosen because they induced immunodominant responses in T cell assays that measure Th1 cytokine production in the blood of latently infected or previously diseased individuals (Brennan & Thole 2012).

Viral vectors expressing selected *M.tb* antigens are also being tested as potential vaccine candidates. Antigens included in these vectors are also selected based on immunodominant responses in T cell assays that measure Th1 cytokine production.

As mentioned earlier, these vaccine candidates are identified for prime-boost heterologous vaccination strategies with BCG, or as immunotherapeutic vaccines, as shown in Table 1, below.

Table 1: TB vaccine candidates in various stages of clinical trials, as at October 2013 (www.pipelinereport.org). Shown are the proposed vaccination strategy, the composition of the vaccine, the sponsors, as well as the clinical trial phase they are in.

Agent	Strategy	Type	Sponsors	Status
M. indicus pranii	Immunotherapeutic	Whole-cell M. indicus pranii	Department of Biotechnology (Government of India), Cadila Pharmaceuticals	Phase III
M. vaccae	Immunotherapeutic	Whole-cell M. vaccae	Anhui Longcom	Phase III pending
MVA85A/ AERAS-485	Prime-boost	Viral vector	Oxford University, Aeras	Phase IIb
M72 + AS01	Prime-boost	Adjuvanted subunit	GSK, Aeras	Phase IIb
Crucell Ad35/ AERAS-402	Prime-boost	Viral vector	Crucell, Aeras	Phase II (formerly phase IIb)
VPM1002	Prime	Live recombinant rBCG	Vakzine Projekt Management GmbH, Max Planck Institute for Infection Biology, TuBerculosis Vaccine Initiative (TBVI), Serum Institute of India	Phase IIa
RUTI	Immunotherapeutic	Fragmented MTB	Archivel Farma	Phase IIa
Hybrid 1 + IC31	Prime-boost	Adjuvanted subunit	Statens Serum Institut (SSI), TBVI, Intercell, European & Developing Countries Clinical Trials Partnership	Phase IIa
Hybrid 56 + IC31	Prime-boost	Adjuvanted subunit	SSI, Aeras	Phase IIa
Hybrid 4 + IC31/ AERAS-404	Prime-boost	Adjuvanted subunit	Aeras, Sanofi Pasteur	Phase IIa
ID93 + GLA-SE	Prime-boost	Adjuvanted subunit	Infectious Disease Research Institute, Aeras	Phase I
Ad5Ag85A	Prime-boost	Viral vector	McMaster University, CanSino	Phase I
MTBVAC	Prime	Live genetically attenuated MTB	University of Zaragoza, Biotabri, TBVI	Phase I
Dar-901	Prime-boost	Whole-cell M. vaccae	Geisel School of Medicine at Dartmouth University	Phase I pending

Note: For each candidate under the prime-boost strategy, trials are evaluating the experimental vaccine in the left-hand column given as a boost to a BCG prime.

The vaccine candidate, MVA85A, is one of the most advanced in the clinical development process. MVA85A is a modified vaccinia Ankara, which is a replication deficient pox virus (Blanchard et al. 1998), and expresses the immunodominant mycobacterial protein antigen 85A (Ag85A). Ag85 is a complex of three secreted proteins with mycoltransferase activity, which is important in maintaining the cell wall integrity of the bacterium. Ag85 is also implicated in playing a role in alveolar macrophage invasion (Wiker & Harboe

1992). Ag85A, B and C are expressed by most mycobacterium species, including *M.tb* and BCG.

Some of the work in this thesis is based on T cell responses induced by MVA85A. At the South African Tuberculosis Vaccine Initiative (SATVI), we have completed five clinical trials of the MVA85A vaccine. MVA85A was shown to be very well tolerated and immunogenic in adults (Hawkridge et al. 2008; Scriba et al. 2012), adolescents and children (Scriba et al. 2010), and infants from a TB endemic area (Tameris et al. 2013; Scriba et al. 2011). In a recently completed phase IIb study in infants, MVA85A was shown to be immunogenic and safe, but had no protective efficacy against *M.tb* infection or TB disease (Tameris et al. 2013). Despite this disappointing result, we used MVA85A as a model vaccine for studying T cell immunity and generating new knowledge that is important for vaccine design.

1.3. Immunity to TB

1.3.1. Innate immunity

The body's first line of defense against pathogens that have permeated the skin or endothelial barrier is known as the innate immune response. This is a rapid response launched to kill or to contain the pathogen and restrict its spread.

Upon inhalation of *M.tb* bacilli, resident cells such as the macrophages and neutrophils are the first to recognise the bacilli through pattern recognition receptors (PRR). These cells have the ability to recognise molecules known as pathogen associated molecular patterns (PAMPs) on the surface of the bacilli as foreign. Recognition is through PRRs such as complement receptor, C-type lectins such as dendritic cell-specific intercellular adhesion molecule-3-grabbing non-integrin (DC SIGN) and through toll like receptors (TLR) (Ernst 1998; Tailleux et al. 2003). This recognition results in uptake of the bacilli by macrophages, as well as recruited dendritic cells and neutrophils. Each one of these cells has a specialised function to eliminate and control the establishment of *M.tb* infection in the lungs.

Macrophages play a pivotal role immediately after inhalation of the bacilli. Macrophages phagocytose the bacteria and sequester the bacilli into the phagosome, which when fused with lysosomes, facilitates acidification of the phagolysosome resulting in death of the bacilli (van Crevel et al. 2002). Macrophages can also use autophagy to sequester *M.tb* bacilli in the cytoplasm, into a double membrane autophagosome, which when activated increases the acidification of the phagosome and leads to killing of the mycobacteria (Kundu & Thompson 2008; Gutierrez et al. 2004). However more and more studies have shown that *M.tb* has the ability to stop phagosome-lysosome fusion, survive, and replicate within the macrophage.

Neutrophils have been shown to play multiple roles in controlling *M.tb* infection. Neutrophils are highly efficient at phagocytosis after which they undergo apoptosis forming debris which is taken up by macrophages to control spread of the bacterium (Morel et al. 2008). Neutrophils are able to kill *M.tb* through production of antimicrobial peptides such as cathelicidin (Martineau et al. 2007). Studies in the mouse have shown that neutrophils may play a role in the recruitment of other cells, such as T cells, through a chemoattractant mechanism (Seiler et al. 2003). *M.tb* has been shown to subvert immune control mechanisms, and one way is by preventing the apoptosis of neutrophils, promoting its survival (Blomgran et al. 2012).

On its own, the innate response is not sufficient to effectively control or eliminate *M.tb*, and efficient control of *M.tb* is dependent on induction of an adaptive immune response. Dendritic cells are the professional antigen presenting cells (APC) that initiate priming of T cells (Banchereau & Steinman 1998). DCs thus act as a link between the innate and adaptive immune system. After *M.tb* infection, DCs are recruited to the lung by activated macrophages that secrete chemokines. In the lung, DCs take up *M.tb* bacilli and upregulate expression of cell surface markers involved in migration to lymph nodes and co-stimulation of T and B cells, such as CCR7, CD80, CD86, and CD40. These DCs then mature and traffic to draining lymph nodes where they present *M.tb* antigen in the context of HLA molecules to prime T cells (Hickman-Miller & Yewdell 2006; Steinman & Swanson 1995), initiating

adaptive immunity.

1.3.2. Adaptive Immunity: T cell subsets and functions

Upon exposure to antigen, naïve T cells to differentiate into different T cell subsets, which have a wide range of functions and produce multiple cytokines. This differentiation is influenced by the cytokine milieu present when the cells experience antigen for the first time, as well as the nature of the antigen (Mosmann & Coffman 1989). The cytokine milieu is largely influenced by cytokines being secreted by DCs that are delivering and presenting antigen to the naive cells.

A few CD4 T cell subsets have been characterised in depth and belong to well defined differentiation lineages. This sub-setting was based on patterns of cytokine expression in effector T cells as well as lineage specific transcription factors, as shown in Figure 4. These transcription factors regulate the generation, function and cytokine production, as well as the inhibition of differentiation of other lineages of helper T cells (Oestreich & Weinmann 2012). The most characterised helper T cell lineages to date are Th1, Th2, Th17 and Tregs.

Th1 cells are required and essential for clearance or control of intracellular pathogens such as bacteria and viruses (Fietta & Delsante 2009). Th1 cells are generated when naïve T cells are primed in the presence of IL-12, resulting in expression of the transcription factor, T-Bet (Szabo et al. 2000). This induces the typical Th1 effector cytokine, IFN-γ. Th1 cells predominantly produce IFN-γ, IL-2 and TNF-α (O'Garra et al. 1998), cytokines shown to be very important in orchestrating immune responses. IL-2 promotes T cell proliferation and maintenance of T cell populations. IL-2 has also been implicated in the generation of CD8 T cell memory, ensuring a robust secondary response upon antigen encounter (Williams et al. 2006). IFN-γ activates macrophages resulting in killing of bacteria, as well as further IL-12 production by DCs, resulting in a positive feedback loop that drives expansion of the Th1 population.

Th2 cells play a major role in fighting extracellular parasites, like worms, and are also involved in allergic diseases (Romagnani 1994; De Carli et al. 1994). Th2 cells are induced by priming of naïve T cells in the presence of IL-4, inducing the expression of the transcription factor, GATA-3, which induces production of the cytokines IL-4, IL-5 and IL-13 (Zheng & Flavell 1997; Lantelme et al. 2001; Seder & Paul 1994; O'Garra et al. 1998).

Th1 and Th2 inhibit each other's function and differentiation, and have traditionally been seen as mutually exclusive T cell subsets. However, some data suggests otherwise, since T cell clones that co-produce IFN-γ and IL-4 have been described (Murphy & Reiner 2002). This suggests plasticity in T cell lineages, and that cells are not definitively committed to a lineage and can switch upon particular cues (Murphy & Reiner 2002).

Th17 cells are largely involved in the immune response against extracellular bacteria and fungi. Differentiation of Th17 cells require multiple cytokines, such as various combination of IL-6, TGF-β, IL-1β, IL-21 and IL-23 (Moseley et al. 2003; Korn et al. 2007; Veldhoen et al. 2006; Zhou et al. 2007). Priming of naïve T cells in the presence of these cytokines, results in the expression of RORγt, the master regulator of the T cell lineage. However, several other transcription factors have been implicated in the complete differentiation and lineage commitment of these Th17 cells, as a deficiency in RORγT does not lead to complete interruption of Th17 cytokine expression (Yang et al. 2008). Th17 cells mostly produce the effector cytokines IL-17A, IL-17F and IL-21, which act in an autocrine manner. IL-17 mediates recruitment of neutrophils to sites of infection, and promotes inflammation. (Moseley et al. 2003; Laan et al. 1999). IL-17 is an important effector molecule in chronic inflammatory diseases such as psoriasis (Chiricozzi & Krueger 2013).

Another class of T cells that have been well studied and characterised are the regulatory T cells (Tregs). Two subsets of Tregs have been described. Thymic Tregs, previously named natural Tregs, are derived and develop in the

thymus, and peripheral Tregs (pTregs) (Abbas et al. 2013), previously known as induced Tregs, are derived in the periphery from naïve CD4 T cells (Abbas et al. 2013; Bluestone & Abbas 2003). Priming of naïve T cells in the presence of TGF-β and absence of inflammatory cytokines drives differentiation of naïve cells to Tregs. These cells can be identified by the expression of the transcription factor, FOXP3 as well as high expression of the IL-2 receptor, CD25 (Sakaguchi et al. 1995). Tregs regulate the immune response by regulating inflammation and effector responses and by maintaining tolerance to self-antigens (Sakaguchi 2005). Tregs produce immunomodulatory or suppressive cytokines such as IL-10, IL-35 and TGF-β (Collison et al. 2007; Rubtsov et al. 2008).

Recently, additional subsets, distinct from Th1, Th2 and Th17 subsets, have been identified. These subsets such as Th9 and Th22 are not as well characterised and defined. The Th9 subset is induced by priming of naïve T cells in the presence of IL-4 and TGF-β (Veldhoen et al. 2008; Putheti et al. 2010), and is characterised by production of the effector cytokine IL-9, and not IL-4, IFN-γ or IL-17. Th9 cells primarily express the transcription factor PU.1 upon priming, although IRF4 expression has also been shown to be induced. These IL-9 producing cells have been implicated in allergic asthma and autoimmunity. Surface markers that will allow the isolation of human Th9 cells have not been identified thus far, and hence these cells are still poorly characterised.

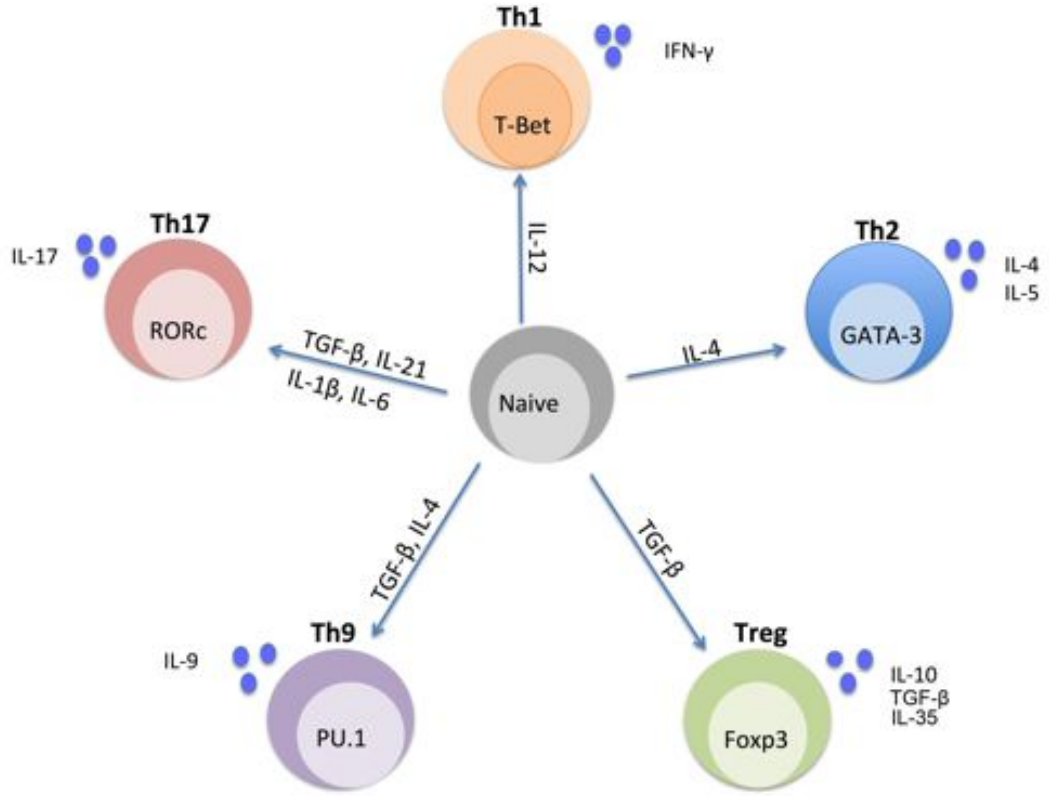

Figure 4: Transcription factors specific to each T cell lineage induce cytokine production. Naïve T cells can be primed to differentiate into multiple T cell subsets in the presence of different cytokines. Cytokines influencing the differentiation of naïve T cells to specific lineages are shown adjacent to the arrows. Transcription factors specific to T cell linages are shown, as well as the effector cytokines produced by specific T cell lineages.

1.3.3. The adaptive immune response: CD4 and CD8 T cells in mycobacterial infection.

CD4 and CD8 T cells comprise well-described subsets of T cells known to play important roles in control of mycobacterial infection. These cells are the main focus of this project.

Although comprising only 30-70% of the lymphocytes in the lung as measured in broncheoalveolar lavage (BAL) (Walrath & Silver 2010; Kalsdorf et al. 2009) in healthy infected individuals, CD4 T cells are critical components of granuloma formation and control the replication of *M.tb* bacilli. Mice deficient in CD4 T cells are unable to control bacterial numbers and have more disseminated *M.tb* with higher bacterial burdens in the lung, liver and spleen when challenged intravenously with *M.tb,* compared with wild-type control mice (Caruso et al. 1999). In addition, depletion of CD4 T cells during persistent *M.tb* infection results in increased replication of *M.tb* and breakdown in the granuloma structure, implying that CD4 T cells are also important for maintaining granuloma integrity (Caruso et al. 1999).

The importance of CD4 cells for control of *M.tb* in humans is illustrated by the observation that HIV-infected individuals have a significantly increased risk of developing TB, compared with HIV negative individuals (Lawn et al. 2002). Ongoing viral replication within CD4 T cells is one of the most important parameters driving the massive, systemic depletion of memory CD4 T cells during acute immunodeficiency virus infection (Mattapallil et al. 2005). A recent study showed that *M.tb*-specific CD4 T cells are more rapidly and preferentially infected and depleted by HIV infection (Geldmacher et al. 2010), compared with cytomegalovirus (CMV) specific T cells. HIV infected individuals have reduced frequencies of *M.tb*-specific CD4 T cells in their lungs, and the function of these T cells is impaired (Kalsdorf et al. 2009). This loss and impairment in the function of *M.tb*-specific T cells is likely to be a contributor to the increased risk of TB in HIV infected individuals. This is further corroborated by a study in cynomologous macaques with latent *M.tb* infection. When infected with Simian immunodeficiency virus (SIV), these animals rapidly progressed to TB disease. Depletion in CD4 T cells elevated

risk of progression to disease, further confirming the importance of CD4 T cells in containment and control of *M.tb* (Diedrich et al. 2010).

CD4 T cells mediate their protective functions by secreting effector cytokines, such as the Th1 cytokines, IFN-γ, IL-2 and TNF-α (Hanekom et al. 2007), which regulate other immune cells. IFN-γ is essential for activating macrophages. The importance of IFN-γ in human immunity against mycobacteria is illustrated by individuals with gene mutations in the IFN-γ pathway, such as the IFN-γ receptor and IL-12, who are at high risk of developing severe mycobacterial disease (Ottenhoff et al. 2000). TNF-α is pivotal in cell recruitment, particularly of macrophages to enable granuloma formation and maintenance (Algood et al. 2005). The importance of TNF-α is further demonstrated in studies where the anti-TNF antibody, Infliximab, was used to treat rheumatoid arthritis and Crohn's disease in individuals latently infected with *M.tb.* In these studies, it was noted that many of these individuals developed TB disease within a short period of receiving anti-TNF treatment (Keane et al. 2001; Wallis et al. 2004). IL-2 was shown to be important in the development of long term T cell memory, which is essential for long-lived immunological protection (Ottenhoff et al. 1998).

CD4 T cells are also necessary for development of functional cytotoxic CD8 T cells. Mice deficient in CD4 T cells had impaired CD8 T cell cytotoxic activity in their lungs in an acute model of *M.tb* infection (Serbina et al. 2001). CD4 T cells may also have cytotoxic capacity, as they express cytotoxic molecules, which have the ability to restrict *M.tb* growth *in vivo* (Bastian et al. 2008; Canaday et al. 2001; Mutis et al. 1993).

CD8 T cells are also important for immunity to *M.tb*. CD8 T cells share some functions with CD4 T cells since they also express IFN-γ and TNF-α. However, the best-described role of CD8 T cells in controlling infections is via their cytotoxic capacity. Cytotoxic CD8 T cells can induce apoptosis of infected macrophages by releasing cytolytic granules containing perforin (a pore-forming molecule) and granzymes. In addition, the antimicrobial molecule

granulysin, when secreted with perforin, can lead to direct intracellular killing of *M.tb* (Stenger et al. 1999; Mohagheghpour et al. 1998). The importance of CD8 T cells in humans has recently been shown in patients suffering from autoimmune diseases, who were treated with anti-TNF therapy and presented with increased susceptibility to developing TB. These patients had a reduction in CD8 T cells with the ability to kill *M.tb* infected monocytes *in vitro* (Bruns et al. 2009).

Multiple other T cell subsets may be important in the control of *M.tb*. In mice, Th17 cells induced by a novel TB vaccination were shown to mediate protective effects through the recruitment of Th1 cells to the lung upon *M.tb* challenge (Khader et al. 2007). γδT cells (Spencer et al. 2008) and T cells restricted by non-classical molecules such as CD1 and HLA-E may also have roles in protection (Van Rhijn et al. 2009).

In order to identify correlates of protection against TB disease, many studies in humans have assessed anti-mycobacterial T cell immunity, particularly focusing on cytokine expression or T cell phenotype. Studies done by our group have shown that the frequency, as well the cytokine expression profile of T cells in infants vaccinated with BCG and followed up for a period of 2 years, did not correlate with risk of TB disease (Kagina et al. 2010). Our group has also measured cytotoxic markers such as granulysin and perforin in CD4 and CD8 T cells and found no correlation with risk of disease (Keyser et al., unpublished). It is important to recognise that the outcomes measured in the above mentioned studies might not correlate with inhibition of mycobacterial growth or even killing of the pathogen. To address this, several investigators have developed *in vitro* assays aimed at measuring inhibition of mycobacterial growth (Worku & Hoft 2003; Wallis et al. 2001; Kampmann et al. 2000).

1.4 Immunological memory

Immunological memory refers to the maintenance of antigen-experienced, specific T cells that are long-lived, even in the absence of antigen and are

able to proliferate to large numbers of effector T cells upon secondary antigen encounter (Sallusto et al. 2004; Sallusto et al. 2010). The induction of long-lived memory T cells forms the basis for adaptive immunity and vaccination.

Antigen-experienced memory T cells can be categorised into distinct memory subsets according to their function and the expression of specific phenotypic markers. A large number of phenotypic markers have been used to classify T cells into different memory subsets. These include, but are not limited to CD45RA, CCR7, CCR4, IL7-Rα, CD27, CD28 and CD62L, CCR2 and CCR5 (Figure 5, below) (H. H. Zhang et al. 2010; Sallusto et al. 1999; Fritsch et al. 2005; Kaech et al. 2003).

1.4.1. Defining Memory

Naïve T cells are antigen-inexperienced T lymphocytes that recirculate between secondary lymphoid organs in search of antigen presented by dendritic cells. Naïve T cells have a high threshold for antigen stimulation and require co-stimulation in order to be activated. The first phenotypic markers that allowed distinction between naïve, long-lived central memory (T_{CM}) and short-lived effector memory (T_{EM}) cells were CCR7 and/or CD62L in combination with either CD45RA or CD45RO (Sallusto et al. 2000). This classification system defines cells that co-express CD45RA and CCR7, a chemokine receptor that controls T cell homing to secondary lymphoid organs, as naïve T cells. Naïve T cells lose CD45RA expression and up regulate CD45RO upon antigen experience, and differentiate into central memory, effector and effector memory T cells (Sallusto et al. 2000).

T_{CM} cells, which are CD45RA-negative (or CD45RO-positive) but have retained expression of CCR7, are long-lived antigen-experienced cells. T_{CM} cells mainly produce IL-2 and have high proliferative potential upon antigen encounter. T_{CM} usually recirculate between secondary lymphoid organs. T_{CM} have a lower antigen stimulation threshold than naïve T cells and do not require co-stimulation for activation. These cells may differentiate into effector T cells upon antigen exposure or inflammation. Induction of memory cells

bearing a T_{CM} phenotype is thought to be important to induce long lived protection (Sallusto et al. 2000; Lanzavecchia & Sallusto 2005).

Effector memory T cells do not express CCR7 or CD45RA but express chemokine receptors, such as CXCR3, and adhesion molecules, such as $\alpha4\beta1$, $\alpha4\beta7$ and $\alpha E\beta7$, required for homing to inflamed tissues. Thus effector memory T cells are predominantly found at sites of infection and in the periphery. Both CD4 and CD8 effector memory cells produce large amounts of effector cytokines such as IFN-γ within minutes or hours of antigenic stimulation and display immediate cytotoxic function. Unlike T_{CM}, T_{EM} may be short-lived, have limited proliferative capacity and are more prone to apoptosis upon antigen stimulation (Sallusto et al. 1999; Lanzavecchia & Sallusto 2005).

A fourth subset is termed terminally differentiated memory T cells (T_{EMRA}). These are antigen-experienced effector cells, which re-express CD45RA, and are thus $CD45RA^{+}CCR7^{-}$. Based on their limited functionality and short telomere lengths, indicating that these cells have undergone extensive division, this subset is the most differentiated of the antigen-experienced populations (Fritsch et al. 2005; Geginat et al. 2003). T_{EMRA} are thought to be the last step before cell death, and are limited in function, producing only very low levels of cytokines, and are unable to proliferate. This subset of T cells is well described in CD8 T cells but not in CD4. T_{EMRA} are associated with persistent or chronic infections such as CMV, Hepatitis B virus (HBV) and HIV infection (Walker et al. 2013; Harari et al. 2004).

Other markers and cytokine/chemokine receptors that can be used to characterise T cells into memory phenotypes have been described. One such marker is CD27. CD27 is a member of the TNF receptor family and is used to delineate T cell differentiation stages in both CD4 and CD8 T cells. It is expressed at high levels on naïve T cells and upon stimulation T cells lose the expression of CD27. In CD4 T cells this marker has been well characterised in the differentiation pathway (Fritsch et al. 2005).

Many more markers are used as shown in Figure 5 below, adding to the complexity of defining memory T cell subsets. In this study, we aimed to characterise memory T cells induced by MVA85A vaccination and natural *M.tb* infection by measuring expression of a number of markers.

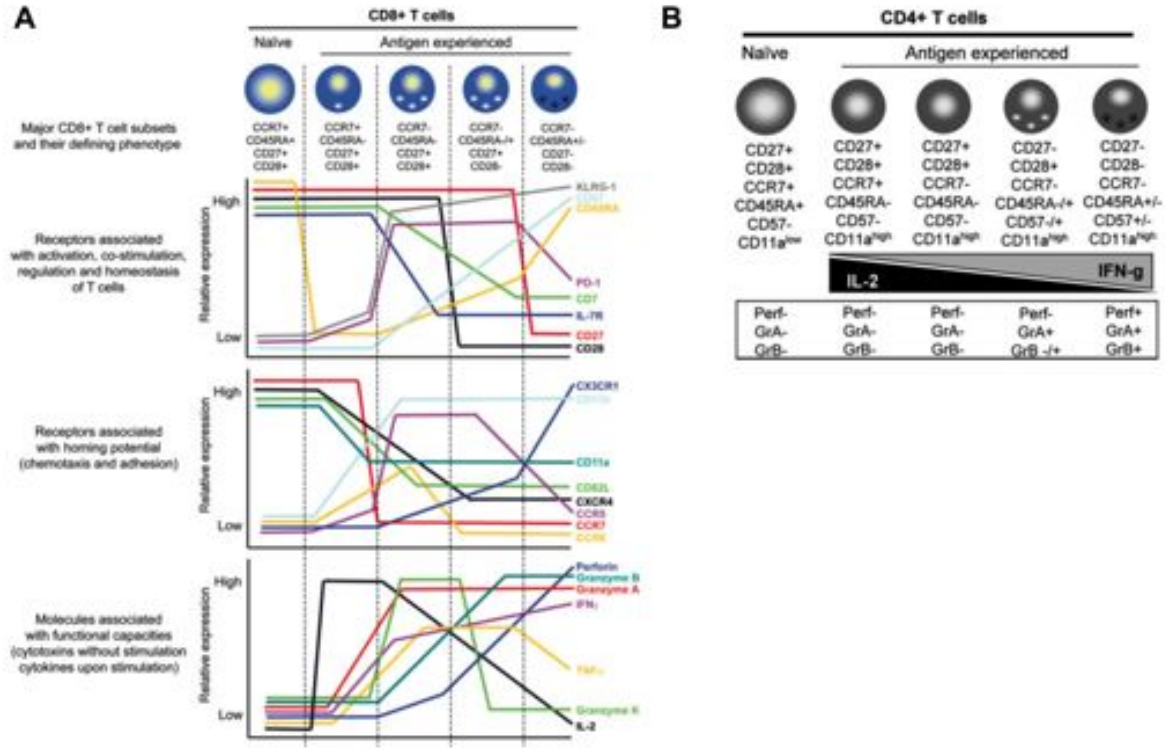

Figure 5: Phenotypic and functional attributes of T cells in the differentiation pathway. (A) CD8 T cells as classified by the phenotypic markers CD45RA, CCR7, CD27 and CD28. Functional and other phenotypic properties are shown below. (B) CD4 T cells as classified by the phenotypic markers CD45RA, CCR7, CD27, CD28 as well as CD57 and CD11a. Functional properties such as cytokine production and cytotoxic capabilities are shown (Adapted from Appay et al., (Appay et al. 2008)).

1.4.2. Memory T cells in mycobacterial infection

The risk of progressing from infection to TB disease is highest immediately after primary infection and then wanes over time (Wiker et al. 2010). Mathematical models have been used to investigate this reduction in risk, which varies in different studies (Colijn et al. 2006). Some reports have suggested that the risk of active TB disease following TB exposure is significantly reduced in individuals with established latent *M.tb* infection, compared with uninfected persons (Andrews et al. 2012; Stead 1967; Chiang & Riley 2005; Brooks-Pollock et al. 2011). The hypothesis that latent infection

may be protective against TB upon re-exposure is supported by recent studies of isoniazid preventative therapy (IPT) in high endemic TB areas, where IPT was given to clear latent infection to reduce the incidence of TB. The results surprisingly showed that cumulative incidence of TB disease was not different between persons on IPT and untreated persons, most likely due to reinfection (Samandari et al. 2011; Churchyard et al. 2014). One explanation may be that clearing *M.tb* infection results in reduced effector memory T cell populations that may have protected against disease upon reinfection.

These epidemiological findings suggest that *M.tb*-specific immune responses in persons with established infection, who did not develop TB within the first 1-2 years after exposure, may protect against TB disease. In an attempt to understand which T cell memory subsets may be required to prevent progression from infection to disease, many human studies have characterised the function and phenotype of *M.tb*-specific T cell responses in asymptomatic latent *M.tb* infection and/or in active TB disease (Harari et al. 2011; Day et al. 2011; Rozot et al. 2013; Rueda et al. 2010; Sutherland et al. 2010).

M.tb-specific CD8 T cells predominantly display effector memory phenotype in patients with active TB disease and a terminally differentiated phenotype in LTBI individuals (Rozot et al. 2013). In children with active TB, the direct ex vivo phenotype of CD8 T cells was greatly skewed to an effector memory phenotype, when compared with latently infected and uninfected children (Jacobsen et al. 2007). Reduced proliferative capacity of *M.tb*-specific CD8 T cells has been observed in individuals with smear-positive TB as compared to individuals with LTBI or smear negative TB (Day et al. 2011). Treatment of smear positive TB cases resulted in gradual restoration of proliferative capacity of *M.tb*-specific T cells, suggesting that mycobacterial load may drive functionality and differentiation of memory T cells.

In healthy latently infected adults and children, mycobacteria-specific Th1 CD4 T cells predominantly display an effector memory phenotype, whereas

IL-17 and IL-22 producing CD4 T cells predominantly displayed a central memory phenotype (Scriba et al. 2008; Tena-Coki et al. 2010; Mueller et al. 2008). In another study, the authors showed that LTBI healthy individuals had higher frequencies of antigen-specific CD4 T cells that displayed a late-stage differentiated (CD45RA-CD27-) effector memory phenotype and the cells expressed PD-1, a marker associated with exhaustion or activation of T cells in virus models (Adekambi et al. 2012). A study of pleural fluid cells from patients with active TB disease also suggested that *M.tb*-specific CD4 T cells display an effector memory phenotype (Li et al. 2011).

Spontaneous healing from TB disease has been documented in the pre-antibiotic era. In one of these studies, ESAT6 and CFP10-specific CD4 T cells were detected up to 50 years after healing. Effector responses were detected in most participants and were attributed to incomplete clearance of *M.tb*. In a minority of participants, T cell responses were detectable only upon *in vitro* expansion of *M.tb*-specific T cells and were attributed to central memory lymphocytes (Millington et al. 2010). Understanding properties of memory cells that may have conferred the ability to heal TB disease may be critical for advancing our knowledge of TB pathogenesis in humans.

However, phenotypes of *M.tb*-specific cells may also not always fit the model described for other infections. An unusual population of mycobacteria-specific memory T cells, with phenotypic characteristics of naïve lymphocytes, has been described in numerous human studies. These “naïve-like” (NL) memory T cells express effector cytokines such as IFN-γ and TNF-α, but display a CD45RA+CCR7+CD27+ “naïve” phenotype (Kagina et al. 2009; Caccamo et al. 2006; Soares et al. 2008; Soares et al. 2013). These cells have been observed after vaccination and during natural infection (Kagina et al. 2009; Caccamo et al. 2006; Tena-Coki et al. 2010; Soares et al. 2008; Soares et al. 2013). Phenotypic and functional properties of these naïve-like T cells in *M.tb* infection have not been explored, and are the focus of Chapter 5.

The above-mentioned studies of T cell phenotypes were limited by the necessity for T cell stimulation in order to identify antigen-specific T cells through cytokine production. A caveat to this is that activation of cells by antigen stimulation may have altered expression of key phenotypic markers and thus influenced the outcomes and the interpretation of the data (Mallone & Nepom 2004). On the other hand, CD4 T cells expressing different cytokines may belong to different memory subsets, as observed for Th1 and Th17 cells (Scriba et al. 2008). Identification of mycobacteria-specific CD4 T cells by expression of one or few cytokines may therefore bias expression patterns of phenotypic markers. Measurement of phenotypic markers on mycobacteria-specific T cells directly *ex vivo* would eliminate these limitations.

1.4.3. Memory responses after vaccination

It is thought that a long-lived T cell response characterised by central memory T cells may be important for protection against TB disease. With this in mind, it has been postulated that a TB vaccine should aim to induce antigen-specific central memory CD4 T cells (Orme 2010). Hence, many groups have studied the memory phenotype of T cells after vaccination with novel TB vaccines.

Scriba et al. report a dominant effector memory phenotype of MVA85A-induced CD4 T cells after vaccination and this phenotype remained unchanged up to 56 days after vaccination in adolescents and children. Ag85A-specific central memory CD4 T cells were virtually undetectable 2 months after vaccination in these participants (Scriba et al. 2010). Another study of MVA85A-induced T cells in the United Kingdom also characterised Ag85A-specific T cells using different markers and found that these cells displayed a relatively immature ($CD45RO^{+}CD27^{int}CD57^{-}$) memory phenotype (Beveridge et al. 2007).

Soares et al. showed that, in 10-week old BCG vaccinated infants, mycobacteria-specific CD4 T cells predominantly displayed an effector memory phenotype (Soares et al. 2008). Kagina et al. observed predominantly an effector memory phenotype in infants who received BCG, either at birth or at 10 weeks of age. Central memory responses were very

low in these infants up to 1 year after vaccination (Kagina et al. 2009). However, in a more recent study, Soares et al. showed that BCG-specific cells mainly expressed a central memory phenotype 27 weeks after vaccination (Soares et al. 2013). This study highlighted two important differences. Firstly, the time at which T cell phenotype is assessed is very important, as the immune responses evolve from an early effector phase to establish the memory pool. Secondly, the antibody clones for CCR7 used in these studies were different and may have affected interpretation of the results. Orme et al., have hypothesised that one of the reasons for poor long-term protection conferred by BCG may reside in the prevalent induction of effector memory cells. In this model, constant re-exposure in TB endemic settings drives effector memory cells to differentiate into short lived effector cells, which are not replenished by central memory T cells (Orme 2010). The reason for BCG not protecting against pulmonary TB disease remains unclear.

To protect against TB disease, we propose that a TB vaccine should induce T cells that are long lived, have high proliferative potential, express Th1 cytokines and be able to traffic to the lung upon antigen re-exposure. We aimed to characterise the memory phenotype of *M.tb*-specific CD4 T cells in natural infection and after vaccination using tools that do not require T cell activation.

1.5 Tissue homing of T cells

The capacity of memory T cells to rapidly traffic to the relevant tissue or site of infection is likely to be a critical factor in protective immunity. Many studies have shown that the site at which a T cell is primed influences the expression of markers required for homing (Kantele et al. 1997; Kantele et al. 1999; Campbell & Butcher 2002; Kaufman et al. 2008). For example, T cells that are primed in the mesenteric lymph node, in the gut, possess the ability to traffic back to the gut (Kantele et al. 1999). This gut homing potential was shown to be dependent on co-expression of the integrins $\alpha 4$ and $\beta 7$. In a comparative study of oral and parenteral vaccination with Salmonella typhi Ty21a antigen, antigen-specific T cells were committed to migrating to mucosal

compartments and expressed $\alpha4\beta7$ after oral vaccination. By contrast, antigen-specific T cells induced by parenteral vaccination were directed to the systemic compartment (Kantele et al. 1997). It has also been observed that skin homing receptors, such as cutaneous lymphocyte antigen (CLA), are preferentially induced when T cells are primed in dermal peripheral lymph nodes (Campbell & Butcher 2002). A study suggested that T cell expression of $\alpha4\beta1$ may mark T cells that home to sites of inflammation, including the lung, but not the gut which requires $\alpha4\beta7$ (Feng et al. 2000). A recent study by Silver et al., showed that a large proportion of the *M.tb*-specific CD4 T cells in the lung after PPD challenge expressed $\alpha4\beta1$, further suggesting these integrins to be important in localising the CD4 T cells to the lung (Walrath & Silver 2010).

The studies cited above based their interpretation on the premise that tissue homing is programmed. However, studies suggest that the compartmentalisation of T cell responses is less categorical. In mice and rhesus macaques vaccinated intramuscularly with a recombinant adenovirus-based vaccine, antigen-specific T cell responses were found both systemically and at multiple mucosal surfaces (Kaufman et al. 2008). The ability to generate a potent mucosal immune response is an important goal of vaccination against pathogens acquired via mucosal transmission such as *M.tb*. Hence a better understanding of how the site of vaccination could influence the trafficking pattern of antigen-specific cells is critical. Optimal disease control would involve recruitment of specific T cells to the site of infection, such as the lung in *M.tb* infection, to carry out their protective functions immediately upon exposure.

The studies referred to above suggest that T cells with lung homing capacity will be observed in natural *M.tb* infection, whereas intra-dermal administration with a vaccine may prime cells expressing skin homing markers. We aimed to investigate homing marker expression by CD4 T cells after vaccination.

1.6 Detection of antigen-specific cells

In order to quantify immune responses induced by vaccinations or natural infection, multiple assays that measure T or B cell functions have been developed. These assays measure up regulation of effector functions such as cytokine production (Hanekom et al. 2004), or proliferation upon *in vitro* stimulation of cells with specific antigens. As T cells are likely key players in mediating *M.tb*-specific control, immunological assays to measure responses to *M.tb* vaccines or infection are mostly directed at T cells. The easiest compartment to assess these immune responses is the peripheral blood. Accessing other compartments, such as the lung or lymph nodes, is invasive and more challenging. Each assay can be highly informative in some ways. However assays are subject to limitations as will be outlined for each assay employed for this study, which are informed by the scientific question to be answered.

1.6.1. Whole blood vs Peripheral Blood Mononuclear Cell (PBMC) based assays.

In humans, whole blood or purified PBMCs are typically used to measure antigen-specific T cells and their functions. Whole blood must be stimulated fresh shortly after collection, followed by lysing of red blood cells and, optionally, fixation and cryopreservation of leukocytes. PBMCs can be isolated, cryopreserved without fixation and retain viability for subsequent stimulation and analysis. Cells are stimulated for different lengths of time (from a few hours up to 7 days) depending on the functional outcome assessed (Hanekom et al. 2008).

Vaccinologists advocate simplification and harmonisation of assays used to measure immunogenicity, with the aim to compare results across sites and across vaccines.

An advantage of whole blood assays (WBA) is that they allow assessment of T cell functions in the context of all components in the blood. The detected immune responses result from the interaction between all cell subsets normally present in the blood. PBMC preparations contain only mononuclear cells which allows for de-convolution of possible subsets responsible for

effector molecule production, however cryopreservation of the cells may introduce variability in their capacity to respond to *in vitro* stimulation (Hanekom et al. 2008).

1.6.2. Intracellular cytokine stimulation assay

The intracellular cytokine assay (ICS) is commonly used to detect antigen-specific cells that are producing cytokines in response to antigenic stimulation. Cells are stimulated for a period of time (typically 12 hours in our assays) with the antigen of interest during which time the protein secretion inhibitor, Brefeldin A, is added to block secretion of cytokines. Cells are then fixed, permeabilised, and intracellular cytokines stained with fluorescently conjugated antibodies, and detected by flow cytometry (Hanekom et al. 2004). In ICS assays, both intracellular cytokines and surface markers can be stained, allowing simultaneous interrogation of T cell phenotype and function. Many investigators have used this method or an adaptation of it, to interrogate the memory phenotype of cells after vaccination or infection (Kagina et al. 2009; Tena-Coki et al. 2010; Beveridge et al. 2007; Soares et al. 2010; Scriba et al. 2011; Scriba et al. 2012).

A limitation of this assay is that it depends on stimulation in order to identify antigen-specific cells, and the cellular activation may result in changes in the cell phenotype. Stimulation has been shown to affect the expression of some memory markers, including CD28 and CCR7 (Chao et al. 1997; Sallusto et al. 2004; Vallejo et al. 1999). Another limitation of this assay is that not all antigen-specific cells can be expected to produce the cytokines measured. A particular proportion of the antigen-specific cells may therefore remain undetected.

In this study, a 12-hour whole blood assay was used to assess the functionality of CD4 T cells after vaccination with a novel TB vaccine, MVA85A.

1.6.3. ELISpot assay

The Enzyme-linked Immunosorbent Spot (ELISpot) assay detects production and release of IFN-γ by T cells after a short term *in vitro* stimulation of PBMC with specific antigens. It was first described 30 years (Czerkinsky et al. 1983) ago and has become one of the most commonly used assays to measure cell specific immune responses (Slota et al. 2011). This is a highly reproducible, robust and sensitive assay to enumerate cells with immediate effector functions. An individual spot on the membrane in the well represents an individual cytokine-producing cell. The spots can be counted manually or using an automated reader and quantified.

ELISpot assays can be performed on freshly isolated or cryopreserved cells. ELISpots can be adapted in two ways: the short term assay to detect cytokine expression (direct *ex vivo*) or the cultured ELISpot assay which detects cytokines after the cells are cultured for an extended period of time (12-13 days) in the presence of antigen. Cells may be cultured in the presence of antigen to promote expansion of antigen-specific cells before performing a direct *ex vivo* ELISpot. The cultured ELISpot allows detection of antigen-specific cells that are at very low frequencies by expanding this population to become readily detectable.

As for IFN-γ release assays in stimulated whole blood, this assay does not allow identification of the cellular source of IFN-γ, unless it is performed after depletion of cell subsets from the PBMCs.

In this study, a cultured ELISpot assay was used to determine which *M.tb*-specific epitopes were recognised by latently infected individuals, to facilitate the development of HLA class II tetramers.

1.6.4. Proliferation Assay

One of the key characteristics of long-lived memory cells is the ability of cells to proliferate more readily than naïve T cells as they require less stimulation. Therefore, by assessing the proliferative capacity of cells, one can infer some memory properties of antigen-specific cells.

Initially the proliferation assay, a longer term assay, was used to identify antigen-specific cells, as cells were cultured with antigen for a period of 6 days, then assessed for proliferation. The proliferation assay can also be used to assess effector functions of expanded T cells. Many different techniques are available to assess *in vitro* proliferation of antigen-specific T cells. In this study, we used an assay based on dilution of a fluorescent dye upon cell division. This assay involves staining of PBMCs with the fluorescent dye 5,6-carboxyfluorescein diacetate succinimidyl ester (CFSE) or its derivative, Oregon green, which covalently bind intracellular proteins. As cells divide, the dye is diluted between the daughter cells, and as a consequence, its fluorescence intensity is halved with each division (Lyons 1999). The proportion of cells that proliferate and the number of divisions that have occurred in response to stimulation with a particular antigen can then be estimated by flow cytometry (Lyons 1999).

In vitro expansion of antigen-specific cells also allows measurement of cells that may be present at frequencies too low to detect with a short-term assay.
The proliferation assay is useful to address questions about induction of memory and long-lived responses. Although this assay can also be combined with staining of other cell markers to identify specific T cell populations, the long-term stimulation affects the expression of memory markers.
In this study, a proliferation assay was used to assess the proliferative capacity of MVA85A induced CD4 T cells.

1.6.5. HLA tetramers

HLA tetramers are multimeric peptide-HLA molecule complexes that physically bind directly to the cognate T cell receptor (TCR) expressed on antigen-specific T cells (Figure 6). The use of tetramers takes advantage of co-operative binding to simultaneously bind more than one TCR on a specific cell, resulting in a slower dissociation rate between peptide-HLA and the TCR. This property makes tetramers labeled with a fluorochome suitable for direct staining and detection of antigen-specific T cells, without a requirement for cell activation. Another advantage of using tetramers is the ability to detect antigen-specific cells regardless of their functional abilities.

HLA class I tetramers were developed first (Altman et al. 1996). They have been used extensively to study virus-specific CD8 T cell function and phenotype. Much has been learnt about the development and different phases of chronic and acute viral infections from the use of class I tetramers (Klenerman, Lucas, et al. 2002b; Kantzanou et al. 2003). HLA class II tetramers have been more challenging to develop and only recently has the use of HLA class II tetramers increased due to technological advancements. The largest hindrance in developing HLA class II tetramers has been the technical difficulty of synthesising the alpha and beta polymorphic chains of the HLA molecule in *E.coli* (Ferlin et al. 2000). The use of mammalian cell lines brought about much progression in development of HLA class II tetramers (Crawford et al. 1998; Novak et al. 1999). The full potential of HLA class II tetramers has not yet been realized, and is likely to revolutionise the study of CD4 T cells.

In this thesis, we used HLA class II tetramers to detect *M.tb*-specific T cells to answer a number of novel questions about mycobacteria-specific T cell immunity.

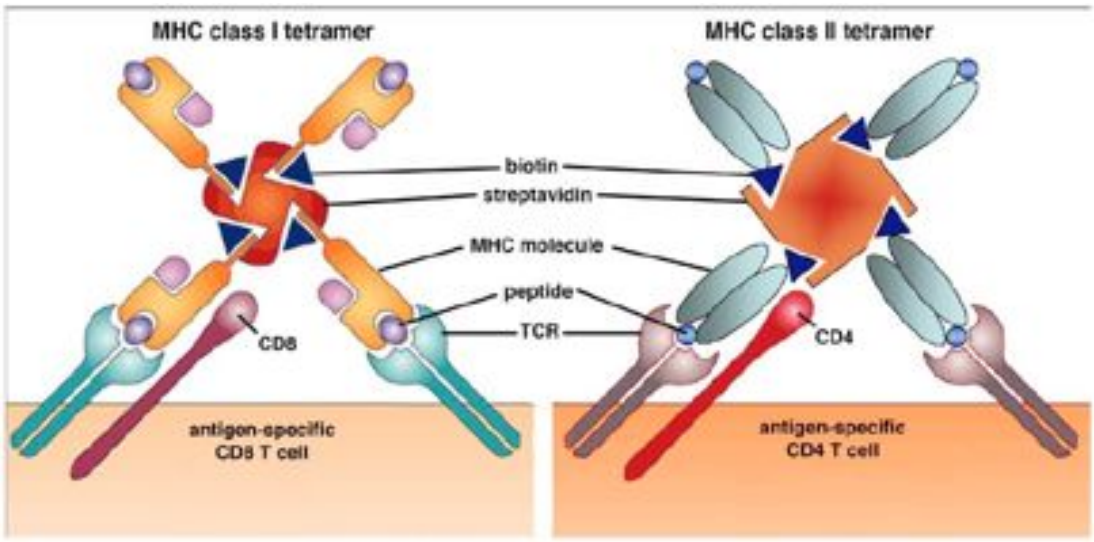

Figure 6: MHC monomers with a single peptide from the antigen of interest are biotinylated, to allow for up to 4 monomers to be complexed together on streptavidin to form a tetramer, to make use of co-operative binding. The tetramer is then fluorescently labeled allowing for detection by flow cytometry. (Adapted from Klenermann et al., (Klenerman et al. 2002a))

1.6.6. Gene expression by qPCR

Current flow cytometry-based techniques are limited in the number of different molecules that can be simultaneously measured. Another way to characterise cell subsets is to measure gene expression. By sorting T cell into different memory subsets based on phenotypic marker expression, and perfoming transcriptional analysis on these memory subsets, genes have been identified that are present only in specific T cell subsets and completely absent in other subsets. These genes can be used to classify and differentiate T memory cell subsets from each other. Appay et al. used gene expression profiles to define the transcriptional differentiation stages of CD4 T cells as they differentiate from naïve (antigen-inexperienced) to antigen-experienced cells (Appay et al. 2007). A recent study by Gattinoni et al. also utilised gene expression profiles to characterise a novel subset of T memory stem cells in humans, and to compare them to antigen-specific effector memory and central memory T cell subsets (Gattinoni et al. 2011).

Advances in the field of real time polymerase chain reactions (RT-PCR) allow interrogation of gene expression even at a single cell level. Fluidigm has developed the BioMark HD high-throughput real time qPCR platform that allows simultaneous quantification of 96 transcripts in 96 samples on a single microfluidic chip.

In this study, we characterise gene expression in sorted tetramer labeled T cell subsets to gain a better understanding of the transcriptional complexity in mycobacteria-specific CD4 T cells.

Objectives of this thesis:

i.) Map and identify Ag85A, ESAT6 and CFP10-specific CD4 T cell epitopes and determine HLA restriction elements of these epitopes to design HLA class II tetramers (Chapter 2).

ii.) Optimise HLA class II tetramer staining protocols for specific and sensitive detection and characterisation of *M.tb*-specific CD4 T cells (Chapter 2).

iii.) Comprehensive delineation of the phenotype and function of MVA85A-specific CD4 T cells (Chapter 3).

iv.) Develop and optimise protocols for mRNA expression profiling in sorted antigen-specific CD4 T cells (Chapter 4).

v.) Determine phenotypic properties and transcriptional profiles of naïve-like *M.tb*-specific CD4 T cells (Chapter 5).

Chapter 2: Tetramer development

2.1. Introduction

CD4 T cells are crucial for protection against *M.tb*, however whether a particular memory phenotype of these cells is associated with protection remains a point of debate. To start addressing this question, we sought to characterise memory subsets of *M.tb*-specific CD4 T cells after MVA85A vaccination and in natural, asymptomatic *M.tb* infection. We chose to use MHC class II tetramers to avoid or minimize activation of lymphocytes and obtain a measure of the direct *ex vivo* phenotype of *M.tb*-specific CD4 T cells irrespective of their functionality (Chao et al. 1997; Sallusto et al. 2004; Vallejo et al. 1999).

This chapter describes how we identified immunodominant *M.tb* specific CD4 T cell epitopes and their HLA class II allele restriction in order to develop tetramers. Further, optimisation of staining conditions required to detect T cells with these tetramers is also described.

We focused on Ag85A, the antigen contained in MVA85A vaccine, which is expressed by most mycobacteria, including BCG and *M.tb.* To characterise immune responses induced by natural infection with *M.tb*, we focused on two well known immunodominant antigens, ESAT6 and CFP10, which are not expressed by BCG and most non-tuberculous mycobacteria (Behr et al. 1999)

2.2. Aims

Because binding of different peptides is HLA allele restricted, in order to design HLA class II tetramers to be used in our study we aimed to:

i.) Identify immunodominant CD4 T cell epitopes, within mycobacterial proteins Ag85A, ESAT6 and CFP10.

ii.) Determine HLA restriction of selected epitopes.

iii.) Optimise staining conditions for HLA class II tetramers

2.3. Materials and Methods

The work in this chapter was performed by the candidate unless otherwise stated.

2.3.1. Study participants for MVA85A vaccine trials performed in Dr Helen McShanes' laboratory at Oxford University, United Kingdom

Data generated from vaccine trials performed in the United Kingdom were used to determine HLA restrictions of epitopes, as described below. These trials aimed to determine the safety and immunogenicity profiles of the MVA85A vaccine in healthy adults.

MVA85A vaccine trial (TB005): BCG-vaccinated adults were recruited under protocols approved by the Oxfordshire Research Council Ethics Committee. The age range for inclusion was 18–55 years. All participants tested sero-negative for HIV, hepatitis B virus (HBV) and hepatitis C virus (HCV) and had a Heaf test reaction not greater than grade II at screening. The Heaf test involved the injection of PPD into the forearm of an individual using a gun, which had needle points dipped in the PPD. The test was read between 2-7 days after injection. If upon reading 6 minute punctures were found, this was considered a negative result, and participants were unlikely to be *M.tb*-infected. If 4-6 papules were found at the injection site, this was also considered negative (Grade I). However, if a confluence of papules formed undurating the ring, this was considered positive (Grade II), and participants likely to be *M.tb*-infected. A central filling that formed a disc was also considered positive (Grade III). The largest grading was a Grade IV, which was characterised by a disc >10mm with or without blistering and this was considered strongly positive. Subjects received a single intradermal inoculation with MVA85A at a dose of $5x10^7$ plaque forming units (pfu). The median time between BCG vaccination and immunisation with MVA85A was 18 years (range: 0.5–38 years) (Beveridge et al. 2007).

MVA85A vaccine Trial (TB009): BCG-vaccinated adults with no evidence of *M.tb* infection, as defined by a maximum Heaf test reaction grade II and a negative early secretory antigen target 6 (ESAT6) and culture filtrate protein-10 (CFP10) ELISpot assay, were recruited under protocols approved by the

Oxfordshire Research Ethics Committee. The age range for inclusion was 18-50 years; all subjects were required to be seronegative for HIV, hepatitis B virus and hepatitis C virus. Subjects received a single intradermal inoculation with MVA85A at a dose of $1x10^8$ pfu (Beveridge et al. 2008).

2.3.2. Study participants for MVA85A vaccine trials performed at the South African Tuberculosis Vaccine Initiative (SATVI)

PBMCs from the following participants were used for the proliferation assays, data mining as well as for the tetramer staining discussed in Chapter 3.

Participants were enrolled into phase I/IIa clinical trials of the MVA85A vaccine in South Africa. These trials were aimed at determining the safety and immunogenicity profiles of the MVA85A vaccine in healthy adults (Hawkridge et al. 2008) and adolescents (Trial TB008) (Scriba et al. 2010) from the SATVI clinical site in Worcester, Western Cape. The trials were approved by the Research Ethics Committees of the University of Cape Town and Oxford University and conducted according to International Conference on Harmonisation/Good Clinical Practice guidelines. The trials were externally monitored by an independent contract research organisation and all protocols and subsequent amendments were approved by the Medicines Control Council of South Africa.

Written, informed consent was obtained from all adults. Written, informed consent was also obtained from parents or legal guardians of all adolescents while written, informed assent was obtained from all adolescents who were judged to have a good understanding of the study. Enrolled participants were all HIV negative and had no evidence of *M.tb* infection, as defined by absence of PBMC reactivity to ESAT6 and CFP10 in an ELISpot assay and a tuberculin skin test (TST) of less than 15mm. TST involves the intradermal injection of a standard dose of purified protein derivative (PPD), a tubercule extract, in the forearm. After 48-72 hours the injection site is examined and the induration around it is measured. All participants had a normal chest X-ray and had received BCG at birth, as is routine in South Africa.

All individuals received an intra-dermal dose of $5x10^7$ pfu of MVA85A. Adults and adolescents were followed up for 12 months. Blood products were obtained and stored at all post-vaccination time points indicated in Table 2.

Table 2: Time points of study visits at which blood products were isolated and stored

Participants	No. of participants	Time points (days after vaccination)
Adolescents	12	Baseline, 7, 14, 28, 56, 84, 168 and 364
Adults	24	Baseline, 7, 14, 28, 56, 84, 168 and 364

2.3.3. Study participants for natural *M.tb* infection studies

We aimed to enrol healthy latently infected donors under the healthy donor protocol (UCT HREC ref: 126/2006). Donors had to be HIV negative, not on any chronic medication and not pregnant. All donors had to have a QuantiFERON TB-GOLD In tube (QFT) result greater than 0.35IU/mL, which is considered positive for *M.tb* infection, as well as a TST induration greater than 15mm. Donors had to have given consent for HLA typing. Blood samples were collected and PBMCs isolated and cryopreserved as described in section 2.3.4, below. PBMCs were used for epitope mapping of ESAT6 and CFP10.

2.3.4. PBMC isolation and cryopreservation

Blood was collected from participants by venipuncture into heparinised tubes. Blood was diluted 1:1 with phosphate buffered saline (PBS, Lonza) and slowly layered onto 15mL of Ficoll (histopaque) to a maximum total volume of 45mL in a 50mL conical tube. This tube was then centrifuged at 800g for 30 minutes at room temperature with the brake off, to separate the PBMC from the other cells. PBMC were aspirated at the ficoll interface using a 5mL pipette and transfered to a 50mL tube and topped up with PBS and inverted 3 times. This tube was centrifuged for 10 min at 596g at 22°C with the brake on “max/high”. The supernatant was decanted and cells were resuspended in 1mL of PBS and gently pipetted up and down. The tube was topped up with PBS and centrifuged for 10 min at 596g at 22°C with brake on “max/high”. Supernatant was decanted and PBMCs were then cryopreserved in 10% DMSO (Sigma)

and 10% Foetal calf serum (FCS, Lonza) in RPMI (Lonza) media. Ten million PBMCs were cryopreserved per vial.

2.3.5. Peptides used for epitope mapping

We designed 15mer peptides overlapping by 10 amino acids to cover the whole proteins Ag85A (66 peptides), CFP10 (18 peptides) and ESAT6 (17 peptides) (Maecker et al. 2001). Peptides were used at a concentration of 2μg/mL for stimulation of PBMCs in the direct *ex vivo* IFN-γ ELISpot and at a concentration of 1μg/mL for the cultured IFN-γ ELISpot.

2.3.6. Direct ex vivo ELISpot

PBMCs from MVA85A participants in all the vaccine trials were thawed into 10mL of 10%AB+ human serum (Sigma) in RPMI containing DNase (50U/mL, Sigma). Cells were spun down at 596g for 10 minutes and then washed once by resuspending in 10mL of PBS. Cells were spun down at 596g for 10 minutes and then resuspended into 10%FCS/RPMI media. Plates (Millipore) were coated with anti-IFN-γ mAb antibody (15μg/mL, MAbTech), at 4°C overnight. Plates were then washed with PBS and blocked with 10%FCS/RPMI for 3 hours at 37°C. Three hundred thousand cells in 10%FCS/RPMI were added into each plate well and were left unstimulated (uns) as a negative control or stimulated with a pool of MVA85A peptides (2μg/mL) or Phytohaemagglutinin (PHA)(10μg/mL, Remel) as positive control. Stimulations were done in duplicate wells and plates were incubated at 37°C with 5% CO_2 for 18 hours. Plates were developed according to the manufacturers instructions (Bio-Rad). Briefly, the plates were washed 5 times with 0.05% Tween 20 in PBS. We then added 50μL of a 1/1000 dilution of biotin-anti IFN-γ antibody to each well. The plates were incubated for 2 hours at room temperature in the dark. The plates were then washed 5 times with 0.05% Tween 20 in PBS and 50μL of a 1/1000 dilution of streptavidin-ALP (alkaline phosphatase) solution was added to each well and allowed to incubate for 1 hour at room temperature. The plate were washed again in 0.05% Tween 20 in PBS. Fifty microlitres of developing buffer was added to each well and incubated for 8 minutes at room temperature until blue spots

developed. Washing the plates in tap water, four times, terminated the colour reaction. The plates were then allowed to dry overnight on the bench. Results were read on an ELISpot reader (AID). A positive response had to be greater than 17 spot forming cells (SFC)/million PBMCs after subtracting the unstimulated response. In wells where the response was too large to quantify the well was given a maximum value of 500/well or 1667 SFC/million PBMC, as previously described (McShane et al. 2004).

2.3.7. Cultured IFN-γ ELISpot for *in-vitro* expansion of antigen-specific cells

Cryopreserved PBMCs from healthy *M.tb* latently infected participants were thawed into 10%AB+/RPMI medium containing DNase (50U/mL). Cells were washed once and then resuspended into 10%AB+/RPMI media. Two million PBMC were resuspended in 2mL of media and stimulated with ESAT6 or CFP10 15mer peptide pools (1μg/mL). Cells were incubated at 37°C with 5% CO_2 for 12 days and 1mL of media was removed every 3 days and replaced. On day 3 and 6, IL-2 (50U/mL) was added with replenishment of media. On the 12th day, 1mL of media was removed and replaced with fresh media without IL-2 and left overnight at 37°C with 5% CO_2. Plates (Millipore) were coated with anti-IFN-γ mAb antibody at 4°C overnight. Plates were washed with PBS and then blocked with 10%FCS/RPMI for 3 hours at 37°C, according to the manufacturers protocol (MAbTech). On the 13th day, 50000 cells in 10%FCS/RPMI were added into each plate well, were left unstimulated as a negative control or stimulated with single ESAT6 or CFP10 peptides (1μg/mL) or PHA (10μg/mL) as a positive control. Stimulations were performed in duplicate wells and plates were incubated at 37°C with 5% CO_2 for 18 hours. Plates were developed according to the manufacturers instructions (Bio-Rad). Results were read on an ELISpot reader, as described in section 2.3.6 (AID). A response was considered positive if it was 2.5x greater than the unstimulated, as had been previously determined for cultured ELISpots in our laboratory (M. Musvosvi et al., unpublished). Briefly, in a previous study, a cultured IFN-γ ELISpot was performed in individuals before and after *M.tb* infection using ESAT6 peptides to stimulate PBMCs. The fold increase of the ESAT6 response divided by the responses in the unstimulated

condition was determined and receiver operating characteristics (ROC) curve analysis was done. Discrimination between before and after infection and the area under the curve was significant at 0.98. The sensitivity and specificity for discriminating between pre and post infection, using various fold increase cut off was plotted. A fold increase value of 2.5 gave the maximum sensitivity and specificity, as shown in Figure below.

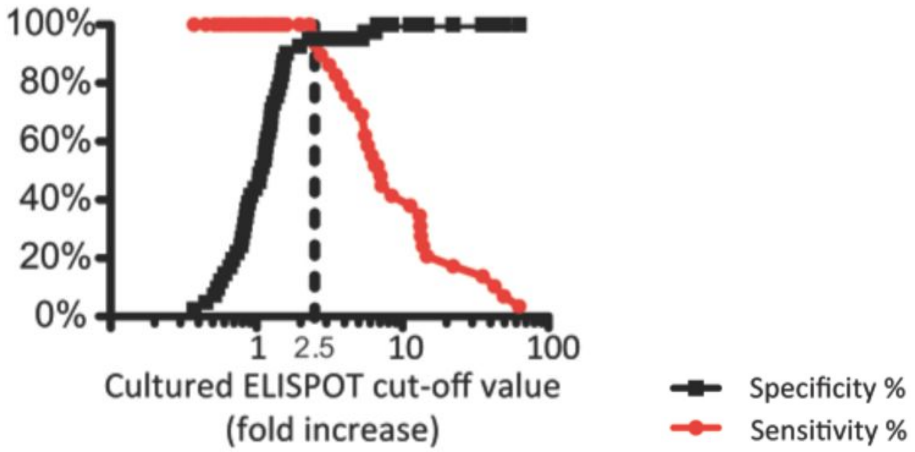

Figure 7: Receiver operating characteristic curve analysis to determine a cut off for cultured IFN-γ ELISpots. The sensitivity (red) and specificity (black) is shown for different cut offs. A cut off of 2.5x was considered optimal. (Courtesy of M. Musvosvi).

2.3.8. Human leukocyte antigen class I and II typing

Deoxyribonucleic acid (DNA) was extracted from PBMC using the Qiagen Mini-blood DNA isolation kit, following the manufacturers protocol. DNA was sent to the National Institute of Communicable Diseases (Johannesburg, South Africa) for high resolution Human Leukocyte Antigen (HLA) class II typing by DNA sequencing. Alternatively, DNA extracted from healthy *M.tb*-infected participants was sent to our collaborators (Alex Sette et al.,) at the La Jolla Institute of Allergy and Immunology for high resolution HLA class II typing (La Jolla, California, USA).

2.3.9. HLA class II epitope prediction

Single peptides that were recognised by at least 30% of the responders to any antigen in the protein were considered immunodominant and were used as potential targets for tetramer development. Amino acid sequences of selected

peptides were analysed using epitope prediction software to determine the putative binding epitopes to different HLAs.

Epitope prediction databases used for this analysis included:

- SYFPEITHI. Binding scores are arbitrary and are based on the binding affinity between amino acids in peptides and different HLA types. Amino acids that bind with high affinity are given a positive score and poor binding residues a negative score. The overall score is then calculated. The maximum achievable score is 40.
- IEDB Analysis Resource, http://tools.immuneepitope.org/mhcii/. The median percentile rank calculates a consensus rank from three prediction methods (neural network-based alignment (NN_align), stabilization matrix alignment method (SMM_align) and Sturniolo), for each peptide. The median percentile rank is generated by comparing the peptide's score against the scores of five million random 15 mers selected from SWISSPROT database. A small numbered percentile rank indicates high affinity. The NN-align and SMM align scores are given as predicted binding affinity (half maximal inhibitory concentration 50, IC_{50}) to each HLA allele, in nM. Peptides with IC_{50} values <50nM are considered high affinity, <500nM intermediate and <5000nM low affinity. The prediction result of Sturniolo is an arbitrary raw score, the higher the score, the greater the affinity.
- PROPED (http://www.imtech.res.in/raghava/propred/) uses quantitative matrices derived from published literature by Sturniolo et. al., (Sturniolo et al. 1999) to predict HLA Class-II binding regions in an antigen sequence. It also locates promiscuous binding regions within an antigen sequence. The higher the percentage score an epitope is given to a particular HLA allele, the greater the probability of it binding that allele (Singh & Raghava 2001).

2.3.10. HLA-peptide binding assays

Our collaborators (Alex Sette et al.,) at the La Jolla Institute for Allergy and Immunology in San Diego, USA, performed the HLA-peptide binding assays, for the selected epitopes.

Assays to quantitatively measure peptide binding to HLA class II molecules are based on the inhibition of binding of a high affinity radiolabeled peptide to purified HLA molecules (Sidney et al. 2001). Briefly, 0.1-1nM of radiolabeled peptide was co-incubated at room temperature or 37°C with 1μM to 1nM of purified HLA in presence of a cocktail of protease inhibitors. Following a 2-4 day incubation, the percent of HLA bound radioactivity was determined by capturing HLA/peptide complexes on LB3.1 (DR), L243 (DR), HB180 (DR/DP/DQ), SPV-L3 (DQ) or B7/21 (DP) antibody coated Optiplate, and bound counts per minute (cpm) measured using the TopCount microscintillation counter. Under the conditions utilised, where [label]<[HLA] and IC_{50}≥[HLA], the measured IC_{50} are reasonable approximations of the true K_d values.

2.3.11. HLA class II tetramers

DRB1*03:01 iTag HLA class II tetramers were obtained from Beckman Coulter. The tetramers were conjugated to PE and supplied at a concentration of 100μg/mL. ESAT6 and CFP10 tetramers were obtained from the NIH Tetramer Core Facility at Emory University, GA, USA. ESAT6 and CFP10 tetramer concentrations varied and are shown in Table 3, below. All tetramer staining was done at a final concentration of 2μg/mL.

Table 3: HLA class II tetramer concentrations

HLA allele	Peptide number	Protein	Peptide Sequence	Concentration
DRB5*01:01	11	$CFP10_{(51-65)}$	AQAAVVRFQEAANKQ	1.3mg/mL
DRB5*01:01		Clip	PVSKMRMATPLLMQA	1.3mg/mL
DRB1*0401	15	$CFP10_{(71-85)}$	EISTNIRQAGVQYSR	0.8mg/mL
DRB1*0401		Clip	PVSKMRMATPLLMQA	1.3mg/mL
DRB1*0301	12/13	$Ag85A_{(55-75)}$	VPSPSMGRDIKVQFQSGGAN	100μg/mL
DRB1*0301		Apolipoprotein$B_{(2877-2894)}$ (ApoB)	ISNQLTLDSNTKYFHK LN	100μg/mL

2.3.12. HLA class II tetramer staining

Cryopreserved PBMCs were thawed into 10%AB+ serum/RPMI medium containing DNase (50U/mL). Cells were spun down at for 7 minutes and then washed once by resuspending in 10mL of PBS. Cells were spun down at 596g for 7 minutes. PBMCs were resuspended in 1mL of PBS and stained for 30 minutes with LIVE/DEAD Fixable Violet Dead Cell Stain (ViViD, Molecular Probes, Invitrogen). Cells were then washed once in PBS and stained with 2μg/mL of HLA class II tetramer at 37°C or room temperature (RT) for 1 hour in a total volume of 100μL of 2%FCS/PBS containing 0.05% sodium azide (Sigma) and 2mM ethylenediaminetetraacetic acid (EDTA, Sigma). Incubation length and temperature were optimised for each tetramer as shown in this chapter. Cells were washed and stained with all other antibodies, for which each panel is listed in the relevant chapter, at room temperature for 30 minutes unless otherwise stated. Cells were washed, resuspended and fixed with 1% paraformaldehyde, unless otherwise stated. Cells were acquired on a BD Biosciences LSRII flow cytometer.

2.3.13. Antibodies

The antibody concentrations for each panel were titrated and the volume chose based on staining saturation and best signal-to-noise index, to ensure minimal background staining and best resolution of the positive and negative populations. Fluorescence minus one (FMO) staining was done for all fluorescent conjugated antibodies used in this panel. In such FMO experiments, a sample is stained with all fluorescent conjugated antibodies except one of the antibodies, which is left out. This is repeated for each individual antibody. This method allows identification of spillover fluorescence from all secondary antibodies (as well as auto fluorescence) into each primary detector in the absence of the primary antibody. This method also aids positioning of gates to distinguish a positive population from the negative, since spillover fluorescence and auto fluorescence can be accounted for (Roederer 2002). All antibody panels described in this thesis were optimised in this manner.

2.3.14. Flow cytometer instrument configuration

The BD Biosciences LSRII flow cytometer was set up to ensure the following: i) we had the optimal optical filters, ii) the laser beam shape and location was optimal and iii) that resolution and sensitivity of photoelectron detection was maximal as described (Perfetto et al. 2012). Optimal voltages were determined for each fluorochrome and for each detector in the instrument to ensure optimal resolution of populations. A quality assurance routine was set up to monitor and ensure consistent and optimal functioning of the machines was maintained over the period of use, and to ensure reproducibility. Cytometer setup and tracking Beads (BD Biosceinces) that fluoresce in each channel at a predetermined median fluorescence intensity (MFI) were run daily to ensure that these settings and MFI are maintained (Perfetto et al. 2012). Photomultiplier tube (PMT) voltages were adjusted daily to ensure that consistent MFIs were maintained, using Rainbow fluorescent particle (Spherotech) beads. Compensation beads were acquired daily before acquisition of samples, to allow post-acquisition compensation. Shown below in Figure 8, are the configurations used on the BD LSRII flow cytometer.

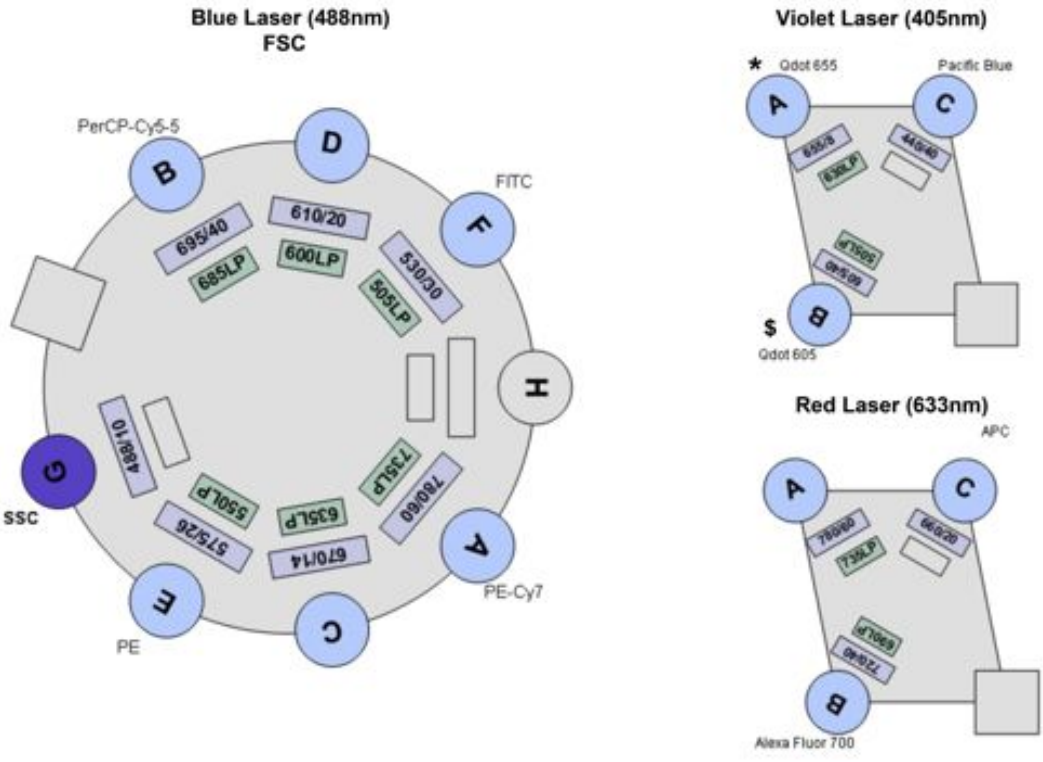

Figure 8: Filter and laser configuration of the BD LSRII flow cytometer. The dichroic mirrors are shown in green and the band pass filters in lilac. The detectors are shown as circles with the alphabetic letters dictating the light path.

2.3.15. Flow cytometry data analysis

Flow cytometry data were analysed using Flowjo v9.1 to v9.7.1. Compensation on the flow cytometer was done using single stained beads and automatically calculated and applied to all samples in Flowjo.

2.4. Results

2.4.1. Study participants for MVA85A vaccine trials

A total of 24 adults and 12 adolescents were enrolled into the TB008 trial. Demographic characteristics of these adults and adolescents are shown in Table 4, below.

Table 4: Demographic characteristics of enrolled adults and adolescents in the MVA85A TB008 vaccine trial.

		Adults (n=24)	Adolescents (n = 12)
Male, n (%)		8 (33)	6 (50)
Median age in years (range)		35.5 (20.7-48.7)	14.4 (13.3-15.0)
Race, n (%)	Black	5 (21)	9 (75)
	Mixed race	10 (42)	3 (25)
	White	9 (38)	0 (0)
Median body mass index in kg/m^2 (range)		27.6 (21.8-39.2)	21.1 (17.5-31.4)

We did not have access to the demographics from the MVA85A vaccine trials performed in Oxford. All participants were white adults.

2.4.2. MVA85A tetramer design

To design HLA class II tetramers bearing peptides of commonly recognised, immunodominant Ag85A epitopes, epitope identification and the HLA restriction of each epitope had to be determined. We analysed direct *ex vivo* IFN-γ ELISpot data from routine immunogenicity outcomes measured in previous trials of the MVA85A vaccine, completed at Oxford (TB005 (Beveridge et al. 2007) and TB009 (Beveridge et al. 2008)), and at SATVI (TB008) (Hawkridge et al. 2008; Scriba et al. 2010). Fifteen-mer peptides encoding Ag85A, overlapping by 10 amino acids, were either used individually or were divided into 7 different pools to stimulate PBMCs. As this was done as part of a vaccine trial, ELISpots were performed on freshly isolated PBMCs. In the Oxford vaccine trials (TB005 and TB009), which included 36 participants, 25 of the 66 Ag85A peptides were recognised by at least one individual in either of the trials, whereas 23 peptides were recognised by at least one individual in both trials. The proportions of MVA85A vaccinees that had a

positive T cell response against the peptides are shown below (Figure 9). Peptides that were recognised by 30% or more of the cohort in both trials were considered immunodominant and investigated further.

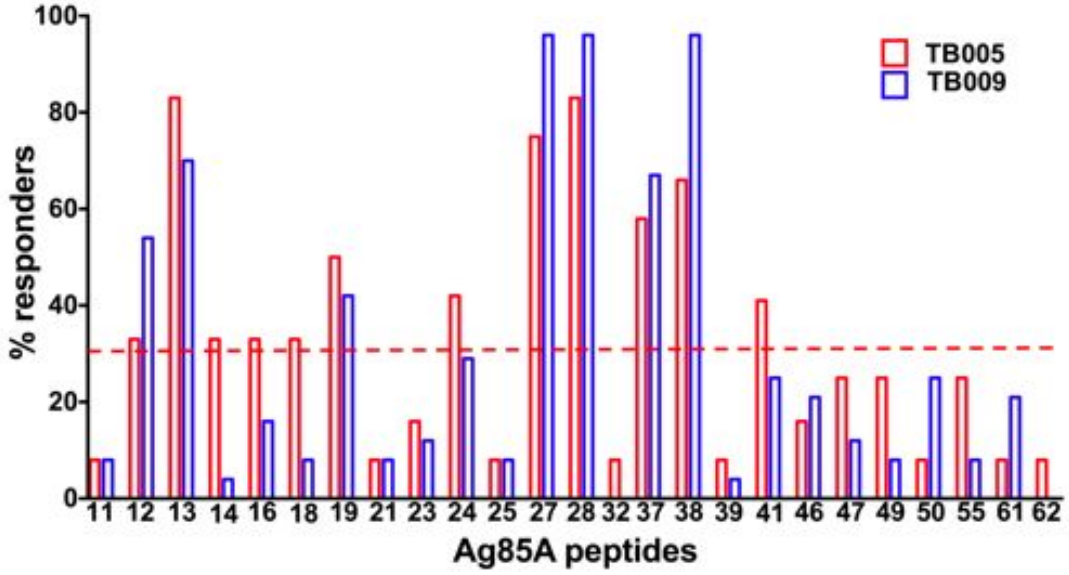

Figure 9: Peptide mapping in 36 adults who received the MVA85A vaccine (12 participants in trial TB005, in red; 24 participants in trial TB009, in blue). Responses were measured by IFN-γ ELISPOT assay in PBMCs collected 7 days after vaccination. Responses greater than 17 SFC/million PBMC were considered positive as defined previously (Beveridge et al. 2007). Only peptides recognised by at least one vaccinee are shown. The number of individuals from all 36 trial participants with a response to a peptide is shown as % responders.

Three Ag85A regions, encompassing peptides 12/13, 27/28 and 37/38, appeared to be immunodominant (Table 5). It is likely that these regions represent epitope(s) that are common to the overlapping amino acid regions in these flanking peptides. For each region we therefore combined the two 15mer amino acid sequences into single 20mer peptides for further HLA restriction and binding prediction analysis.

Table 5: Ag85A peptides recognised by at least 30% of the cohort (TB005 and TB009).

Peptide number	Amino acid position	Sequence	% responders (No.) in TB005 (n=12)	% responders (No.) in TB009 (n=24)
12	56-70	VPSPSMGRDIKVQFQ	35 (4)	54 (13)
13	61-75	MGRDIKVQFQSGGAN	83 (10)	70 (17)
27	131-145	GKAGCQTYKWETFLT	75 (9)	96 (23)
28	136-150	QTYKWETFLTSELPG	83 (10)	96 (23)
37	181-195	YHPQQFVYAGAMSG	58 (7)	67 (16)
38	186-200	FVYAGAMSGLDPSQ	66 (8)	96 (23)

We then determined associations between HLA alleles and peptide responses. We observed a strong association between T cell responses to peptide 12/13 and individuals bearing the DRB1*03:01 allele (Figure 10). Such clear associations between specific HLA alleles and responses to peptides were not observed with P27/28 or P37/38. However, T cell responses to P27/28 were observed in donors bearing DRB1*15:01, and responses to P37/38 were observed in donors bearing DRB1*04:01 (data not shown).

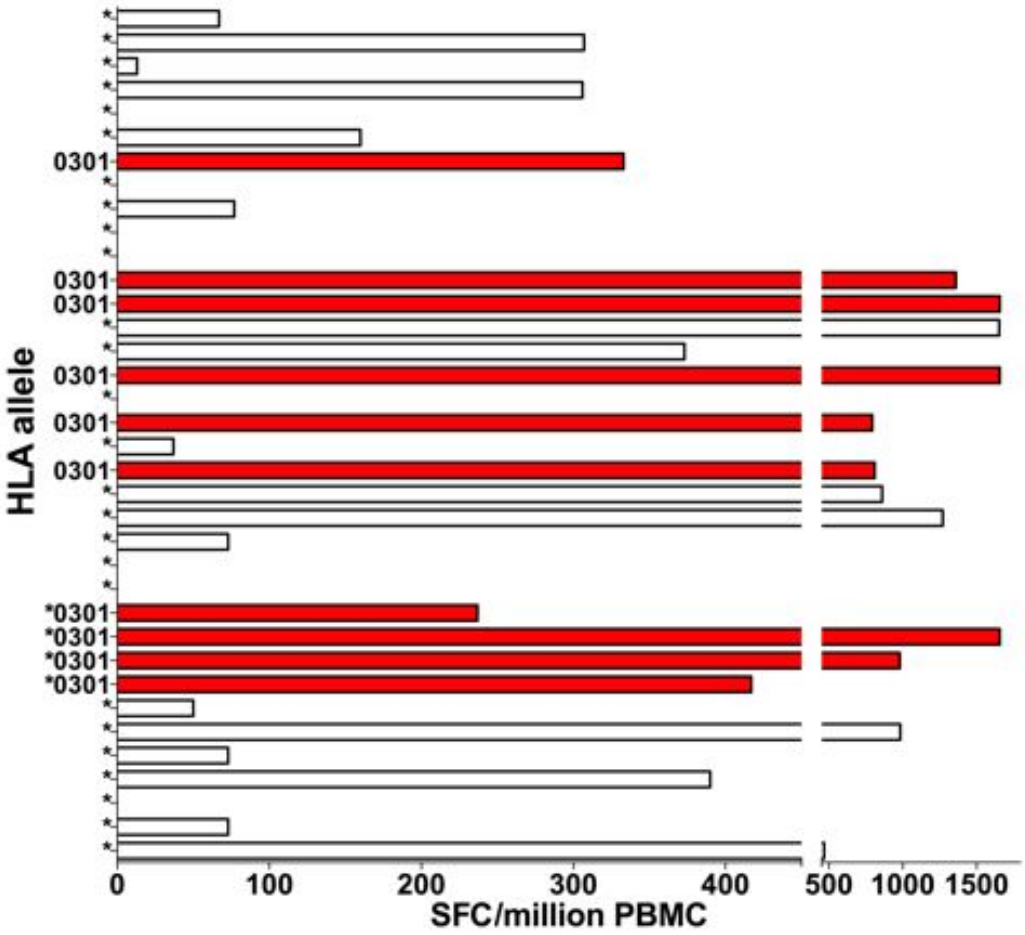

Figure 10: IFN-γ ELISpot responses to Ag85A peptide 12/13 measured in 36 MVA85A vaccines from the TB005 and the TB009 vaccine trials. Only the HLA allele for donors bearing HLA DRB1*03:01 are shown and their responses to peptide 12/13 are highlighted in red. White bars represent donors who had responses to peptide 12/13 but who did not have the HLA DRB1*03:01 allele. A response was considered positive if it was greater than 17 SFC/million PBMC (Beveridge et al. 2007).

Binding of peptides to HLA class II molecules is known to be promiscuous; an individual peptide may bind multiple, unrelated HLA alleles. This is attributed to the degenerate binding motif found within class II HLA molecules (Godkin et al. 2001; Wang et al. 2008) and makes precise determination of allele restriction challenging. To biologically determine the HLA restriction of the 3 immunodominant 20mer Ag85A peptides, we investigated whether responsiveness to each peptide was associated with expression of specific HLA DR alleles (Table 6). We found a significant association between the presence of DRB1*03:01 and responsiveness to peptide 12/13 in 48 MVA85A vaccinees (from TB005, TB008 and TB009 trials). By contrast, no such associations were found between responsiveness to peptide 27/28 and

DRB1*15:01 or peptide 37/38 and DRB1*04:01. However, due to the promiscuity of HLA class II peptide binding, this result does not exclude these alleles as restricting HLAs for these peptides. These epitopes may be restricted by multiple HLA alleles.

Table 6: HLA restrictions of MVA85A vaccinee peptide responses

Peptide and HLA DR allele	Responsiveness (IFN-γ ELISpot assay response)	Vaccinees not bearing allele, n	Vaccinees bearing allele, n	p-value (Fisher exact test)
Ag85A P12/13 DRB1*03:01	yes	12	12	p < 0.001
	no	24	0	
Ag85A P27/28 DRB1*15:01	yes	32	9	p = 0.176
	no	4	3	
Ag85A P37/38 DRB1*04:01	yes	36	4	p = 0.427
	no	7	1	

We therefore used multiple epitope prediction algorithms to estimate the putative HLA allele binding affinity of the three immunodominant Ag85A 20mer peptides, P12/13, P27/28 and P37/38, to DRB1*03:01, DRB1*15:01 and DRB1*04:01, as well as other alleles. The results for each prediction algorithm are shown in Table 7, below. The consensus percentile rank, which calculates a consensus binding score from 3 prediction algorithms was shown to allow more reliable HLA binding prediction than any single prediction algorithm (Wang et al. 2008).

Table 7: Predicted HLA allele binding scores or ranks for each 20mer Ag85A peptide from 5 different algorithms and the combined consensus percentile rank.

Peptide	HLA class II DRB1 allele	SYFPEITHI	Consensus Percentile	SMM Align *	NN_a Align*	Sturniolo Score
P12/13	*0301	35	0,13	254	60,4	5,9
P27/28	*0401	22	3,55	335	234,5	2,9
	*1501	24	28,21	1766	829,9	2,26
P37/38	*0401	28	3,39	322	172,5	2,7
	*0701		1,2	84	8,1	-
	*1501	24	13,81	683	317,7	-
Apo-B	*0301	38	0,4	73	9,8	2,9

*The MHCII binding predictions were made using the IEDB analysis resource Consensus tool. The Peptides with IC_{50} values <50nM are considered high affinity (red), <500nM intermediate (yellow) and <5000nM low affinity (green). SYFPEITHI, consensus percentile and Sturniolo scores are ranked from highest (green) to lowest (red).

In order to narrow down possible candidates for tetramers, we focused on alleles that were prominent in our South African cohort.

HLA allele DRB1*03:01 showed a high affinity for P12/13, as it had the highest percentile score, an intermediate SMM align and NN_a align score, a high Sturniolo score and a high Propred score, as well as a high SYFPEITHI score, suggesting it is very likely to be restricted by this HLA allele. As biological results also confirmed this association, the Ag85A 20mer, which spanned P12 and P13, was selected to continue further for tetramer synthesis. Furthermore, based on the peptide binding data published by Malcherek et al (Malcherek et al. 1993), Apolipoprotein B-100 (2877-2894), a self peptide, was selected as a negative control peptide for the DRB1*03:01 tetramer. Binding scores for this peptide to the DRB1*03:01 allele are also shown in Table 6, above.

The SYFPEITHI predictions for P27/28 suggested that it was restricted by DRB1*04:01, however analysis with the IEDB database, suggested that it had low affinity binding to this HLA allele, based on the SMM_align, NN_a align and Sturniolo score. Its percentile rank score of 28.21 was indicative of low binders as well. Propred gave a relatively low percentage binding probability, and SYFPEITHI also yielded an intermediate score. This suggested that this peptide was not a strong binder to this HLA allele. Interestingly, this peptide showed better binding affinity to DRB1*15:01 when we analysed its

SMM_align, NN_a align and Sturniolo score. It had higher Propred binding probability percentage to the DRB1*04:01 allele, and a lower SYFPEITHI score (Table 7). This further supported the finding that class II epitopes are promiscuous. We opted to continue with the synthesis of the DRB1*15:01 tetramer.

Alleles such as DRB1*07:01 showed a high affinity for P37/38, as they had a high percentile rank, as well as a low SMM align and NN_a align score, however this allele was not present in our cohort and thus this combination was not considered.

While our biological data suggested that P37/38 was not restricted by the DRB1*04:01 HLA allele, we observed an intermediate binding affinity predicted by SMM_align, NN_a align and Sturniolo scores. Furthermore, the SYFPEITHI score given to this peptide binding to the DRB1*04:01 HLA allele was moderate. Its probability of binding this allele, as predicted by Propred, was low though (Table 7). These results were not conclusive, but suggested that it could be restricted by this allele. We went forward with the synthesis of this tetramer.

Though the prediction binding software tools were informative about peptide restrictions and binding probabilities, they are known not to give a definitive answer. A combination of biological data and prediction tool results guided our tetramer selection.

Selected tetramers (Table 8) were synthesised by Beckman Coulter. The class II invariant chain-associated peptide (CLIP), a self protein which is found naturally bound to peptide-free HLA molecules, and plays a role in stabilising the HLA molecule during HLA processing and loading during antigen presentation, was selected as a control tetramer for the DRB1*04:01 and the DRB5*01:01 tetramers.

Table 8: Selected tetramers.

HLA allele	Peptide number	Protein	Peptide Sequence
DRB1*03:01	12/13	$Ag85A_{(56-75)}$	VPSPSMGRDIKVQFQSGGAN
DRB1*03:01		Apolipoprotein $B_{(2877-2894)}$ (ApoB)	ISNQLTLDSNTKYFHK LN
DRB1*04:01	27/28	$Ag85A_{(131-150)}$	GKAGCQTYKWETFLTSELPG
		clip	PVSKMRMATPLLMQA
DRB1*15:01	37/38	$Ag85A_{(181-200)}$	YHPQQFVYAGAMSGLLDPSQ
		clip	PVSKMRMATPLLMQA

2.4.3. Study participants for natural *M.tb* infection studies

Epitope mapping for ESAT6 and CFP10 was performed on cryopreserved PBMC samples that were available from a previous study. We used these samples, as we knew the *M.tb* infection status of the participants. Twenty-two healthy latently infected adolescents were enrolled. The demographics of the participants are shown in Table 9 below.

Table 9: Demographic characteristics of enrolled donors in the natural *M.tb* infection epitope mapping.

		Adolescents (n = 22)
Male, n (%)		9 (41)
Median age in years (range)		16.8 (14.4-19.3)
Race, n (%)	Black	1 (4,5)
	Mixed race	21 (95,5)
	White	0 (0)

2.4.4. ESAT6 and CFP10 epitope mapping

To study *M.tb*-specific CD4 T cells elicited by natural infection, we focused on responses to ESAT6 and CFP10, which are expressed by *M.tb* and not BCG. To design HLA class II tetramers, we aimed to identify immunodominant ESAT6 and CFP10 epitopes and their HLA restriction in healthy, latently *M.tb*-infected donors. We performed epitope mapping by using a 12day cultured IFN-γ ELISpot, where cryopreserved PBMCs were stimulated with single 15mer peptides from ESAT6 and CFP10. We have recently shown that when using the direct *ex vivo* ELISpot, fewer antigen-specific responses are

detected as compared to the cultured ELISpot (Figure 11) (M. Musvosvi et al., unpublished). The process of culturing cells for 12 days allowed the expansion of antigen-specific memory T cells, increasing the sensitivity of detection of rare T cell clones. An example of the cultured ELISpot responses is shown in Figure 12. The cultured ELISpot showed a greater magnitude of responses to single peptides when compared to the directly *ex vivo* ELISpot.

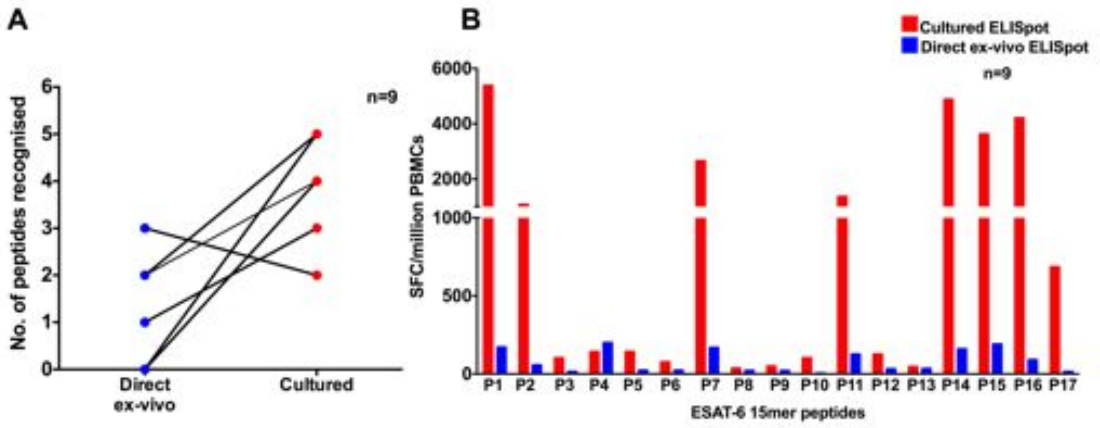

Figure 11: Direct comparison of the number of ESAT6 peptides recognised, in a direct *ex vivo* IFN-γ ELISpot as compared to a 12 day cultured IFN-γ ELISpot, in 9 latently infected donors (courtesy of M. Musvosvi et al., unpublished). All 17 ESAT6 peptides were used to stimulate PBMCs. (A) A greater number of peptides were recognised by the direct culture compared with direct *ex vivo* ELISpot. (B) The summed magnitude of the responses to single ESAT6 peptides.

When a positive response was regarded as at least 2.5 fold higher SFC/million PBMCs than the unstimulated, at least one individual recognised all CFP10 peptides. The median unstimulated response was 50 SFC/million PBMCs (Figure 12B).

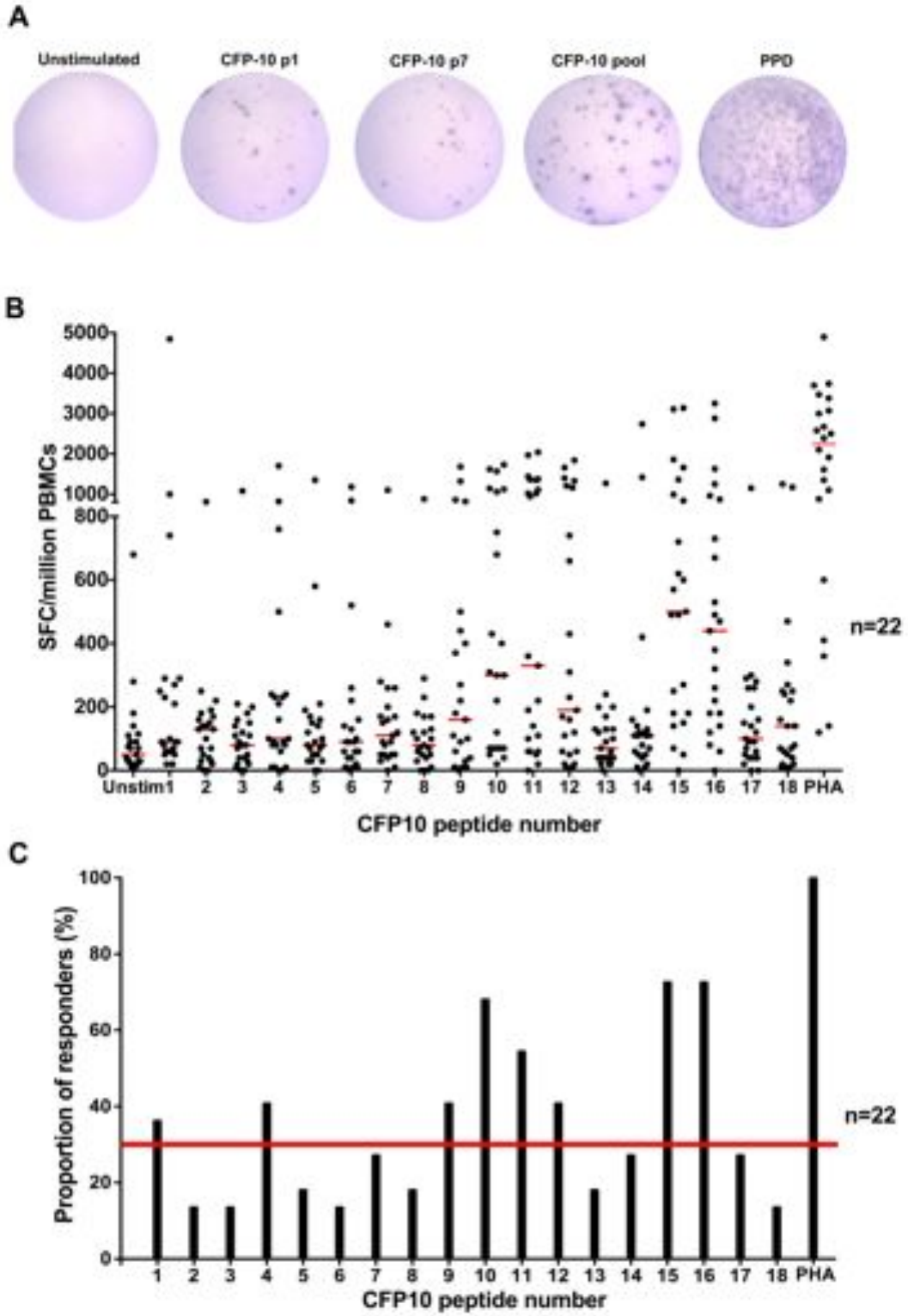

Figure 12: Mapping CFP10 responses by cultured IFN-γ ELISpot. (A) Representative results of a single individuals PBMCs, where single CFP10 15mer peptides were used for stimulation. Negative control (unstimulated), complete CFP10 peptide pool and positive control (PHA) are also shown. (B) ELISpot response (SFC/million PMBCs) before background subtraction. (C) Proportion of the cohort that had responses to the single CFP10 15mer peptides is shown (n=22). At least 30% of the cohort had to have a response for that peptide to be considered further; the red line indicates the cut off.

Eight CFP10 peptides were recognised by 30% or more responders (Figure 12C). These peptides were selected as candidates for determination of HLA restriction and are listed in the Table 10.

Table 10: CFP10 peptides recognised by at least 30% of the cohort.

Peptide number	Amino acid position	Sequence	No. of responders (out of 22), and (%)
1	1-15	MAEMKTDAATLAQEA	8 (36)
4	16-25	GNFERISGDLKTQID	9 (41)
9	41-55	GQWRGAAGTAAQAAV	9 (41)
10	46-60	AAGTAAQAAVVRFQE	15 (68)
11	51-65	AQAAVVRFQEAANKQ	12 (55)
12	56-70	VRFQEAANKQKQELD	9 (41)
15	71-85	EISTNIRQAGVQYSR	16 (73)
16	76-90	IRQAGVQYSRADEEQ	16 (73)

ESAT6 peptide mapping was also performed and, as for the CFP10, a positive response was defined as being 2.5x greater than the unstimulated. The median response in unstimulated samples was 40 SFC/million PBMCs. All ESAT6 peptides were recognised by at least one individual (Figure 13B).

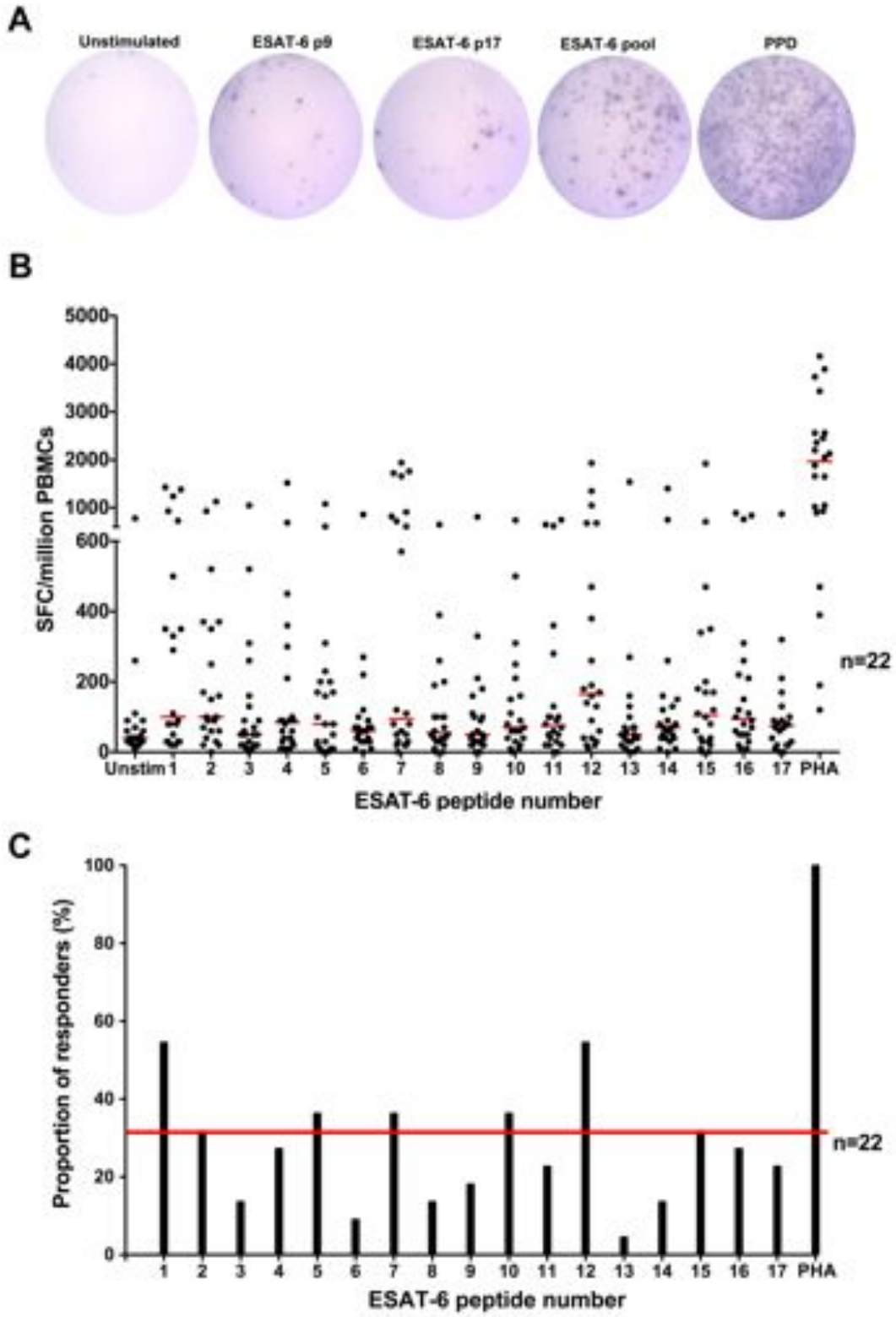

Figure 13: Mapping ESAT6 responses by cultured IFN-γ ELISpot. (A) Representative results for a single individual's PBMCs, where single ESAT6 15mer peptides were used for stimulation. Negative control (unstimulated), complete peptide pool and positive control (PHA) are also shown. (B) ELISpot response (SFC/million PMBCs) before background subtraction. (C) Proportion of the cohort that had responses to the single ESAT6 15mer peptides is shown (n=22). At least 30% of the cohort had to have a response for that peptide to be considered further; the red line indicates the cut off.

Seven of the 17 peptides screened were recognised by greater than 30% of the cohort (Figure 13C). These peptides were selected further for HLA restriction determination (Table 11).

Table 11: ESAT6 peptides recognised by at least 30% of the cohort.

Peptide number	Amino acid position	Sequence	No. of responders (out of 22), (%)
1	1-15	MTEQQWNFAGIEAAA	12 (55)
2	16-25	WNFAGIEAAASAIQG	7 (32)
5	21-35	NVTSIHSLLDEGKQS	8 (36)
7	31-45	EGKQSLTKLAAAWGG	8 (36)
10	46-60	SGSEAYQGVQQKWDA	8 (36)
12	56-70	QKWDATATELNNALQ	12 (55)
15	71-85	NLARTISEAGQAMAS	7 (32)

2.4.5. Determination of HLA restriction of selected epitopes

Instead of using prediction software, our collaborators (Alex Sette et al.,) at La Jolla Institute of Allergy and Immunology performed epitope binding assays using 15mer overlapping peptides spanning the whole ESAT6 and CFP10 proteins for every HLA allele in our cohort. Results for our peptides of interest are shown in Table 12. We considered IC_{50} scores below 100 (as highlighted in Table 12) as high affinity binders, showing a likely HLA restriction. As HLA class II peptides are known to be promiscuous, it was not surprising that the same peptide was putatively restricted by multiple HLA alleles.

Table 12: Binding of peptides to DR HLA alleles. IC_{50} scores below 100nM are considered high affinity binders to that HLA allele, and are highlighted

Protein		Sequence	Pos	DQB1 *0201	DQB1 *0301	DQB1 *0402	DQB1 *0602	DRB1 *0101	DRB1 *0301	DRB1 *0401	DRB1 *0405	DRB1 *0802	DRB1 *0901	DRB1 *1101	DRB1 *1201	DRB1 *1302	DRB1*1501	DRB3 *0101	DRB3 *0202	DRB4 *0101	DRB5 *0101
CFP10		MAEMKTDAATLAQEA	1	3344	9439	364	476	57	76	58	586	60	920	583	6135	64	1261	9.0	82	512	8684
	P4	GNFERISGDLKTQID	16	61	-	7044	2213	354	123	701	2463	6236	841	899	21506	2215	7030	643	5367	2039	153
	P9	GQWRGAAGTAAQAAV	41	426	13	33	23	4.6	-	74	411	2707	35	74	36643	-	5127	3803	65	13508	48
	P10	AAGTAAQAAVVRFQE	46	2889	17	614	154	174	-	867	10451	1872	406	8560	9487	7882	3681	6869	1479	508	90
	P11	AQAAVVRFQEAANKQ	51	30170	3016	9780	692	583	-	4555	21895	981	3431	30914	19791	24297	7355	-	16166	747	81
	P12	VRFQEAANKQKQELD	56	4853	37930	13219	26908	12516	-	2102	8000	11822	6943	6535	-	42431	-	4969	24694	17959	11
	P15	EISTNIRQAGVQYSR	71	5382	91	444	74	245	893	44	204	27	1223	1067	2023	1228	1687	11241	4695	81	1601
	P16	IRQAGVQYSRADEEQ	76	105	6357	4676	2834	10365	19154	1912	8308	243	30682	38502	18401	31543	38969	13981	-	5198	28295
ESAT6																					
	P1	MTEQQWNFAGIEAAA	1	656	187	145	208	69	-	326	2981	23776	261	1189	13897	29397	7146	26477	-	11500	13851
	P5	NVTSIHSLLDEGKQS	21	6947	8905	2776	1344	2581	34059	3091	68	1202	14451	2304	90a3	5588	6475	571	23869	34	1774
	P7	EGKQSLTKLAAAWGG	31	26067	5899	52	42	11	-	4627	591	532	61	255	33	-	5678	-	-	7055	4118
	P10	SGSEAYQGVQQKWDA	46	1793	5565	3278	3296	6640	-	26425	2803	-	6716	33441	37854	-	21016	8303	-	31215	2512
	P12	QKWDATATELNNALQ	56	4864	14835	258	323	2335	35013	515	3875	-	10221	23011	-	-	-	-	16421	35976	-
	P15	NLARTISEAGQAMAS	71	19378	101	2405	4965	722	3886	1778	-	538	630	6739	19379	30426	14102	4451	-	9351	13551

When a single peptide bound multiple alleles, we reverted back to our ELISpot data, to determine which allele was dominant in individuals who responded to that particular peptide. For example, CFP10 peptide 1, bound the alleles in Table 13 below.

Table 13: HLA alleles for which CFP10 peptide 1 bound in the binding assays

Peptide	HLA allele	Binding IC_{50} (nM)
CFP-10 P1	DRB1*01:01	57
	DRB1*03:01	76
	DRB1*04:01	58
	DRB1*08:02	60
	DRB1*13:02	64
	DRB3*01:01	9
	DRB3*02:02	82

In our ELISpot results, DRB1*04:01 was the only HLA allele observed in more than one responder to CFP10 P1 (3/8 responders). This suggested that in our cohort it was most likely that CFP10 peptide 1 was restricted by DRB1*04:01. To biologically determine the HLA restriction of the CFP10 peptide, we investigated whether responsiveness to each peptide was associated with expression of specific HLA DR alleles (Table 14). We found a significant association between the presence of DRB1*04:01 and responsiveness to peptide 1 in 22 *M.tb* infected individuals.

Table 14: CFP10 peptide 1 responses for HLA restrictions

Peptide and HLA DR allele	Responsiveness (IFN-γ ELISpot assay response)	Individuals not bearing allele, n	Individuals bearing allele, n	p-value (Fisher exact test)
CFP10 P1 DRB1*04:01	yes	5	3	p=0.036
	no	14	0	

The same analysis was repeated for all ESAT6 and CFP10 peptides that were selected based on the epitope mapping. Table 15, below, displays all peptide-HLA pairs that we determined to be potential tetramer reagents.

Table 15: HLA restrictions for ESAT6 and CFP10 peptides

HLA allele	Peptide number	Protein	Peptide Sequence	IC_{50} (nM)*
DRB5*01:01	11	$CFP10_{(51-65)}$	AQAAVVRFQEAANKQ	81
DRB1*04:01	2	$ESAT6_{(6-20)}$	WNFAGIEAAASAIQG	39
	1	$CFP10_{(1-15)}$	MAEMKTDAATLAQEA	58
	9	$CFP10_{(41-55)}$	GQWRGAAGTAAQAAV	74
	15	$CFP10_{(71-85)}$	EISTNIRQAGVQYSR	44
DRB3*02:02	1	$CFP10_{(1-15)}$	MAEMKTDAATLAQEA	82
	9	$CFP10_{(41-55)}$	GQWRGAAGTAAQAAV	65
DRB4*01:01	5	$ESAT6_{(21-35)}$	NVTSIHSLLDEGKQS	34
	15	$CFP10_{(71-85)}$	EISTNIRQAGVQYSR	81
DQB1*06:02	2	$ESAT6_{(6-20)}$	WNFAGIEAAASAIQG	52
	7	$ESAT6_{(31-45)}$	EGKQSLTKLAAAWGG	42
	9	$CFP10_{(41-55)}$	GQWRGAAGTAAQAAV	23
	15	$CFP10_{(71-85)}$	EISTNIRQAGVQYSR	74

These tetramers were all synthesised by the NIH tetramer core facility.

2.4.6. Optimisation of tetramer staining conditions

A wide variety of conditions and concentrations for antigen-specific tetramer staining are reported in the literature. Some investigators have reported using tetramer concentrations as high as 20μg/mL (J. J. Yang et al. 2004; Day et al. 2003; Novak et al. 1999), while others used concentrations as low as 1μg/mL (Scriba et al. 2005; Novak et al. 1999). Furthermore, the temperatures used for staining were variable, with 3 temperatures being commonly used for staining: 4°C, room temperature (20-23°C) or 37°C. The duration of staining varied from 10 minutes to as long as 20 hours. Due to this variation in conditions, the optimal tetramer concentration, staining temperature and duration of staining were determined for each tetramer.

Firstly, PBMCs were stained with a range of tetramer concentrations, in a two-fold dilution series from 4µg/mL to 0.5µg/mL for 1 hour at room temperature or 37°C, in a total volume of 100µL of staining media (Figure 15). The gating strategy is shown in Figure 14.

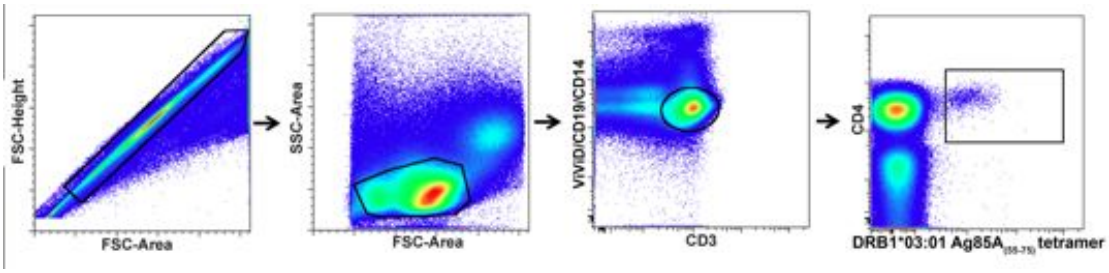

Figure 14: Flow cytometric analysis and gating strategy of tetramer stained CD4 T cells. Representative density plots showing the gating strategy employed to identify live, $CD3^+$, small CD4 lymphocytes. Cell doublets were excluded using forward scatter-area (FSC-A) versus forward scatter-height (FSC-H) parameters, small lymphocytes were then selected before gating on $CD19^-$ and $CD14^-$ live ($ViViD^{low}$), $CD3^+$ T cells. Finally, $CD4^+$ T cells were selected.

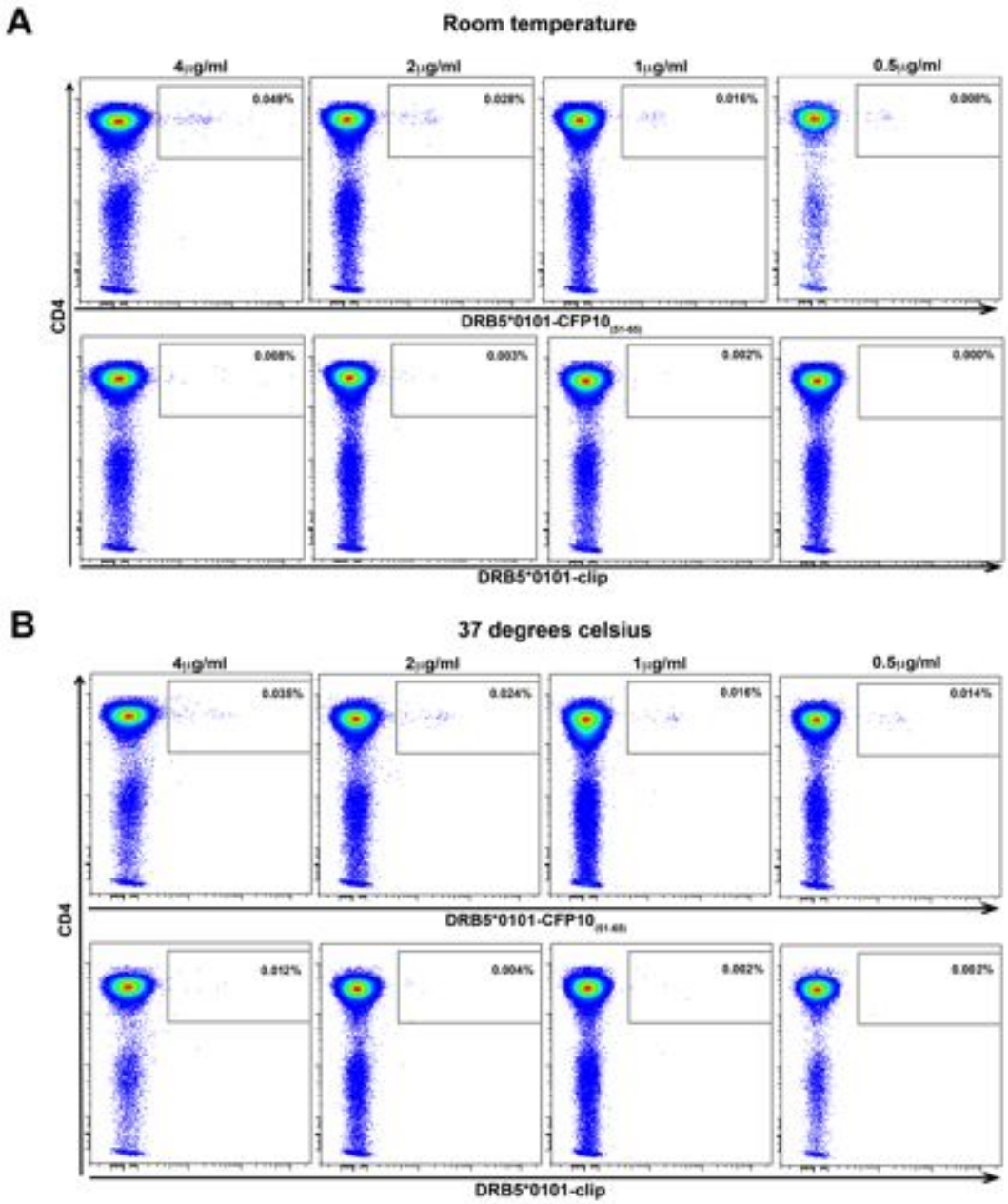

Figure 15: Optimisation of HLA class II tetramer staining concentrations. Representative figure of PBMCs stained with 2-fold dilutions of class II tetramer concentrations, starting at 4μg/mL. The top panel shows staining with the DRB5*01:01 tetramer bearing the $CFP10_{(51-65)}$ peptide and the lower panel shows staining with the control tetramer (clip). Tetramer staining was performed at room temperature for a period of one hour (A) or at 37 degrees Celsius for a period of 1 hour (B). The frequencies of $tetramer^{+}$ CD4 T cells are shown in each box.

Although variation was observed, 2μg/mL of tetramer was sufficient to label the antigen specific cells in PBMCs, with low background or unspecific staining. At higher tetramer concentrations, the amount of background or unspecific staining increased (Figure 16).

It has been shown that the tetramer can also be internalised at 37°C and in order to avoid this, we chose to stain at room temperature as the frequencies of tetramer+ CD4 T cells were comparable between the two conditions. Furthermore, staining at room temperature minimises T cell stimulation.

The DRB1*03:01-Ag85A$_{(56-75)}$ tetramer acquired from Beckman Coulter showed more distinct labelling at 37°C for 1 hour as compared to room temperature (data not shown), whereas all the other HLA class II tetramers stained as efficiently at room temperature for 1 hour.

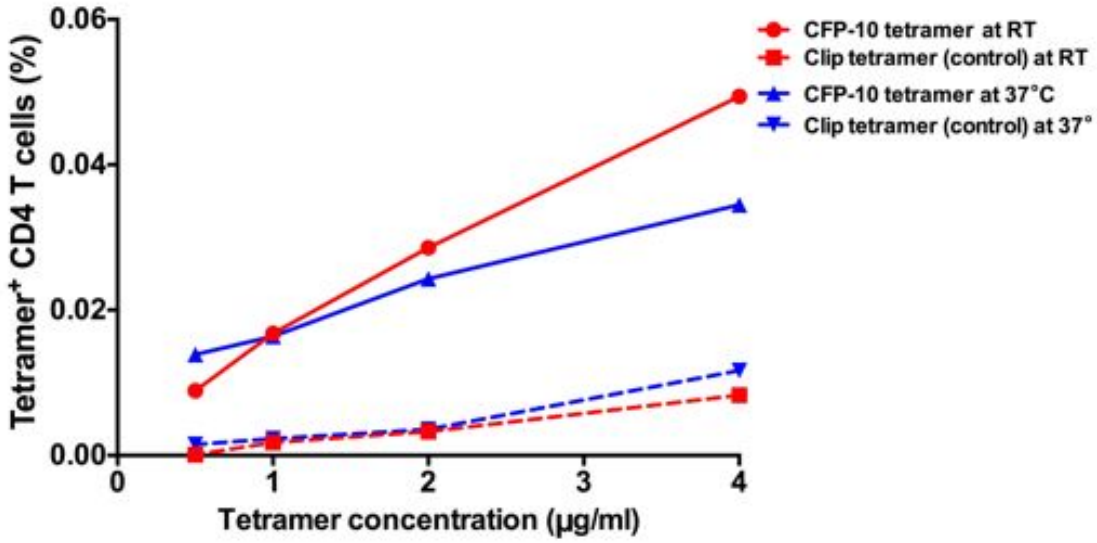

Figure 16: Frequencies of tetramer+CD4+ T cells recorded for the DRB5*01:01-CFP10$_{(51-65)}$ and the DRB5*01:01-clip (control) tetramers shown as dotted lines, at room temperature and at 37°C after a 1 hour incubation period.

To determine if longer incubation periods with the tetramers resulted in increased frequencies and brighter staining of the tetramer specific T cells, we stained PBMCs for either 1 hour or 2 hours. Although longer incubation periods resulted in brighter staining (increased median fluorescent intensity (MFI)) the frequencies of antigen specific tetramer+ CD4 T cells were similar. There was also an increase in non-specific background staining, and MFI of the non-specific staining, with longer incubation periods (Figure 17). Based on these results, all staining was done for a period of 1 hour in all studies in this thesis unless otherwise stated.

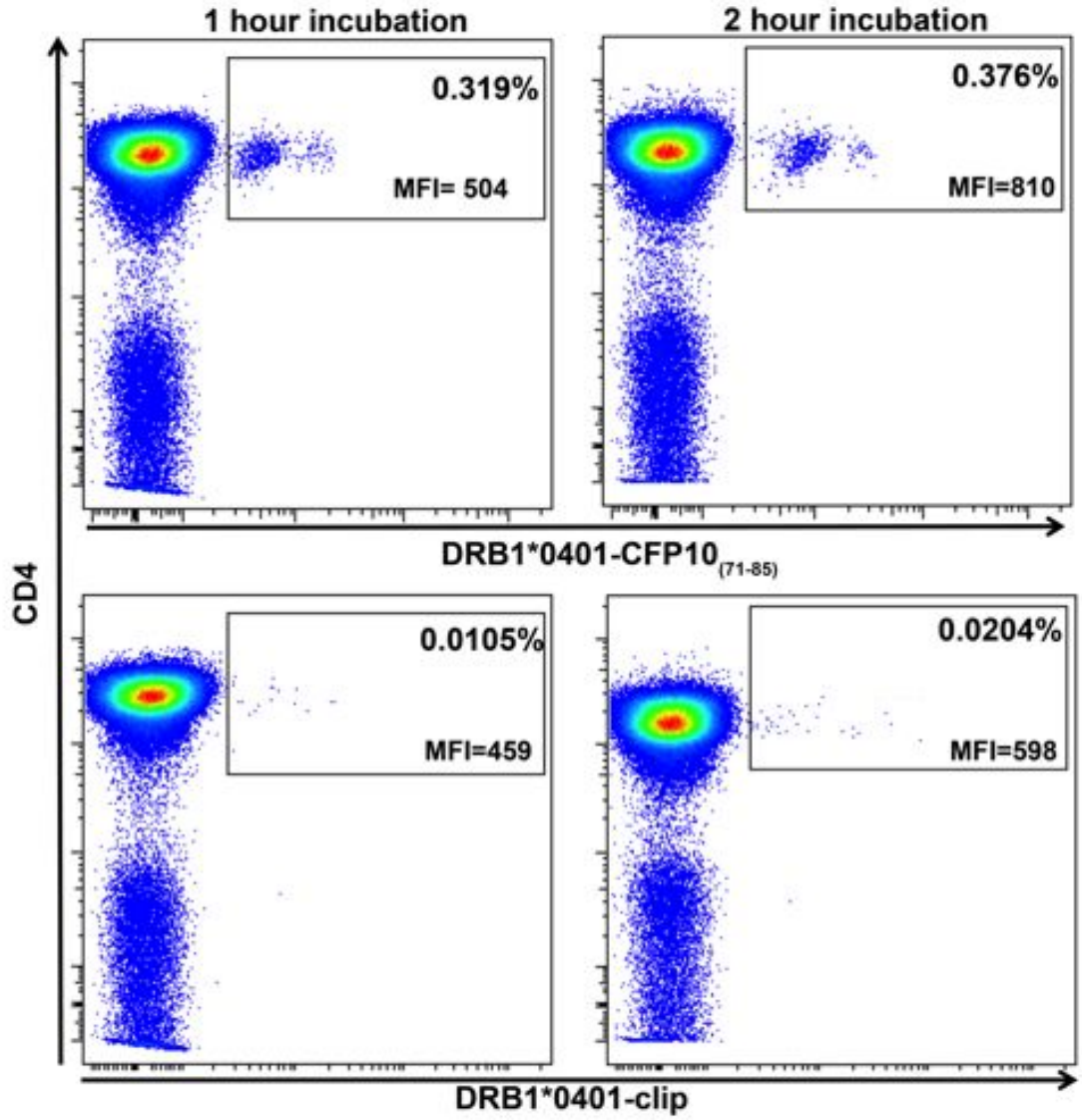

Figure 17: Optimisation of HLA class II tetramer staining conditions. Representative dot plots of PBMCs stained with 2μg/mL of tetramer at room temperature for a period of 1 hour or 2 hours. The frequencies of tetramer+ CD4 T cells are shown in the plots, as well as the median fluorescence intensities (MFI) of the tetramer+ CD4 T cells.

2.4.7. Final tetramer selection

Using the above-mentioned methods we validated the use of only 3 out of the 13 selected tetramers, as listed below in Table 16. We could not rule out that the other ESAT6 and CFP10 tetramers may be specifically binding antigen-specific T cells, as we did not have a sufficient sample size of donors with the correct HLA alleles to definitively show this. The Ag85A P27/38 tetramer and the Ag85A P37/38 tetramer failed to work after multiple attempts of staining PBMCs from multiple donors in various conditions, no further work was done with these tetramers.

Table 16: Tetramers utilised in this thesis for Chapters 3,4 and 5.

HLA allele	Peptide number	Protein	Peptide Sequence
DRB5*01:01	11	$CFP10_{(51-65)}$	AQAAVVRFQEAANKQ
DRB5*01:01		Clip	PVSKMRMATPLLMQA
DRB1*0401	15	$CFP10_{(71-85)}$	EISTNIRQAGVQYSR
DRB1*0401		Clip	PVSKMRMATPLLMQA
DRB1*0301	12/13	$Ag85A_{(56-75)}$	VPSPSMGRDIKVQFQSGGAN
DRB1*0301		$ApolipoproteinB_{(2877-2894)}$ (ApoB)	ISNQLTLDSNTKYFHK LN

2.5. Discussion

Tetramers are extremely powerful tools to directly characterise antigen-specific T cells with minimal *in vitro* manipulation. However, unlike class I tetramers, HLA class II tetramers have been challenging to develop and use.

The work described in this chapter aimed to identify *M.tb*-specific CD4 T cell epitopes that are commonly recognised in our cohort, and to determine which HLA alleles restrict the identified epitopes, to develop tetramer reagents.

While identifying epitopes in *M.tb* antigens has been a major focus in recent years (Arlehamn et al. 2012; Geluk & van Meijgaarden 2000; Commandeur et al. 2011), primarily to identify suitable antigens to develop new TB vaccines, determining the HLA restrictions of these epitopes has not been given an equal amount of attention. Of the studies that have sought to determine which HLA alleles restrict *M.tb*-specific epitopes (Pathan et al. 2001; Mustafa et al. 2000), very few have published on synthesis of tetramer reagents with this data (Arlehamn et al. 2012; Hohn et al. 2007). Many of the studies have confirmed the epitopes identified in this chapter and some have even confirmed their HLA restrictions (Pathan et al. 2001; Hohn et al. 2007). .

We identified 3 Ag85A epitopes that were recognised by more than 30% of participants of MVA85A vaccine trials. More than 30% of latently *M.tb*-infected donors recognised 7 different ESAT6 epitopes and 8 CFP10 epitopes. With the exception of 2 ESAT6 epitopes, similar results were reported by Arlehamn et al. (Arlehamn et al. 2012) and Pathan et al. (Pathan et al. 2001).

Many of the peptides described in this chapter bound multiple HLA alleles confirming the promiscuity of class II peptides (Mustafa et al. 2000). This promiscuous binding of class II peptides has been observed across a wide range of antigens, and is not exclusive to bacterial antigens. However we were able to use biological data to confirm binding to HLA alleles that were common in our cohort, which is representative of the population. This aided in narrowing down the options of HLA allele peptide restrictions to those that may be applicable to our cohort.

Due to the large discrepancy in literature on the use and conditions used for MHC class II tetramer staining, we next aimed to optimise the conditions to

utilise for staining. Studies have reported dramatic variations in incubation times for HLA class II tetramers, ranging from 1 to 20 hours (Arlehamn et al. 2012; Novak et al. 1999; Day et al. 2003; Reijonen & Kwok 2003; Crawford et al. 1998; Cameron et al. 2002; Cameron et al. 2001). In this thesis, optimal staining was seen after 1 hour, and longer incubation periods were associated with increased non-specific staining.

Different studies have reported specific staining at 4°C, at room temperature and at 37°C (Scriba et al. 2005; Day et al. 2003; Cameron et al. 2002). For the Ag85A tetramer, more efficient staining was observed when performed at 37°C for 1 hour, whereas for the CFP10 tetramers, incubation at room temperature resulted in more efficient staining and lower background. In accordance with other studies (Cameron et al. 2001; Cunliffe et al. 2002; Lemaître et al. 2004), very little staining was observed at 4°C and higher tetramer concentrations were necessary (data not shown). This difference in staining temperatures is possibly influenced by differential binding affinities of the TCR/pMHC complex (Reichstetter et al. 2000). These studies suggest that only high affinity TCRs are bound by the tetramer at 4°C.

We were unable to detect tetramer+ CD4 T cells with Ag85A p27/28 and p37/38 tetramers, as well as all the DRB1*04:01, DRB4*01:01 and DQB1*06:02 ESAT6 epitope bearing tetramers. There were no known issues with the synthesis of the tetramers; they were shown to have the peptide loaded on the correctly folded HLA molecule. Multiple staining conditions were attempted with no success. The reasons for this lack of staining are unclear and many groups have reported similar experiences. This lack of staining may be due to poor binding of pHLA to the TCR, or due low T cell frequencies too low to detect.

In conclusion, we generated and validated staining with 3 HLA class II tetramers, which have then been used to address the aims of this project.

2.6. Contributions

Helen McShane allowed access to the data generated in the MVA85A vaccine trials at the University of Oxford

Alex Sette's lab at the La Jolla Institute of Allergy and Immunology in San Diego, USA performed part of the HLA typing of participants, as well as the epitope binding assays.

Part of the HLA typing was performed at the National Institute for Communicable Disease in Johannesburg, South Africa.

Chapter 3: Heterologous vaccination against human tuberculosis modulates antigen-specific $CD4^+$ T-cell function

This data had been published and the paper is attached as an appendix.

3.1. Introduction

After clean water, vaccination is the most effective global public health intervention (Plotkin SA 1999). While protection by most currently licensed vaccines correlates with levels of induced antibodies, protection against pathogens such as HIV-1 and *M.tb* is thought to rely, at least in part, on specific T-cell responses (Kaufmann & McMichael 2005; Walzl et al. 2011). Heterologous prime-boost regimens, involving priming with either BCG or an improved live mycobacterial vaccine, followed by an adjuvanted subunit or viral vectored boost, may constitute the most promising vaccination strategy against TB (Kaufmann 2010; Lambert et al. 2009; Hatherill 2011).

It is currently not known exactly which T-cell response vaccines should induce for protection against TB disease (Kaufmann & McMichael 2005; Walzl et al. 2011). In phase I and II clinical trials of new TB vaccines, the frequencies of vaccine-induced antigen-specific T helper type 1 (Th1) cytokine-expressing CD4 and/or CD8 T cells are usually quantified with the premise that vaccination-induced responses should be higher than the pre-vaccination response (Hanekom et al. 2008). The pattern of effector cytokine expressed by specific T cells is also commonly measured (Hanekom et al. 2008; Abel et al. 2010; Soares et al. 2008). However, we recently showed that a Th1 response-inducing vaccination strategy in infants, which involves a BCG prime at birth and a boost with the novel poxvirus-vectored TB vaccine candidate, MVA85A, showed no evidence of efficacy against TB disease or *M.tb* infection (Tameris et al. 2013). These results suggest that features other than frequencies and cytokine-expression patterns of induced T cells should be explored as correlates of vaccine-induced immunity. For example, it is thought that the capacity to expand after T cells re-encounter antigen is an important function that may be measured in vaccine trials (Esser et al. 2003). It is thought that memory T cells, which are long-lived and have the capacity to proliferate rapidly upon antigen encounter, should be a desirable vaccine-

induced response. However, in recent years many in the field have been debating whether having a constant population of effector T cells may be a more efficient way to control new *M.tb* infections. Thus this is being actively investigated.

In areas with a high incidence of TB, where most of the population is already infected with *M.tb*, the success of heterologous boost vaccines may depend on the modulation of the existing mycobacteria-specific T-cell repertoire to possess more “favourable” functional characteristics, rather than inducing de novo T-cell responses. In TB endemic countries, CD4 T cells specific for conserved immunodominant antigens such as Ag85A are detectable in most individuals beyond infancy (Scriba et al. 2011). These cells could have been induced by BCG vaccination and/or exposure to environmental mycobacteria and/or *M.tb* or even cross-reactive bacteria (Abel et al. 2010; Scriba et al. 2012; Scriba et al. 2011). We propose two minimum criteria for a potentially successful heterologous vaccination strategy: (1) the boost vaccine should modify or reprogram the T-cell response to display different functional and/or phenotypic characteristics to the pre-vaccination response; (2) the induced T cell response should be long-lived. We also propose that the ability of the cells to home to the lungs is critical. Very little is known about whether cells primed in the dermis have the capacity to home to the lung mucosa or whether programming of the cells at the dermis is mutually exclusive to the capability to home to the lung.

In this chapter, we comprehensively characterised mycobacteria-specific CD4 T cells before and after vaccination with MVA85A using HLA class II tetramers.

3.2. Aims

The need to develop a vaccine against TB that is better than BCG is evident and a priority in the vaccine field. However, the T cell characteristics that a vaccine should induce remain elusive and a point of debate. Understanding the immune responses induced by the current vaccines in clinical trials is very important and critical for informing rational vaccine design. The goal of this chapter was to enhance our understanding of the responses induced by a novel TB vaccine, MVA85A.

Specific aims:

i.) To delineate MVA85A-specific CD4 T cell memory phenotype

ii.) To characterise the expression of tissue-homing markers on MVA85A-specific CD4 T cells

iii.) To describe the T cell effector function and proliferative capacity of MVA85A induced CD4 T cells.

3.3. Materials and Methods

The work in this chapter was performed by the candidate unless otherwise stated.

3.3.1. Study participants, vaccination and follow-up, blood collection and HLA typing.

We accessed cryopreserved samples from a subset of participants (24 adults, 12 adolescents (TB008) and 24 children (TB014), Table 21) who were enrolled in to two completed phase I/IIa trials of MVA85A (Hawkridge et al. 2008; Scriba et al. 2010). Participants were all vaccinated with BCG at birth, were all HIV negative and had no evidence of *M.tb* infection, as defined by a negative ESAT6/CFP10 ELISpot and a TST induration of <15 mm, and all had a normal chest X-ray. Participants received a single intra-dermal dose of $5x10^7$ pfu of MVA85A over the deltoid region of the left arm, and were followed up for a minimum of 6 months (Hawkridge et al. 2008; Scriba et al. 2010). None converted to a positive ESAT6/CFP10 response during follow-up. DNA was extracted from PBMCs as described in chapter 2 section 2.3.8. and sent for HLA typing.

3.3.2. Direct *ex vivo* IFN-γ ELISpot assay

The frequency of IFN-γ-expressing cells was measured by *ex vivo* ELISpot assay. Briefly, antigens included pooled Ag85A peptides (2μg/mL each) and *M.tb* purified protein derivative (PPD, from Statens Serum Institute, used at 20μg/mL). Medium alone served as negative control and phytohaemagglutinin A (PHA, Remel, 10μg/mL) as positive control. Results were expressed as the number of spot forming cells (SFCs) per million PBMCs above the negative control. The cut-off for a positive response was 17 SFC per million PBMCs, after the frequency of cells in the unstimulated sample had been subtracted.

3.3.3. Lymphoproliferation assay

PBMCs were thawed in 12.5%AB+/RPMI media containing DNAse (20 μg/mL), washed and rested overnight at 37°C with 5% CO2 in medium in a 15mL tube. The next day, the tube was topped up to 10 mL with 12.5% AB+/RPMI and centrifuged for 10 min at 596g at 22°C with brake on

"max/high". The supernatant was decanted and cells were resuspended in 1mL of PBS and gently pipetted up and down. The tube was topped up with PBS and centrifuged for 10 min at 596g at 22°C with brake on "max/high". PBMCs were then stained with 0.5μg/mLCellTrace Oregon Green 488 (Molecular Probes, Invitrogen) a cytoplasmic dye, per $1x10^7$ cells for 30 minutes in the dark, in a volume of 1mL. Tube was topped up with PBS and centrifuged for 10 min at 596g at 22°C. Stained cells were resuspended in 12.5%AB+/RPMI and incubated either with medium alone (negative control), 66 pooled 15mer peptides overlapping by 10 amino acids spanning the mycobacterial Ag85A protein (1μg/mL each, Peptide Protein Research Ltd.) or PPD (used as positive control at 2μg/mL) for 6 days at 37°C with 5% CO2. After 6 days the cells were washed once in PBS and then stained with the live/dead, Violet Fixable Viability dye (Vivid, Molecular Probes, Invitrogen), fixed using FACSLysing Solution (BD Biosciences), permeabilised with BD Perm/Wash buffer (BD Biosciences) and stained with fluorescence-conjugated antibodies (Table 17). Antibody panels had been optimised as described in Chapter 2 section 2.3.13. Stained samples were acquired on an LSRII flow cytometer, (see configuration in Chapter 2 section 2.3.14).

Table 17: Panel of fluorochrome-conjugated antibodies and dyes used to stain cells for the lymphoproliferation assay.

Marker	Clone	Manufacturer	Fluorochrome/dye	Volume/concentration used
CD3	UCHT1	Invitrogen	Quantum Dot 605	0.5μL
CD8	SK1	BD Biosciences	PerCP-Cy5.5	3μL
Proliferation		Invitrogen	Oregon Green	0.5μg/mL
Live/dead		Invitrogen	ViViD	0.5μg/mL

3.3.4. Whole blood intracellular cytokine assay

This assay was performed as previously described (Plotkin SA 1999; Hanekom et al. 2004), with minor modifications. Briefly, 1mL of heparinized whole blood was incubated immediately after collection in the presence of anti-CD28 and anti-CD49d (each at 0.5μg/mL, BD Biosciences). Pooled Ag85A peptides (2μg/mL per peptide) or viable BCG (Strain Danish 1331, Statens Serum Institute, 1.2×10^6 cfu/mL) were used as antigens. No antigen

was used as a negative control, and Staphylococcal enterotoxin B (SEB, 5μg/mL, Sigma-Aldrich) as a positive control. After 7 hours, Brefeldin A (10μg/mL, Sigma-Aldrich) was added and samples were incubated for a further 5 hours. EDTA (Sigma) was added at 2mM to break cell clumps, followed by high speed vortexing for 10 s, incubation at room temperature for 15 minutes, and repeat of the vortexing. Erythrocytes were lysed and white cells fixed using FACSLysing Solution (BD Biosciences), before cryopreservation in 10%FCS/RPMI and 10%DMSO. Cells were thawed in batch, washed in PBS, permeabilised with BD Perm/Wash buffer and stained with fluorescent antibody panel optimised as described in Chapter 2 section 2.3.13, in a total volume of 100μL (Table 18 below), and acquired on the LSRII flow cytometer.

Table 18: Panel of fluorochrome-conjugated antibodies used to stain cells for the whole blood intracellular cytokine assay.

Marker	Clone	Manufacturer	Fluorochrome/dye	Volume used
CD3	UCHT1	BD Biosciences	Pacific Blue	1μL
CD8	SK1	BD Biosciences	PerCP-Cy5.5	3μL
CD4	SK3	Invitrogen	QuantumDot605	0.5μL
IFN-γ	K3	BD Biosciences	AlexaFluor700	1μL
IL-2	5344.11	BD Biosciences	FITC	5μL

3.3.5. HLA class II tetramers and staining

Custom ordered PE-conjugated iTag MHC class II tetramers (100 μg/mL) were obtained from Beckman Coulter. HLA-DRB1*03:01 tetramers were complexed either to the mycobacterial Ag85A 20mer peptide, VPSPSMGRDIKVQFQSGGAN (DRB1*03:01-Ag85A$_{(56-75)}$), or the human apolipoprotein B-100 peptide, ISNQLTLDSNTKYFHKLN, (DRB1*03:01-ApoB$_{(2877-2894)}$, negative control tetramer) (Malcherek et al. 1993; Rammensee et al. 1999). Cryopreserved PBMCs were thawed, washed and stained with Violet or Aqua LIVE/DEAD Fixable Dead Cell Stain. Cells were stained with 2μg/mL iTAg class II tetramer at 37°C for 1 hour as previously optimised in Chapter 2. Tetramer-stained cells were washed and stained with surface marker antibodies for 40 minutes at 4°C in a total volume of 100μL, except for staining with anti-CCR7-APC, which was done separately at 37°C for 20

minutes, before the other monoclonal antibodies were added for 40 minutes at 4°C (Table 19 or Table 20).

Table 19. Panel of fluorochrome-conjugated antibodies and dyes used to stain cells for MVA85A T cell memory phenotype studies.

Marker	Clone	Manufacturer	Fluorochrome	Volume/concentration Used
CD3	UCHT1	BD Biosciences	Alexa Fluor 700	1μL
CD4	S3.5	Invitrogen	Quantum Dot 605 (Qdot 605)	0.5μL
CD45RA	HI1700	eBiosciences	PerCP Cy5.5	0.5μL
CCR7	150503	R&D Systems	Allophycocyanin (APC)	5μL
CD27	CLB-27/1	Invitrogen	Quantum Dot 655	0.1μL
CD38	HB7	BD Biosciences	PeCy7	0.5μL
CD14	MΦP9	BD Biosciences	V450	1.25μL
CD19	HIB19	BD Biosciences	V450	0.3μL
Live/dead		Invitrogen	ViViD	0.5μg/mL

Table 20. Panel of fluorochrome-conjugated antibodies and dyes used to stain cells for MVA85A T cell homing and activation phenotype studies.

Marker	Clone	Manufacturer	Fluorochrome	Volume Used
CD3	UCHT1	BD Biosciences	Alexa Fluor 700	1μL
CD4	S3.5	Invitrogen	Quantum Dot 605	0.5μL
CLA	HECA-452	Biolegend	Fluorescein isothiocyanate (FITC)	1.25μL
Integrin Beta 1	HB7R	AbD Serotec	Biotinilyated	0.5μL
Streptavidin		BD Biosciences	PECy7	0.15μL
Integrin Beta 7	FIB504	eBiosciences	eFluor 650	0.3μL
Integrin Alpha4	44H6	AbD Serotec	Alexa Fluor 647	0.3μL
CD14	HCD14	Biolegend	PerCP Cy5.5	1.25μL
CD19	HIB19	BD Biosciences	V450	0.3μL
Live/dead		Invitrogen	ViViD	0.5μg/mL

Finally, cells were washed and fixed in 100μL of 1% paraformaldehyde in PBS and acquired on the BD LSRII.

3.3.6. Flow cytometry analysis

Stained cells were immediately acquired on a LSRII flow cytometer (BD Biosciences), configuration shown in Chapter 2 section 2.1.14. Flow cytometry data analysis was performed using FlowJo version 9.2 (TreeStar). Unstained cells and single stained mouse κ beads were used as controls and to calculate compensations for every run. Cell doublets were excluded using forward scatter (FSC)–area versus FSC–height parameters (Figure 21);

acquisition time gating was applied to exclude data with inconsistent fluorescence and antibody aggregates were gated out using “keeper” gating. Boolean gating was employed to discern memory populations (Figure 23).

3.1.7. Statistical considerations

For the intracellular cytokine staining assay, the cut-off for a positive CD4 T cell response was above 0.01%, after frequencies of cells in the unstimulated sample had been subtracted. Phenotypic data were included for analysis only for samples with specific tetramer+ CD4 T cell frequencies above 0.01%, the limit of detection of the flow cytometer and absolute numbers of tetramer^{+} CD4 T cells of ≥35 cells. Statistical tests were performed using Prism v.5.0a (GraphPad). Paired and unpaired comparisons were done using the non-parametric Wilcoxon Matched Pairs, or the Mann Whitney U tests, respectively.

3.4. Results

3.4.1 Study participants

PMBCs from the following subset of participants, who were enrolled in previous MVA85A clinical trials (TB008 and TB014), were utilised in this chapter. Table 21 below, describes the demographics of the participants, as well which assays were performed on their PBMCs.

Table 21. Details of trial participants

Donor No.	Age (years)	Gender	Ethnicity	MVA85A Vaccine trial	Assays performed	HLA-DRB1 genotype
DN01-1051	21	F	Black African	TB008	Tetramer[a)], Elispot[b)]	*03:01, *11:01
DN01-1078	42	M	Caucasian	TB008	Tetramer, Elispot	*03:01, *12:01
DN01-1117	49	M	Mixed Race	TB008	Tetramer, Elispot	*03:01, *12:01
DN04-1002	2	M	Mixed race	TB014	Tetramer, Elispot	*03:01, *04:03
DN04-1011	6	M	Mixed race	TB014	Tetramer, Elispot	*03:01, *15:03
DN02-1002	13	M	Black	TB008	Tetramer, Elispot, Proli[c)], ICS[d)]	*03:01, *13:02
DN02-1006	15	F	Mixed race	TB008	Tetramer, Elispot, Proli, ICS	*03:01, *13:02
DN02-1001	13	F	Black African	TB008	Elispot, Proli, ICS	*03:02, *15:03
DN02-1003	13	M	Black African	TB008	Elispot, Proli, ICS	*11:01, *14:01
DN02-1005	14	M	Black African	TB008	Elispot, Proli, ICS	*03:02, *12:01
DN02-1007	15	M	Black African	TB008	Elispot, Proli, ICS	*09:01, *13:01
DN02-1009	14	F	Black African	TB008	Elispot, Proli, ICS	*04:05, *13:01
DN02-1011	15	F	Black African	TB008	Elispot, Proli, ICS	*01:02, *12:01
DN02-1017	15	F	Black African	TB008	Elispot, Proli, ICS	*15:01, *15:03
DN02-1020	15	M	Mixed race	TB008	Elispot, Proli, ICS	*11:01, *13:01
DN02-1023	14	F	Mixed race	TB008	Elispot, Proli, ICS	*03:02, *03:02
DN02-1025	15	M	Black African	TB008	Elispot, Proli, ICS	*01:02, *03:02

[a)] *Ex vivo* HLA class II tetramer staining and phenotyping.
[b)] *Ex vivo* IFN-γ ELISpot assay.
[c)] *In vitro* proliferation assay.
[d)] Whole blood intracellular cytokine staining assay.

3.4.2. *Ex vivo* detection of Ag85A-specific CD4 T cells by DRB1*03:01-Ag85A$_{(56-75)}$ HLA class II tetramer staining

Because the antigen-induced activation of T cells during *in vitro* stimulation may change the expression of certain phenotypic markers (Chao et al. 1997; Sallusto et al. 2004; Vallejo et al. 1999), we employed HLA class II tetramers to detect and characterise CD4 T cells directly *ex vivo*, in the absence of T-cell activation. To establish whether CD4 T cell binding to the DRB1*03:01-Ag85A$_{(56-75)}$ HLA class II tetramer was specific, we thawed PBMCs collected 7-14 days after MVA85A vaccination from 7 individuals bearing the HLA-

DRB1*03:01 allele. Cells were stained either with the DRB1*03:01-Ag85A$_{(56-75)}$ tetramer, or the DRB1*03:01-ApoB$_{(2877-2894)}$ control tetramer, which is complexed to a peptide spanning amino acids 2877–2894 from apolipoprotein B, a human protein involved in cholesterol transport (Malcherek et al. 1993). DRB1*03:01-Ag85A$_{(56-75)}$ tetramer+ CD4 T cells were detected in all 7 vaccinees at frequencies between 0.015% and 0.53% as shown in Figure 1B. By contrast, DRB1*03:01-ApoB$_{(2877-2894)}$ tetramer+ CD4 T cells were detected at a median frequency of 0.017% (maximum frequency 0.024%) in these individuals (Figure 18 B). We also stained PBMCs from 6 HLA-DRB1*03:01 non-bearing MVA85A vaccinees, who had robust Ag85A-specific CD4$^+$ T-cell responses observed previously by IFN-γ ELISpot assay (data not shown (Scriba et al. 2010)). No specific DRB1*03:01-Ag85A$_{(56-75)}$ tetramer staining was observed in these samples; frequencies of tetramer$^+$ CD4 T cells were consistently observed below 0.02% (data not shown).

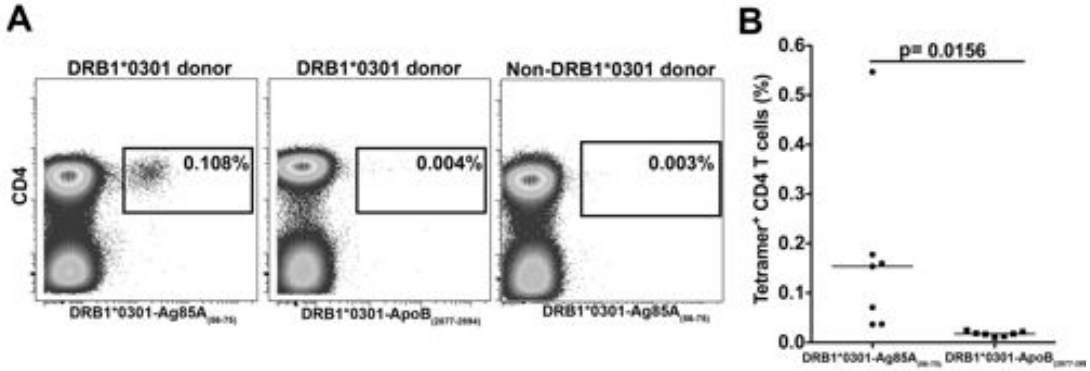

Figure 18: Direct *ex vivo* detection of mycobacterial Ag85A-specific CD4 T cells by HLA class II tetramer staining. PBMCs from MVA85A-vaccinated individuals were stained with the DRB1*03:01-Ag85A$_{(56-75)}$ tetramer or the DRB1*03:01-ApoB$_{(2877-2894)}$ control tetramer. Flow cytometry plots show data gated on CD14$^-$, CD19$^-$, live (ViViD$^-$), CD3$^+$ lymphocytes. The gating strategy is shown in Figure 21. (A) HLA class II tetramer staining of PBMCs 7 days after MVA85A vaccination, from a single donor with or without the HLA-DRB1*03:01 allele is shown. (B) The frequencies of DRB1*03:01-Ag85A$_{(56-75)}$ or DRB1*03:01-ApoB$_{(2877-2894)}$ tetramer+ CD4 T cells from 7 HLA-DRB1*03:01-bearing donors 7 days after MVA85A vaccination are shown. Each symbol represents an individual donor and bar represents the mean.

3.4.3. Frequencies of Ag85A-specific CD4 T cells peak 7 days after MVA85A vaccination

Previous MVA85A studies in humans have measured cytokine expressing cells to determine the magnitude and kinetics of the Ag85A-specific T cell response after MVA85A vaccination (Hawkridge et al. 2008; Scriba et al. 2010). We stained PBMCs collected before, and at multiple time points up to

1 year after MVA85A vaccination with the DRB1*03:01-Ag85A$_{(56-75)}$ tetramer. Pre-vaccination frequencies of DR3-Ag85A-specific CD4 T cells were mostly low (Figure 19A and B). Following MVA85A vaccination, frequencies of DRB1*03:01-Ag85A$_{(56-75)}$-specific CD4 T cells increased markedly in all vaccinees (Figure 19A and B). The response peaked 7 days post-vaccination and had returned to pre-vaccination levels after 2 months (Figure 19B). This kinetic profile was remarkably similar to that of specific CD4 T-cell frequencies measured by IFN-γ ELISpot assay, following incubation of PBMCs with peptides spanning the entire Ag85A protein (Figure 19C). However, Ag85A-specific CD4 T cells detected by ELISpot assay remained at higher frequencies than those observed pre-vaccination for the entire follow-up period (Figure 19C), indicating greater magnitude when T cell responses to the entire Ag85A protein are measured, and/or possibly greater sensitivity of the ELISpot assay.

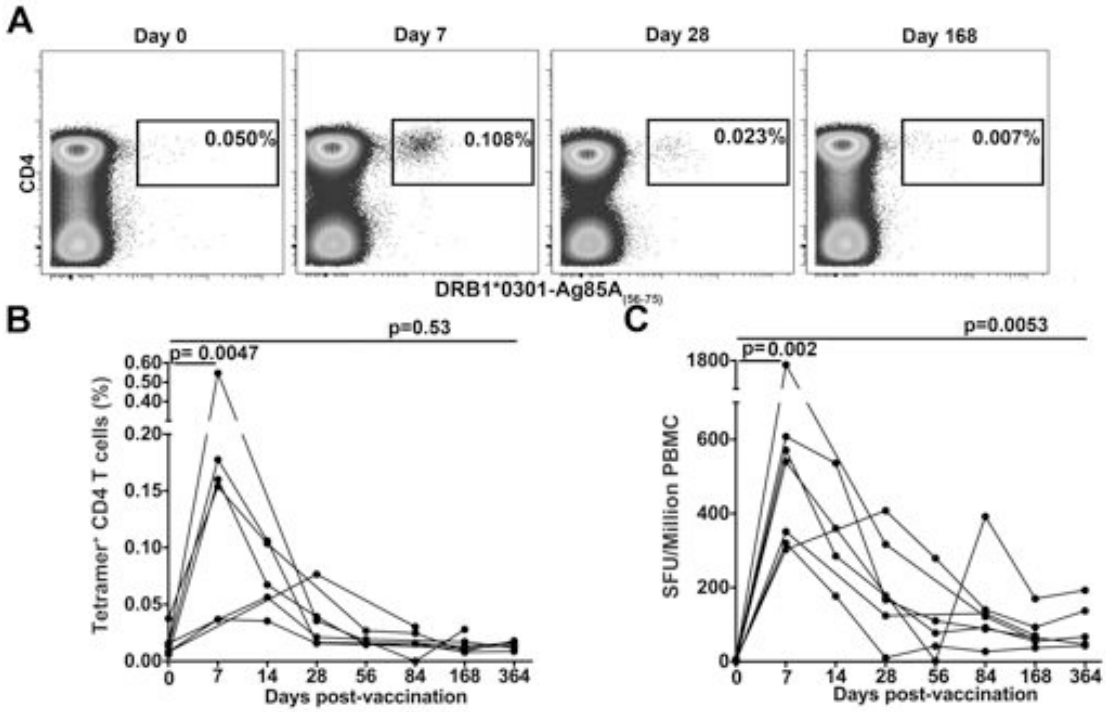

Figure 19: Direct *ex vivo* detection of mycobacterial Ag85A-specific CD4 T cells by HLA class II tetramer staining. PBMCs from MVA85A-vaccinated individuals were stained with the DRB1*03:01-Ag85A$_{(56-75)}$ tetramer or the DRB1*03:01-ApoB$_{(2877-2894)}$ control tetramer. (A) Representative flow cytometry plots of DRB1*03:01-Ag85A$_{(56-75)}$ tetramer staining of PBMCs collected before, and at the indicated time points, after MVA85A vaccination are shown from a single individual. (B) Longitudinal follow-up of DRB1*03:01-Ag85A$_{(56-75)}$ tetramer+ CD4 T-cell frequencies in 7 HLA-DRB1*03:01-bearing donors before, and up to 1 year after, MVA85A vaccination is shown. (C) The frequencies of IFN-γ-expressing T cells in the same 7 HLA-DRB1*03:01-bearing donors, measured by ELISpot assay after stimulation of PBMCs with 15-mer peptides spanning the entire Ag85A protein are shown.

3.4.4. CD4 T cell activation after MVA85A vaccination is short-lived

To investigate the kinetics and duration of T cell activation after vaccination, we measured expression of the activation marker CD38 on tetramer$^+$ CD4 T cells (Figure 20). T-cell activation increased markedly by 7 days post-vaccination and was short-lived, as CD38 expression levels returned to baseline levels in most vaccinees by 14 days (Figure 20A and B). These low CD4 T cell activation levels persisted throughout the remaining follow up period.

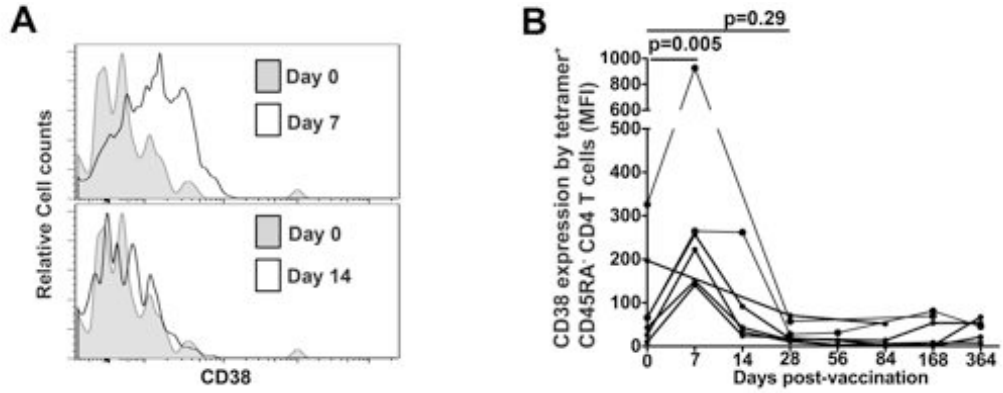

Figure 20: Direct *ex vivo* detection of CD38 expression on Ag85A-specific CD4 T cells. PBMCs from MVA85A-vaccinated individuals were stained with the DRB1*03:01-Ag85A$_{(56-75)}$ tetramer. Flow cytometry plots show data gated on CD14^{-}, CD19^{-}, live (ViViD^{-}), CD3^{+} DRB1*03:01-Ag85A$_{(56-75)}$ tetramer+ CD4 T lymphocytes. (A) Representative flow cytometry plots of CD38 expression on Ag85A-specific CD4^{+} T cells before (Day 0)and 7 or 14 days after MVA85A vaccination are shown for an individual. (B) Longitudinal post-vaccination follow-up of Ag85A-specific CD4 T-cell activation in the 7 HLA-DRB1*03:01-bearing donors are shown. Activation was measured as CD38 median fluorescence intensity on DRB1*03:01-Ag85A$_{(56-75)}$ tetramer+ CD4 T cells. P-values were calculated using the Wilcoxon matched pairs test.

3.4.5. Activated MVA85A-induced CD4 T cells express a skin-homing phenotype

The capacity of antigen-specific T cells to traffic to the site of infection-induced inflammation is critical for protective immunity. To determine the tissue homing potential of Ag85A-specific CD4 T cells induced by intradermal MVA85A vaccination, we measured expression of homing markers associated with trafficking to skin (cutaneous lymphocyte antigen, CLA (D. J. Campbell & Butcher 2002)), gut ($\alpha4\beta7$ (Kantele et al. 1999)) and lung ($\alpha4\beta1$ (Walrath & Silver 2010)) on DRB1*03:01-Ag85A$_{(56-75)}$ tetramer+ CD4 T cells (Figure 22A). The gating strategy used to discern T cell populations is shown in Figure 21.

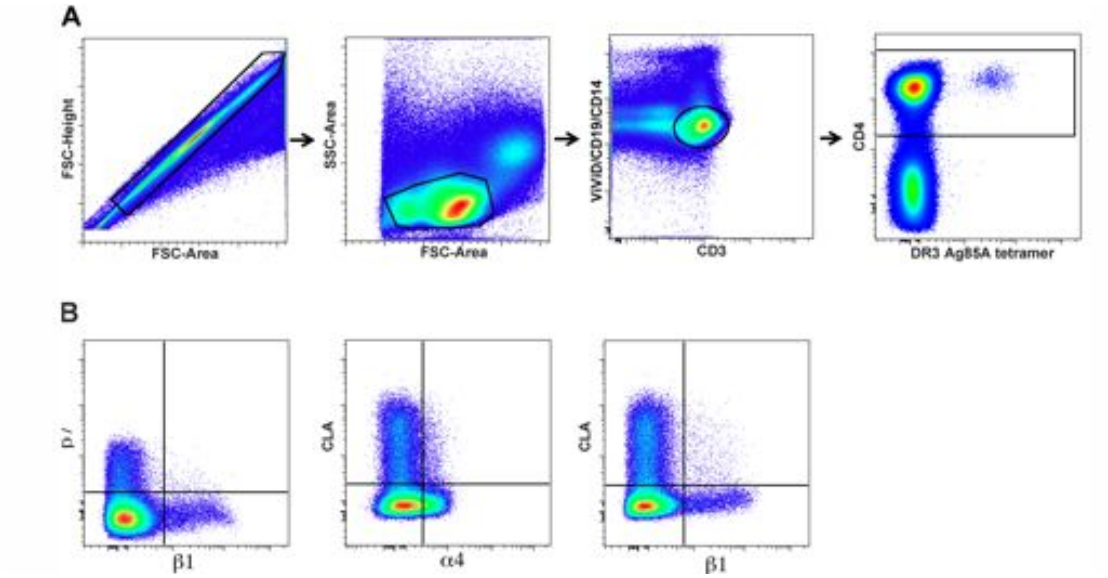

Figure 21: Flow cytometric analysis and gating strategy of CD4 T cells. (A) Representative density plots showing the gating strategy employed to identify live, $CD3^+$, small CD4 lymphocytes. Cell doublets were excluded using forward scatter-area (FSC-A) versus forward scatter-height (FSC-H) parameters, small lymphocytes were then selected before gating on $CD19^-$ and $CD14^-$ live ($ViViD^{low}$), $CD3^+$ T cells. Finally, CD4 T cells were selected. (B) Representative flow cytometry plots showing CD4 T cell co-expression of the homing markers β7, β1, α4 and CLA.

During the peak response, 7 days post-vaccination, Ag85A-specific $CD4^+$ T cells predominantly expressed CLA, while a minority expressed α4β1 (Figure 22B). This expression pattern was short-lived and mirrored T-cell activation; by day 14 post-vaccination the proportion of CLA-expressing cells had returned from ~70% to pre-vaccination levels of ~20%, and remained at this level throughout the duration of follow-up (Figure 22C). The proportion of α4β1-expressing tetramer+ CD4 T cells remained relatively consistent at ~20% during follow-up. Ag85A-specific T cells expressing the gut homing marker, α4β7, were infrequent or not detectable, at all time-points (Figure 22B). Of note, more than 60% of the tetramer+ CD4 T cells detected 14 days after vaccination expressed none of the homing markers analysed.

An important observation was that expression of CLA, α4β1 and α4β7 was not distinct; many cells co-expressed these markers. Seven days post-vaccination, CLA-expressing Ag85A-specific CD4 T cells co-expressed the integrins α4β1, α4 alone or β1 alone (Figure 22). This co-expression pattern was not observed in the total CD4 T-cell population.

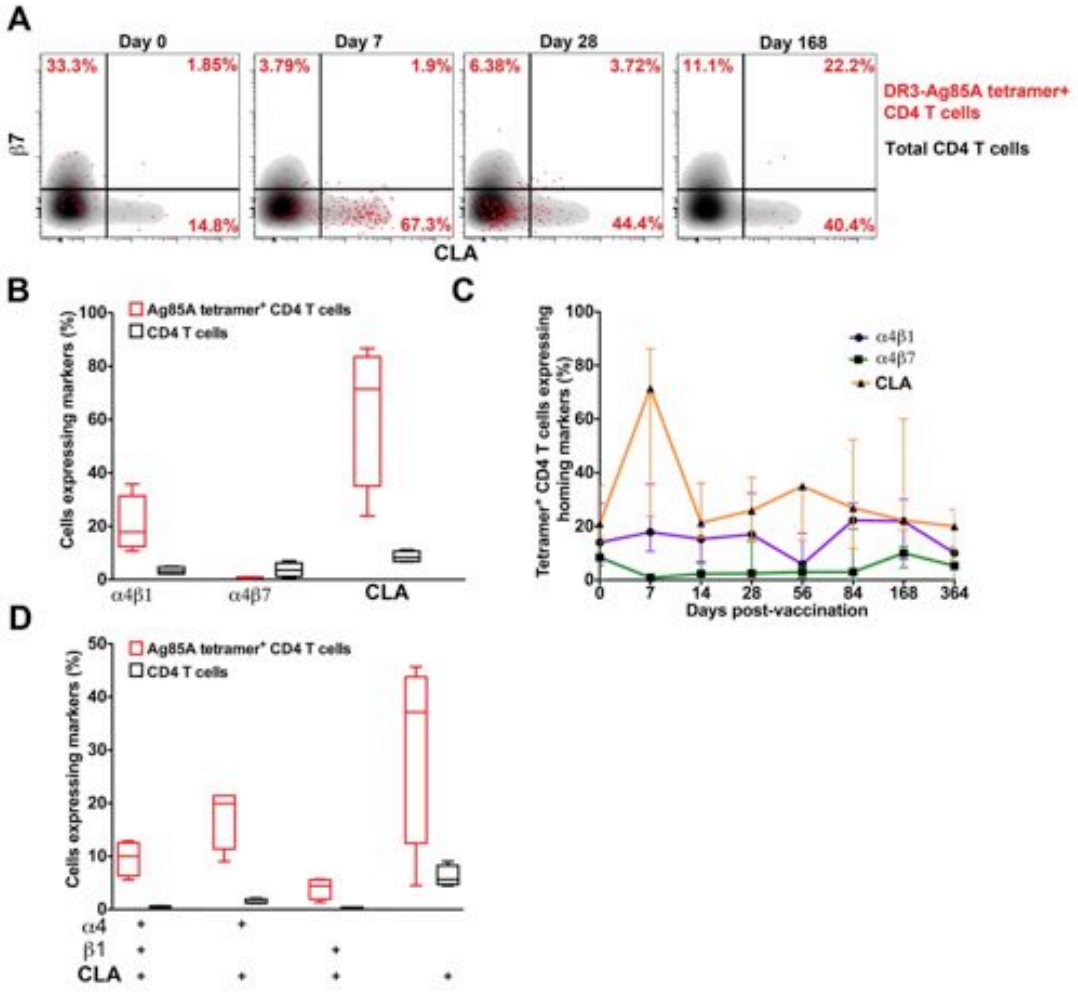

Figure 22: Homing marker expression by Ag85A-specific $CD4^+$ T cells. (A) The expression of the T-cell homing markers CLA and integrin β7 on DRB1*03:01-$Ag85A_{(56-75)}$ tetramer+ CD4 T cells (red dots) or the total CD4 T cell population (grey background) before or after MVA85A vaccination is shown for a single individual. Red numbers indicate proportions of DRB1*03:01-$Ag85A_{(56-75)}$ tetramer+ CD4 T cells in each quadrant. (B) The expression of α4β1, α4β7 and CLA on DRB1*03:01-$Ag85A_{(56-75)}$ tetramer+ CD4 T cells, and the total CD4 T cell population, in 7 HLA-DRB1*03:01-bearing individuals 7 days after MVA85A-vaccination is shown. Horizontal lines represent the medians; boxes the inter-quartile range (IQR) and whiskers represent the range. (C) Longitudinal homing marker expression by DRB1*03:01-$Ag85A_{(56-75)}$ tetramer+ CD4 T cells in the 7 MVA85A recipients, before and up to 1 year after MVA85A vaccination. Lines represent medians and error bars represent the IQR. (D) Co-expression of α4β1, α4 or β1 by CLA^+ DRB1*03:01-$Ag85A_{(56-75)}$ $tetramer^+$ CD4 T cells, in the 7 MVA85A recipients 7 days after MVA85A-vaccination.

3.4.6. MVA85A-induced CD4 T cells display an effector phenotype

Vaccines that protect for decades, such as smallpox, induce a long-lived memory T-cell response (Esser et al. 2003; Crotty et al. 2003; J. D. Miller et al. 2008; Akondy et al. 2009). Such long-lived central memory (T_{CM}) CD4 cells, which home to lymph nodes by virtue of high CCR7 expression, produce

mostly IL-2 and possess greater proliferative potential compared with effector (T_E) or effector memory (T_{EM}) CD4 cells (Wrammert et al. 2009; Sallusto et al. 1999). The latter subsets migrate to sites of infection and predominantly express effector molecules, such as IFN-γ (Wrammert et al. 2009; Sallusto et al. 1999).

To characterise the memory phenotype of MVA85A-induced T cells, we measured expression of CD45RA, CCR7 and CD27 on DRB1*0301-Ag85A$_{(56-75)}$ tetramer+ CD4 T cells (Figure 24). The gating strategy utilised to discern T cell memory populations is shown below in Figure 23.

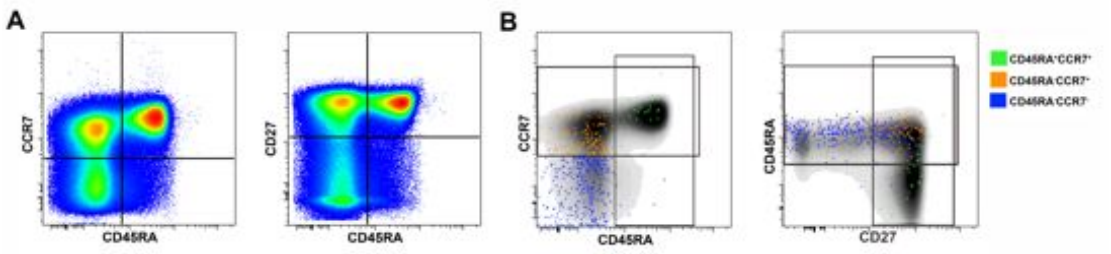

Figure 23: Flow cytometric gating strategy of CD4 T cell memory populations. (A) Representative flow cytometry plots showing CD4 T cell co-expression of the memory markers CD45RA, CCR7 and CD27. (B)Representative flow cytometry plots showing the boolean gating strategy used to identify memory populations. Expression of CD45RA, CCR7 and CD27 on DRB1*03:01-Ag85A$_{(56-75)}$ tetramer+ CD4 T cell subsets (coloured dots) overlayed on the total CD4 T cell population (grey background) are shown.

Ag85A-specific CD4 T cells detected before MVA85A vaccination predominantly displayed either a CD45RA+CCR7+CD27+ phenotype, typical of naïve T cells (Wrammert et al. 2009; Sallusto et al. 1999), and thus termed "naïve-like" T cells, or a CD45RA$^-$CCR7$^+$CD27$^+$ T_{CM} phenotype (Figure 24A and B). During the acute post-vaccination response, when Ag85A-specific CD4 T cells were highly activated (Figure 20B), these cells predominantly displayed a CD45RA−CCR7−CD27− effector phenotype (Figure 24B and C). As this effector response waned, DRB1*03:01-Ag85A$_{(56-75)}$ tetramer+ CD4 T cells reverted to displaying either the CD45RA+CCR7+CD27+ (Figure 24B and D) or CD45RA−CCR7+CD27+ T_{CM} (Figure 24B and E) phenotype, which predominated before vaccination.

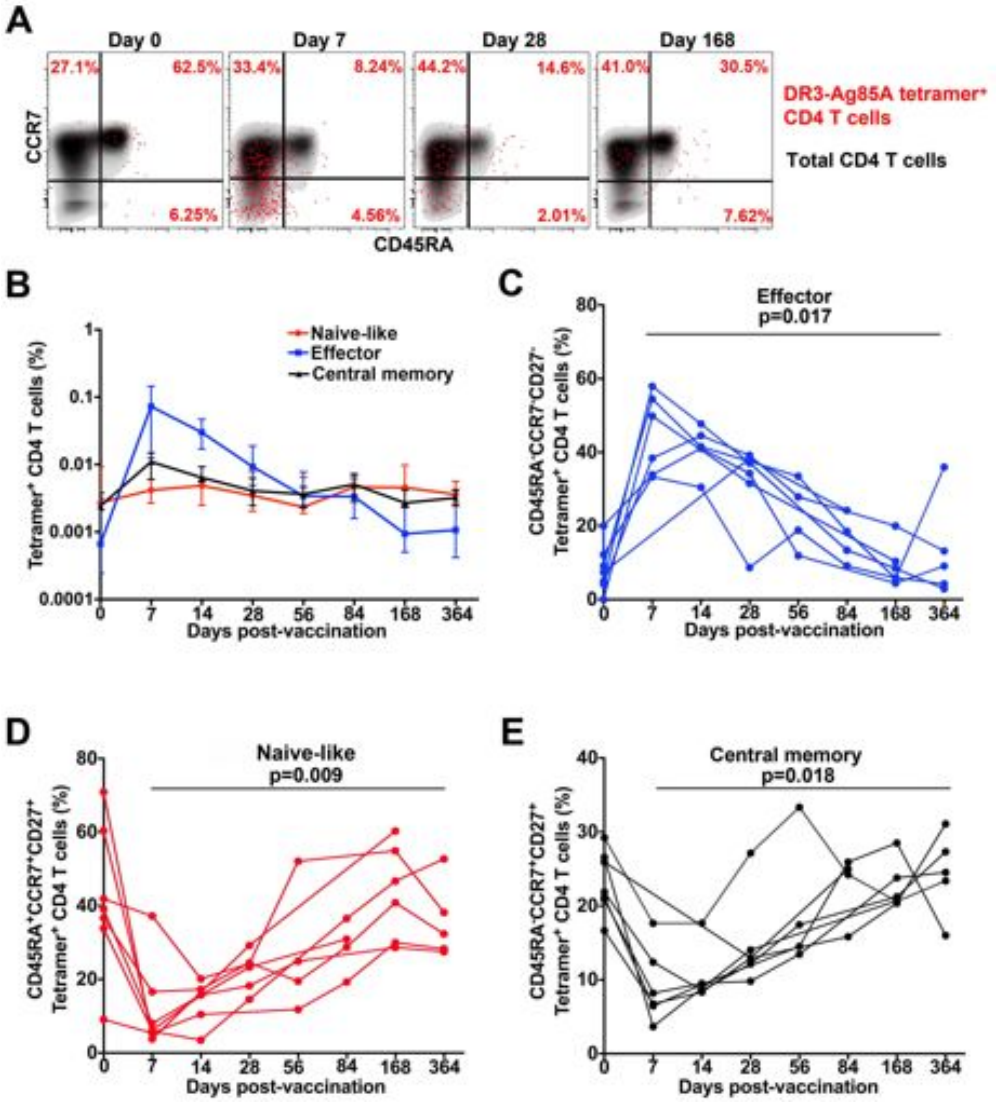

Figure 24: Memory phenotype of Ag85A-specific CD4 T cells. (A) Longitudinal changes in expression of CD45RA and CCR7 by DRB1*03:01-Ag85A$_{(56-75)}$ tetramer+ CD4 T cells (red dots) or the total CD4 T-cell population (grey background) before or after MVA85A vaccination (n=7). Red numbers indicate relative proportions of DRB1*03:01-Ag85A$_{(56-75)}$ tetramer+ CD4 T cells in each quadrant. (B) Kinetic changes in frequencies of DR3-Ag85A tetramer+ CD4 T cells expressing an effector phenotype (CD45RA–CCR7–CD27–), a "naive-like phenotype (CD45RA+CCR7+CD27+) or a central memory phenotype (CD45RA–CCR7+CD27+) at the indicated time points after MVA85A vaccination. Data are shown as median and IQR of the 7 donors. (C-E) Kinetic changes in the proportions of DRB1*03:01-Ag85A$_{(56-75)}$ tetramer+ CD4 T cells expressing (C) an effector phenotype (CD45RA–CCR7–CD27–), (D) a "naive-like" phenotype (CD45RA+CCR7+CD27+) or (E) a central memory phenotype (CD45RA–CCR7+CD27+) are shown. P-values were calculated using the Wilcoxon matched pairs test.

3.4.7. Increased proliferation and IL-2 expression of Ag85A-specific memory $CD4^+$ T cells post-vaccination.

To determine whether the phenotypes of pre- and post-vaccination Ag85-specific CD4 T cells were associated with differential T-cell proliferative capacity, we measured *in vitro* proliferation in response to Ag85A peptides before and up to 1 year after MVA85A vaccination (Figure 25A and B). Pre-vaccination proliferation of Ag85A-specific CD4 T cells was very low. Upon vaccination, Ag85A-specific *in vitro* proliferation of CD4 T cells increased gradually and peaked between 28 and 168 days post-vaccination. Frequencies of proliferating specific CD4 T cells remained above pre-vaccination levels up to 12 months post-vaccination (Figure 25B and C).

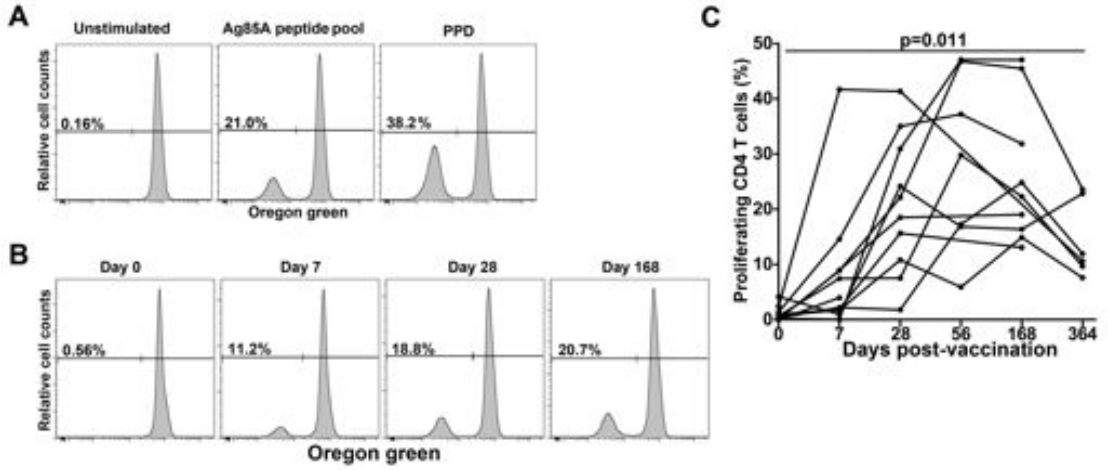

Figure 25: Lymphoproliferation of Ag85A-specific $CD4^+$ T cells before and after MVA85A vaccination. PBMCs from MVA85A-vaccinated adolescents were stimulated with Ag85A peptide pool, PPD or left unstimulated for 6 days. Proliferation was measured by dye dilution of Oregon Green. (A) Flow cytometry plots of specific $CD4^+$ T-cell proliferation from a representative donor, 28 days after MVA85A vaccination are shown. Numbers indicate proportions of Oregon $Green^{low}$, proliferating CD4 T cells. (B) Ag85A-specific CD4 T cell proliferation before and after MVA85A vaccination, from a representative adolescent. (C) Longitudinal kinetics of Ag85A-specific CD4 T cell proliferation before and after MVA85A vaccination in 10 adolescents are shown.

CD4 T cells that preferentially express IFN-γ generally have lower proliferative capacity, while predominant IL-2 expression is associated with greater proliferation (Sallusto et al. 2000; Harari et al. 2004). To further characterise the function of MVA85A-induced memory cells, we measured the relative proportions of Ag85A-specific CD4 T cells expressing IFN-γ and/or IL-2 at 7, 28 and 168 days after MVA85A vaccination (Figure 26A). Ag85A-specific CD4

T cells at the pre-vaccination time point were too infrequent to analyse relative proportions of cytokine-expressing cells definitively (see methods). The acute response, 7 days post-vaccination, was characterised by similar proportions of CD4 T cells expressing IL-2 and/or IFN-γ. The waning of T_E cells after the peak response was associated with increasing proportions of Ag85A-specific IL-2-expressing cells and decreasing proportions of IFN-γ-expressing cells (Figure 26A and B). However, most antigen-specific CD4 T cells co-expressed IFN-γ and IL-2 (Figure 26A).

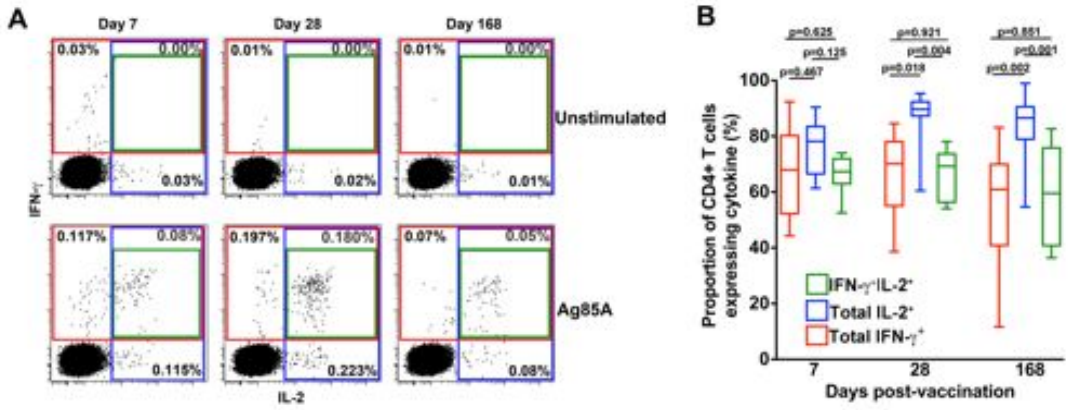

Figure 26: Vaccine induced CD4 T cell cytokine responses as measured by flow cytometry, in 12 adolescents. (A) Representative plots of IFN-γ and IL-2 expression by unstimulated or Ag85A peptide pool stimulated CD4 T cells, at the indicated time points after MVA85A vaccination. The red gate indicates IFN-γ-expressing $CD4^+$ T cells; the blue gate indicates IL-2-expressing CD4 T cells while the green gate indicates co-expression of both cytokines. Numbers indicate the frequencies of $CD4^+$ T cells falling into these gates. (B) The relative proportions of total Ag85A-specific $cytokine^+$ CD4 T cells expressing total IFN-γ (red) or total IL-2 (blue) or both cytokines (green), at the indicated time points after MVA85A vaccination in 12 participants are shown as median, IQR (box) and range (whiskers). P-values were calculated using the Wilcoxon matched pairs test.

3.5.Discussion

We characterised antigen-specific CD4 T cell response induced by MVA85A boost vaccination in adults, adolescents and children from a TB endemic setting, where BCG is routinely administered at birth. It is not known which characteristics of the T-cell response may mediate superior protection against TB than those primed by BCG or natural infection (Kaufmann & McMichael 2005; Walzl et al. 2011). We proposed that a boost vaccine should induce long-lived modifications to the functional and/or phenotypic characteristics of pre-existing mycobacteria-specific T cell.

We showed that Ag85A-specific CD4 T cells predominantly co-expressed IFN-γ and IL-2, skin homing integrins and activation markers during the effector response, which was short-lived. Contraction of the immune response was marked by a transition to predominantly IL-2-expressing, CD45RA-CCR7+CD27+ or CD45RA+CCR7+CD27+ specific CD4 T cells.

The proportion of Ag85A-specific CD4 T cells bearing effector or central memory phenotypes was similar before and one year after vaccination, but functional differences could be shown: Ag85A-specific CD4 T cell proliferative capacity was markedly higher 6-12 months after MVA85A than before vaccination, highlighting discordance between proliferative function and memory phenotype.

The short duration of Ag85A-specific CD4 T cell activation observed during the acute response to MVA85A was not surprising. Given the replication-deficient nature of the MVA vector (Sutter & Moss 1992), the presence of antigen is likely to be very short-lived. The kinetics of this effector response are consistent with those reported for vaccination with live, rapidly cleared smallpox and yellow fever vaccines (J. D. Miller et al. 2008). Predictably, the duration of CLA expression by these effector cells also reflected the short-lived nature and location of the inflammatory response, which typically resolves within 7 days of vaccination and presents as redness and swelling at the intradermal injection site (Scriba et al. 2010; Hawkridge et al. 2008). Only a small proportion of DRB1*03:01-Ag85A$_{(56-75)}$-specific T cells expressed $\alpha4\beta1$, while $\alpha4\beta7$ expression was negligible. We found that the homing markers CLA, $\alpha4$ and $\beta1$ were co-expressed on Ag85A-specific CD4$^+$ T cells

during the acute response. The majority of previous studies have reported distinct expression patterns of these markers, implying that specific T cells possess homing potential to a single tissue site only Kantele et al. 1999; D. J. Campbell & Butcher 2002; Walrath & Silver 2010; J. A. Burns et al. 2001). One study reported a similar finding in mice and humans, showing transient co-expression of CLA, and $\alpha 4\beta 7$ (Masopust et al. 2010). Whether cells co-expressing homing markers may home to multiple sites is possible, but not definitive. These observations suggest that expression of homing markers may be more complex than previously acknowledged, and that studies of T-cell homing should take co-expression of these makers into account, especially whilst inflammation is present at the site of infection or vaccination.

Waning of the MVA85A-induced effector response coincided with a transition to CD45RA-CCR7+CD27+ T_{CM} and CD45RA+CCR7+CD27+ naïve-like phenotypes, which also predominated the Ag85A CD4 T cell response before MVA85A vaccination.

The observed T_{CM} phenotype of Ag85A-specific $CD4^+$ T cells following MVA85A vaccination contradicts our previous finding in adolescents, which showed that antigen-specific T cells predominantly displayed a T_E-cell phenotype up to 2 months post-vaccination (Hanekom et al. 2008; Scriba et al. 2010; Abel et al. 2010; Soares et al. 2008). This discrepancy is likely due to the different assays employed to detect Ag85A-specific T cells. In our previous study, Ag85A-specific T cells were identified as cytokine-expressing CD4 T cells following 12 hours of *in vitro* re-stimulation with Ag85A peptides (Tameris et al. 2013; Scriba et al. 2010). Short-term *in vitro* T-cell stimulation has been shown to alter expression of certain phenotypic markers (Chao et al. 1997; Vallejo et al. 1999; Fritsch et al. 2005), and may be a potential confounder in our peripheral blood measurements. By contrast, *ex vivo* detection of specific T cells by HLA tetramers offers more accurate measurement of T-cell phenotype, since it does not rely on T-cell activation. Regardless, our current data of Ag85A-specific T-cell phenotype, cytokine expression and proliferative potential following MVA85A vaccination support the well-described differences in function between T_E and T_{CM} cells Sallusto et al. 1999; Sallusto et al. 2000; Harari et al. 2004).

Whether long-lived memory cells with excellent proliferative potential, rather than effector functions, may confer better protection against TB is not known. A gradual loss of BCG-induced T cells through attrition has been mooted as an underlying reason for the waning of BCG-induced protection against TB observed during adolescence (Orme 2010). Long-lived T_{CM} responses can provide protection for decades as illustrated by successful prophylactic vaccines, such as those against tetanus toxoid (Cellerai et al. 2007), yellow fever (J. D. Miller et al. 2008) and smallpox (J. D. Miller et al. 2008). The high proliferative potential observed up to 1 year after MVA85A vaccination may thus reflect an ability to rapidly generate large numbers of specific effector cells upon infection, which may improve longevity of anti-mycobacterial immunity. Such longevity is further supported by our finding that elevated frequencies of Ag85A-specific CD4 T cells persist up to 5 years after MVA85A vaccination, even in infants (Tameris et al. 2014). However, no evidence for efficacy against TB disease or *M.tb* infection was observed in infants after MVA85A vaccination in a recent phase IIb trial (Tameris et al. 2013). It is not known why MVA85A failed to confer protection over and above newborn BCG vaccination in this infant trial, or whether MVA85A would be more efficacious in the older populations studied here, who have greater frequencies of Ag85A-specific responses before and after MVA85A vaccination than infants (Scriba et al. 2011). The possible reasons underlying the observed lack of efficacy in infants, which may include route and/or age of administration, dose of the vaccine, the high rate of *M.tb* transmission in the trial population, or the magnitude, function and/or phenotype of the induced immune response, have been discussed in detail (Tameris et al. 2013; Dye & Fine 2013).

Induction and maintenance of a persistent, specific T_{EM} response, by chronic antigen stimulation, has also been suggested as an effective strategy against chronic infections (Hansen et al. 2011), including *M.tb*. The partially protective effect of BCG vaccination against *M.tb* challenge in mouse models may support this: BCG persists and replicates in mice (Mittrucker et al. 2007) and thus maintains a consistent population of T_{EM} cells (Kaveh et al. 2011). The reason for a more protective response may be the preferential homing of T_{EM} cells to peripheral sites of inflammation, such as the lung. This is supported by

results from murine vaccination with a recombinant BCG vaccine that expresses the membrane-perforating listeriolysin and is devoid of the urease C gene (Desel et al. 2011). This vaccine was shown to recruit more antigen-specific cells to the lung and enhance protection against *M.tb* than parental BCG. Regardless, studies are needed to determine which phenotypic and/or functional attributes of T-cell responses induced by BCG and novel vaccine candidates may be associated with long-lived protection in humans.

We decided to focus on vaccine-induced antigen-specific CD4 T cell responses because previous studies showed that MVA85A induced low or undetectable Ag85A-specific CD8 T cell responses (Scriba et al. 2010; Scriba et al. 2011). Other prime-boost strategies, such as those employing recombinant BCG or adenoviral Aeras402 (Hoft et al. 2012; Abel et al. 2010), did induce antigen-specific CD8 T-cell responses.

Substantial proportions of mycobacteria-specific CD45RA+CCR7+CD27+ or CD45RA+CCR7+ naïve-like CD4 T cells have been reported in multiple studies (Soares et al. 2008; Tena-Coki et al. 2010; Kagina et al. 2009; Caccamo et al. 2006), but have not been characterised. BCG-specific naïve-like CD4 T cells expressed cytokines in response to antigen stimulation (Soares et al. 2008; Tena-Coki et al. 2010; Kagina et al. 2009) and were present at frequencies considerably greater than those described for pathogen-specific naïve T cells (Geiger et al. 2009; Kwok et al. 2012). Additional studies are required to delineate the functional attributes of naïve-like CD4 T cells and how they fit into the ontology of T-cell differentiation. We further characterise these naïve-like CD4 T cells in Chapter 5.

A limitation of our study was that our analyses were confined to T cells circulating in the peripheral blood. It is likely that, early after vaccination, most antigen-specific T cells traffic to the vaccination site and are thus not circulating in the periphery.

Another limitation of our approach was the use of a single tetramer complexed to a single Ag85A epitope. We cannot rule out that CD4 T cells recognising different Ag85A epitopes may yield different results to the ones reported here.

In conclusion, we report that a prime-boost vaccination strategy against TB in children, adolescents and adults modulates the function of long-lived memory

CD4 cells and endow them with the capacity to proliferate readily upon secondary antigen encounter. Our recent phase IIb trial results suggest that these memory CD4 cells may not be sufficient for protection against TB in infants (Tameris et al. 2013). More studies are needed to explore whether a greater magnitude, a qualitatively different, or a completely new immunological response is needed for protection against TB.

3.6. Contibutions

HLA typing of MVA85A vaccines was performed at the National Institute for Communicable Disease in Johannesburg, South Africa.

Chapter 4: Optimisation of high throughput microfluidic qRT-PCR platform (Fluidigm) and T cell sorting

4.1. Introduction

Next, we aimed to characterise the interesting and novel mycobacteria specific naïve-like CD4 T cells observed in Chapter 3, by comparing mRNA expression with those of naïve, central memory, effector T cells as well as other *M.tb*-specific CD4 T memory cell populations.

Gene expression profiling of cells has given us the ability to simultaneously investigate many cell characteristics, which uniquely define and identify cell subsets (Bedognetti et al. 2010). Measurement of only a few markers, though informative, may underestimate complexity and limit understanding of the roles of specific T cells. This is exemplified by the initial reports that T helper (Th) cell subsets fell into 2 subsets only, Th1 and Th2 (Mosmann & Coffman 1989). Due to technological advancements, it is now known that measurement of a handful of phenotypic and functional markers may not be sufficient to define the great complexity in Th cells subsets especially in the context of immune interactions with *M.tb*. The scientific community is showing a strong drive to delve deeper into intricate signalling pathways, gene expression profiles and regulation thereof in disease or after vaccination. Until very recently, DNA microarrays were the best tools to interrogate expression of a large number of genes. However, this method has been historically hindered by a requirement for large numbers of cells or input material.

The development of high throughput qRT-PCR has revolutionised the capability to study cells at a transcriptional level. The BioMark microfluidic qRT-PCR platform (Fluidigm) allows simultaneous quantification of 96 mRNA transcripts in 96 samples in a single chip. By combining the sensitivity and dynamic range of single cell qRT-PCR with the multiplexing of microarrays, BioMark technology overcomes the need for large amounts of starting material. With a PCR reaction volume of 3nL, this platform facilitates analyses of transcriptional profiles using very little starting material, even down to single cells. When combined with the ability to sort rare populations of antigen-

specific cells, this technology provides an invaluable tool for scrutiny of transcriptional complexity amongst T cell subsets. This novel platform has been used disparately and, until recently, no optimal and quantitative application of this technology had been detailed (Flatz et al. 2011). A recent study was the first to publish rigorous methodology to assess quantitative application of this technique to measure gene expression in small cell populations (Dominguez et al. 2013).

In this chapter, we set out to develop and optimise methodology for quantification and comparison of mRNA expression patterns amongst different subsets of antigen-specific T cell memory populations, sorted by FACS. Quantification of mRNA depends on accurate, reliable and linear measurement of each transcript, necessitating qualification of each set of primers and probes required to detect specific gene transcripts.

4.2. Aims

To analyse the transcriptional profile of T cell memory subsets, including the newly described naïve-like CD4 T cells, antigen-specific T cells had to be sorted according to expression patterns of established memory surface markers. We also sought to optimise conditions required for qRT-PCR assays, and to qualify the Taqman primer/probe sets used in BioMark Fluidigm technology. Finally, determining the minimum number of cells required to yield reliable detection of gene transcripts, given our limited input material, was essential.

To establish methods for mRNA expression profiling in sorted antigen-specific cells, we had to:

i) Select genes for transcriptional profiling of T cells
ii) Qualify and validate the primer/probes for detection of selected genes
iii) Optimise simultaneous and efficient sorting of four distinct CD4 T cell populations
iv) Sort different T cell numbers and determine the reliability of gene transcript detection
v) Determine if HLA class II tetramer binding of antigen-specific T cells results in mRNA transcript expression changes

4.3. Materials and methods

The work in this chapter was performed by the candidate unless otherwise stated.

4.3.1. Gene selection

We aimed to determine if *M.tb*-specific naïve-like CD4 T cells, which shared a memory phenotype profile with naïve CD4 T cells, had a transcriptional profile distinct from truly naïve CD4 T cells, effector and central memory CD4 T cells. We therefore selected genes to quantify mRNA expression by genes that differentiate naïve, effector and central memory CD4 T cells from each other, based on published literature. In-depth criteria for gene selection are described in section 4.4.1 of this chapter.

4.3.2. PBMC stimulation and RNA extraction for primer/probe qualification

PBMCs from healthy donors were thawed into 10mL of 10%AB+/RPMI media containing DNase (50U/mL). Cells were spun down at 596g for 10 minutes and then washed once by re-suspending in 10mL of PBS. Cells were spun at 596g for 10 minutes and then re-suspended into 10%AB+/RPMI media. A vial of 10 million PBMCs was split into 2 aliquots, one aliquot was left unstimulated and the second aliquot was stimulated with PHA (10µg/mL) for 5 hours at 37°C in a 5% CO_2 incubator. Cell aliquots were then combined at the end of the stimulation and RNA was extracted using the Qiagen RNeasy Plus kit following the manufacturers' protocol (Qiagen).

4.3.3. Primer/probe qualification

RNA extracted from the combined, unstimulated and stimulated cells was diluted in a 12-point two-fold serial dilution ranging from a concentration of 80ng/mL to 0.02ng/mL. Each dilution series was loaded in 8 replicate wells across a 96 well plate. RNA was reverse transcribed to cDNA using the First strand cDNA synthesis kit following the manufacturers' protocol (Invitrogen). cDNA synthesis was then confirmed as described below in section 4.3.4., at random from a few dilutions on the plates. The cDNA was then loaded onto a Fluidigm 96.96 gene expression chip and run as described below. Threshold expression (Et) values are used as they are the reciprocal of the Ct values, and this eases interpretation of data, as a high value is high mRNA transcript

levels. The raw Et (40-Ct) values were then plotted against RNA input and the slope of the line as well as the correlation coefficient determination (R^2), were calculated across any 5 or more points, using R version 3.0.1 according to the method published by Dominguez et al (Dominguez et al. 2013).

4.3.4. cDNA synthesis and amplification for qRT-PCR from low cell numbers

The CellsDirect One-Step qRT-PCR kit (Invitrogen) was used. This kit is ideal for gene expression analysis in a single cell and up to 10000 cells per reaction (Fox et al. 2012; Dominguez et al. 2013). T cell populations were sorted directly into 9µL of the Reverse Transcribe Specific Target Amplification (RT-STA) mix that contained the reagents in Table 22.

Table 22: RT-STA mix (CellsDirect One-step qRT-PCR kit).

Reagent	Per reaction volume
CellsDirect 2x reaction mix	5µL
Superscript III RT/Platinum Taq mix	0.5µL
0.2x primer/probe mix	2.5µL
DNA suspension buffer	1µL
Total	9µL

Polymerase chain reaction (PCR) tubes containing the RT-STA mix and cells were placed in a thermal cycler and following thermal profile in Table 23 was used for the reverse transcriptase (RT) reaction, followed by an 18 cycle pre-amplification step. The pre-amplification step is required to increase the level of mRNA transcripts of genes of interest without bias, as all 96 primer probes are included. Because the sample is split 96 ways in the microfluidic chip, pre-amplification is performed to ensure even distribution of rare template across the 96 reactions.

Table 23: Reverse transcription and pre-amplification thermal cycling protocol.

	RT	Taq activation	Specific target Amplification (18 cycles)	
Temperature	50°C	95°C	95°C	60°C
Time	20 minutes	2 minutes	15 seconds	4 minutes

Upon completion of the thermal cycling, the cDNA was diluted with 40µl of molecular biology grade water to dilute out the primer/probes used for pre-amplification to very low levels (1:5 dilution). Dilution of cDNA was performed

to drastically reduce the probability of non-specific amplification of particular transcripts due to remaining primer/probes from the pre-amplification step. To confirm successful reverse transcription to cDNA and pre-amplification, a PCR with a single primer was performed to detect PCR product. The following reagents, Table 24 below, and thermal cycling protocol was used according to the TaqMan protocol (Table 25).

Table 24: Reagents for confirmation of successful cDNA synthesis and pre-amplification.

Reagent	Per reaction volume
TaqMan Universal PCR master mix (Applied Biosciences)	10µL
20x TaqMan gene expression assay	1µL
Pre-amplified cDNA (1:5 dilution, from above)	4µL
Water	5µL
Total	20µL

Table 25: Thermal cycling profiling for conventional PCR on Rotorgene light cycler following the TaqMan gene expression assay protocol.

	Initial Setup		Denature	Anneal/Extend
	HOLD	HOLD	40 Cycles	
Temperature	50°C	95°C	95°C	60°C
Time	2 minutes	10 minutes	15 seconds	1 minutes

Once cDNA pre-amplification was confirmed, cDNA samples were mixed with the reagents listed below (Table 26) and 5µL of the sample mix was loaded into each sample well of the Fluidigm 96.96 gene expression chip. The single primer/probes were also mixed with the assay reagents (Table 27) and 5µL was loaded into each assay well on the Fluidigm 96.96 gene expression chip, shown in Figure 27.

Table 26: Sample preparation for Fluidigm 96.96 gene expression chip run

Reagent	Per sample volume
TaqMan universal PCR master mix	5.55µL
DA sample loading reagent (Fluidigm)	0.55µL
cDNA sample	5µL
Total	11.1µL

Table 27: Assay preparation for Fluidigm 96.96 gene expression chip run

Reagent	Per sample volume
20x TaqMan gene expression	5.55µL
DA sample loading reagent (Fluidigm)	0.55µL
cDNA sample	5µL
Total	11.1µL

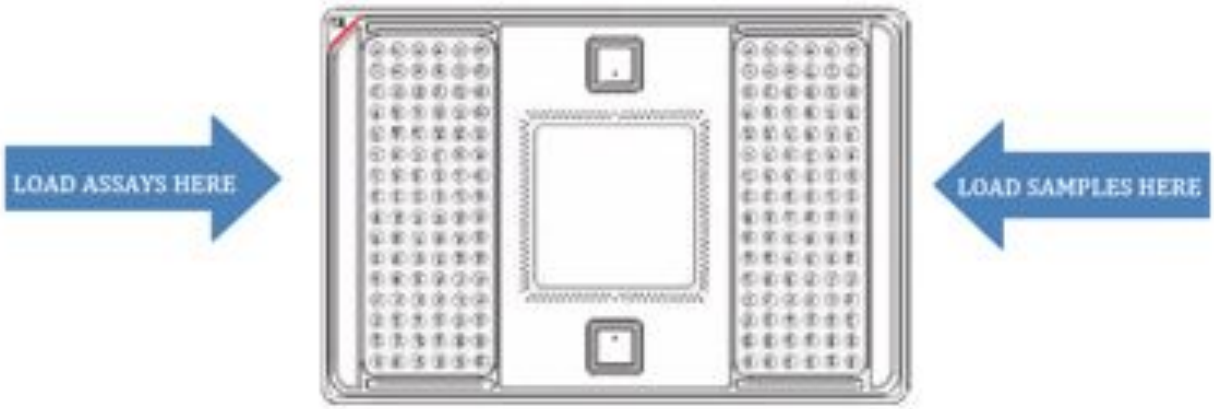

Figure 27: The Fluidigm 96.96 gene expression chip layout demonstrating where the samples and assays are loaded. The single primer probes in assay reagent are loaded on the left of the chip and the pre-amplified cDNA samples in sample reagent are loaded into the wells on the right.

4.3.5 Selection of candidate primer/probes for qualification

The following primer/probes were selected as candidates for qualification based on their ability to discriminate between T cell memory subsets. Those that qualified, as described in section 4.4.2 of this chapter, were then selected to address our aims.

Table 28: The 109 primer/probe assays included in qualification experiments.

Gene	Applied biosystems™ assay
ARGHEF	Hs00248726_m1
AXIN	Hs00610344_m1
BCL2	Hs00608023_m1
BCL2L11	Hs00708019_s1
BTLA	Hs00699198_m1
CAMK4	Hs00174518_m1
CCR2	Hs01560352_m1
CCR5	Hs00152917_m1
CCR6	Hs01890706_s1
CCR7	Hs01013469_m1
CCR9	Hs01890924_s1
CD137	Hs00155512_m1
CD154	Hs00163934_m1
CD27	Hs00386811_m1
CD28	Hs00174796_m1
CD38	Hs01120071_m1
CD4	Hs01058407_m1
CD69	Hs00934033_m1
CD8A	Hs00233520_m1
CTLA4	Hs03044418_m1
CXCL10	Hs01124251_g1
CXCR3	Hs01847760_s1
CXCR6	Hs00174843_m1
EPHA4	Hs00177874_m1
FAS	Hs00236330_m1
FOXO3A	Hs00818121_m1
FOXP3	Hs01085834_m1
GATA3	Hs00231122_m1
GNLY	Hs00246266_m1
GZMA	Hs00989184_m1
GZMB	Hs01554355_m1
GZMK	Hs00157878_m1
ICOS	Hs00359999_m1
IFNGR1	Hs00988304_m1
IL-10	Hs00961622_m1
IL12RB2	Hs01548202_m1
IL2RA	Hs00907779_m1
IL2RB	Hs01081697_m1
IL2RG	Hs00953624_m1
IL6	Hs00985639_m1
IL7R	Hs00902334_m1
ITGAX	Hs01015070_m1
ITK	Hs00960634_m1
JNK	Hs00177083_m1
KI67	Hs01032443_m1
LEF1	Hs01547250_m1
LTB	Hs00242737_m1
MAN1C1	Hs00220595_m1
NFKB1	Hs00765730_m1
NR3C1	Hs00966655_m1
PTPRK	Hs00267788_m1
NRCAM	Hs01031598_m1
PPIBP2	Hs00900559_m1

Gene	Applied biosystems™ assay
STAT4	Hs01028017_m1
STAT5A	Hs00234181_m1
STAT5B	Hs00273500_m1
STAT6	Hs00598625_m1
TBX21	Hs00894392_m1
TCF3	Hs00413032_m1
TCF7	Hs00175273_m1
TCF7L2	Hs01009044_m1
TFRC	Hs00951083_m1
TGFB1	Hs00998133_m1
CD31	Hs00169777_m1
BETA CATENIN	Hs00355049_m1
CD44	Hs01075861_m1
B2M	Hs00984230_m1
HPRT	Hs01003267_m1
G6PD	Hs00166169_m1
GAPDH	Hs02758991_g1
Glob	Hs00361202_s1
GPR15	Hs00922903_s1
CCL5	Hs00174575_m1
ENTPD1	Hs00969559_m1
TIMD4	Hs00293316_m1
FCER1G	Hs00175408_m1
IGF1R	Hs00609566_m1
FAM129A	Hs00223000_m1
PRR5L	Hs01029928_m1
CCR4	Hs00747615_s1
GFPT2	Hs01049561_m1
BAG-1	Hs00185390_m1
JUNB	Hs00357891_s1
PLA2	Hs00185926_m1
IFNG	Hs00989291_m1
IL-2	Hs00174114_m1
TNF-a	Hs01113624_g1
CD200	Hs01033303_m1
IL4	Hs00929862_m1
PDCD1	Hs01550088_m1
PRF1	Hs00169473_m1
PRKCA	Hs00925195_m1
PTPRC	Hs00365634_g1
RHOH	Hs00180265_m1
RORA	Hs00536545_m1
RORC	Hs01076112_m1
SELL	Hs00174151_m1
SOCS1	Hs00705164_s1
STAT1	Hs01013996_m1
STAT3	Hs01047580_m1
RBM11	Hs00376405_m1
MEST	Hs00602654_m1
DSC1	Hs00245189_m1
MYB	Hs00920556_m1
AUTS2	Hs01688766_m1
PTPRM	Hs00267809_m1
FOS	Hs04194186_s1

4.3.6. Flow cytometer configuration

A BD FACS Aria II flow cytometer was utilised for sorting T cell memory populations for microfluidic qRT-PCR. Optimal voltages were determined for each fluorochrome and for each detector to ensure optimal resolution of stained cell populations. A quality assurance routine was set up to monitor and ensure consistent and optimal functioning of the instrument and was maintained over the period of use, and to ensure consistent and reproducible measurements. Cytometer setup and tracking (BD Biosciences) beads that fluoresce in each channel at a predetermined median fluorescence intensity (MFI) were run daily to ensure target MFI and signal CVs are maintained (Perfetto et al. 2012). Photomultiplier tube (PMT) voltages were adjusted daily to ensure that consistent MFIs were maintained, using Rainbow fluorescent particle (Spherotech) beads. Compensation beads were also acquired daily before acquisition of samples, to allow pre-acquisition compensation. Shown below in Figure 28, are the mirror and filter configurations used on the BD FACS Aria II flow cytometer.

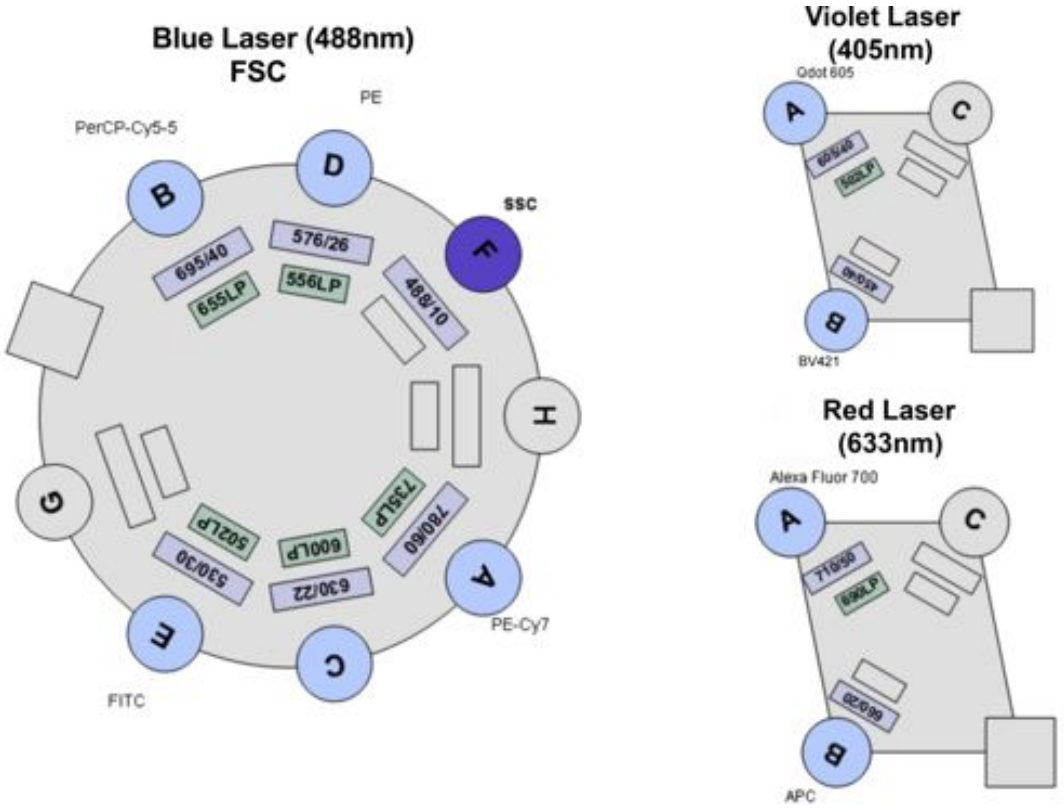

Figure 28: Filter and mirror configuration for each laser of the BD FACS Aria II flow cytometer. The dichroic mirrors are shown in green and the band pass filters in lilac.

4.3.7. Antibodies

Fluorescence-conjugated antibody panels utilised for cell sorting experiments are shown in Table 29. Panels were optimised as described in Chapter 2 section 2.3.13.

Table 29: Panel of fluorochrome-conjugated antibodies and HLA class II tetramer used for cell sorting studies.

Marker	Clone	Manufacturer	Fluorochrome	Volume/concentration used (in 100µL final staining volume)
CD14 (dump)	M5E2	Biolegend	Brilliant Violet 421	0.5µL
CD19 (dump)	HIB19	BD Biosciences	Brilliant Violet 421	0.25µL
CD8 (dump)	RPA-T8	BD Biosciences	Brilliant Violet 421	0.5µL
CD335 (dump)	9E2	Biolegend	Brilliant Violet 421	0.5µL
Live/dead (dump)		Invitrogen	ViViD	0.5µg/mL
CD4	S3.5	Invitrogen	Quantum Dot 605	0.5µL
CD95	DX2	Biolegend	APC	1.25µL
CD3	UCHT1	BD Biosciences	Alexa Fluor 700	1µL
CD27	M-T271	BD Biosciences	FITC	1.25µL
Tetramer		NIH tetramer core facility	PE	2µg/mL
CCR7	150503	BD Biosciences	PerCP Cy5.5	1.25µL
CD45RA	HI100	eBiosciences	PECy7	0.05µL

The markers CD14, CD19, CD335 and CD8 were all conjugated to the same fluorescent molecule to exclude them from analysis, this is known as a dump channel. This channel is also used for the live/dead, to exclude dead cells.

4.3.8. Four-way sorting of CD4 T cell populations

PBMC were stained with the memory phenotype antibody panel in Table 8 (except tetramer). Tube adaptors were evaluated for their capacity to capture single cells being sorted into collection tubes of varied sizes. We sorted bulk naïve CD4 T cells (CD45RA+CCR7+CD27+), effector CD4 T cells (CD45RA-CCR7-CD27-/+), central memory CD4 T cells (CD45RA-CCR7+CD27+) and $CD3^{+}CD8^{-}CD4^{-}$ T cells.

4.3.9. Sorting of different cell numbers

PBMC were stained with the memory phenotype antibody panel in Table 8 (except tetramer). Twenty-five and 50 cells from each cell population were sorted directly into RT-STA mix, containing all 96 selected primer probes. We

sorted bulk naïve CD4 T cells (CD45RA+CCR7+CD27+), effector CD4 T cells (CD45RA-CCR7-CD27-), central memory CD4 T cells (CD45RA-CCR7+CD27+) and CD3+CD8-CD4- T cells. This was replicated numerous times, depending on the experiment.

4.3.10. Tetramer staining for determination of effects on gene expression

PBMCs from healthy donors were thawed into 10mL of 10%AB+/RPMI containing DNase (50U/mL). Cells were spun down at 596g for 10 minutes and then washed once by re-suspending in 10mL of PBS. Cells were spun at 596g for 10 minutes and then re-suspended into 10%AB+/RPMI media. Washed PBMCs were split into 6 aliquots of 2 million PBMC each. Tetramer staining was performed following the protocol described in Chapter 2 section 2.3.12, except that tetramer staining periods were varied as follows: one aliquot was stained with the DRB1*04:01-CFP10$_{(71-85)}$ tetramer for 10 minutes, another for 30 minutes, another for 60 minutes, another for 2 hours and another for 4 hours at RT. The last aliquot was stimulated with PMA (15ng/mL) and Ionomycin (740ng/mL) for 4 hours at 37°C in a 5% CO_2 incubator. Cells were washed once in 2%FCS/PBS after specified periods to stop staining and the rest of the protocol followed. Thirty DRB1*04:01-CFP10$_{(71-85)}$ tetramer+ cells were sorted in triplicate directly into Cellsdirect RT-STA mix for each condition, and then run on the microfluidic qRT-PCR platform as described in section 4.3.4 above.

4.3.11. Data analysis (performed in collaboration with M. Musvosvi, SATVI).

The R^2 of Et (40-Ct) values for the dilution series of cells and efficiency values for qualification of the primer/probe sets were calculated using R v3.0.1, across any 5 or more points, as explained in the results section. Data were expressed as Et values to facilitate intuitive interpretation of results, because high Et values depict high mRNA transcript levels. Et values are therefore the converse of Ct values. The Mann-Whitney test was used to compare different conditions in cell sort efficiency and cell number requirements, using R v3.0.1. In the tetramer stimulation experiment where we wanted to determine the effects of tetramer staining of gene expression, data for all genes was normalised to B2M and delta Ct values were used to calculate fold indices

and p-values. The t-test was used to compare tetramer results in the tetramer stimulation experiment due to the small sample size of sorts (n=3). A Mann Whitney test could not be used as a sample size of greater than 4 is required per condition/sort to utilise this statistical test (De Winter 2013).

4.4. Results

4.4.1. Gene selection

To characterise naïve-like *M.tb*-specific T cells at a transcriptional level, we sought to measure mRNA expression of genes that are differentially expressed between naïve, effector, central memory and T memory stem cells. Genes encoding proteins that are traditionally different between memory subsets, such as functional and effector molecules were selected, as well as genes involved in T cell migration, activation markers, apoptosis, cell signalling, effector molecules and transcription factors. Housekeeper genes, which are genes expressed at highly consistent levels in all cell subsets, were used as reference genes for normalising gene expression data. We selected reference genes (GAPDH, B2M, HPRT, G6PD) based on published literature (de Jonge et al. 2007).

Many publications were considered for gene selection. Furthermore, a recent publication by Gattinoni et al., described the transcriptional profile of CD8 T memory stem cells (T_{SCM}) in humans. The authors published a list of genes that distinguished T_{SCM} from all other memory populations, as well as from truly naïve T cells (Gattinoni et al. 2011). This T memory stem cell population shares a phenotypic profile similar to that of the naïve-like cells we sought to characterise, namely CD45RA+CCR7+CD27+. The fact that the Gattinoni published gene list was derived from CD8 T cell subsets was not ideal as we aimed to study naïve-like CD4 T cells. However, since this was the only published comprehensive set of genes, we reasoned that many of the genes may also apply to differentiation of CD4 T cell memory subsets. We selected genes that highly differentiated truly naïve T cells from T memory stem cells based on fold difference in expression and a significant p-value, as well as from the other memory populations to include in our panels. Genes selected from this publication are shown in Table 30.

Another study, by Appay et al., described cell surface markers that were differentially expressed on CD4 cells as they transitioned from antigen inexperienced, naïve cells to memory cells, and then described genes that were differentially expressed in these subsets (Appay et al. 2007). We also

incorporated genes from their results, which were differentially expressed between naïve cells and cells in an early memory differentiation stage, as well as cells in a late differentiation stage. Genes selected from this publication are shown in Table 30.

There was considerable overlap between genes selected form the Gattinoni et al., and the Appay et al., lists and those selected from other published literature (Lanzavecchia & Sallusto 2005; Sallusto et al. 2004; H. H. Zhang et al. 2010; Seiler et al. 2003; Song et al. 2005; Latta et al. 2007; Guarda et al. 2007; Acosta-Rodriguez et al. 2007; Ahmed & Akondy 2011; Akondy et al. 2009; Baekkevold et al. 2005; Caccamo et al. 2006; Campbell & Butcher 2002; J. J. Campbell et al. 1999; Cui & Kaech 2010; Esser et al. 2003; Gattinoni et al. 2009; Geginat et al. 2001; Hand & Kaech 2009; Harari et al. 2005; Mohan et al. 2005; Rivino et al. 2004; Sallusto et al. 2000; Sallusto et al. 1999). Transcripts that were unique to the Gattinoni et al., and Appay et al., gene lists are shown in Table 30. Many of the genes shown in Table 30 have multiple roles, and were classified according to their functions in T cells.

Table 30:Genes selected according to published gene literature and T cell function

Activation	**Chemokine Receptor**	**Effector Molecules**	**Lineage Markers**
CD154	CCR2	GNLY	CD4
CD38	CCR4	GZMA	CD8A
CD69	CCR5	GZMB	CD45
ICOS	CCR6	GZMK	
KI67	CCR7	PRF1	**Transcription Factor**
TFRC	CCR9	CD160	FOXO3A
	CXCR3		FOXP3
Apoptosis	CXCR6	**Homing/Cell Trafficking**	NFKB1
BCL2		ITGAX	RORA
BCL2L11	**Cytokine Receptor**	SELL	RORC
BTLA	IFNGR1	CD44	RHOH
CD137	IL12RB1	CD31	STAT1
FAS	IL12RB2	B-CATENIN	STAT3
PDCD1	IL2RA	ARHGEF18	STAT4
BID	IL2RB	MCAM	STAT5A
TNFSF10	IL2RG	RASGRF2	STAT5B
	IL7R	CD62L	STAT6
Gattinoni/Appay			TBX21
Glob	**Cytokines/Chemokine**	**Kinases/ receptor Kinase**	TCF3
GPR15	IFNG	CAMK4	TCF7L2
ENTPD1	IL10	EPHA4	TGFB1
FCER1G	IL2	ITK	GATA3
IGF1R	IL4	PRKCA	LEF1
FAM129A	IL6	JNK	TCF7
PRR5L	TNFA	ZAP70	
GFPT2	LTB		**Misc**
BAG-1	IL15	**Housekeeper**	MAN1C1
JUNB	IL17A	B2M	
IPLA2	IL21	G6PD	**Co-stimulatroy molecules**
TIMD4	IL22	GAPDH	CD27
CCL5	CXCL10	HPRT	CD28
	Inhibition		
	CTLA4		
	SOCS1		
	CD200		
	AXIN2		
	PKIA		

4.4.2. Primer/probe qualification

The primer and probe combinations used to detect and quantify mRNA transcripts by qRT-PCR must be qualified to ensure they meet the minimum requirements for quantitative analysis. The efficiency of a primer/probe set relies on its ability to consistently amplify a gene product, doubling the product after each cycle during the logarithmic phase of the amplification reaction. A primer/probe set with a perfect PCR efficiency (100%) would demonstrate a reduction or increase in 3.3 Et values when comparing templates that differ by 1 log (10 fold) in concentration. This efficiency across a 10-fold dilution series

is calculated as the slope (Dominguez et al. 2013). An efficiency between 90% and 110% is considered to be acceptable, corresponding to a slope of 3.1-3.6. Secondly, the signal should be proportionate to the RNA input, a property known as “linearity”, expressed as the R^2 across a dilution series. The R^2 was calculated from the slope, where the logarithm of the RNA input was plotted against the amplification cycles (Et = 40-Ct). To meet linearity requirements, the coefficient of determination (R^2) had to be greater or equal to 0.97 across any 5 consecutive points in the dilution series. Both efficiency and linearity criteria had to be met for a primer/probe to be qualified in any of the 8 replicate dilution series. An example of the dilution series and evaluation of the slope and R^2 value across >5 points is shown in Figure 29. The primer/probe R^2 and slopes for all tested primer/probe sets are represented in Figure 30.

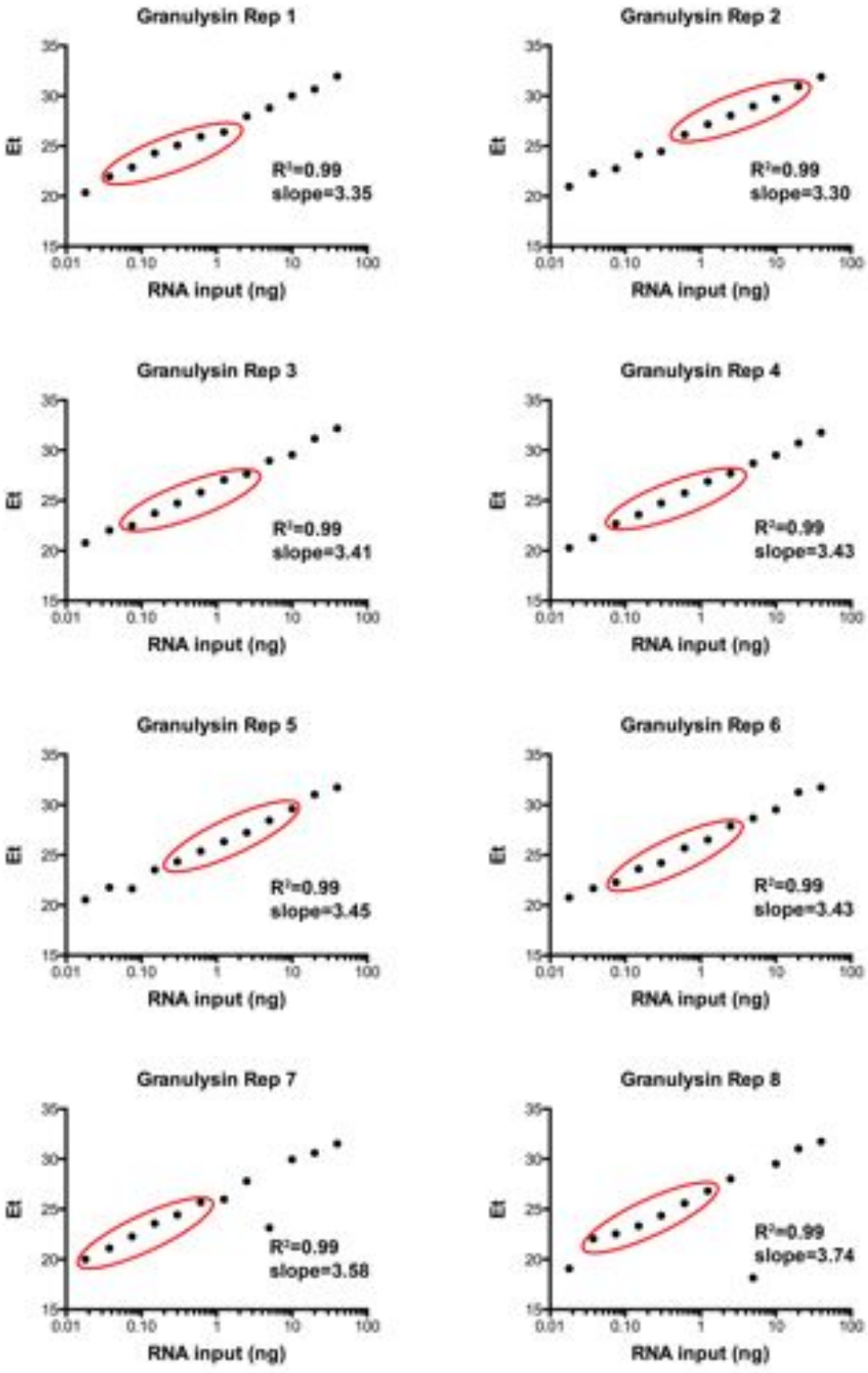

Figure 29: Primer/probe qualification method. A broad range (0.02ng-80ng) of RNA template concentrations was plotted against their corresponding observed Et (40-Ct) values. We evaluated segments of >5 points where amplification is efficient. Efficiency is defined as points in a segment where the signal doubles with every PCR cycle. To pass, the R^2 representing linearity, had to be greater than 0.97 and the slope had to fall between 3.1–3.6. When one segment within a replicate dilution series, in any one of these replicates, met these criteria, the primer was deemed qualified.

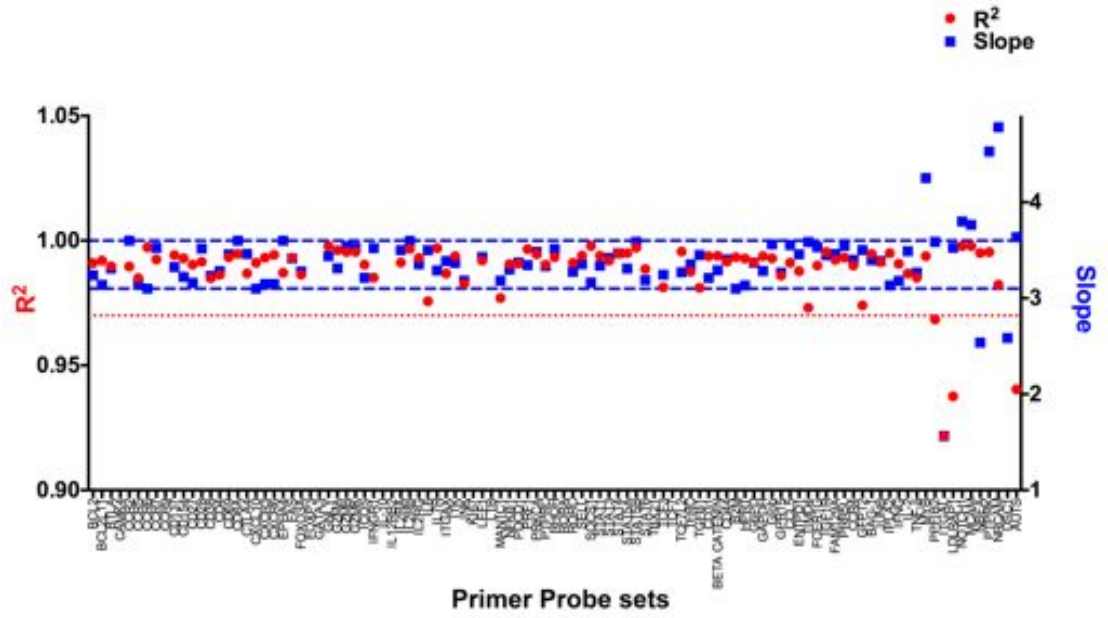

Figure 30: Qualification of primer/probe sets. R^2 values for each primer probe set are plotted on the left Y-axis and slopes are plotted on the right Y-axis. Primer probe sets (n = 4) with the R^2 values below the threshold (shown in red dashed line at 0.97) where excluded. Similarly, primer/probe sets (n = 8) with slopes above or below the threshold (shown in blue dashed lines at 3.1-3.6) where excluded.

We tested a total of 109 primer-probe sets. After excluding the sets that did not qualify, 96 genes were selected for our panel. The final genes selected are shown in Table 31, below.

Table 31: Final list of genes selected for transcriptional profile studies.

Gene			
ARGHEF18	FAS	NFKB1	CD44
AXIN2	FOXO3A	PDCD1	B2M
BCL2	FOXP3	PRF1	HPRT
BCL2L11	GATA3	PRKCA	G6PD
BTLA	GNLY	PTPRC	GAPDH
CAMK4	GZMA	RHOH	Glob
CCR2	GZMB	RORA	GPR15
CCR5	GZMK	RORC	CCL5
CCR6	ICOS	SELL	ENTPD1
CCR7	IFNGR1	SOCS1	TIMD4
CCR9	IL-10	STAT1	FCER1G
CD137	IL12RB2	STAT3	IGF1R
CD154	IL2RA	STAT4	FAM129A
CD27	IL2RB	STAT5A	PRR5L
CD28	IL2RG	STAT5B	CCR4
CD38	IL6	STAT6	GFPT2
CD4	IL7R	TBX21	BAG-1
CD69	ITGAX	TCF3	JUNB
CD8A	ITK	TCF7	IPLA2
CTLA4	JNK	TCF7L2	IFNG
CXCL10	KI67	TFRC	IL-2
CXCR3	LEF1	TGFB1	TNF-a
CXCR6	LTB	CD31	CD200
EPHA4	MAN1C1	B-CATENIN	IL4

4.4.3. Cell sorting (4-way vs 1-way)

Frequencies of antigen-specific CD4 T cells in peripheral blood are extremely heterogeneous and depend on a number of variables including the antigen, nature of infection, and length of persistence of infection. Regardless, most CD4 T cells that bear the TCR for a single epitope restricted by a single HLA allele are very infrequent. Our previous work showed that when using a sample of 10 million PBMC, a range of 0-1000 tetramer-positive CD4 T cells were detected using an Ag85A DRB1*03:01 HLA class II tetramer. Given these very low frequencies and the limited numbers of cryopreserved PBMC from study participants, it was clear that simultaneous sorting of tetramer positive T cells within the different memory T cell populations was necessary. Furthermore, the low frequencies dictated that the Cells-direct method of RNA analysis should be followed, which required sorting of cells directly into a volume of 9µL of Cells-direct solution. Such a small volume limited the type of

tube the BD FACS Aria II flow cytometer could sort cells into, as compatible tube adaptors are limited. A 0.6mL tube adaptor from the BD FACS Aria I was modified to fit the Aria II. Many collection tubes were tested previously on the BD FACS Aria II adaptors and none yielded optimal cell sorts, as determined by sorting a defined number of cells and determining whether gene transcripts were detectable (described in more detail below). The modified 0.6mL Eppendorf tube adaptor performed with the highest sorting efficiency (data not shown). These tubes were selected for further sorting experiments.

While sorting of cells into a single tube was relatively straightforward, sorting of 4 cell populations simultaneously presented more challenges. The BD FACS Aria can sort cells into four streams of micro-droplets containing a single cell (Figure 31). The distance between the streams is manually adjustable.

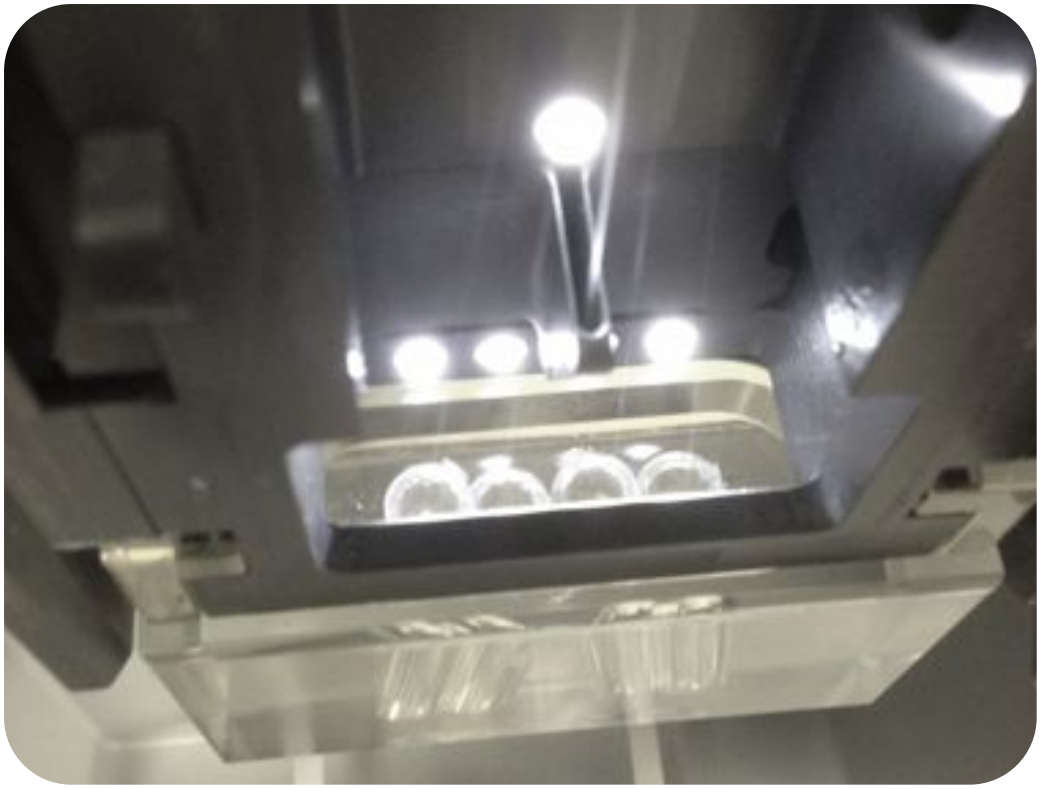

Figure 31: Photo of the BD FACS Aria II sorting layout used in our experiments. The adaptor holds four 0.6mL Eppendorf tubes. The distance between the streams is manually adjusted to ensure that cells are deposited into each tube.

An important aspect of our optimisation experiments was to ensure that equal cell sorting efficiencies (i.e. accurate cell deposition) could be achieved for all

four tube adaptors. We tested whether simultaneous sorting of four populations at a range of pre-determined cell numbers yielded similar mRNA transcript detection compared to one-way sorting (Figure 32).

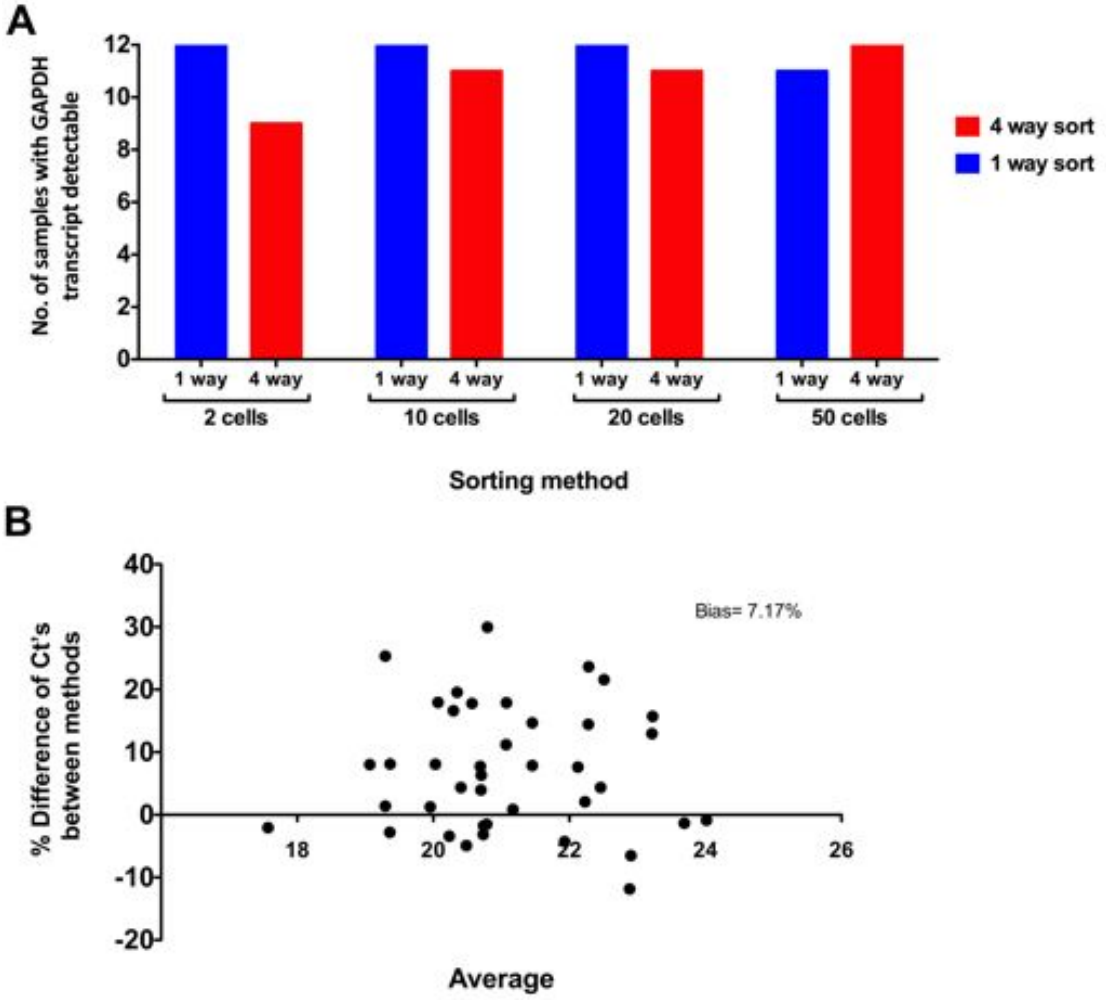

Figure 32: Comparison of 4-way T cell sorting method with 1-way T cell sorting. (A) Twelve replicates of 2, 10, 20 or 50 T cells were sorted using 1-way or 4-way sorting and GAPDH transcripts were detected by qRT-PCR. No statistical differences were observed. (B) Bland Altman plot of the percentage difference of the average raw GAPDH Ct values between the two sort methods for all the samples.

Different numbers (2, 10, 20 and 50 cells) of bulk CD4+ T cells were sorted using 1-way or 4-way sorting and GAPDH transcripts were detected by qRT-PCR. We chose the reference gene, GAPDH, because it is known to be expressed at highly consistent levels in most cells (de Jonge et al. 2007). We sorted each cell number 12 times to have a large enough sample size to detect differences. Using the 1-way sorting method, all twelve cell sorts of 2 cells yielded detectable GAPDH transcript, compared with 9 out of 12 samples when using the 4-way sorting method. However, with increasing cell

numbers, the number of samples with detectable GAPDH transcripts was more consistent between the 1-way and 4-way sorting methods (Figure 32). We therefore concluded that the 4-way sorting method could be applied to analyse antigen-specific CD4 T cells from each memory population, provided at least 10 cells were sorted for each experiment.

To further confirm this finding, we performed a Bland Altman test to determine how similar the results of 4 way sorting were to 1 way sorting. The percentage difference of the average raw GAPDH Ct values between the two sort methods for all the samples were plotted Figure 32B. We observed a 7.8% bias towards one way sorting as compared to 4 way sorting. We did not view this result as a concern as all samples were to be sorted using the 4 way method, given its advantages, and thus the bias would be eliminated as a factor.

Next, we sought to determine whether sorting of different T cell memory cells, based on their distinct expression of surface molecules, also yielded consistent sort accuracies. We again compared the 4-way and 1-way sorting methods with bulk T cell memory populations, naïve CD4 T cells ($CD45RA^{+}CCR7^{+}CD27^{+}$), effector CD4 T cells ($CD45RA^{-}CCR7^{-}CD27^{-/+}$), central memory CD4 T cells ($CD45RA^{-}CCR7^{+}CD27^{+}$) and $CD3^{+}CD8^{-}CD4^{-}$ T cells (Figure 33). This was assessed by quantifying all 96 genes on the Fluidigm 96.96 gene expression platform.

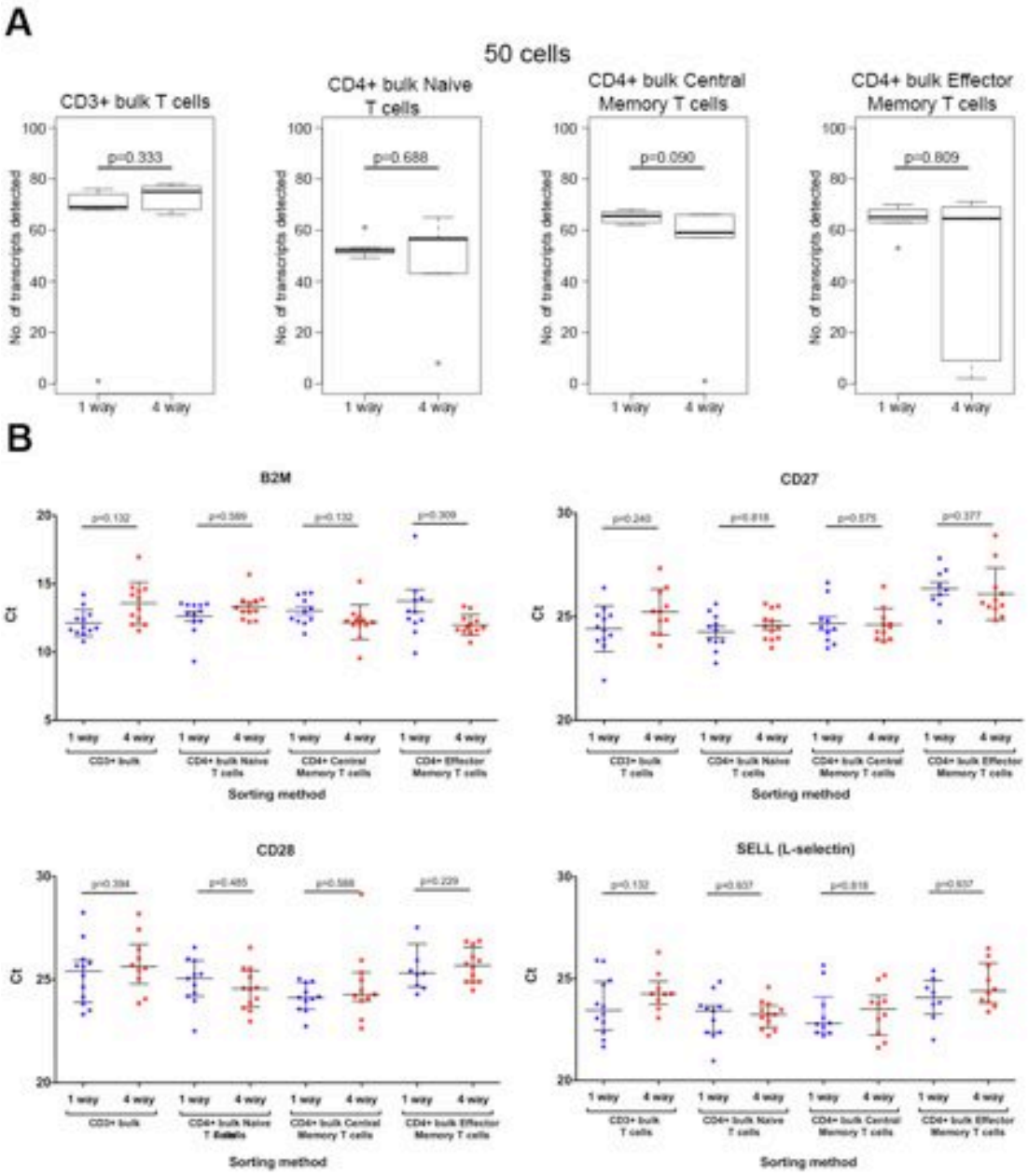

Figure 33: Determination of sorting efficiency of distinct CD4 T cell memory subsets. (A) The number of transcripts detected in 50 cells sorted either by the 1-way cell sorting method or the 4-way cell sorting method are shown. T cell memory populations were sorted and gene transcript levels for 96 genes were detected by microfluidic qRT-PCR. (B) Representative plots of the raw Ct values, for 4 of the 96 genes, for the 4 way sort and 1 way sort. Each T cell memory population was sorted 12 times per sorting method. The Mann-Whitney test was used to calculate p-values.

No significant differences in the number of gene transcripts were detected in any of the sorted T cell memory populations when the two different cell-sorting methods were compared. Furthermore, we assessed whether mRNA transcripts were detected at similar levels in both methods within each aorted

T cell population. Gene transcript levels were similar for all 96 genes (Figure 33B and data not shown).

4.4.4. Cell numbers required for efficient transcript quantification

As mentioned above, the frequencies of mycobacteria-specific CD4 T cells in persons with latent *M.tb* infection are typically very low and highly variable. Another important consideration was the minimum number of cells required to allow reliable detection of mRNA transcripts amongst the different mycobacteria-specific CD4 T cell memory subsets. Using different cell numbers to analyse gene expression may introduce bias among different subsets, as differential transcript expression may not reflect real inter-subset differences but rather differences due to different cell numbers. By keeping cell numbers consistent in each cell population eliminates this. From previous experience, we expected to detect a maximum of 20-50 cells for the most infrequent tetramer+ CD4 T cell memory subset, namely naïve-like cells, from 10 million PBMC. We sorted 25 and 50 cells from each memory CD4 T cell population using the 4-way cell sorting method and measured mRNA expression by microfluidic qRT-PCR.

No differences in the number of transcripts detected between the 25 cells and 50 cells were detected (Figure 34).

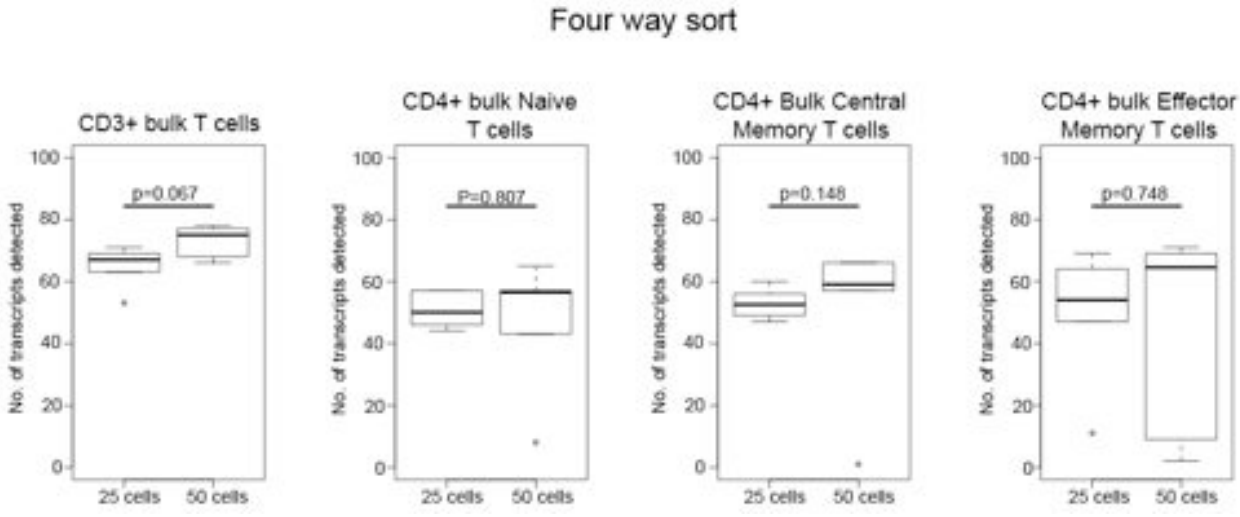

Figure 34: Comparison of mRNA transcript detection in 25 and 50 sorted T cells. Bulk CD3+CD8-CD4- T cells and naïve, central memory or effector memory CD4+ T cell populations were sorted using 4-way sorting on the BD FACs Aria II. The number of transcripts detected in each cell number was determined for 12 replicates of each memory population. The Mann-Whitney test was used to calculate p-values.

Because the number of transcripts detected between 25 cells and 50 cell sorts were not different, we concluded that transcriptomic analyses could be performed on sorted CD4 T cell memory populations consisting of 25 cells. Since previous experiments performed on 5-10 million PBMC, consistently yielded more than 30 tetramer+ CD4 T cells of each memory subset, we decided to sort exactly 30 cells per memory population for all experiments going forth in this thesis.

4.4.5. Changes in transcript expression after staining with tetramers

MHC class II tetramers engage the TCR, suggesting that it could potentially activate cells. Previous work has shown that tetramer staining does not alter the expression of phenotypic markers of T cells (Chao et al. 1997; Sallusto et al. 2004; Vallejo et al. 1999). Whether tetramer staining affects the transcriptional profile of cells is not known. Because we were interested in mRNA expression by antigen-specific T cells detected with HLA class II tetramers, we sought to determine if tetramer staining would affect mRNA transcript levels.

PBMCs were stained with the DRB1*04:01-CFP10$_{(71-85)}$ HLA class II tetramer for varied time periods and mRNA transcript levels measured for all 96 genes. Samples stained with tetramer for 10 minutes were treated as the baseline, since this was the minimum required to allow detection of tetramer+ T cells for analysis. mRNA transcript levels for all genes, at all other time points were measured in relation to those of the 10 minute time point sample, to calculate the fold change in expression. P-values were calculated using the Student t-test. Gene expression was considered different when the fold change was greater than or equal to 2, and the p-value was less than 0.05.

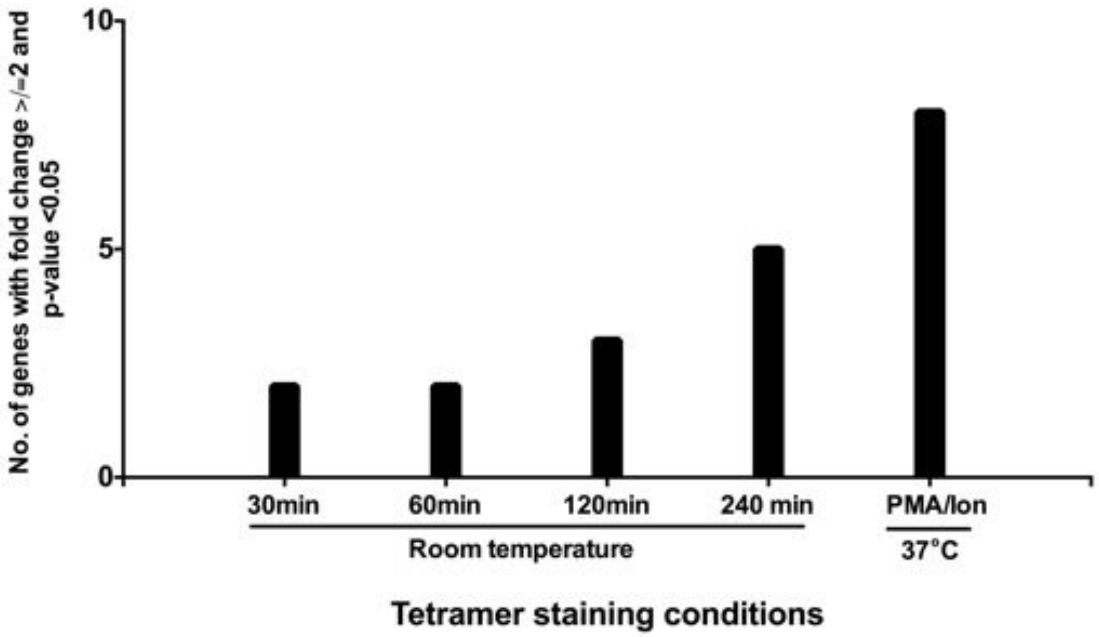

Figure 35: Influence of tetramer staining on mRNA gene transcript levels. T cells were stained with the DRB1*04:01-CFP10$_{(71-85)}$ tetramer for the indicated time periods and temperatures. The fold change was calculated as transcript levels of cells at each condition relative to the 10-minute tetramer stain. Data represents 3 sorts of 30 cells for each condition, all from 1 individual.

For the T cells stained with the DRB1*04:01-CFP10$_{(71-85)}$ HLA class II tetramer at room temperature (RT) for 30 minutes, mRNA transcript levels from 2 genes (NFKB1 and STAT3) were significantly different. Following 1 hour of staining at RT, expression of two genes (PRKCA and FAM129A) was different. Following 2 and 4 hours staining at RT, 3 (BCL2L11, CD28 and IFNG) and 5 (AXIN2, EPHA4, SELL, TCF7L2 and GPR15) genes were expressed at different levels, respectively (Figure 35).

Cells stimulated with PMA/Ionomycin for 4 hours at 37°C before tetramer staining were used as a positive control. mRNA expression of 8 genes (CCR7, CXCL10, G6PD, GZMK, IFNGR1, RHOH, TBX21, and CCR4) was different in the PMA/Ionomycin stimulated T cells (Figure 35).

This data suggested that staining with tetramer for 1 hour would have negligible impact on mRNA transcript levels in our experiments.

4.5. Discussion

The development of high throughput qRT-PCR has revolutionised our ability to study cells on a transcriptional level. The Fluidigm microfluidic platform allows simultaneous quantification of 96 gene transcripts on 96 samples in a single chip. This platform has been successfully utilised for transcriptional analyses of single cells (Dominguez et al. 2013). We combined this microfluidic qRT-PCR platform with sorting of rare tetramer-stained CD4 T cells to allow characterisation of mycobacteria-specific CD4 T cell memory subsets, including the novel naïve-like cells described in Chapter 3. Our methodology combines the sensitivity of single cell qRT-PCR with the multiplexing capability of microarrays and thus circumvents the need for large amounts of starting material. The work in this chapter describes the optimisation of conditions required to combine these two methods to optimally perform transcriptional profiling of mycobacteria-specific T cells (manuscript in preparation).

While the Fluidigm platform has been used in a few studies, until recently no optimal and quantitative application of this technology had been detailed (Flatz et al. 2011). A recent study described protocols to assess the quantitative application of this technique with rigorous methodology (Dominguez et al. 2013). We followed the procedure described by Dominguez et al., to qualify our selected primer/probe sets. The cut-off for efficiency was set at 0.97 for our study, and for linearity, the slope had to lie between 3.1 and 3.6. Of the 109 primer/probe sets selected, 96 passed the qualification criteria and were selected for further experiments. All inventoried Taqman primer/probe sets supplied by Applied Biosystems are reported to have an amplification efficiency of 100%. However, some of these inventoried primer/probe sets did not meet our qualification criteria. The reasons for this discrepancy remain unclear. We postulate that one of the reasons for this discrepancy could be the difference in the qRT-PCR platform used for qualifying the primer/probes. While the manufacturer of the primer/probes have used multiple different systems to determine their efficiency, at the time of submission of this thesis, no efficiency analysis had been done by Applied

Biosystems using the Fluidigm platform. As we will study low cell numbers, we only used the primer/probe sets that passed our qualification criteria to ensure that our experiments yield reliable and accurate transcriptomic measurements.

From previous experience in our lab, we know that the frequencies of mycobacteria-specific CD4 T cells detected using MHC class II tetramers are low, ranging from 0 to 0.53%. We determined the minimum number of cells required for consistent and reliable detection of gene transcripts in sorted CD4 T cell memory subsets. Further, given the limited availability of PBMC, our planned transcriptional analyses of different mycobacteria-specific memory CD4 T cell subsets would have to be done on a single vial of PBMC, necessitating 4-way FACS. We therefore demonstrated that sorting four subsets simultaneously would be as efficient and accurate as sorting each subset individually in a 1-way sort. At cell numbers below 10, the 1-way sort was more efficient and more transcripts were detectable than using the 4-way sorting method. However, for analyses of cell numbers above 10, 4-way sorting was as efficient as the 1-way sorting method and we continued with the 4-way sorting method.

It was also important to establish the minimum number of cells required for accurate detection of gene transcripts amongst the different memory T cell populations. No significant differences in the number of transcripts detected in 25 and 50 cell sorts were observed for all the sorted memory T cell subsets.

Previous experiments in our group showed that at least 30 antigen-specific tetramer+ naïve-like T cells could consistently be detected when staining 10 million PBMCs. Transcriptional patterns in different memory subsets can only be compared when cell numbers within each subset are kept constant, as the likelihood of detecting rare gene transcripts is greater with higher cell numbers. By contrast, in very low cell numbers detection may become stochastic. Sorting constant cell numbers eliminates this issue. Our results suggested that 4-way sorting of 30 cells per subset would yield reliable and consistent transcriptomic profiling.

Finally, it was important to determine whether staining with the tetramer would influence mRNA transcript levels since the HLA class II tetramer engages the

TCR of the T cell. It had been suggested that the tetramer might be able to activate stained cells. We assessed if tetramer staining time and temperature could affect the transcriptional profile of tetramer stained CD4 T cells. mRNA transcript levels did not change when staining at RT for 1 hour; only FAM129A and IGF1R were different. The result that only 2 genes were differentially expressed after 60 minutes provided confidence that tetramer staining had minimal effects on mRNA expression. We acknowledged this difference and took it into account in our experiments going forth.

The methods optimised in this chapter were taken further to address the questions in Chapter 5.

4.6. Contributions

Munyaradzi Musvosvi contributed to the qualification of primer/probes sets, as well as to the analysis of the qRT-PCR data generated in this chapter.

Chapter 5: Phenotypic and transcriptional profile analysis of antigen-specific naïve-like CD4 T cells

5.1. Introduction

Antigen-experienced or memory T cells have been classified into central memory and effector/effector memory T cells, based on their functions, such as proliferative capacity, cytokine secretion and tissue homing. Several groups, including our own, who have studied human immune responses against *Mycobacterium tuberculosis*, have reported an unusual population of mycobacteria specific T cells, with phenotypic characteristics of naïve T cells. These "naïve-like" (NL) T cells, which express effector cytokines but display a naïve CD45RA+CCR7+CD27+ phenotype, have been identified across different age groups (Kagina et al. 2009; Caccamo et al. 2006; Tena-Coki et al. 2010; Soares et al. 2008). A novel, long-lived T cell population, memory stem T (T_{SCM}) cells, has recently been described in animals (Gattinoni et al. 2009; Y. Zhang et al. 2005) and humans (Gattinoni et al. 2011). These cells, which share phenotypic characteristics with CD45RA+CCR7+ naive T cells, possess an enhanced capacity for self-renewal and multipotent ability to derive T_{CM}, T_{EM} and T_E cells (Gattinoni et al. 2011).

In Chapter 3 we described detection of naive-like cells after MVA85A vaccination. We now seek to characterise this unusual subset of mycobacteria-specific naïve-like CD4 T cells using methodology optimised in Chapter 4, which we propose may be an important target for new TB vaccines and may help in elucidating the complexity of *M.tb*-specific memory T cell differentiation.

5.2. Aims

The aim of this chapter was to characterise the naïve-like CD4 T cells observed in natural *M.tb* infection or after vaccination against TB disease.

Specific aims:

i.) To determine if naïve-like *M.tb*-specific CD4 T cells share phenotypic properties with memory stem T cells.

ii.) To elucidate and compare the transcriptional profile of these naïve-like *M.tb*-specific CD4 T cells with those of naïve, central memory and effector memory CD4 T cells.

5.3. Materials and Methods

The work in this chapter was performed by the candidate unless otherwise stated.

5.3.1. Study participants for phenotypic profiling of MVA85A induced NL T cell studies

We retrieved cryopreserved samples from a subset of 12 adolescents (TB008) who were enrolled into a completed phase I/IIa trial of MVA85A (Scriba et al. 2010). Participants were all vaccinated with BCG at birth, were all HIV negative and had no evidence of *M.tb* infection, as defined by a negative ESAT6/CFP10 ELISpot and a TST induration of <15 mm, and all had a normal chest X-ray. Participants received a single intra-dermal dose of $5x10^7$ pfu of MVA85A over the deltoid region of the left arm, and were followed up for 1 year (Scriba et al. 2010). None converted to a positive ESAT6/CFP10 response during follow-up.

5.3.2. Study participants for natural *M.tb* infection studies

We enrolled healthy donors with asymptomatic *M.tb* infection, under the healthy donor protocol approved by the Human research ethics committee of UCT (HREC 160/2006). All donors had to be HIV negative, not on any chronic medication and not pregnant. The donors had to have a QuantiFERON TB-GOLD In-tube (QFT) result greater than 0.35IU/mL, to be considered positive for *M.tb* infection. Donors had to give consent for HLA typing. For those who met these criteria, blood samples were collected and PBMCs isolated and cryopreserved as described in chapter 2, section 2.3.4.

5.3.3. HLA typing

DNA was extracted from PBMCs and sent to our collaborators, Alex Sette et al., at La Jolla Institute of Allergy and Immunology (LIAI) for HLA typing , as described in chapter 2, section 2.3.8.

5.3.4. HLA class II tetramer staining

Ten to 20 million PBMCs from each donor were thawed and stained with tetramers as described in chapter 2, section 2.3.12. Briefly, PBMCs were thawed and washed. PBMCs were stained with anti-CCR7 antibody for 30

minutes at 37°C, and then washed once in 2%FCS/PBS. PBMCs were then stained with 2µg/mL of tetramer (Table 32) for 1 hour at room temperature, in a total volume of 100µL. PBMCs were then washed and stained with the rest of the antibodies listed in section 5.3.5. of this chapter, as previously described.

Table 32: HLA class II tetramers used to stain PBMCs for cell sorting of CFP10-specific CD4 T cells.

HLA allele	Peptide number	Protein	Peptide Sequence
DRB5*01:01	11	$CFP10_{(51-65)}$	AQAAVVRFQEAANKQ
DRB1*04:01	15	$CFP10_{(71-85)}$	EISTNIRQAGVQYSR

5.3.5. Antibodies

Fluorescence-conjugated antibody panels utilised for cell sorting experiments are shown in Table 33. Antibody panels were optimised as described in Chapter 2, section 2.3.13.

Table 33: Panel of fluorescence-conjugated antibodies and dyes used to stain cells for the natural *M.tb* infection T cell phenotype tetramer staining and cell sorting studies.

Marker	Clone	Manufacturer	Fluorochrome	Volume Used (in final staining volume of 100µl)
CD3	UCHT1	BD Biosciences	Alexa Fluor 700	1µL
CD4	S3.5	Invitrogen	Quantum Dot 605	0.5µL
CD45RA	HI100	eBiosciences	PECy7	0.05µL
CCR7	150503	BD Biosciences	PerCP Cy5.5	1.25µL
CD95	DX2	Biolegend	APC	1.25µL
CD27	M-T271	BD Biosciences	FITC	1.25µL
CD14 (dump)	M5E2	Biolegend	Brilliant Violet 421	0.5µL
CD19 (dump)	HIB19	BD Biosciences	Brilliant Violet 421	0.25µL
CD8 (dump)	RPA-T8	BD Biosciences	Brilliant Violet 421	0.5µL
CD335 (dump)	9E2	Biolegend	Brilliant Violet 421	0.5µL
Live/dead (dump)		Invitrogen	ViViD	0.5µg/mL

The markers CD14, CD19, CD335 and CD8 were all conjugated to the same fluorescent molecule to exclude them from analysis, this is known as a dump channel. This channel is also used for the live/dead, to exclude dead cells. Cells were acquired and sorted on the BD FACS Aria II flow cytometer, as described in Chapter 4, section 4.4.3.

5.3.6. CD4 T cell sorting

Thirty cells from each bulk CD4 T cell memory populations, as well as from each antigen-specific tetramer+ CD4 T cell subset were sorted directly into 9µL of Cells-direct solution as described in chapter 4 section 4.3.4. Four replicates of each population were sorted, with the exception of naïve-like antigen-specific CD4 T cells which were too infrequent; for these we sorted 1 or 2 replicates of 30 cells. cDNA was synthesised and reverse transcribed as described in Chapter 4 section 4.3.4. was followed.

5.3.7. Data analysis (performed in collaboration with M. Musvosvi, SATVI).

Flow cytometry data was analysed using Flowjo version and Graphpad Prism version 6. Analysis of all the qRT-PCR data was performed in R version 3.0.1.

As a first step in performing quality control on our data, samples that did not express CD4 or B2M mRNA transcript were excluded from any further analysis. Identification of outlier samples, which were excluded from analysis, is described in detail in section 5.3.4 in this chapter. The delta Ct was calculated by subtracting the B2M Ct value from the Ct of your gene in that sample, to normalise the data. We then calculated a delta Et (25-delta Ct) for each gene for all the samples. By plotting the data in a reciprocal manner, the data is read intuitively, since a high delta Et value represents higher transcript numbers and lower delta Et values, lower transcript numbers. All analyses going forward in this Chapter were performed and reported using delta Et. We then performed a Kruskal-Wallis test to identify significant differences in transcript abundance between cell populations. The Benjamini Hochberg (Benjamini & Hochberg 1995) test was used to correct for multiple comparisons, with a stringent false discovery rate ($q<0.05$).

Principal component analysis (PCA) is a statistical procedure of identifying patterns in data and expressing the data in a way that highlights similarities and differences in the data. PCAs were performed in R version 3.0.1.

5.4. Results

5.4.1 Study participants for natural *M.tb* infection studies

Demographics of the 7 healthy *M.tb* latently infected donors are shown in Table 34.

Table 34: Demographic characteristics of enrolled healthy donors

		Adults (n=7)
Male, n (%)		1 (15)
Median age in years (range)		25.4 (22-42)
Race, n (%)	Black	2 (29)
	Mixed race	5 (71)

5.4.2. Naïve-like Ag85A-specific $CD4^+$ T cells are not memory stem T cells

Because CD95 was shown to discern T_{SCM} from naïve CD4 T cells, we measured CD95 expression by DRB1*03:01-$Ag85A_{(56-75)}$ tetramer+ CD45RA+CCR7+CD27+ CD4 T cells in PBMCs from adolescents who received MVA85A (Figure 36A), as described in section 5.3.1. We combined all data we had from different time points after vaccination because limited samples were remaining from the TB008 vaccine trial, and because similar frequencies of NL-Ag85A-specific CD4 T cells were observed at different time points (Figure 36B). Naïve-like Ag85A-specific CD4 T cells were detected at frequencies 10-20 fold lower than Ag85A-specific $CD45RA^-$ memory CD4 T cells. In turn, $CD95^+$ T_{SCM} comprised at most 5-10% of this naïve-like CD4 T cell subset, while being undetectable in some vaccinees (Figure 36B). These data suggest that most of the CD45RA+CCR7+CD27+ naive-like memory CD4 T cells are not T_{SCM} cells.

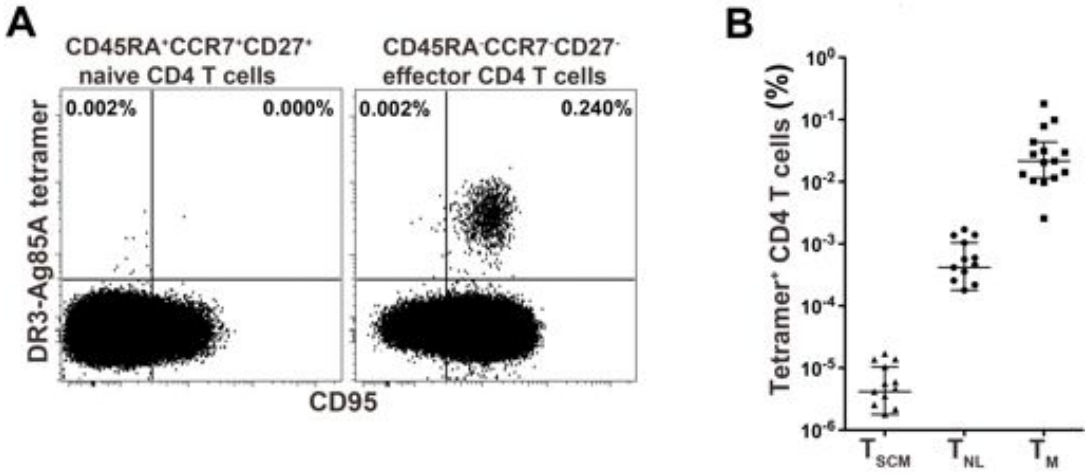

Figure 36: Phenotypic characterisation of naïve-like Ag85A-specific CD4 T cells.
(A) Representative flow cytometry plots of CD95 and DRB1*03:01-Ag85A$_{(56-75)}$ tetramer staining of CD4 T cells in PBMCs collected 14 days after MVA85A vaccination from an individual adolescent. Shown are cells gated on total CD45RA+CCR7+CD27+ naïve CD4 T cells (left) and cells gated on total CD45RA^{-} CCR7–CD27– T_E CD4 cells (right). (B) Frequencies of DRB1*03:01-Ag85A$_{(56-75)}$ tetramer^{+} CD4 T cells classified as T_{SCM} cells, naïve-like memory (T_{NL}) CD4 T cells. and CD45RA- memory (T_M) CD4 T cells in 4 HLA-DRB1*03:01-bearing participants, All post-vaccination time points are shown. The values for 3 samples in the T_{SCM} were 0, and are therefore not plotted on the logarithmic scale. Horizontal lines represent the medians, and error bars the IQR.

5.4.3. Sorting of CD4 T cell populations

To assess transcriptional profiles of antigen-specific naïve-like CD4 T cells, thirty cells from bulk CD4 T cell memory populations, as well as from antigen-specific tetramer+ CD4 T cell memory populations were sorted. T_{SCM} were too infrequent to sort. The gates used for cell sorting are shown in Figure 37, below. We sorted the following populations:

- Bulk naïve CD4 T cells (CD45RA+CCR7+CD27+CD95-)
- Bulk central memory CD4 T cells (CD45RA-CCR7+CD27+CD95+/-)
- Bulk effector CD4 T cells (CD45RA-CCR7-CD27+/-CD95+/-)
- CFP10-specific naïve-like CD4 T cells (tetramer+CD45RA+CCR7+CD27+CD95-)
- CFP10-specific central memory CD4 T cells (tetramer+CD45RA-CCR7+CD27+CD95+/-)
- CFP10-specific effector CD4 T cells (tetramer+CD45RA-CCR7-CD27+/-CD95+/-)

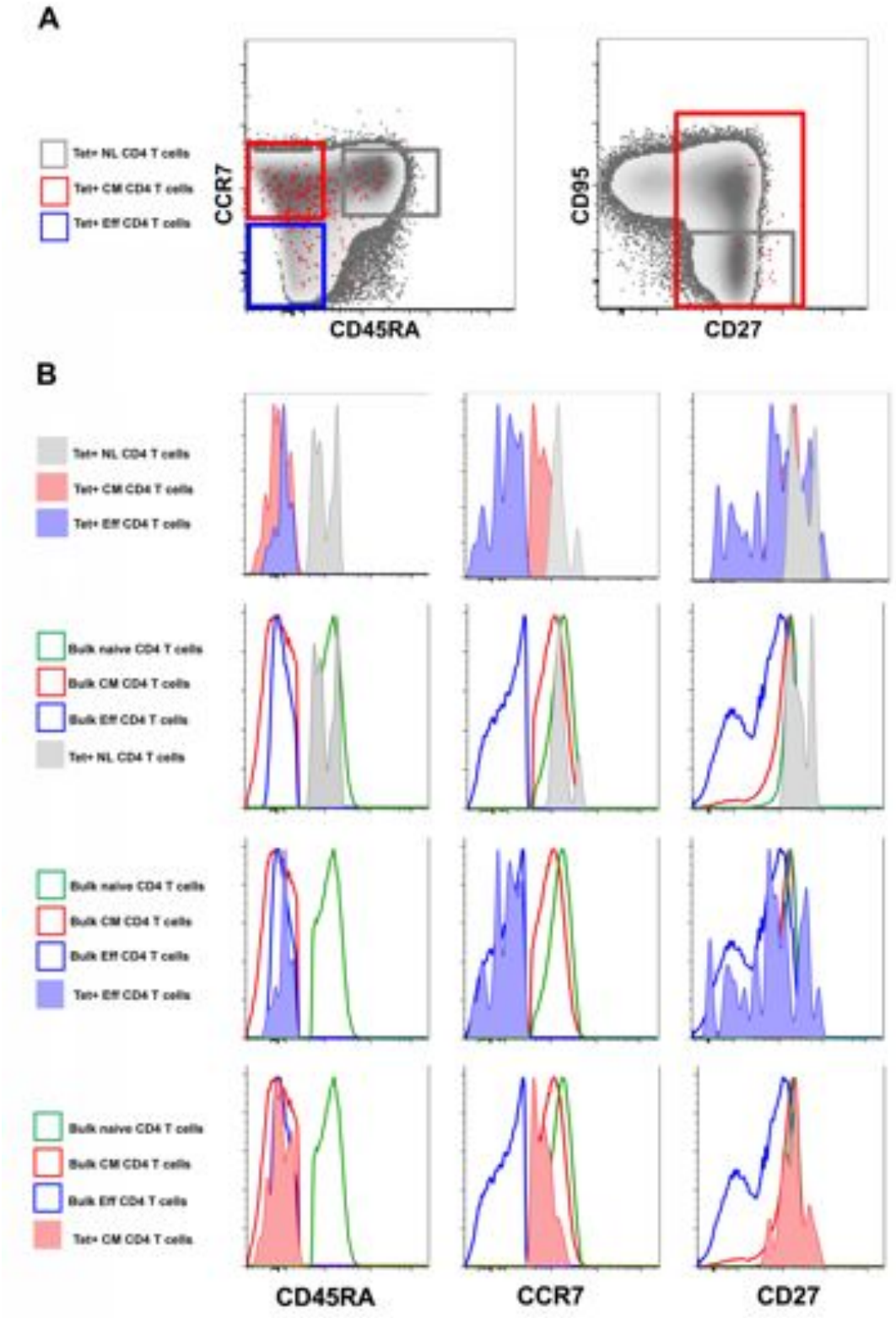

Figure 37: Sorting of CD4 T cell memory populations based on cell surface phenotypic marker expression. (A) Representative flow cytometry plots depicting placement of gates to select and sort the different CD4 T cell bulk memory populations (grey background), and the tetramer+ T cell populations (red). The grey gate selected the NL tetramer+ CD4 T cell population, the red indicates the gate utilised to sort central memory tetramer+ CD4 T cells and the blue gate effector tetramer+ CD4 T cells. (B) Flow cytometry plots indicating expression of the surface markers CD45RA, CCR7 and CD27.

5.4.4. Exclusion/inclusion criteria for samples from qRT-PCR

It has been shown that many factors contribute to measurement error in qRT-PCR. Technical errors as well as flaws in the experimental design add to variability within the data and have to be taken into account during data handling and interpretation. One of the key steps is identification of outlier samples, since inclusion of atypical samples may lead to data skewing and misinterpretation of results. To identify outliers in our data sets, we used the method described by Burns et al (Burns et al. 2005).

Data generated from all experiments were analysed in the following manner. Firstly we sought to identify transcripts with consistent expression across all the different sorted T cell subsets, to allow identification of outlier data that did not follow the expected mRNA expression pattern of these transcripts. We calculated the coefficient of variation (CV) of Ct values for all mRNA transcripts in all the samples before normalisation, and selected genes with a CV of 15% or less (Figure 38). The genes selected were B2M, TGFB1, CD4, LEF1, CD44 and STAT5B. IL4 was not included in this analysis, as no expression of IL4 was observed in any of the sorted samples.

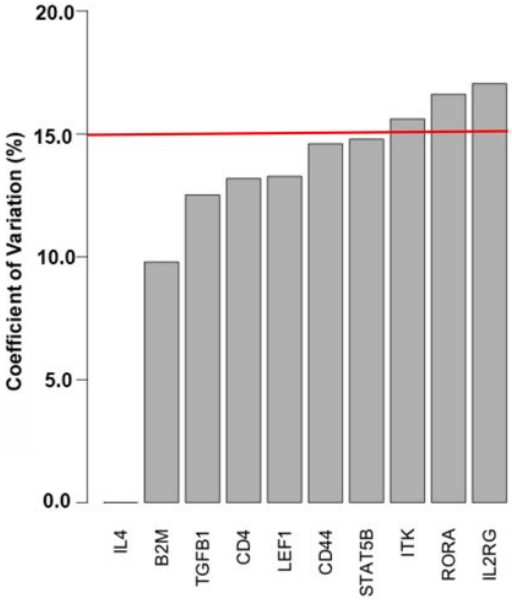

Figure 38: Analysis of the coefficient of variation (CV) of mRNA transcripts to allow for identification of transcript expression patterns, for outlier exclusion. The bar graph represents the CVs for 10 of the 96 most consistently expressed genes. Six of the 10 genes shown had a CV below 15%. The red horizontal line depicts the cut off. Raw Ct values were used to calculate the CV.

We followed the method for exclusion of outliers based on RT-PCR data published by Burns et al (Burns et al. 2005). We then calculated the geometric mean of the Et (40-Ct) values for these 6 genes, for all the samples, and plotted on a box and whisker plot (Figure 39).

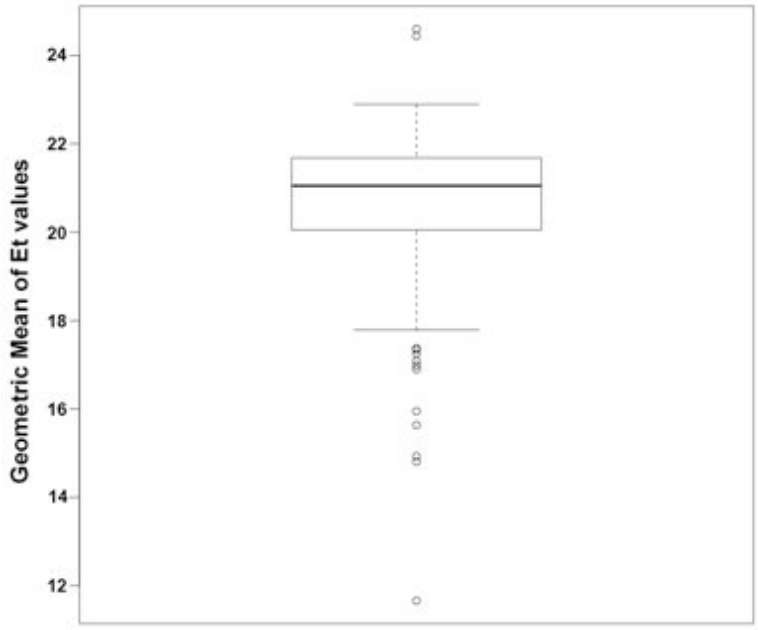

Figure 39: Determination of outlier samples. Distribution of the geometric mean of the Et (40-Ct) values of the 6 genes with a CV below 15% for all T cell sorts. The bold line represents the median and the box around the median represents the interquartile range. The whiskers extend out as far as the last data point that lies within the range of 1.5 times the IQR. Samples that lay below the lower or above the upper whisker were considered outliers, and excluded from the data analysis (n=13) (Burns et al. 2005).

The whiskers extend out as far as the last data point that lies within the range, of 1.5 times the IQR. All data points that lay above or below the whiskers were considered outliers and excluded from any further analysis (M. J. Burns et al. 2005). Outlier samples that were ultimately excluded are depicted in green on the heatmap in Figure 40, a supervised hierarchal clustering analysis.

Because the samples from each sort were loaded as technical duplicates on the Fluidigm chip, Ct values from duplicates were averaged. Where one of the duplicates was excluded based on our exclusion/inclusion criteria, the remaining duplicate was used for further analysis.

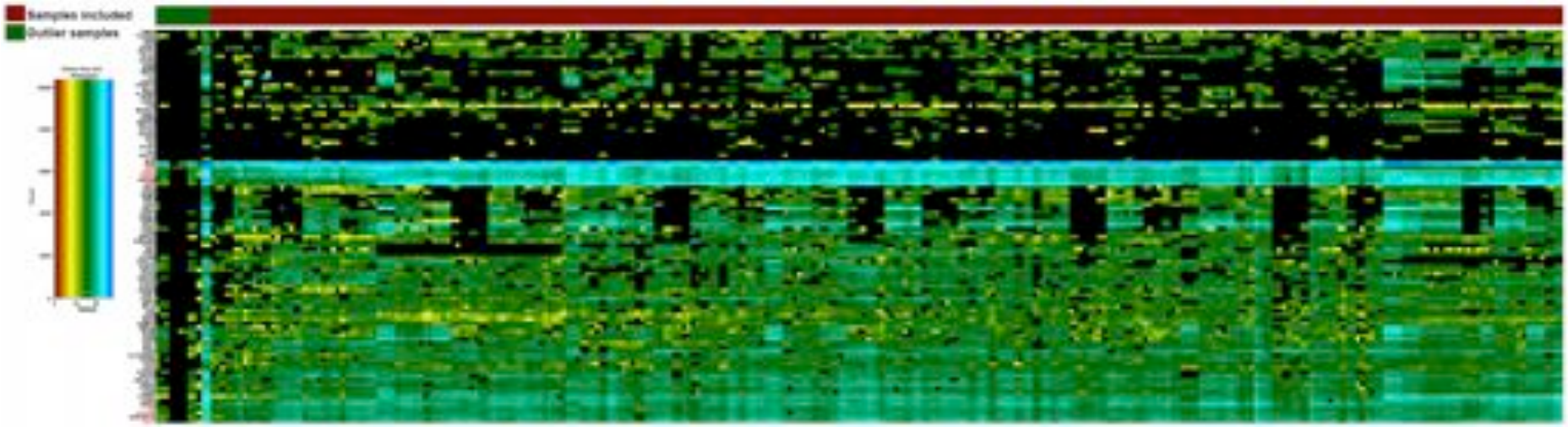

Figure 40: Supervised hierarchal clustering of all 96 mRNA transcripts for all CD4 T cell sorts, depicting outlier data samples for ultimate exclusion. Samples shown in green were designated as outliers and excluded from further analysis. Samples shown in red were taken further for analysis. The histogram shows the distribution of the delta Et values for all the samples. The colour key designates delta Et values. The 6 genes selected to determine outliers, are highlighted in red.

5.4.5. Confirmation of expression of transcripts of surface markers used for T cell memory subset sorting.

To confirm that our cell sorting and transcriptional analysis methodology yielded expected results, we quantified mRNA expression of genes encoding the memory markers CCR7, CD27 and CD62L (SELL). Many groups have also used SELL (L-selectin/CD62L) to differentiate T cell memory subsets (Zhang et al. 2013). CCR7, CD27 and SELL mRNA transcript levels were higher in bulk naïve and central memory cells than in bulk effector CD4 T cells. CFP10-specific naïve-like CD4 T cells expressed similar mRNA transcript levels of these genes to bulk naïve T cells (Figure 41A). However, CFP10-specific naïve-like CD4 T cells expressed significantly higher levels of these mRNA transcripts than CFP10-specific central memory and effector subsets (Figure 41B). These data confirmed that our sorting methods and quantification of mRNA expression in sorted cells yielded expected results.

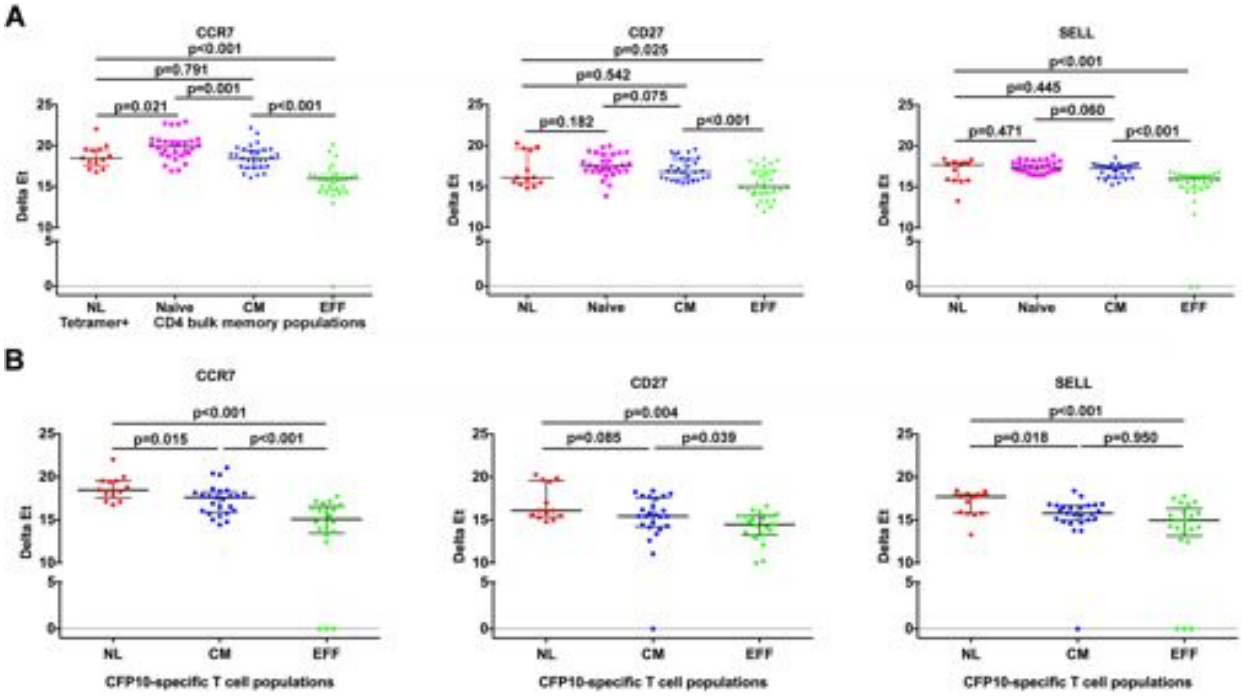

Figure 41: CCR7, CD27 and SELL (encoding CD62L) mRNA transcript levels in sorted CD4 T cell memory populations. (A) mRNA transcript levels of the DRB1*04:01-CFP10$_{(71-85)}$ and DRB5*01:01-CFP10$_{(51-65)}$ tetramer+ naïve-like CD4 T cells, bulk naïve, central memory and effector memory CD4 T cells. (B) mRNA transcript levels of CFP10-specific naïve-like, central memory and effector CD4 T cells. Results from seven donors are expressed as delta Et values (normalised to B2M) in each sort of 30 cells. P-values were calculated using the Mann-Whitney test, after adjusting for multiple comparisons with the Benjamini Hochberg method. P values below 0.05 were considered significant.

5.4.6. Naïve-like T cells have a transcriptional profile distinct from truly naïve cells.

We sought to determine if naïve-like *M.tb*-specific CD4 T cells shared mRNA expression profiles with bulk naïve CD4 T cells. We performed unbiased clustering analyses of sorted DRB1*04:01-CFP10$_{(71-85)}$ and DRB5*01:01-CFP10$_{(51-65)}$ tetramer+ NL cells and bulk naïve, central memory and effector CD4 T cells from 7 donors. We identified 50 genes that were differentially expressed between the four T cell populations. CFP10-specific NL cells clustered together and away from the truly naïve cells. This suggests that the NL cells are more similar to each other than to truly naïve, central memory or effector CD4 T cells. Naïve-like cells clustered more closely with the bulk effector CD4 T cells (Figure 42), suggesting they may have effector functions.

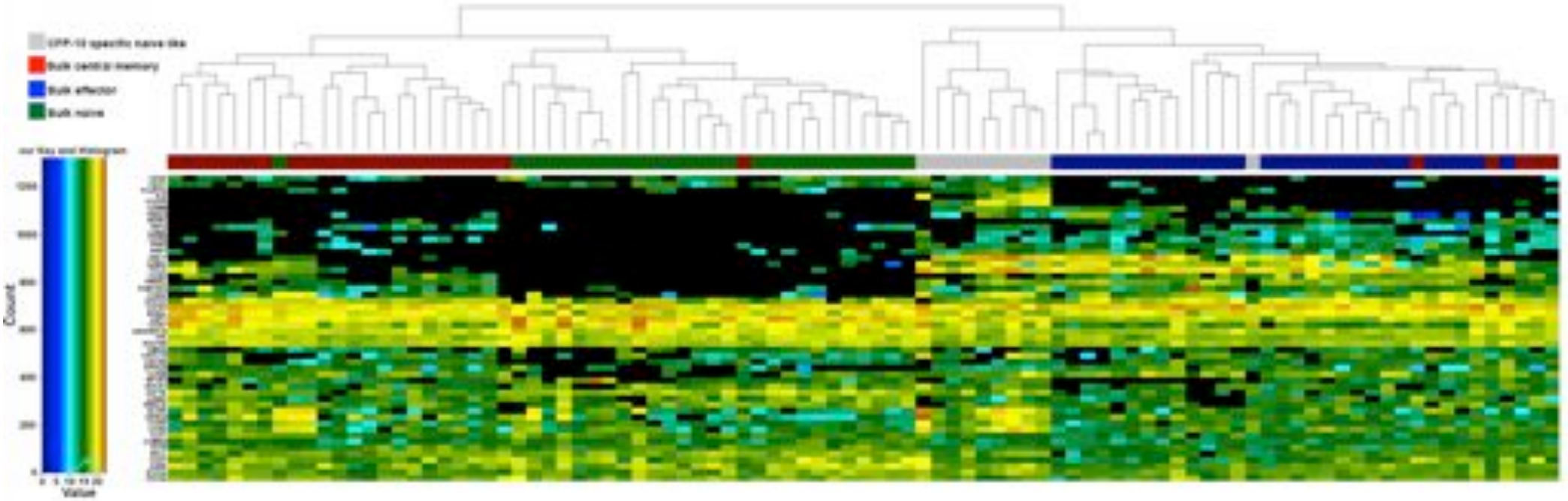

Figure 42: Unsupervised hierarchal clustering of transcriptional profiles of bulk CD4 T cell populations and antigen specific, DRB1*04:01-CFP10$_{(71-85)}$ and DRB5*01:01-CFP10$_{(51-65)}$ tetramer+, naïve like CD4 T cells shown as delta Et values. Fifty genes were differentially expressed between antigen-specific naïve-like CD4 T cells (grey), bulk central memory CD4 T cells (red), bulk effector CD4 T cells (blue) and truly naïve bulk CD4 T cells (green). Heatmap rows = genes, columns = T cell population per sample.

To gain further insight into similarities or differences between NL cells and bulk naïve, central memory and effector CD4 T cells, we performed another unsupervised technique, principal component analysis (PCA). Tetramer stained CFP10-specific naïve-like cells did not cluster with the truly naïve CD4 T and clustered away from bulk CD4 T cell populations (Figure 43). This further suggested that the CFP10-specific naïve-like T cells are very different to truly naïve T cells. When considering PC1, the CFP10-specific NL cells lie between central memory and effector cells, but PC2 suggests that the NL cells are also different to all the bulk subsets, although the differences are in different genes than those that separate truly naïve from central memory and effector CD4 T cells.

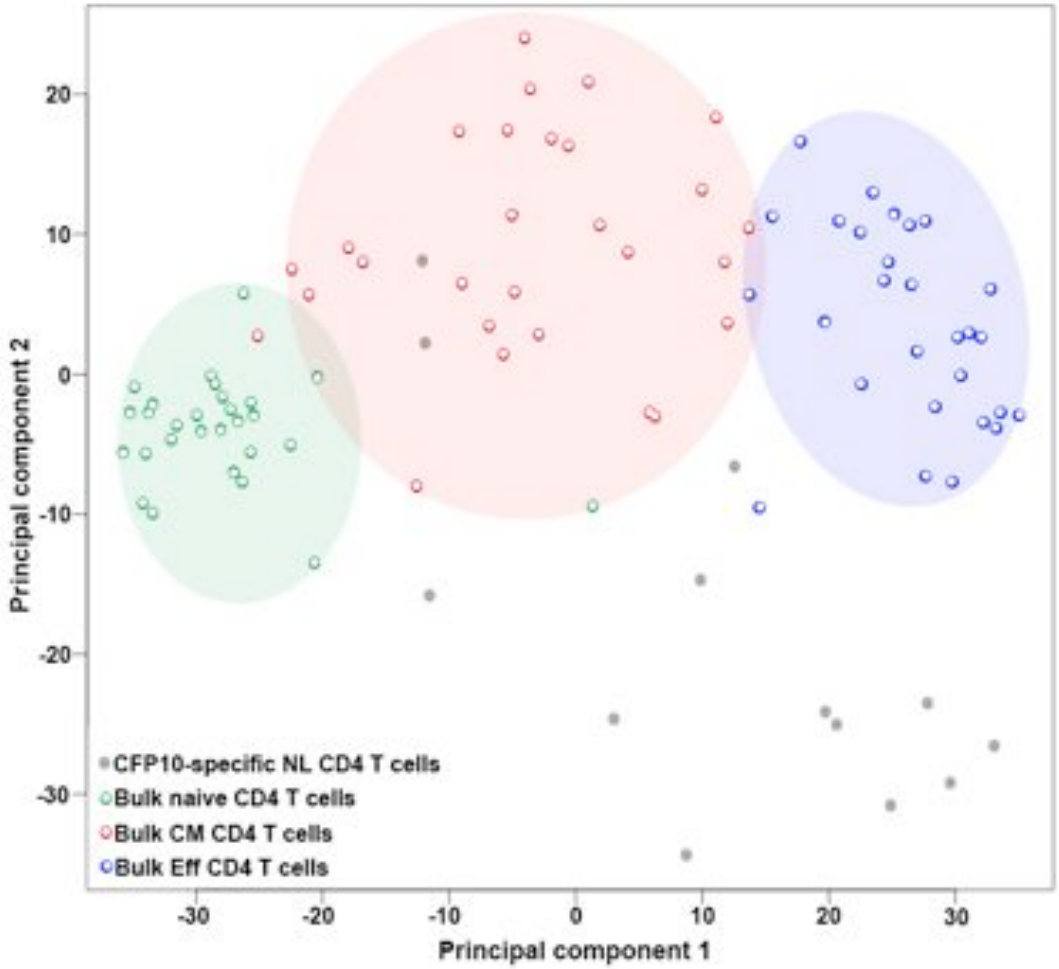

Figure 43: Principal component analysis of the tetramer stained CFP10-specific naive-like CD4 T cells (grey), bulk central memory CD4 T cells (red), bulk effector CD4 T cells (blue) and truly naïve bulk CD4 T cells (green).

In depth analysis of transcriptional profiles of these cell subsets showed particular patterns of gene expression. Firstly, seven chemokine receptors

were differentially expressed between CFP10-specific naïve-like CD4 T cells and bulk CD4 T cell populations. We observed higher expression of CCR4, CCR6 and CCR9 by CFP10-specific NL CD4 T cells compared with truly naïve bulk CD4 T cells, while a subset of CFP10-specific NL CD4 T cells expressed CCR2, CCR5 and CXCR6. The chemokine receptors CCR2 and CCR5 where not expressed by bulk naïve CD4 T cells. CCR7 was expressed at a lower level in CFP10-specific naïve-like cells compared with truly naïve bulk CD4 T cells, whereas CXCR6 expression levels were not different (Figure 44). CFP10-specific NL CD4 T cells expressed significantly higher levels of CCR6 and CCR9 compared to bulk central memory CD4 T cells, lower levels of CXCR6, and similar levels of the other chemokine receptors.

Chemokine receptor mRNA expression by CFP10-specific NL CD4 T cells was also distinct from effector CD4 T cells. NL cells expressed higher levels of CCR6; CCR7 and CCR9 transcripts compared with bulk effector CD4 T cells, but significantly lower levels of CCR2, CCR5 and CXCR6 transcripts (Figure 44). Interestingly, CCR4, a receptor for the chemokines MIP-1 and RANTES, was not significantly different between CFP10-specific NL cells and effector T cells.

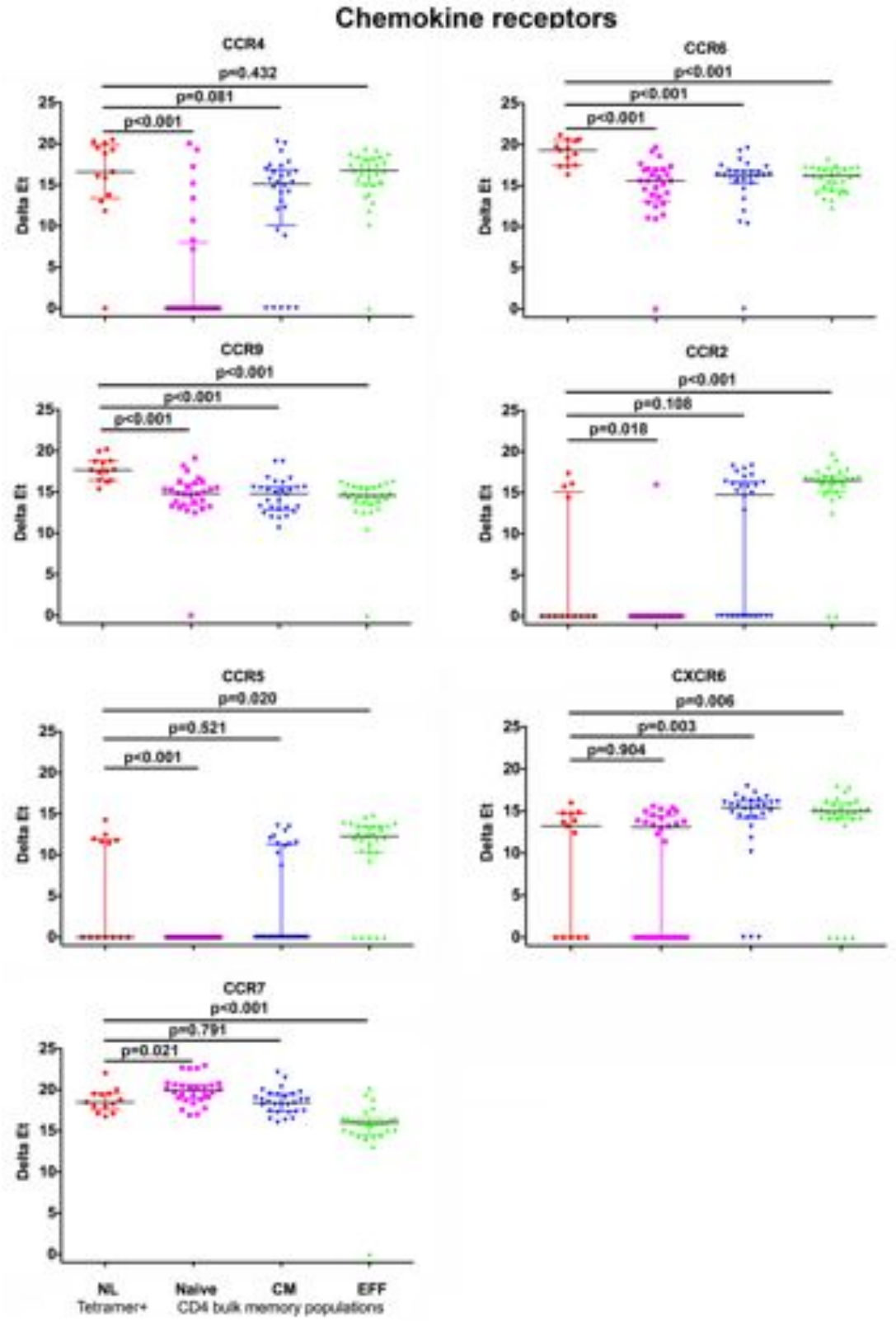

Figure 44: Chemokine receptor mRNA transcript levels in *M.tb*-specific NL and bulk memory CD4 T cell populations expressed as delta Et values. Each dot represents a sort of 30 cells from 7 LTBI volunteers. Results from seven donors are expressed as delta Et values (normalised to B2M) in each sort of 30 cells. P-values were calculated with the Mann-Whitney test, after correcting for multiple comparisons with the Benjamini Hochberg method with an FDR of 0.05 (q-value). P-values below 0.05 were considered significant.

Eight mRNA transcripts encoding cytokine and cytokine receptors were differentially expressed between CFP10-specific NL CD4 T cells and bulk CD4 T cell populations. The mRNA transcript levels of IFN-γ, TNF-α, CCL5 (RANTES), CXCL10 (IP-10) and IL2RB were significantly higher in CFP10-specific NL CD4 T cells compared with truly naïve bulk CD4 T cells. However, LTB (TNF-C), IL2RG and IL7R were expressed at significantly lower levels in CFP10-specific naïve-like CD4 T cells (Figure 45).

CFP10-specific NL CD4 T cells appeared to be adapted for effector functions, since mRNA transcript levels of IFN-γ, CCL5 and CXCL10 were higher compared with bulk central memory CD4 T cells. LTB (TNFC) and IL2RG were significantly lower in CFP10-specific naïve-like CD4 T cells. mRNA transcript levels of TNF-α, IL2RB and IL7R were not different between these two populations (Figure 45).

The apparent effector characteristics of NL cells were further supported by the finding that mRNA transcript levels of IFN-γ, CCL5 and CXCL10 were not different to those expressed by effector cells. LTB and IL2RG did not follow this pattern; their mRNA levels were significantly lower in CFP10-specific NL CD4 T cells (Figure 45).

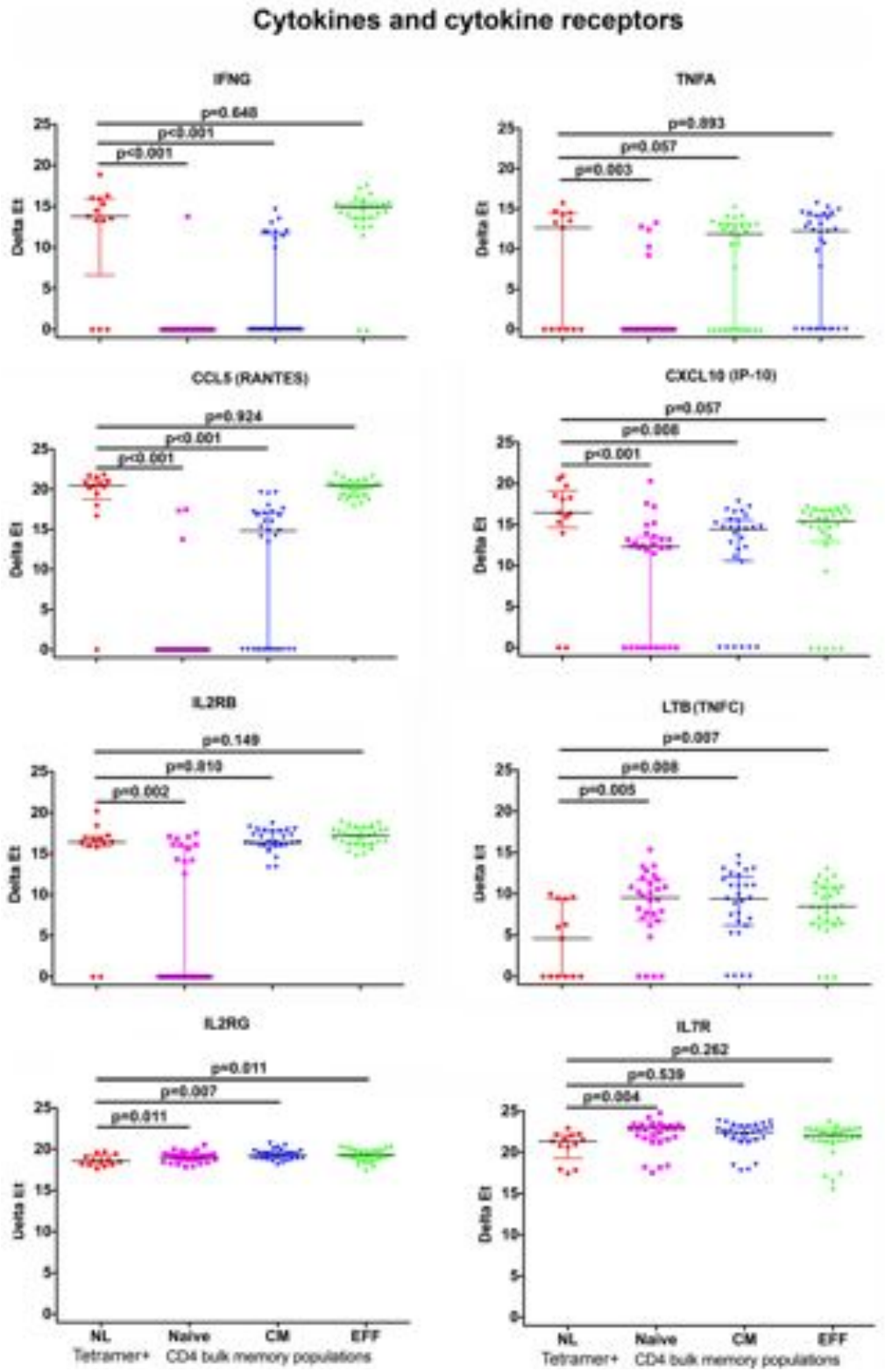

Figure 45: Cytokine and cytokine receptor mRNA transcript levels in *M.tb*-specific NL and bulk memory CD4 T cell populations expressed as delta Et values. Each dot represents a sort of 30 cells from 7 LTBI volunteers. Results from seven donors are expressed as delta Et values (normalised to B2M) in each sort of 30 cells. P-values were calculated with the Mann-Whitney test, after correcting for multiple comparisons with the Benjamini Hochberg method with an FDR of 0.05 (q-value). P-values below 0.05 were considered significant.

The finding that CFP10-specific NL CD4 T cells expressed effector cytokines prompted us to investigate other effector molecules. The effector molecules Granulysin (GNLY), Granzyme A (GZMA) and B (GZMB), and Perforin (PRF1) mRNA transcript expression were higher in NL compared to bulk naïve and central memory CD4 T cells, but expressed at similar levels as effector cells. Granzyme K (GZMK) was the only molecule that was different between NL CD4 T cells and effector cells (Figure 46).

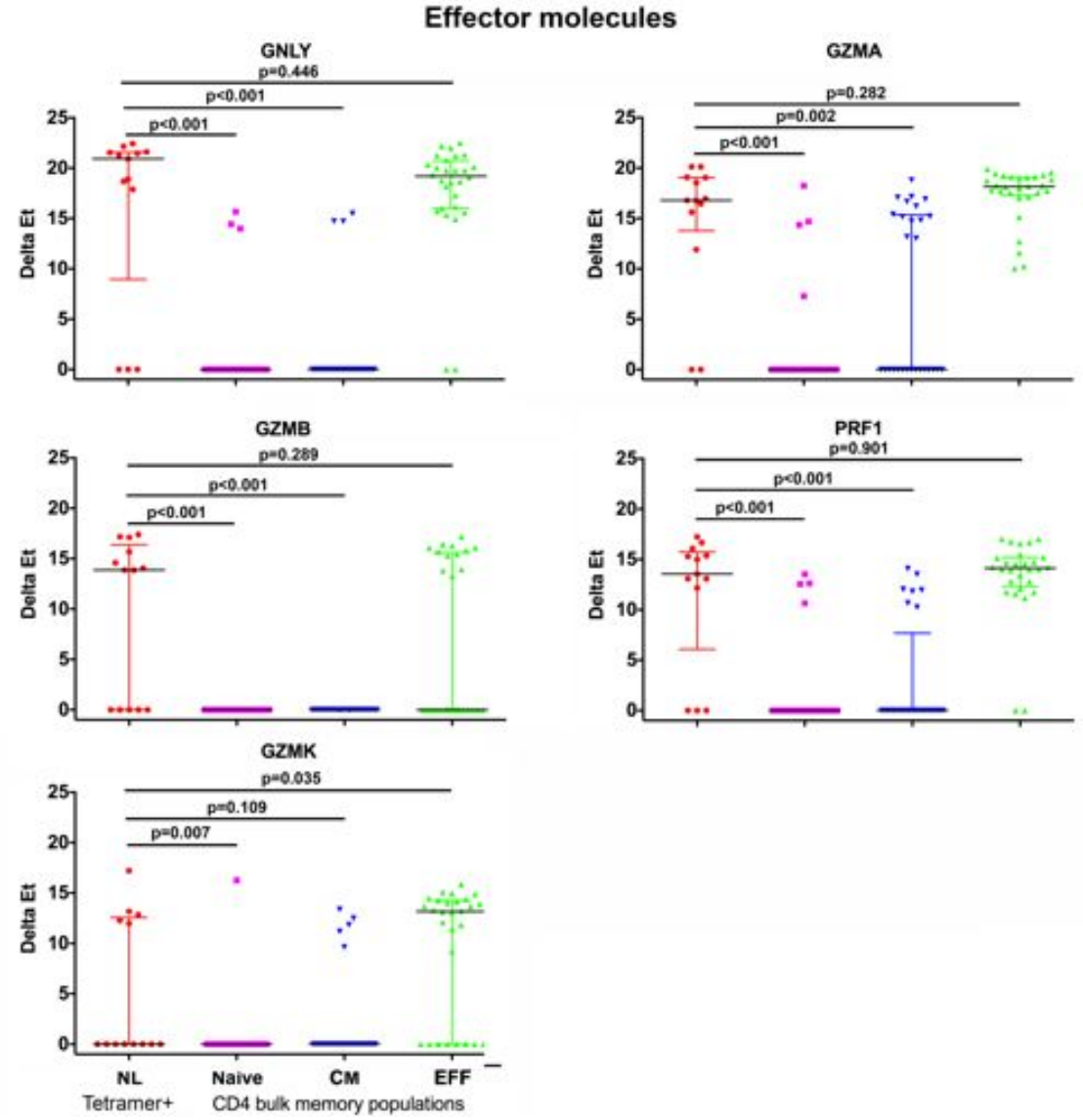

Figure 46: Effector molecule mRNA transcript levels in *M.tb*-specific NL and bulk memory CD4 T cell populations expressed as delta Et values. Each dot represents a sort of 30 cells from 7 LTBI volunteers. Results from seven donors are expressed as delta Et values (normalised to B2M) in each sort of 30 cells. P-values were calculated with the Mann-Whitney test, after correcting for multiple comparisons with the Benjamini Hochberg method with an FDR of 0.05 (q-value). P-values below 0.05 were considered significant.

Other mRNA transcripts levels (median and IQR) that were differentially expressed between the CD4 T cell subsets are listed in Table 35.

Table 35. Differentially expressed gene transcripts in antigen-specific naïve-like CD4 T cells and bulk CD4 T cell populations. Shown are the median and IQR for each population. Transcript levels more abundant in the CFP10-specific naïve-like population compared with the other populations are highlighted in red. Transcript level less abundant in CFP10-specific naïve-like population than bulk T cell populations are highlighted in green. P-values were calculated with the Mann-Whitney test, after correcting for multiple comparisons with the Benjamini Hochberg method with an FDR of 0.05 (q-value). P-values below 0.05 were considered significant.

	Tet+	Bulk CD4					
GENE	Naive-like median [IQR]	Naïve median [IQR]	CM median [IQR]	Eff median [IQR]	Tet+ NL VS Bulk Naïve	Tet+ NL VS Bulk CM	Tet+ NL VS Bulk Eff
ARGHEF18	18.23 [17.47-19.06]	18.99 [18.59-19.66]	18.81 [18.37-19.32]	18.08 [17.78-18.56]	0.000	0.004	>0.999
AXIN2	13.74 [0.00-15.25]	16.63 [15.02-17.64]	15.60 [14.09-16.92]	14.55 [11.93-16.10]	0.000	0.001	0.360
BCL2L11	17.88 [17.18-19.27]	17.57 [16.62-18.70]	16.91 [15.67-17.48]	16.88 [16.32-17.57]	0.429	0.001	0.001
BTLA	15.64 [14.30-16.92]	15.34 [13.74-16.56]	15.29 [14.50-15.85]	14.01 [12.83-15.32]	0.394	0.224	0.001
CAMK4	13.94 [12.72-15.51]	15.48 [14.86-16.47]	14.71 [13.63-15.33]	14.21 [13.59-14.89]	0.001	0.604	0.767
CD154	16.32 [15.12-17.01]	17.38 [16.79-17.99]	17.21 [16.53-17.65]	16.70 [16.79-17.99]	0.000	0.001	0.2325
CD38	13.87 [0.00-14.80]	13.59 [0.00-14.80]	5.18 [0.00-13.62]	0.00 [0.00-0.00]	0.916	0.131	0.000
EPHA4	13.05 [5.51-13.46]	0.00 [0.00-13.55]	15.38 [13.89-16.03]	15.69 [13.58-16.38]	0.115	0.000	0.000
GATA3	17.22 [15.90-17.70]	17.78 [16.23-18.42]	18.42 [17.66-18.88]	19.09 [18.34-19.48]	0.272	0.000	<0.001
ICOS	14.34 [13.59-15.97]	16.32 [15.69-17.01]	16.44 [15.66-16.81]	15.40 [14.26-16.20]	0.001	0.000	0.488
ITGAX	15.88 [0.00-19.54]	0.00 [0.00-0.00]	0.00 [0.00-0.00]	0.00 [0.00-0.00]	<0.001	<0.001	<0.001
ITK	17.93 [17.45-18.80]	18.92 [18.08-19.19]	18.16 [17.69-18.69]	17.69 [17.24-18.08]	0.002	0.718	0.007
LEF1	19.34 [18.77-20.60]	21.12 [20.60-21.72]	19.98 [19.25-20.51]	18.30 [17.72-18.98]	<0.001	0.267	0.000
NFKB1	13.07 [0.00-16.44]	15.44 [14.55-16.56]	14.45 [13.26-15.54]	13.03 [0.00-14.29]	0.215	0.568	0.266
PRKCA	15.73 [0.00-16.80]	17.15 [15.76-17.88]	16.82 [15.65-17.78]	15.66 [14.56-16.66]	0.000	0.001	0.631
RORA	18.93 [17.82-20.11]	19.05 [18.23-19.54]	19.63 [19.28-19.87]	19.57 [19.11-19.89]	0.697	0.003	0.009
RORC	0.00 [0.00-0.00]	0.00 [0.00-0.00]	13.72 [0.00-15.42]	0.00 [0.00-14.09]	0.317	0.168	0.001
SOCS	16.28 [15.16-17.19]	16.67 [15.32-17.63]	14.71 [13.65-15.90]	15.37 [12.93-16.50	0.538	0.001	0.006
STAT4	17.15 [16.66-18.08]	17.40 [16.13-18.25]	16.40 [16.12-16.98]	16.92 [16.33-17.16]	0.855	0.000	0.128
STAT5B	17.77 [17.24-18.80]	18.5 [18.10-18.98]	18.46 [18.02-19.08]	18.17 [17.74-18.52]	0.002	0.001	0.211
TBX21	10.98 [0.00-14.49]	0.00 [0.00-0.00]	0.00 [0.00-0.00]	12.15 [1.34-15.22]	<0.001	0.000	0.479
TCF7	15.21 [14.52-16.27]	16.42 [15.89-16.86]	15.68 [15.20-16.89]	14.75 [13.61-15.24]	0.000	0.164	0.205
CD31	15.05 [0.00-15.88]	14.88 [12.92-15.51]	0.00 [0.00-0.00]	0.00 [0.00-0.00]	0.729	0.000	<0.001
GLOB	19.41 [17.18-20.73]	14.37 [13.00-17.09]	14.77 [11.60-15.54]	14.66 [13.62-15.82]	<0.001	<0.001	<0.001
GPR15	18.43 [16.43-19.47]	13.04 [11.34-16.00]	16.94 [14.09-18.23]	15.88 [14.70-16.61]	<0.001	0.003	<0.001
TIMD4	0.00 [0.00-14.17]	15.07 [0.00-16.22]	12.97 [0.00-14.13]	13.33 [0.00-14.17]	0.004	0.5626	0.525
FCER1G	15.25 [6.52-16.78]	0.00 [0.00-0.00]	0.00 [0.00-0.00]	0.00 [0.00-0.00]	<0.001	<0.001	<0.001
IGF1R	16.93 [16.65-17.92]	18.17 [17.72-18.94]	16.75 [14.99-17.66]	13.80 [3.19-15.52]	0.000	0.237	<0.001
FAM129A	13.27 [0.00-15.60]	0.00 [0.00-0.00]	14.30 [11.88-15.05]	15.55 [13.66-16.24]	0.000	0.895	0.004
PRR5L	16.46 [0.00-17.50]	0.00 [0.00-0.00]	14.72 [0.00-16.00]	17.53 [17.08-18.13]	<0.001	0.125	0.001
JUNB	17.50 [16.90-18.79]	18.56 [17.64-19.10]	17.02 [16.05-17.99]	16.58 [15.84-17.17]	0.267	<0.001	0.000

5.3.7. CFP10-specific CD4 T cell transcriptional profiles

Our finding that CFP10-specific naïve-like cells shared transcript characteristics with bulk effector cells was surprising. We also wanted to compare the transcriptional profile of CFP-10 specific NL CD4 T cell subsets with CFP10-specific central memory and effector CD4 T cells detected by HLA class II tetramer staining. We identified 22 genes that were differentially expressed between the three CFP10-specific T cell populations (Figure 47). Unsupervised hierarchical clustering, performed on expression data of these 22 genes showed that these antigen-specific subsets sorted according to surface CCR7, CD27 and CD45RA marker expression, did not fall into discrete clusters (Figure 47).

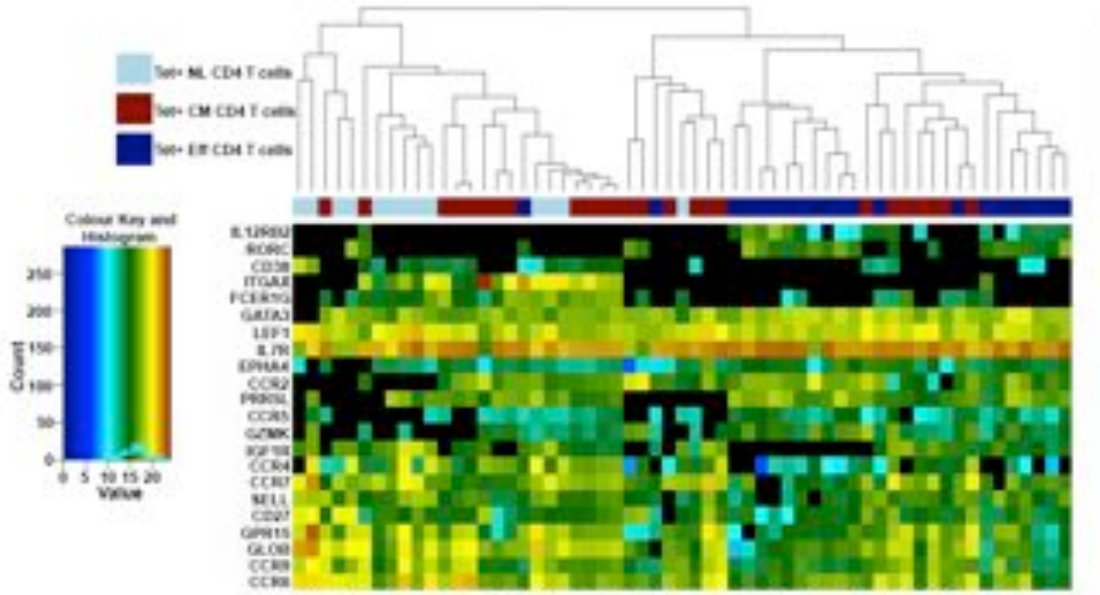

Figure 47: Unsupervised hierarchal clustering of the transcriptional profile of CFP10-specific, DRB1*04:01-CFP10$_{(71-85)}$ and DRB5*01:01-CFP10$_{(51-65)}$ tetramer+, naïve like, central memory and effector CD4 T cell populations shown as delta Et values. Twenty-two genes were differentially expressed between CFP10-specific naïve-like CD4 T cells (grey), central memory CD4 T cells (red) and effector CD4 T cells (blue). Heatmap rows = genes and columns = T cell population per sample.

Some central memory cells clustered with NL CD4 T cells while others clustered with the effector CD4 T cell population. This suggested substantial heterogeneity within CFP10-specific CD4 T cells, even when cells are sub-setted according to commonly used memory markers.

To investigate this further, we performed PCA. The PC1 and PC2 parameters defined in the PCA of the NL and bulk populations were applied to the analysis of the CFP10-specific NL, central memory and effector CD4 T cell populations. We reasoned that this analysis would allow interpretation of transcriptional signatures of CFP10-specific cells in relation to the bulk T cell populations. The CFP10-specific naïve-like CD4 T cell cluster overlapped somewhat with the CFP10-specific central memory population. CFP10-specific central memory cells also overlapped with the CFP10-specific effector population (Figure 48).

The CFP10-specific naïve-like and central memory cells had low PC2 values, which constituted the main factors differentiating them from bulk populations, whereas the CFP10-specific effector cells overlapped with bulk effector CD4 T cells.

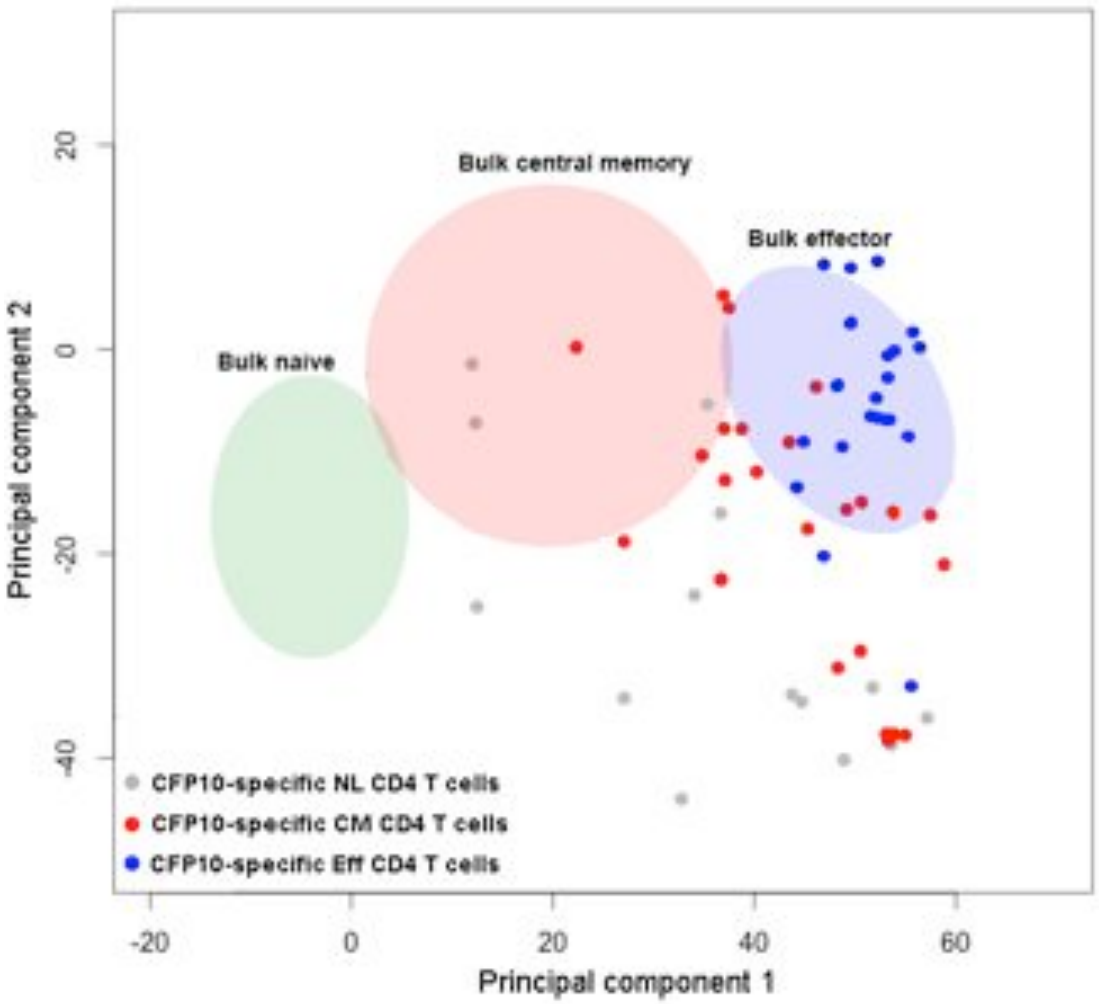

Figure 48: Principal component analysis of the CFP10-specific naive-like, CFP10-specific central memory and effector populations. Shown are the CFP-10 -specific naïve-like CD4 T cells (grey), the CFP-10 specific central memory CD4 T cells and the CFP-10 specific effector CD4 T cells (blue) overlaid over the bulk CD4 T cell populations, shown as shaded ellipses in the background.

To gain a better understanding of how NL cells differed from central memory and effector cells, within the *M.tb*-specific compartment, we compared gene expression levels of cell trafficking molecules. Six chemokine receptors were significantly different between the CFP10-specific T cell populations. We observed no differences in expression CCR4, CCR5, CCR6 and CCR9 levels in CFP10-specific NL cells and central memory T cells, while a subset of NL cells did not express CCR5. However, the expression of these markers in NL cells was higher than in effector cells. CCR2 levels were higher in effector T cells when compared to NL cells, and only a subset of NL cells expressed detectable CCR2 mRNA. Transcript levels of CCR7, a marker for lymph node

trafficking, were higher in NL CD4 T cells when compared with central memory and effector CD4 T cells (Figure 49).

This gene expression pattern of the cell trafficking molecules suggested that in CFP10-specific NL cells shared a similar expression profile with CFP10-specific central memory cells, rather than effector cells.

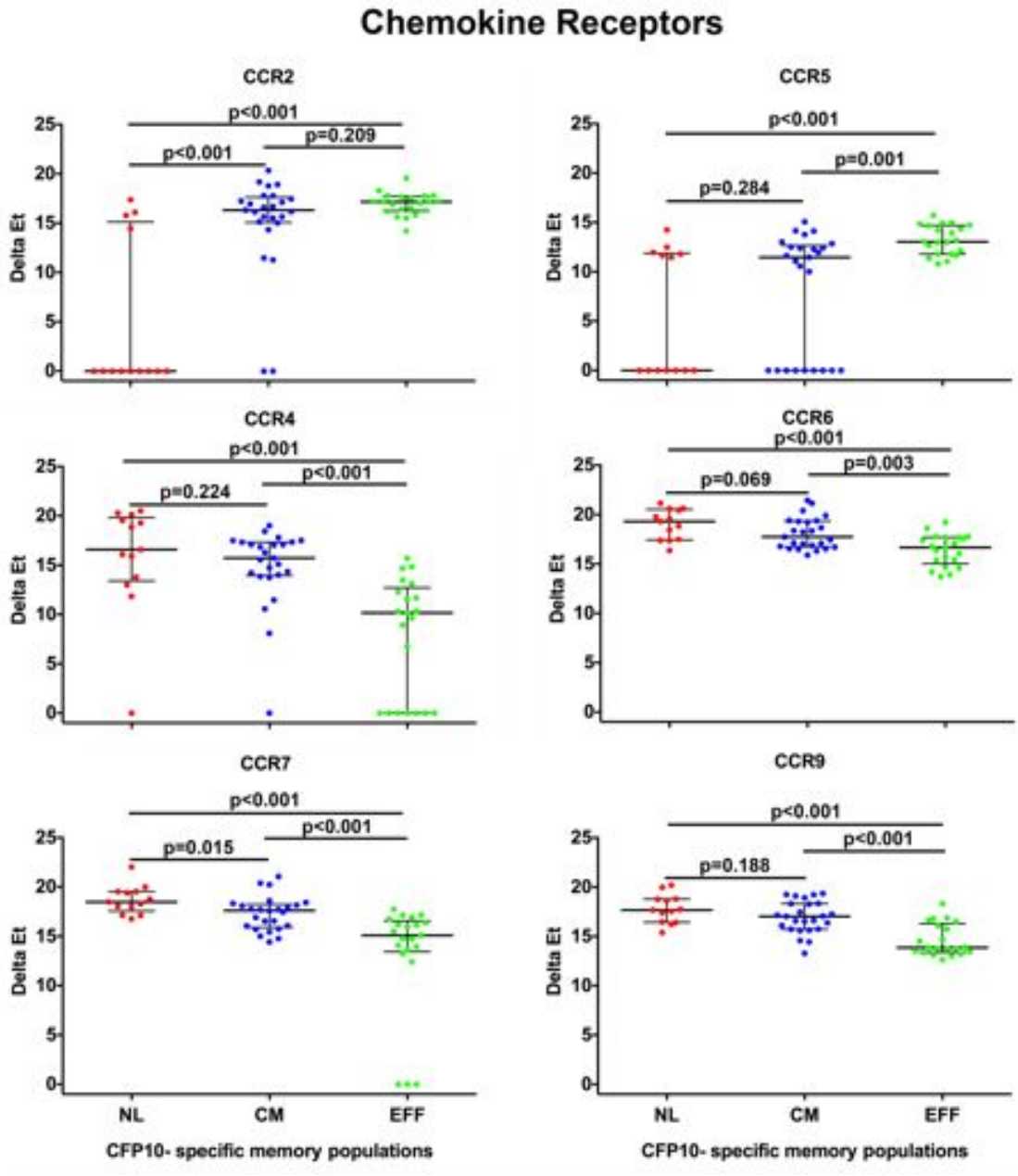

Figure 49: Chemokine receptor mRNA transcript levels in *M.tb*-specific naïve-like, central memory and effector CD4 T cell populations expressed as delta Et values. Each dot represents a sort of 30 cells from 7 LTBI volunteers. Results from seven donors are expressed as delta Et values (normalised to B2M) in each tetramer sort of 30 cells. P-values were calculated with the Mann-Whitney test, after correcting for multiple comparisons with the Benjamini Hochberg method with an FDR of 0.05 (q-value). P-values below 0.05 were considered significant.

Furthermore, we did not observe any significant differences in the expression of transcription factor mRNA levels between the CFP10-specific naïve-like CD4 T cells and CFP10-specific central memory CD4 T cells (Figure 50). GATA3 and RORC transcript levels were higher in CFP10-specific effector

CD4 T cells, compared with CFP10-specific naïve-like CD4 T cells, while LEF1 was higher in CFP10-specific naïve-like CD4 T cells.

GATA3 and RORC transcript levels were significantly higher in CFP10-specific effector CD4 T cells, compared with CFP10-specific central memory CD4 T cells, while LEF1 was expressed at similar levels between the two populations (Figure 50). This data further suggested that CFP10-specific NL cells appear to display a transcriptional profile similar to CFP10-specific central memory cells rather than effector cells.

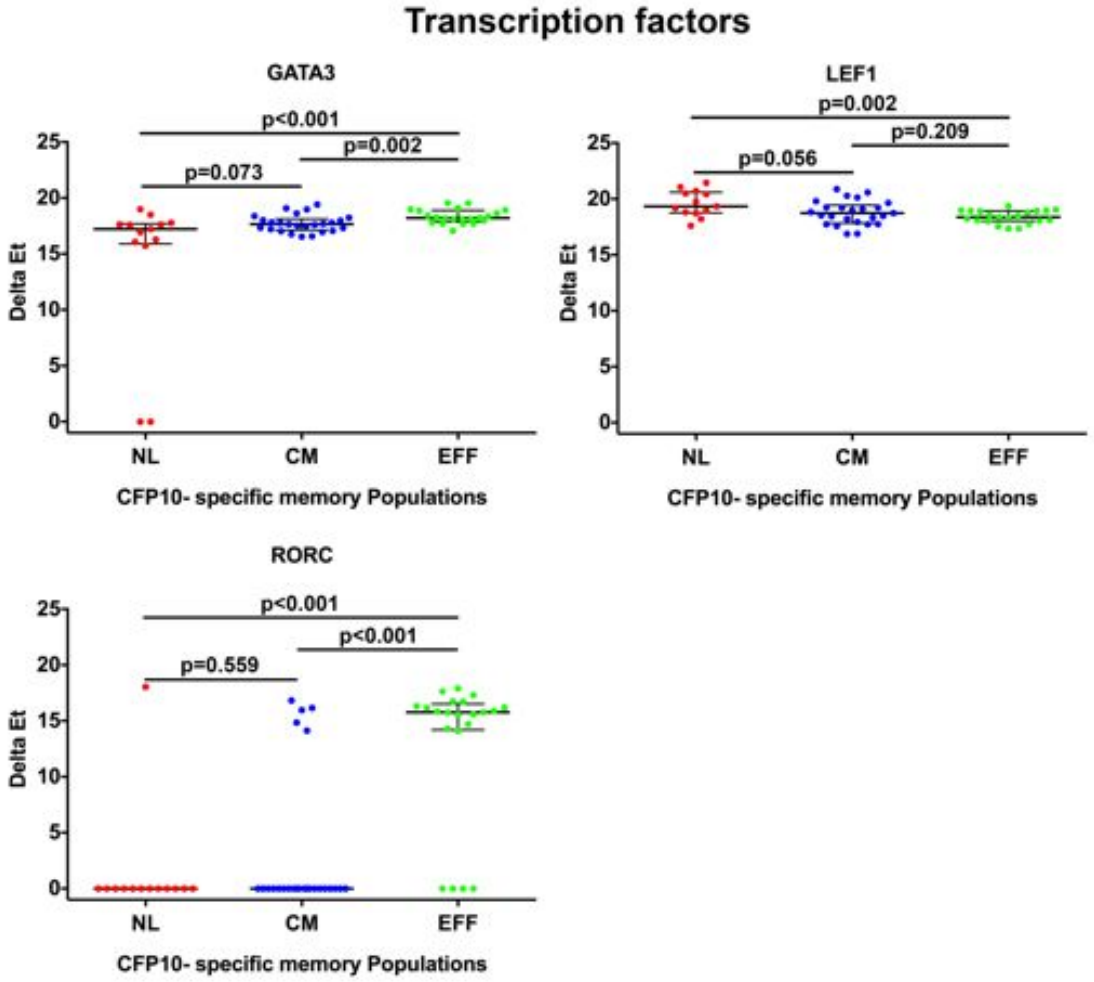

Figure 50: Transcription factor mRNA transcript levels in *M.tb*-specific NL, central memory and effector CD4 T cell populations expressed as delta Et values. Each dot represents a sort of 30 cells from 7 LTBI volunteers. Results from seven donors are expressed as delta Et values (normalised to B2M) in each tetramer sort of 30 cells. P-values were calculated with the Mann-Whitney test, after correcting for multiple comparisons with the Benjamini Hochberg method with an FDR of 0.05 (q-value). P-values below 0.05 were considered significant.

As the data suggested that CFP10-specific NL cells shared a transcriptional profile similar to that of central memory cells rather than effector cells, prompted us to investigate the expression of effector molecules and effector cytokines. The only effector molecule for which mRNA transcriptional levels were different between the CFP10-specific T cell populations was Granzyme K (GZMK). GZMK was expressed at significantly higher levels by antigen-specific effector and central memory CD4 T cells compared with naïve-like CD4 T cells, many of which did not express detectable levels of GZMK. However, transcript levels of GZMK were not significantly different between CFP10-specific effector and central memory CD4 T cells (Figure 51).

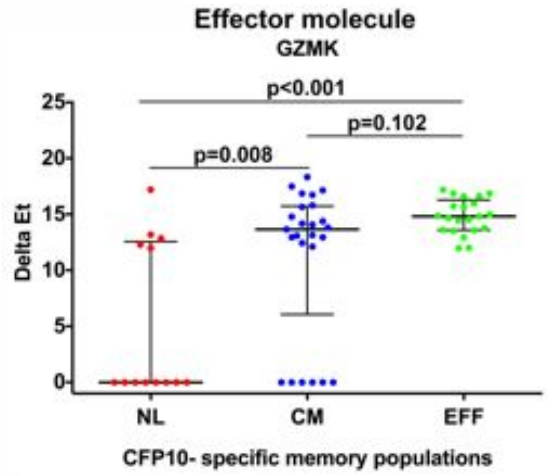

Figure 51: Granzyme K mRNA transcript levels in *M.tb*-specific NL, central memory and effector CD4 T cell populations expressed as delta Et values. Each dot represents a sort of 30 cells from 7 LTBI volunteers. Results from seven donors are expressed as delta Et values (normalised to B2M) in each tetramer sort of 30 cells. P-values were calculated with the Mann-Whitney test, after correcting for multiple comparisons with the Benjamini Hochberg method with an FDR of 0.05 (q-value). P-values below 0.05 were considered significant.

CFP10-specific naïve-like cells expressed significantly lower levels of the cytokine receptor, IL7R, than CFP10-specific central memory and effector CD4 T cell populations, while the latter expressed significantly higher levels of IL7R transcript, compared with the central memory population (Figure 52).

IL12RB2 transcript levels were not different between CFP10-specific NL and CM CD4 T cell populations, and virtually no expression was observed in these

two populations. However, it was expressed at significantly higher levels in CFP10-specific effector CD4 T cells.

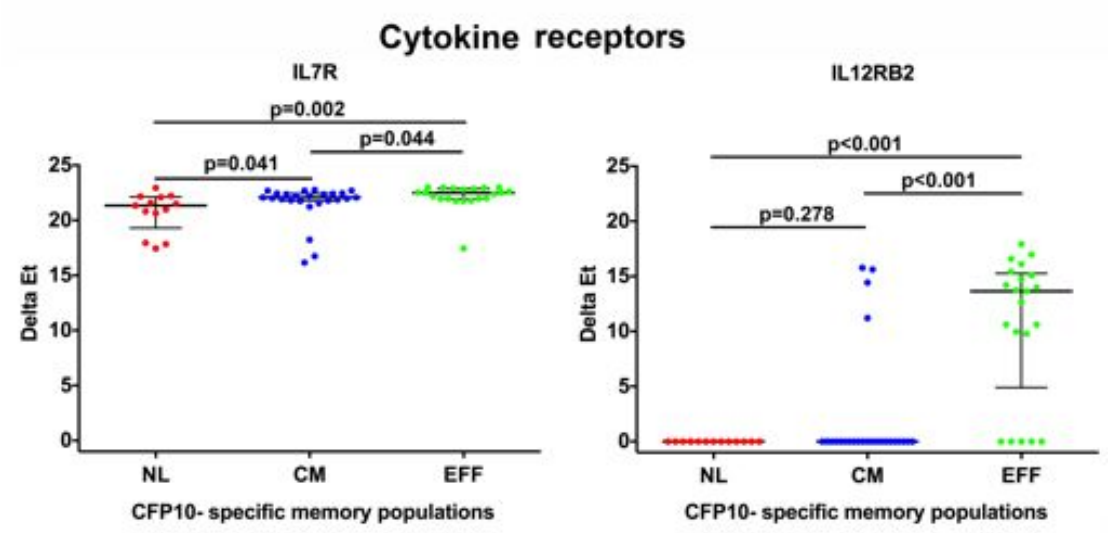

Figure 52: Cytokine receptor mRNA transcript levels in *M.tb*-specific NL, central memory and effector CD4 T cell populations expressed as delta Et values. Each dot represents a sort of 30 cells from 7 LTBI volunteers. Results from seven donors are expressed as delta Et values (normalised to B2M) in each tetramer sort of 30 cells. P-values were calculated with the Mann-Whitney test, after correcting for multiple comparisons with the Benjamini Hochberg method with an FDR of 0.05 (q-value). P-values below 0.05 were considered significant.

Differences in mRNA transcript levels of other genes are shown in Table 36. Significant differences between CFP10-specific memory subsets were observed in genes involved in T cell activation and cell trafficking, as well as genes that were selected based on the Gattinoni et al., and Appay et al., gene lists. The data in Table 36, further suggests that CFP10-specific naïve-like CD4 T cells share a transcriptional profile with CFP10-specific central memory cells.

Table 36: Differentially expressed gene transcript levels in CFP10-specific naïve-like CD4 T cells compared with CFP10-specific central memory and effector CD4 T cells. Shown are the median and IQR for each population. Transcript levels more abundant in the CFP10-specific naïve-like population compared with the other populations are highlighted in red. Transcript level less abundant in CFP10-specific naïve-like population than other CFP10-specific T cell populations are highlighted in green. Values shown in red, are significant differences observed between CFP10-specific effector and central memory T cells. P-values were calculated with the Mann-Whitney test, after correcting for multiple comparisons with the Benjamini Hochberg method with an FDR of 0.05 (q-value). P-values below 0.05 were considered significant.

Gene	Tet+ Naive-like median [IQR]	Tet+ CM median [IQR]	Tet+ Effector median [IQR]	Tet+ NL VS Tet+ CM	Tet+ NL VS Tet+ Eff	Tet+ CM VS Tet+
CD38	13.87 [0.0-14.80]	0.00 [0.0-13.91]	0.00 [0.0-0.0]	0.134	<0.001	0.022
EPHA4	13.05 [5.5-13.46]	13.49 [11.61-14.72]	14.48 [13.79-15.58]	0.105	<0.001	0.021
ITGAX	15.88 [0.0-19.54]	0.00 [0.0-18.46]	0.00 [0.0-0.0]	0.416	0.002	0.014
GLOB	19.41 [17.18-20.73]	18.39 [17.03-19.03]	15.76 [12.85-16.60]	0.133	<0.001	<0.001
GPR15	18.43 [16.43-19.47]	17.25 [16.02-18.71]	15.38 [12.71-16.47]	0.199	<0.001	0.003
FCER1G	15.25 [6.52-16.78]	14.21 [0.0-16.73]	0.0 [0.0-11.73]	0.622	<0.001	0.001
IGF1R	16.93 [16.65-17.92]	14.55 [0.0-16.19]	13.34 [0.0-15.42]	<0.001	<0.001	0.165
PRR5L	16.46 [0.0-17.50]	15.85 [0.0-16.67]	17.04 [16.28-18.00]	0.351	0.183	<0.001

5.5. Discussion

In this chapter we characterised the transcriptional profile of CFP10-specific naïve-like CD4 T cells in natural *M.tb* infection. We hypothesised that CFP10-specific naïve-like CD4 T cells had a transcriptional profile distinct from truly naive, bulk central memory, bulk effector as well as the CFP10-specific central memory and effector CD4 T cell populations. We have showed that CFP10-specific naïve-like CD4 T cells: i) had a transcriptional profile distinct from truly naïve bulk CD4 T cells, ii) displayed a functional and trafficking molecule patterns similar to that of bulk effector CD4 T cells and iii) had a transcriptional profile similar to that of the CFP10-specific central memory T cell.

We have shown that Ag85A-specific naïve-like $CD4^+$ T cells were mostly CD95-negative, a hallmark marker for T_{SCM} along with CCR7, CD27 and CD45RA expression, suggesting that these mycobacteria-specific cells are not T_{SCM} cells (Gattinoni et al. 2011). Our experiments to determine if NL cells were T_{SCM} cells were performed on limited numbers of cryopreserved PBMCs from MVA85A-vaccinated subjects. Since T_{SCM} cells typically occur at very low frequencies in peripheral blood (Gattinoni et al. 2011), we cannot definitively rule out whether these cells exist in the mycobacteria-specific repertoire. By contrast, Ag85A-specific naïve-like $CD4^+$ T cells were surprisingly abundant.

The combination of T cell sorting by flow cytometry and multiplexed microfluidic qRT-PCR (Fluidigm) allows thorough interrogation of transcriptional profiles of rare cell subsets (Dominguez et al. 2013). We developed methodology to combine tetramer-stained cell sorting and microfluidic qRT-PCR, as well as data analysis and quality control measures to explore the transcriptional profile of *M.tb*-specific NL CD4 T cells. Patterns of mRNA expression of the phenotypic surface markers CCR7, SELL (CD62L) and CD27 confirmed that our methodology and analysis pipeline yielded expected results. We could not measure CD45RA transcriptional levels because this is an isoform of the CD45 protein.

We aimed to determine if CFP10-specific naïve-like CD4 T cells were distinct from truly naïve bulk CD4 T cells. We identified 50 genes that were differentially expressed between naïve and memory T cell populations. These genes included chemokine receptors, cytokines and cytokine receptors, inhibitory molecules, kinases involved in signaling, a co-stimulatory molecule, molecules involved in tissue homing, effector molecules and transcription factors. Nine of the 13 genes selected based on literature published by Gattinoni (Gattinoni et al. 2011) and Appay (Appay et al. 2007) were differentially expressed in these populations and mostly at higher levels in CFP10-specific naïve like CD4 T cells than in other bulk T cell populations.

Several lines of evidence suggest that NL cells are not truly naïve cells. Unsupervised hierarchal clustering of the T cell populations showed that CFP10-specific CD4 T cells did not cluster with naïve bulk CD4 T cells, but rather clustered with bulk effector CD4 T cells. Principal component analysis confirmed this clustering behaviour, showing CFP10-specific CD4 T cells clustering alone, but within close proximity to bulk effector CD4 T cells. CFP10-specific naïve-like CD4 T cells displayed a transcriptional profile that resembled that of bulk effector CD4 T cells, expressing effector molecules and cytokines, suggesting that they may have effector function. High expression levels of chemokine receptors also suggest that CFP10-specific naïve-like CD4 T cells may have ability to rapidly traffic to tissues and play a role in inflammatory processes during *M.tb* infection. The high expression levels of cytokines and effector molecules observed further support this possible role in inflammation.

Analysis of CFP10-specific naïve-like, central memory and effector populations identified 22 genes that were differentially expressed between the 3 populations. These genes included chemokine receptors, transcription factors, an effector molecule, a co-stimulatory molecule, homing markers, a cytokine receptor, a kinase receptor and 5 of the genes selected based on the literature published by Gattinoni (Gattinoni et al. 2011), and Appay (Appay et al. 2007). Unsupervised hierarchal clustering showed that CFP10-specific naïve-like CD4 T cells clustered with CFP10-specific central memory CD4 T

cells rather than with CFP10-specific effector T cells. Principal component analysis of the CFP10-specific population showed all three populations clustering closely together and with bulk effector CD4 T cells. CFP10-specific naïve-like CD4 T cells had transcriptional profiles similar to both CFP10-specific central memory and effector memory cells. Interestingly, CFP10-specific central memory cells also clustered with the bulk effector T cell population rather than with bulk central memory T cells. The amount of overlap observed in these memory subsets suggests a substantial degree of heterogeneity.

Closer analysis of the CFP10-specific CD4 T cell populations showed heterogeneity within these populations. Unlike mRNA levels of CCR7, CD27 and SELL (CD62L), which were homogeneously expressed in all cells of a given subset, levels of other transcripts, such as chemokine receptors, were very heterogeneous across multiple sorts of the same cell subset. This heterogeneity may be addressed by performing single cell sorting and transcriptional profiling in future.

In addition, to delineate this naïve-like memory T cell population further, spectratyping of the complementary DNA (cDNA) across the TCR third complementary determining region (CDR3) region could generate information about the relative frequencies of different CDR3 length products. As various T-cell clones have different sequences or lengths of CDR3, analysis of the CDR3 could be used to determine the overall TCR repertoire diversity of this population (Ciupe et al. 2013; Pannetier et al. 1995). Furthermore, using an antigen-specific T cell control population, such as cells detected by CMV-specific HLA class II tetramers would be important to interpret transcriptional profiles and in determining if our results reflect attributes of antigen-specific cells or *M.tb*-specific patterns.

Further experiments are required to understand the functional properties of *M.tb*-specific naïve-like CD4 T cells. The observation that CFP10-specific NL cells express mRNAs encoding cytotoxic molecules and pro-inflammatory cytokines, similar to that of effector cells, suggest that these cells may have

effector functions. Future experiments should explore intracellular expression of these molecules by flow cytometry upon cell stimulation. Chemokine receptor cell surface expression should also be measured by flow cytometry. To determine how differentiated these cells really are, another option may be measurement of T cell telomere lengths, as highly differentiated cells have short telomeres when compared with naïve cells, or cells that have only recently recognised antigen (Weng et al. 1995; Son et al. 2000; Hodes et al. 2002).

5.6. Contributions:

Munyaradzi Musvosvi contributed to the analysis of the data generated in this chapter.

Chapter 6. General conclusion

6.1. Conclusion

The objective of this thesis was to characterise *M.tb*-specific CD4 T cells after MVA85A vaccination and in natural, asymptomatic *M.tb* infection. Because it is not known exactly which CD4 T cell characteristics are important for protection, we aimed to assess T cell memory phenotype, homing marker expression, effector functions and proliferative capacity. We postulated that long-lived memory CD4 T cells with high proliferative capacity and the ability to home to the site of infection upon re-exposure to antigen may protect against TB, and that TB vaccines should aim to induce this phenotype of T cells. We chose to use HLA class II tetramers to avoid or minimise activation of lymphocytes and obtain a snap shot of the direct *ex vivo* phenotype of CD4 T cells. To be able to achieve this aim, we first generated tetramer reagents. Using data from previously completed MVA85A vaccine trials, as well as healthy LTBI individuals, we were able to identify commonly recognised epitopes in the *M.tb* proteins, Ag85A, ESAT6 and CFP10 and determine their HLA restriction. The epitopes defined in these three antigens were then used to synthesise multiple tetramers of which 3 were selected for further studies in this thesis. Given the paucity of published HLA class II tetramers with highly specific T cell binding properties, this work should be of value to the field of mycobacterial immunology.

Armed with these new detection tools, we identified and characterised Ag85A-specific CD4 T cells after MVA85A vaccination. We showed that early after vaccination cells predominantly displayed an effector phenotype, that waned, and T cells reverted to either a naïve-like or central memory phenotype. The observed higher proportion of Ag85A-specific $CD45RA^{-}CCR7^{+}$ CD4 T_{CM} cells rather than T_E persisting up to one year after MVA85A vaccination, contradicts our previous finding in adolescents, which showed that antigen-specific T cells predominantly displayed a T_E phenotype up to 2 months post-vaccination (Scriba et al. 2010). We recently completed a long-term follow-up study of MVA85A vaccinees (involving a cohort of adults, adolescents, children and

infants) and reported highly durable Ag85A-specific memory CD4 T cell responses 3-5 years post vaccination. We observed Ag85A-specific CD4 T cells with mixed central and effector memory phenotypes in these individuals (Tameris et al. 2014). These results highlight discordance between memory phenotypes and durability of antigen-specific immune responses, which require investigation.

Another hypothesis is that induction of antigen-specific effector memory T cells that can readily traffic to the site of infection may afford immediate protection against *M.tb* by clearing the pathogen before it is able to replicate and establish persistent infection and disease (Hansen et al. 2011). This priming strategy may be effective against simian immunodeficiency virus (SIV) infection in non-human primates. Picker et al., have shown that use of a CMV-based vaccine vector induced a persistent population of T_{EM} that successfully controlled highly pathogenic SIV infection early after mucosal challenge (Hansen et al. 2011). This strategy may also have application in the field of TB vaccines. However, given the recent data that MVA85A-specific cells predominantly displayed an effector memory phenotype in infants (Tameris et al. 2014), and yet MVA85A did not provide evidence of efficacy against TB disease or *M.tb* infection, argues against this. There are many other possible reasons underlying the observed lack of efficacy in infants that may include route and/or age of administration, dose of the vaccine, the high rate of *M.tb* transmission in the trial population, or the magnitude, function and/or phenotype of the induced immune response. More research is required to understand T cell memory in mycobacterial infection.

We showed that CLA expression by MVA85A-specific effector CD4 T cells was not mutually exclusive to expression of other T cell homing markers, such as α4, β7 or β1. This finding suggests that T cells primed after intradermal vaccination may not be confined to the skin since these cells expressed receptors for homing to other sites of inflammation as it was previously suggested (Kaufmann & McMichael 2005; Kantele et al. 1999; Walzl et al. 2011; D. J. Campbell & Butcher 2002; Walrath & Silver 2010; J. A. Burns et

al. 2001). Regardless, our results suggest that CD4 T cell expression of homing markers may be more complex than previously acknowledged. Importantly, boosting immune responses in the skin, rather than in the respiratory tract, may lead to weaker and delayed T cell responses in the lung, following challenge with *M.tb*. Mice vaccinated intra-nasally with adenovirus expressing Ag85A (Ad85A), after a BCG subcutaneous prime, had lower mycobacterial burdens in their lungs, than mice given an intradermal boost with Ad85A, or mice vaccinated with BCG only (Forbes et al. 2008). This reduced bacterial burden was attributed to higher peripheral/splenic/lung antigen-specific T cell responses and lung-resident T cell responses prior to infection in intra-nasally vaccinated mice, compared with intra-dermally Ad35 boosted mice (Forbes et al. 2008; Santosuosso et al. 2005). Collectively, these observations suggest that a vaccination route that mimics the natural entry portal of the pathogen may be more efficacious by inducing a tissue-resident population of primed T cells.

A limitation of our study of MVA85A induced CD4 T cells was that we could only use a single HLA class II tetramer to identify Ag85A-specific CD4 T cells. We cannot rule out that functional and phenotypic characteristics of CD4 T cells specific for other Ag85A epitopes may be different to the epitope we studied. Despite this, our work highlights the utility of HLA class II tetramers in detecting and characterising vaccine induced responses and how these powerful tools can be used to complement other functional assays. This work therefore adds to the understanding of vaccine induced T cell immunity.

We observed a curious population of naïve-like antigen-specific CD4 T cells in MVA85A vaccinees, as described in Chapter 3. To gain a better understanding of this novel cell subset, we performed transcriptional profiling of sorted bulk and antigen-specific CD4 T cell populations. Interrogation of the gene expression profiles of *M.tb*-specific naïve-like CD4 T cells showed that CFP10-specific naïve-like CD4 T cells were distinct from truly naïve cells and that they were most similar to bulk effector cells. These CFP10-specific naïve-like T cells expressed high levels of transcripts encoding chemokine receptors, cytotoxic molecules, as well as effector cytokines, further supporting their

close resemblance to effector cells. While previous studies had observed expression of effector cytokines upon stimulation of these cells (Kagina et al. 2009; Caccamo et al. 2006; Tena-Coki et al. 2010; Soares et al. 2008), we were surprised to observe high mRNA expression levels of effector molecules directly *ex vivo*.

While these observations require confirmation on a protein expression level, they raise interesting questions regarding functional potential of naïve-like cells and the regulation of these functions. The curious mRNA transcript patterns of naïve-like CD4 T cells could be due to programmed epigenetic modifications of DNA by either methylation or histone modifications, that modulate accessibility of genes for transcription (Youngblood et al. 2013). These mechanisms have recently been shown to modulate transcriptional activation of effector molecules through access restriction to chromatin by transcription factors and polymerases (Youngblood et al. 2013). This mechanism allows rapid recall of effector functions by having a pre-poised accessibility to effector genes and may explain why high transcript levels are present in unstimulated cells. It is tempting to speculate that the high levels of effector molecule transcript expression in naïve-like cells may be in line with this mechanism. However, such transcriptional control does not always translate into protein as many other post-transcriptional mechanisms are also involved (Youngblood et al. 2013). Differential protein expression of CCR7 and CD62L on effector memory and central memory cells has also been attributed to transcriptional regulation of gene products from a subset of genes known as on-off-on genes. On-off-on genes are expressed in naïve cells and repressed in antigen-experienced cells. Their expression is postulated to be due to programming and regulating accessibility to the genes chromatin (Youngblood et al. 2013). Our analysis of CFP10-specific naïve-like, central memory and effector CD4 T cells showed that all three CFP10-specific populations clustered more closely with bulk effector cells, rather than with the respective bulk populations. This suggests that *M.tb*-specific CD4 T cells, irrespective of their surface expression patterns of CCR7, CD27 and CD45RA, appear similarly differentiated to bulk CD45RA-CCR7- effector T cells. The observed effector memory-like characteristics of *M.tb*-specific CD4 T cells may be due to constant re-exposure of the cells to *M.tb,* which is consistent

with the QFT-positive status of these individuals, suggesting persistent *M.tb* infection. Further, transmission rates of *M.tb* are extremely high in this endemic setting in South Africa. Although less likely than persisting *M.tb* infection driving effector responses, our observations may also reflect repeated re-exposure to *M.tb* (Verver et al. 2004). Finally, it is also possible that the highly differentiated *M.tb*-specific CD4 T cells may simply be a unique property of *M.tb*-specific cells. An important addition to future experiments would be inclusion of control tetramers bearing epitopes from other infections agents, such as influenza, EBV or CMV. Phenotypic and transcriptomic characteristics of CD4 T cells specific for cleared and chronic infections may aid interpretation of our results. Since the bulk memory CD4 T cell profile is a mixture of cells specific to other cleared and persistent infections, this subset is not an ideal comparator for our analyses.

Our analyses of gene expression profiles have been highly informative and generated a number of hypotheses about the potential roles and functions of *M.tb*-specific NL T cells. With this in mind, we have proposed a number of further experiments to delineate the possible functions of these cells, as described in Chapter 5, section 5.5.

Possibly the greatest caveat of the work described in this thesis is that the use of tetramers to study T cell populations restricts the breadth of antigen-specific responses and HLA-allele coverage, and therefore only reflects a sub-population of the entire response to the antigen. When possible, it is recommended that multiple tetramers bearing multiple epitopes from the same antigen be utilised together, to gain a better reflection of a broader antigen-specific response. As recently shown, highly multiplexed HLA class II tetramer staining can be combined with mass cytometry (CyTOF) to achieve in-depth protein expression analysis on a single cell level (Newell et al. 2013). Since CyToF allows simultaneous analysis of up to 40 parameters per cell, this technology has enormous potential for exploring the complexity of immunity (Newell et al. 2012). This technology has been recently implemented in our group and will be used for future studies.

Finally, our work suggests that defining memory subsets using well-established memory markers such as CD45RA, CCR7 to pigeon-hole *M.tb*-specific CD4 T cells may not be appropriate, and does not reflect their functionality, as inferred from mRNA expression patterns and functional assays. Even in CD8 T cells, which have been the basis of most memory phenotype and functionality models, it is emerging that phenotype delineation using these markers does not always reflect the functions previously thought to correspond with memory phenotype (Appay et al. 2008). This phenotype-based model, developed mainly while studying virus-specific CD8 T cells, appears to be even less applicable to CD4 T cells. While protein validation is required to back up our transcriptomic results, new markers, or new combinations of markers, are needed to meaningfully define CD4 T cell memory subsets.

References:

Abbas, A.K. et al., 2013. Regulatory T cells: recommendations to simplify the nomenclature. *Nat Immunol*, 14(4), pp.307–308.

Abel, B. et al., 2010. The novel tuberculosis vaccine, AERAS-402, induces robust and polyfunctional CD4+ and CD8+ T cells in adults. *Am J Respir Crit Care Med*, 181(12), pp.1407–1417.

Abu-Raddad, L.J. et al., 2009. Epidemiological benefits of more-effective tuberculosis vaccines, drugs, and diagnostics. *Proc Natl Acad Sci U S A*, 106(33), pp.13980–13985.

Acosta-Rodriguez, E.V. et al., 2007. Surface phenotype and antigenic specificity of human interleukin 17-producing T helper memory cells. *Nat Immunol*, 8(6), pp.639–646.

Adekambi, T. et al., 2012. Distinct effector memory CD4+ T cell signatures in latent Mycobacterium tuberculosis infection, BCG vaccination and clinically resolved tuberculosis. *PLoS One*, 7(4), p.e36046.

Ahmed, R. & Akondy, R.S., 2011. Insights into human CD8(+) T-cell memory using the yellow fever and smallpox vaccines. *Immunol Cell Biol*, 89(3), pp.340–345.

Akondy, R.S. et al., 2009. The yellow fever virus vaccine induces a broad and polyfunctional human memory CD8+ T cell response. *J Immunol*, 183(12), pp.7919–7930.

Algood, H.M., Lin, P.L. & Flynn, J.L., 2005. Tumor necrosis factor and chemokine interactions in the formation and maintenance of granulomas in tuberculosis. *Clin Infect Dis*, 41 Suppl 3, pp.S189–93.

Altman, J.D. et al., 1996. Phenotypic analysis of antigen-specific T lymphocytes. *Science*, 274(5284), pp.94–96.

Andrews, J.R. et al., 2012. Risk of progression to active tuberculosis following reinfection with Mycobacterium tuberculosis. *Clin Infect Dis*, 54(6), pp.784–791.

Appay, V. et al., 2008. Phenotype and function of human T lymphocyte subsets: consensus and issues. *Cytometry A*, 73(11), pp.975–983.

Appay, V. et al., 2007. Sensitive gene expression profiling of human T cell subsets reveals parallel post-thymic differentiation for CD4+ and CD8+ lineages. *J Immunol*, 179(11), pp.7406–7414.

Arlehamn, C.S. et al., 2012. Dissecting mechanisms of immunodominance to the common tuberculosis antigens ESAT-6, CFP10, Rv2031c (hspX), Rv2654c (TB7.7), and Rv1038c (EsxJ). *J Immunol*, 188(10), pp.5020–5031.

Baekkevold, E.S. et al., 2005. A role for CCR4 in development of mature circulating cutaneous T helper memory cell populations. *J Exp Med*, 201(7), pp.1045–1051.

Banchereau, J. & Steinman, R.M., 1998. Dendritic cells and the control of immunity. *Nature*.

Barry, C.E. et al., 2009. The spectrum of latent tuberculosis: rethinking the biology and intervention strategies. *Nat Rev Microbiol*, 7(12), pp.845–855.

Bastian, M. et al., 2008. Mycobacterial lipopeptides elicit CD4+ CTLs in Mycobacterium tuberculosis-infected humans. *J Immunol*, 180(5), pp.3436–3446.

Bedognetti, D. et al., 2010. Gene-expression profiling in vaccine therapy and immunotherapy for cancer. *Expert Rev Vaccines*, 9(6), pp.555–565.

Behr, M.A. et al., 1999. Comparative genomics of BCG vaccines by whole-genome DNA microarray. *Science*, 284(5419), pp.1520–1523.

Ben Youngblood, Hale, J.S. & Ahmed, R., 2013. T-cell memory differentiation: insights from transcriptional signatures and epigenetics. *Immunology*, 139(3), pp.277–284.

Benjamini, Y. & Hochberg, Y., 1995. Controlling the false discovery rate: a practical and powerful approach to multiple testing. *Journal of the Royal Statistical Society Series B …*.

Beveridge, N.E. et al., 2007. Immunisation with BCG and recombinant MVA85A induces long-lasting, polyfunctional Mycobacterium tuberculosis-specific CD4+ memory T lymphocyte populations. *Eur J Immunol*, 37(11), pp.3089–3100.

Beveridge, N.E.R. et al., 2008. A comparison of IFNgamma detection methods used in tuberculosis vaccine trials. *Tuberculosis (Edinb)*, 88(6), pp.631–640.

Blanchard, T.J. et al., 1998. Modified vaccinia virus Ankara undergoes limited replication in human cells and lacks several immunomodulatory proteins: implications for use as a human vaccine. *J Gen Virol*, 79 (Pt 5), pp.1159–1167.

Blomgran, R. et al., 2012. Mycobacterium tuberculosis inhibits neutrophil apoptosis, leading to delayed activation of naive CD4 T cells. *Cell Host Microbe*, 11(1), pp.81–90.

Bluestone, J.A. & Abbas, A.K., 2003. Natural versus adaptive regulatory T cells. *Nature Reviews Immunology*.

Brennan, M.J. & Thole, J., 2012. [CITATION][C]. *Tuberculosis*.

Brooks-Pollock, E. et al., 2011. Epidemiologic inference from the distribution

of tuberculosis cases in households in Lima, Peru. *J Infect Dis*, 203(11), pp.1582–1589.

Bruns, H. et al., 2009. Anti-TNF immunotherapy reduces CD8+ T cell-mediated antimicrobial activity against Mycobacterium tuberculosis in humans. *J Clin Invest*, 119(5), pp.1167–1177.

Burns, J.A. et al., 2001. The alpha 4 beta 1 (very late antigen (VLA)-4, CD49d/CD29) and alpha 5 beta 1 (VLA-5, CD49e/CD29) integrins mediate beta 2 (CD11/CD18) integrin-independent neutrophil recruitment to endotoxin-induced lung inflammation. *J Immunol*, 166(7), pp.4644–4649.

Burns, M.J. et al., 2005. Standardisation of data from real-time quantitative PCR methods - evaluation of outliers and comparison of calibration curves. *BMC biotechnology*, 5, p.31.

Caccamo, N. et al., 2006. Phenotypical and functional analysis of memory and effector human CD8 T cells specific for mycobacterial antigens. *J Immunol*, 177(3), pp.1780–1785.

Cameron, T.O. et al., 2001. Cutting edge: detection of antigen-specific CD4+ T cells by HLA-DR1 oligomers is dependent on the T cell activation state. *J Immunol*, 166(2), pp.741–745.

Cameron, T.O. et al., 2002. Labeling antigen-specific CD4(+) T cells with class II MHC oligomers. *J Immunol Methods*, 268(1), pp.51–69.

Campbell, D.J. & Butcher, E.C., 2002. Rapid acquisition of tissue-specific homing phenotypes by CD4(+) T cells activated in cutaneous or mucosal lymphoid tissues. *J Exp Med*, 195(1), pp.135–141.

Campbell, J.J. et al., 1999. The chemokine receptor CCR4 in vascular recognition by cutaneous but not intestinal memory T cells. *Nature*, 400(6746), pp.776–780.

Canaday, D.H. et al., 2001. CD4(+) and CD8(+) T cells kill intracellular Mycobacterium tuberculosis by a perforin and Fas/Fas ligand-independent mechanism. *J Immunol*, 167(5), pp.2734–2742.

Caruso, A.M. et al., 1999. Mice deficient in CD4 T cells have only transiently diminished levels of IFN-gamma, yet succumb to tuberculosis. *J Immunol*, 162(9), pp.5407–5416.

Cellerai, C. et al., 2007. Functional and phenotypic characterization of tetanus toxoid-specific human CD4+ T cells following re-immunization. *Eur J Immunol*, 37(4), pp.1129–1138.

Chao, C.C., Jensen, R. & Dailey, M.O., 1997. Mechanisms of L-selectin regulation by activated T cells. *J Immunol*, 159(4), pp.1686–1694.

Chiang, C.-Y. & Riley, L.W., 2005. Exogenous reinfection in tuberculosis.

Lancet Infect Dis, 5(10), pp.629–636.

Chiricozzi, A. & Krueger, J.G., 2013. IL-17 targeted therapies for psoriasis. *Expert Opinion on Investigational Drugs*, 22(8), pp.993–1005.

Churchyard, G.J. et al., 2014. A trial of mass isoniazid preventive therapy for tuberculosis control. *N Engl J Med*, 370(4), pp.301–310.

Ciupe, S.M., Devlin, B.H. & Markert, M.L., 2013. Quantification of total T-cell receptor diversity by flow cytometry and spectratyping. *BMC immunology*.

Colditz, G.A. et al., 1994. Efficacy of BCG vaccine in the prevention of tuberculosis. Meta-analysis of the published literature. *JAMA*, 271(9), pp.698–702.

Colijn, C., Cohen, T. & Murray, M., 2006. Mathematical models of tuberculosis: accomplishments and future challenges. … *Symposium on Mathematical and …*.

Commandeur, S. et al., 2011. Identification of human T-cell responses to Mycobacterium tuberculosis resuscitation-promoting factors in long-term latently infected individuals. *Clin Vaccine Immunol*, 18(4), pp.676–683.

Crawford, F. et al., 1998. Detection of antigen-specific T cells with multivalent soluble class II MHC covalent peptide complexes. *Immunity*, 8(6), pp.675–682.

Crotty, S. et al., 2003. Cutting edge: long-term B cell memory in humans after smallpox vaccination. *J Immunol*, 171(10), pp.4969–4973.

Cui, W. & Kaech, S.M., 2010. Generation of effector CD8+ T cells and their conversion to memory T cells. *Immunol Rev*, 236, pp.151–166.

Cunliffe, S.L., Wyer, J.R. & Sutton, J.K., 2002. Optimization of peptide linker length in production of MHC class II/peptide tetrameric complexes increases yield and stability, and allows identification of …. *European journal of …*.

Czerkinsky, C.C. et al., 1983. A solid-phase enzyme-linked immunospot (ELISPOT) assay for enumeration of specific antibody-secreting cells. *J Immunol Methods*, 65(1-2), pp.109–121.

Davis, J.M. & Ramakrishnan, L., 2009. The role of the granuloma in expansion and dissemination of early tuberculous infection. *Cell*, 136(1), pp.37–49.

Day, C.L. et al., 2003. Ex vivo analysis of human memory CD4 T cells specific for hepatitis C virus using MHC class II tetramers. *J Clin Invest*, 112(6), pp.831–842.

Day, C.L. et al., 2011. Functional capacity of Mycobacterium tuberculosis-specific T cell responses in humans is associated with mycobacterial load.

J Immunol, 187(5), pp.2222–2232.

De Carli, M. et al., 1994. Human Th1 and Th2 cells: functional properties, regulation of development and role in autoimmunity. *Autoimmunity*, 18(4), pp.301–308.

de Jonge, H.J.M. et al., 2007. Evidence based selection of housekeeping genes. *PLoS One*, 2(9), p.e898.

De Winter, J., 2013. Using the Student's t-test with extremely small sample sizes. *Practical Assessment*.

Desel, C. et al., 2011. Recombinant BCG ΔureC hly+ induces superior protection over parental BCG by stimulating a balanced combination of type 1 and type 17 cytokine responses. *J Infect Dis*, 204(10), pp.1573–1584.

Diedrich, C.R. et al., 2010. Reactivation of latent tuberculosis in cynomolgus macaques infected with SIV is associated with early peripheral T cell depletion and not virus load. *PLoS One*, 5(3), p.e9611.

Dominguez, M.H. et al., 2013. Highly multiplexed quantitation of gene expression on single cells. *J Immunol Methods*, 391(1-2), pp.133–145.

Dye, C. & Fine, P.E., 2013. A major event for new tuberculosis vaccines. *Lancet*.

Ernst, J.D., 1998. Macrophage receptors for Mycobacterium tuberculosis. *Infect Immun*, 66(4), pp.1277–1281.

Esser, M.T. et al., 2003. Memory T cells and vaccines. *Vaccine*, 21(5-6), pp.419–430.

Feng, C.G. et al., 2000. Up-regulation of VCAM-1 and differential expansion of beta integrin-expressing T lymphocytes are associated with immunity to pulmonary Mycobacterium tuberculosis infection. *J Immunol*, 164(9), pp.4853–4860.

Ferlin, W., Glaichenhaus, N. & Mougneau, E., 2000. Present difficulties and future promise of MHC multimers in autoimmune exploration. *Curr Opin Immunol*, 12(6), pp.670–675.

Fietta, P. & Delsante, G., 2009. The effector T helper cell triade. *Rivista di biologia*, 102(1), pp.61–74.

Fine, P.E., 1995. Variation in protection by BCG: implications of and for heterologous immunity. *Lancet*, 346(8986), pp.1339–1345.

Flatz, L. et al., 2011. Single-cell gene-expression profiling reveals qualitatively distinct CD8 T cells elicited by different gene-based vaccines. *Proc Natl Acad Sci U S A*, 108(14), pp.5724–5729.

Forbes, E.K. et al., 2008. Multifunctional, high-level cytokine-producing Th1 cells in the lung, but not spleen, correlate with protection against Mycobacterium tuberculosis aerosol challenge in mice. *J Immunol*, 181(7), pp.4955–4964.

Fox, B.C. et al., 2012. Comparison of reverse transcription-quantitative polymerase chain reaction methods and platforms for single cell gene expression analysis. *Anal Biochem*, 427(2), pp.178–186.

Fritsch, R.D. et al., 2005. Stepwise differentiation of CD4 memory T cells defined by expression of CCR7 and CD27. *J Immunol*, 175(10), pp.6489–6497.

Gattinoni, L. et al., 2011. A human memory T cell subset with stem cell-like properties. *Nat Med*, 17(10), pp.1290–1297.

Gattinoni, L. et al., 2009. Wnt signaling arrests effector T cell differentiation and generates CD8+ memory stem cells. *Nat Med*, 15(7), pp.808–813.

Geginat, J., Lanzavecchia, A. & Sallusto, F., 2003. Proliferation and differentiation potential of human CD8+ memory T-cell subsets in response to antigen or homeostatic cytokines. *Blood*, 101(11), pp.4260–4266.

Geginat, J., Sallusto, F. & Lanzavecchia, A., 2001. Cytokine-driven proliferation and differentiation of human naive, central memory, and effector memory CD4(+) T cells. *J Exp Med*, 194(12), pp.1711–1719.

Geiger, R. et al., 2009. Human naive and memory CD4+ T cell repertoires specific for naturally processed antigens analyzed using libraries of amplified T cells. *J Exp Med*, 206(7), pp.1525–1534.

Geldmacher, C. et al., 2010. Preferential infection and depletion of Mycobacterium tuberculosis-specific CD4 T cells after HIV-1 infection. *J Exp Med*, 207(13), pp.2869–2881.

Geluk, A. & van Meijgaarden, K.E., 2000. Identification of major epitopes of Mycobacterium tuberculosis AG85B that are recognized by HLA-A* 0201-restricted CD8+ T cells in HLA-transgenic mice and …. *The Journal of ….*

Godkin, A.J. et al., 2001. Naturally processed HLA class II peptides reveal highly conserved immunogenic flanking region sequence preferences that reflect antigen processing rather than peptide-MHC interactions. *J Immunol*, 166(11), pp.6720–6727.

Goo, J.M. et al., 2000. Pulmonary tuberculoma evaluated by means of FDG PET: findings in 10 cases. *Radiology*, 216(1), pp.117–121.

Grassly, N.C. et al., 2007. Protective efficacy of a monovalent oral type 1 poliovirus vaccine: a case-control study. *The Lancet*.

Grode, L. et al., 2005. Increased vaccine efficacy against tuberculosis of

recombinant Mycobacterium bovis bacille Calmette-Guerin mutants that secrete listeriolysin. *J Clin Invest*, 115(9), pp.2472–2479.

Guarda, G. et al., 2007. L-selectin-negative CCR7- effector and memory CD8+ T cells enter reactive lymph nodes and kill dendritic cells. *Nat Immunol*, 8(7), pp.743–752.

Gutierrez, M.G. et al., 2004. Autophagy is a defense mechanism inhibiting BCG and Mycobacterium tuberculosis survival in infected macrophages. *Cell*, 119(6), pp.753–766.

Hand, T.W. & Kaech, S.M., 2009. Intrinsic and extrinsic control of effector T cell survival and memory T cell development. *Immunol Res*, 45(1), pp.46–61.

Hanekom, W.A. et al., 2008. Immunological outcomes of new tuberculosis vaccine trials: WHO panel recommendations. *PLoS Med*, 5(7), p.e145.

Hanekom, W.A. et al., 2004. Novel application of a whole blood intracellular cytokine detection assay to quantitate specific T-cell frequency in field studies. *J Immunol Methods*, 291(1-2), pp.185–195.

Hanekom, W.A., Abel, B. & Scriba, T.J., 2007. Immunological protection against tuberculosis. *S Afr Med J*, 97(10 Pt 2), pp.973–977.

Hansen, S.G. et al., 2011. Profound early control of highly pathogenic SIV by an effector memory T-cell vaccine. *Nature*, 473(7348), pp.523–527.

Harari, A. et al., 2011. Dominant TNF-alpha(+) Mycobacterium tuberculosis-specific CD4(+) T cell responses discriminate between latent infection and active disease. *Nat Med*.

Harari, A. et al., 2005. Functional heterogeneity of memory CD4 T cell responses in different conditions of antigen exposure and persistence. *J Immunol*, 174(2), pp.1037–1045.

Harari, A., Vallelian, F. & Pantaleo, G., 2004. Phenotypic heterogeneity of antigen-specific CD4 T cells under different conditions of antigen persistence and antigen load. *Eur J Immunol*, 34(12), pp.3525–3533.

Hatherill, M., 2011. Prospects for elimination of childhood tuberculosis: the role of new vaccines. *Arch Dis Child*, 96(9), pp.851–856.

Hawkridge, T. et al., 2008. Safety and immunogenicity of a new tuberculosis vaccine, MVA85A, in healthy adults in South Africa. *J Infect Dis*, 198(4), pp.544–552.

Hickman-Miller, H.D. & Yewdell, J.W., 2006. Youth has its privileges: maturation inhibits DC cross-priming. *Nature immunology*.

Hodes, R.J., Hathcock, K.S. & Weng, N.-P., 2002. Telomeres in T and B cells. *Nature Reviews Immunology*, 2(9), pp.699–706.

Hoft, D.F. et al., 2012. A recombinant adenovirus expressing immunodominant TB antigens can significantly enhance BCG-induced human immunity. *Vaccine*, 30(12), pp.2098–2108.

Hohn, H. et al., 2007. MHC class II tetramer guided detection of Mycobacterium tuberculosis-specific CD4+ T cells in peripheral blood from patients with pulmonary tuberculosis. *Scand J Immunol*, 65(5), pp.467–478.

Jacobsen, M. et al., 2007. Clonal expansion of CD8+ effector T cells in childhood tuberculosis. *J Immunol*, 179(2), pp.1331–1339.

Kaech, S.M. et al., 2003. Selective expression of the interleukin 7 receptor identifies effector CD8 T cells that give rise to long-lived memory cells. *Nat Immunol*, 4(12), pp.1191–1198.

Kagina, B.M. et al., 2009. Delaying BCG vaccination from birth to 10 weeks of age may result in an enhanced memory CD4 T cell response. *Vaccine*, 27(40), pp.5488–5495.

Kagina, B.M. et al., 2010. Specific T cell frequency and cytokine expression profile do not correlate with protection against tuberculosis after bacillus Calmette-Guerin vaccination of newborns. *Am J Respir Crit Care Med*, 182(8), pp.1073–1079.

Kalsdorf, B. et al., 2009. HIV-1 infection impairs the bronchoalveolar T-cell response to mycobacteria. *Am J Respir Crit Care Med*, 180(12), pp.1262–1270.

Kampmann, B. et al., 2000. Evaluation of human antimycobacterial immunity using recombinant reporter mycobacteria. *J Infect Dis*, 182(3), pp.895–901.

Kantele, A. et al., 1999. Differential homing commitments of antigen-specific T cells after oral or parenteral immunization in humans. *J Immunol*, 162(9), pp.5173–5177.

Kantele, A. et al., 1997. Homing potentials of circulating lymphocytes in humans depend on the site of activation: oral, but not parenteral, typhoid vaccination induces circulating antibody-secreting cells that all bear homing receptors directing them to the gut. *J Immunol*, 158(2), pp.574–579.

Kantzanou, M. et al., 2003. Viral escape and T cell exhaustion in hepatitis C virus infection analysed using Class I peptide tetramers. *Immunol Lett*, 85(2), pp.165–171.

Kaufman, D.R. et al., 2008. Trafficking of antigen-specific CD8+ T lymphocytes to mucosal surfaces following intramuscular vaccination. *J Immunol*, 181(6), pp.4188–4198.

Kaufmann, S.H., 2010. Future vaccination strategies against tuberculosis:

thinking outside the box. *Immunity*, 33(4), pp.567–577.

Kaufmann, S.H. & McMichael, A.J., 2005. Annulling a dangerous liaison: vaccination strategies against AIDS and tuberculosis. *Nat Med*, 11(4 Suppl), pp.S33–44.

Kaufmann, S.H., Hussey, G. & Lambert, P.H., 2010. New vaccines for tuberculosis. *Lancet*, 375(9731), pp.2110–2119.

Kaufmann, S.H.E., 2012. Tuberculosis vaccine development: strength lies in tenacity. *Trends Immunol*, 33(7), pp.373–379.

Kaveh, D.A. et al., 2011. Systemic BCG immunization induces persistent lung mucosal multifunctional CD4 T(EM) cells which expand following virulent mycobacterial challenge. *PLoS One*, 6(6), p.e21566.

Keane, J. et al., 2001. Tuberculosis associated with infliximab, a tumor necrosis factor alpha-neutralizing agent. *N Engl J Med*, 345(15), pp.1098–1104.

Khader, S.A. et al., 2007. IL-23 and IL-17 in the establishment of protective pulmonary CD4+ T cell responses after vaccination and during Mycobacterium tuberculosis challenge. *Nat Immunol*, 8(4), pp.369–377.

Klenerman, P., Cerundolo, V. & Dunbar, P.R., 2002a. Tracking T cells with tetramers: new tales from new tools. *Nature Reviews Immunology*.

Klenerman, P., Lucas, M., et al., 2002b. Immunity to hepatitis C virus: stunned but not defeated. *Microbes Infect*, 4(1), pp.57–65.

Korn, T. et al., 2007. IL-21 initiates an alternative pathway to induce proinflammatory T(H)17 cells. *Nature*, 448(7152), pp.484–487.

Kundu, M. & Thompson, C.B., 2008. Autophagy: basic principles and relevance to disease. *Annual review of pathology*, 3, pp.427–455.

Kwok, W.W. et al., 2012. Frequency of epitope-specific naive CD4(+) T cells correlates with immunodominance in the human memory repertoire. *J Immunol*, 188(6), pp.2537–2544.

Laan, M. et al., 1999. Neutrophil recruitment by human IL-17 via C-X-C chemokine release in the airways. *J Immunol*, 162(4), pp.2347–2352.

Lambert, P.H., Hawkridge, T. & Hanekom, W.A., 2009. New vaccines against tuberculosis. *Clin Chest Med*, 30(4), pp.811–26– x.

Lantelme, E. et al., 2001. Kinetics of GATA-3 gene expression in early polarizing and committed human T cells. *Immunology*, 102(2), pp.123–130.

Lanzavecchia, A. & Sallusto, F., 2005. Understanding the generation and function of memory T cell subsets. *Curr Opin Immunol*, 17(3), pp.326–332.

Latta, M., Mohan, K. & Issekutz, T.B., 2007. CXCR6 is expressed on T cells in both T helper type 1 (Th1) inflammation and allergen-induced Th2 lung inflammation but is only a weak mediator of chemotaxis. *Immunology*, 121(4), pp.555–564.

Lawn, S.D., Butera, S.T. & Shinnick, T.M., 2002. Tuberculosis unleashed: the impact of human immunodeficiency virus infection on the host granulomatous response to Mycobacterium tuberculosis. *Microbes Infect*, 4(6), pp.635–646.

Lemaître, F.F. et al., 2004. Detection of low-frequency human antigen-specific CD4(+) T cells using MHC class II multimer bead sorting and immunoscope analysis. *Eur J Immunol*, 34(10), pp.2941–2949.

Lin, P.L. et al., 2013. Radiologic responses in cynomolgous macaques for assessing tuberculosis chemotherapy regimens. *Antimicrob Agents Chemother*.

Lyons, A.B., 1999. Divided we stand: tracking cell proliferation with carboxyfluorescein diacetate succinimidyl ester. *Immunol Cell Biol*, 77(6), pp.509–515.

Maecker, H.T. et al., 2001. Use of overlapping peptide mixtures as antigens for cytokine flow cytometry. *J Immunol Methods*, 255(1-2), pp.27–40.

Maglione, P.J. & Chan, J., 2009. How B cells shape the immune response against Mycobacterium tuberculosis. *Eur J Immunol*, 39(3), pp.676–686.

Malcherek, G. et al., 1993. Natural peptide ligand motifs of two HLA molecules associated with myasthenia gravis. *Int Immunol*, 5(10), pp.1229–1237.

Mallone, R. & Nepom, G.T., 2004. MHC Class II tetramers and the pursuit of antigen-specific T cells: define, deviate, delete. *Clin Immunol*, 110(3), pp.232–242.

Martineau, A.R. et al., 2007. Neutrophil-mediated innate immune resistance to mycobacteria. *J Clin Invest*, 117(7), pp.1988–1994.

Masopust, D. et al., 2010. Dynamic T cell migration program provides resident memory within intestinal epithelium. *J Exp Med*, 207(3), pp.553–564.

Mattapallil, J.J. et al., 2005. Massive infection and loss of memory CD4+ T cells in multiple tissues during acute SIV infection. *Nature*, 434(7037), pp.1093–1097.

McShane, H., 2009. Vaccine strategies against tuberculosis. *Swiss medical weekly*, 139(11-12), pp.156–160.

McShane, H. et al., 2004. Recombinant modified vaccinia virus Ankara expressing antigen 85A boosts BCG-primed and naturally acquired antimycobacterial immunity in humans. *Nat Med*, 10(11), pp.1240–1244.

Miller, J.D. et al., 2008. Human effector and memory CD8+ T cell responses to smallpox and yellow fever vaccines. *Immunity*, 28(5), pp.710–722.

Miller, J.L. et al., 2010. The type I NADH dehydrogenase of Mycobacterium tuberculosis counters phagosomal NOX2 activity to inhibit TNF-alpha-mediated host cell apoptosis. *PLoS Pathog*, 6(4), p.e1000864.

Millington, K.A. et al., 2010. Mycobacterium tuberculosis-specific cellular immune profiles suggest bacillary persistence decades after spontaneous cure in untreated tuberculosis. *J Infect Dis*, 202(11), pp.1685–1689.

Mittrucker, H.W. et al., 2007. Poor correlation between BCG vaccination-induced T cell responses and protection against tuberculosis. *Proc Natl Acad Sci U S A*, 104(30), pp.12434–12439.

Mohagheghpour, N. et al., 1998. CTL response to Mycobacterium tuberculosis: identification of an immunogenic epitope in the 19-kDa lipoprotein. *J Immunol*, 161(5), pp.2400–2406.

Mohan, K. et al., 2005. CXCR3 is required for migration to dermal inflammation by normal and in vivo activated T cells: differential requirements by CD4 and CD8 memory subsets. *Eur J Immunol*, 35(6), pp.1702–1711.

Morel, C. et al., 2008. Mycobacterium bovis BCG-infected neutrophils and dendritic cells cooperate to induce specific T cell responses in humans and mice. *Eur J Immunol*, 38(2), pp.437–447.

Moseley, T.A. et al., 2003. Interleukin-17 family and IL-17 receptors. *Cytokine & growth factor reviews*, 14(2), pp.155–174.

Mosmann, T.R. & Coffman, R.L., 1989. TH1 and TH2 cells: different patterns of lymphokine secretion lead to different functional properties. *Annu Rev Immunol*, 7, pp.145–173.

Mueller, H. et al., 2008. Mycobacterium tuberculosis-specific CD4+, IFNgamma+, and TNFalpha+ multifunctional memory T cells coexpress GM-CSF. *Cytokine*, 43(2), pp.143–148.

Murdin, A.D., Barreto, L. & Plotkin, S., 1996. Inactivated poliovirus vaccine: past and present experience. *Vaccine*, 14(8), pp.735–746.

Murphy, K.M. & Reiner, S.L., 2002. The lineage decisions of helper T cells. *Nature Reviews Immunology*, 2(12), pp.933–944.

Mustafa, A.S. et al., 2000. Identification and HLA restriction of naturally derived Th1-cell epitopes from the secreted Mycobacterium tuberculosis antigen 85B recognized by antigen-specific human CD4(+) T-cell lines. *Infect Immun*, 68(7), pp.3933–3940.

Mutis, T., Cornelisse, Y.E. & Ottenhoff, T.H., 1993. Mycobacteria induce CD4+ T cells that are cytotoxic and display Th1-like cytokine secretion

profile: heterogeneity in cytotoxic activity and cytokine secretion levels. *Eur J Immunol*, 23(9), pp.2189–2195.

Newell, E.W. et al., 2013. Combinatorial tetramer staining and mass cytometry analysis facilitate T-cell epitope mapping and characterization. *Nat Biotechnol*, 31(7), pp.623–629.

Newell, E.W. et al., 2012. Cytometry by time-of-flight shows combinatorial cytokine expression and virus-specific cell niches within a continuum of CD8+ T cell phenotypes. *Immunity*, 36(1), pp.142–152.

Novak, E.J. et al., 1999. MHC class II tetramers identify peptide-specific human CD4(+) T cells proliferating in response to influenza A antigen. *J Clin Invest*, 104(12), pp.R63–7.

O'Garra, A. et al., 2013. The immune response in tuberculosis. *Annu Rev Immunol*, 31, pp.475–527.

O'Garra, A., McEvoy, L.M. & Zlotnik, A., 1998. T-cell subsets: chemokine receptors guide the way. *Curr Biol*, 8(18), pp.R646–9.

Oestreich, K.J. & Weinmann, A.S., 2012. Master regulators or lineage-specifying? Changing views on CD4+ T cell transcription factors. *Nat Rev Immunol*, 12(11), pp.799–804.

Orme, I.M., 2010. The Achilles heel of BCG. *Tuberculosis (Edinb)*, 90(6), pp.329–332.

Ottenhoff, T.H. et al., 2000. Human deficiencies in type 1 cytokine receptors reveal the essential role of type 1 cytokines in immunity to intracellular bacteria. *Microbes Infect*, 2(13), pp.1559–1566.

Ottenhoff, T.H., Kumararatne, D. & Casanova, J.L., 1998. Novel human immunodeficiencies reveal the essential role of type-I cytokines in immunity to intracellular bacteria. *Immunol Today*, 19(11), pp.491–494.

Pannetier, C., Even, J. & Kourilsky, P., 1995. T-cell repertoire diversity and clonal expansions in normal and clinical samples. *Immunol Today*, 16(4), pp.176–181.

Pathan, A.A.A. et al., 2001. Direct ex vivo analysis of antigen-specific IFN-gamma-secreting CD4 T cells in Mycobacterium tuberculosis-infected individuals: associations with clinical disease state and effect of treatment. *J Immunol*, 167(9), pp.5217–5225.

Perfetto, S.P. et al., 2012. Quality assurance for polychromatic flow cytometry using a suite of calibration beads. *Nature protocols*, 7(12), pp.2067–2079.

Plotkin SA, O.W., 1999. *Vaccines* 3rd ed., Saunders.

Plotkin, S.A., 2003. Vaccines, vaccination, and vaccinology. *Journal of Infectious Diseases*.

Plotkin, S.A., 2005. Vaccines: past, present and future. *Nat Med*, 11(4 Suppl), pp.S5–11.

Pulendran, B. et al., 2013. Immunity to viruses: learning from successful human vaccines. *Immunol Rev*, 255(1), pp.243–255.

Putheti, P. et al., 2010. Human CD4+ memory T cells can become CD4+ IL-9+ T cells. *PLoS One*.

Ramakrishnan, L., 2012. Revisiting the role of the granuloma in tuberculosis. *Nat Rev Immunol*, 12(5), pp.352–366.

Rammensee, H. et al., 1999. SYFPEITHI: database for MHC ligands and peptide motifs. *Immunogenetics*, 50(3-4), pp.213–219.

Reichstetter, S.S. et al., 2000. Distinct T cell interactions with HLA class II tetramers characterize a spectrum of TCR affinities in the human antigen-specific T cell response. *J Immunol*, 165(12), pp.6994–6998.

Reijonen, H. & Kwok, W.W., 2003. Use of HLA class II tetramers in tracking antigen-specific T cells and mapping T-cell epitopes. *Methods*.

Reiley, W.W. et al., 2008. ESAT-6-specific CD4 T cell responses to aerosol Mycobacterium tuberculosis infection are initiated in the mediastinal lymph nodes. *Proc Natl Acad Sci U S A*, 105(31), pp.10961–10966.

Rivino, L. et al., 2004. Chemokine receptor expression identifies Pre-T helper (Th)1, Pre-Th2, and nonpolarized cells among human CD4+ central memory T cells. *J Exp Med*, 200(6), pp.725–735.

Robertson, B.D. et al., 2012. Detection and treatment of subclinical tuberculosis. *Tuberculosis (Edinb)*, 92(6), pp.447–452.

Rodrigues, L.C., Diwan, V.K. & Wheeler, J.G., 1993. Protective effect of BCG against tuberculous meningitis and miliary tuberculosis: a meta-analysis. *International journal of epidemiology*, 22(6), pp.1154–1158.

Roederer, M., 2002. Compensation in flow cytometry. *Current protocols in cytometry / editorial board, J. Paul Robinson, managing editor ... [et al.]*, Chapter 1, p.Unit 1.14.

Romagnani, S., 1994. Regulation of the development of type 2 T-helper cells in allergy. *Curr Opin Immunol*, 6(6), pp.838–846.

Rozot, V. et al., 2013. Mycobacterium tuberculosis-specific CD8+ T cells are functionally and phenotypically different between latent infection and active disease. *Eur J Immunol*, 43(6), pp.1568–1577.

Rubin, E.J., 2009. The granuloma in tuberculosis--friend or foe? *N Engl J Med*, 360(23), pp.2471–2473.

Rubtsov, Y.P.Y. et al., 2008. Regulatory T Cell-Derived Interleukin-10 Limits

Inflammation at Environmental Interfaces. *Immunity*, 28(4), pp.13–13.

Rueda, C.M. et al., 2010. Characterization of CD4 and CD8 T cells producing IFN-gamma in human latent and active tuberculosis. *Tuberculosis (Edinb)*, 90(6), pp.346–353.

Russell, D.G. et al., 2009. Foamy macrophages and the progression of the human tuberculosis granuloma. *Nat Immunol*, 10(9), pp.943–948.

Sakaguchi, S., 2005. Naturally arising Foxp3-expressing CD25+ CD4+ regulatory T cells in immunological tolerance to self and non-self. *Nature immunology*.

Sakaguchi, S., Sakaguchi, N. & Asano, M., 1995. Immunologic self-tolerance maintained by activated T cells expressing IL-2 receptor alpha-chains (CD25). Breakdown of a single mechanism of self-tolerance causes …. *The Journal of …*.

Sallusto, F. et al., 2010. From vaccines to memory and back. *Immunity*, 33(4), pp.451–463.

Sallusto, F. et al., 2000. Functional subsets of memory T cells identified by CCR7 expression. *Curr Top Microbiol Immunol*, 251, pp.167–171.

Sallusto, F. et al., 1999. Two subsets of memory T lymphocytes with distinct homing potentials and effector functions. *Nature*, 401(6754), pp.708–712.

Sallusto, F., Geginat, J. & Lanzavecchia, A., 2004. Central memory and effector memory T cell subsets: function, generation, and maintenance. *Annu Rev Immunol*, 22, pp.745–763.

Samandari, T. et al., 2011. 6-month versus 36-month isoniazid preventive treatment for tuberculosis in adults with HIV infection in Botswana: a randomised, double-blind, placebo-controlled trial. *Lancet*, 377(9777), pp.1588–1598.

Santosuosso, M. et al., 2005. Mechanisms of mucosal and parenteral tuberculosis vaccinations: adenoviral-based mucosal immunization preferentially elicits sustained accumulation of immune protective CD4 and CD8 T cells within the airway lumen. *J Immunol*, 174(12), pp.7986–7994.

Scriba, T.J. et al., 2012. A phase IIa trial of the new tuberculosis vaccine, MVA85A, in HIV- and/or Mycobacterium tuberculosis-infected adults. *Am J Respir Crit Care Med*, 185(7), pp.769–778.

Scriba, T.J. et al., 2008. Distinct, specific IL-17- and IL-22-producing CD4+ T cell subsets contribute to the human anti-mycobacterial immune response. *J Immunol*, 180(3), pp.1962–1970.

Scriba, T.J. et al., 2011. Dose-finding study of the novel tuberculosis vaccine, MVA85A, in healthy BCG-vaccinated infants. *J Infect Dis*, 203(12),

pp.1832–1843.

Scriba, T.J. et al., 2010. Modified vaccinia Ankara-expressing Ag85A, a novel tuberculosis vaccine, is safe in adolescents and children, and induces polyfunctional CD4+ T cells. *Eur J Immunol*, 40(1), pp.279–290.

Scriba, T.J. et al., 2005. Ultrasensitive detection and phenotyping of CD4+ T cells with optimized HLA class II tetramer staining. *J Immunol*, 175(10), pp.6334–6343.

Seder, R.A. & Paul, W.E., 1994. Acquisition of lymphokine-producing phenotype by CD4+ T cells. *Annual review of immunology*.

Seiler, P. et al., 2003. Early granuloma formation after aerosol Mycobacterium tuberculosis infection is regulated by neutrophils via CXCR3-signaling chemokines. *Eur J Immunol*, 33(10), pp.2676–2686.

Serbina, N.V., Lazarevic, V. & Flynn, J.L., 2001. CD4(+) T cells are required for the development of cytotoxic CD8(+) T cells during Mycobacterium tuberculosis infection. *J Immunol*, 167(12), pp.6991–7000.

Sidney, J. et al., 2001. Measurement of MHC/peptide interactions by gel filtration. *Current protocols in immunology / edited by John E. Coligan ... [et al.]*, Chapter 18, p.Unit 18.3.

Singh, H. & Raghava, G.P., 2001. ProPred: prediction of HLA-DR binding sites. *Bioinformatics*, 17(12), pp.1236–1237.

Slota, M. et al., 2011. ELISpot for measuring human immune responses to vaccines. *Expert Rev Vaccines*, 10(3), pp.299–306.

Soares, A. et al., 2010. Novel application of Ki67 to quantify antigen-specific in vitro lymphoproliferation. *J Immunol Methods*, 362(1-2), pp.43–50.

Soares, A.P. et al., 2008. Bacillus Calmette-Guerin vaccination of human newborns induces T cells with complex cytokine and phenotypic profiles. *J Immunol*, 180(5), pp.3569–3577.

Soares, A.P. et al., 2013. Longitudinal changes in CD4(+) T-cell memory responses induced by BCG vaccination of newborns. *J Infect Dis*, 207(7), pp.1084–1094.

Son, N.H. et al., 2000. Lineage-specific telomere shortening and unaltered capacity for telomerase expression in human T and B lymphocytes with age. *J Immunol*, 165(3), pp.1191–1196.

Song, K. et al., 2005. Characterization of subsets of CD4+ memory T cells reveals early branched pathways of T cell differentiation in humans. *Proc Natl Acad Sci U S A*, 102(22), pp.7916–7921.

Spencer, C.T. et al., 2008. Only a subset of phosphoantigen-responsive gamma9delta2 T cells mediate protective tuberculosis immunity. *J*

Immunol, 181(7), pp.4471–4484.

Stead, W.W., 1967. Pathogenesis of a first episode of chronic pulmonary tuberculosis in man: recrudescence of residuals of the primary infection or exogenous reinfection? *Am Rev Respir Dis*, 95(5), pp.729–745.

Steinman, R.M. & Swanson, J., 1995. The endocytic activity of dendritic cells. *J Exp Med*, 182(2), pp.283–288.

Stenger, S. et al., 1999. Granulysin: a lethal weapon of cytolytic T cells. *Immunol Today*, 20(9), pp.390–394.

Sturgill-Koszycki, S. et al., 1994. Lack of acidification in Mycobacterium phagosomes produced by exclusion of the vesicular proton-ATPase. *Science*, 263(5147), pp.678–681.

Sturniolo, T. et al., 1999. Generation of tissue-specific and promiscuous HLA ligand databases using DNA microarrays and virtual HLA class II matrices. *Nat Biotechnol*, 17(6), pp.555–561.

Sudfeld, C.R., Navar, A.M. & Halsey, N.A., 2010. Effectiveness of measles vaccination and vitamin A treatment. *International journal of epidemiology*, 39 Suppl 1(Supplement 1), pp.i48–i55.

Sutherland, J.S. et al., 2010. Production of TNF-alpha, IL-12(p40) and IL-17 can discriminate between active TB disease and latent infection in a West African cohort. *PLoS One*, 5(8), p.e12365.

Sutter, G. & Moss, B., 1992. Nonreplicating vaccinia vector efficiently expresses recombinant genes. *Proc Natl Acad Sci U S A*, 89(22), pp.10847–10851.

Szabo, S.J. et al., 2000. A novel transcription factor, T-bet, directs Th1 lineage commitment. *Cell*, 100(6), pp.655–669.

Tailleux, L. et al., 2003. DC-SIGN is the major Mycobacterium tuberculosis receptor on human dendritic cells. *J Exp Med*, 197(1), pp.121–127.

Tameris, M. et al., 2014. The Candidate TB Vaccine, MVA85A, Induces Highly Durable Th1 Responses. *PLoS One*, 9(2), p.e87340.

Tameris, M.D. et al., 2013. Safety and efficacy of MVA85A, a new tuberculosis vaccine, in infants previously vaccinated with BCG: a randomised, placebo-controlled phase 2b trial. *Lancet*.

Tena-Coki, N.G. et al., 2010. CD4 and CD8 T-cell responses to mycobacterial antigens in African children. *Am J Respir Crit Care Med*, 182(1), pp.120–129.

Vallejo, A.N. et al., 1999. Modulation of CD28 expression: distinct regulatory pathways during activation and replicative senescence. *J Immunol*, 162(11), pp.6572–6579.

van Crevel, R., Ottenhoff, T.H.M. & van der Meer, J.W.M., 2002. Innate immunity to Mycobacterium tuberculosis. *Clinical microbiology reviews*, 15(2), pp.294–309.

Van Rhijn, I. et al., 2009. Low cross-reactivity of T-cell responses against lipids from Mycobacterium bovis and M. avium paratuberculosis during natural infection. *Eur J Immunol*, 39(11), pp.3031–3041.

VANDIVIERE, H.M. et al., 1956. The treated pulmonary lesion and its tubercle bacillus. II. The death and resurrection. *The American journal of the medical sciences*, 232(1), pp.30–7– passim.

Veldhoen, M. et al., 2006. TGFbeta in the context of an inflammatory cytokine milieu supports de novo differentiation of IL-17-producing T cells. *Immunity*, 24(2), pp.179–189.

Veldhoen, M. et al., 2008. Transforming growth factor-β“reprograms” the differentiation of T helper 2 cells and promotes an interleukin 9–producing subset. *Nature*.

Velmurugan, K. et al., 2007. Mycobacterium tuberculosis nuoG is a virulence gene that inhibits apoptosis of infected host cells. *PLoS Pathog*, 3(7), p.e110.

Verver, S. et al., 2004. Transmission of tuberculosis in a high incidence urban community in South Africa. *International journal of epidemiology*, 33(2), pp.351–357.

Walker, L.J. et al., 2013. CD8αα Expression Marks Terminally Differentiated Human CD8+ T Cells Expanded in Chronic Viral Infection. *Frontiers in immunology*, 4, p.223.

Wallis, R.S. et al., 2001. A whole blood bactericidal assay for tuberculosis. *J Infect Dis*, 183(8), pp.1300–1303.

Wallis, R.S., Broder, M.S. & Wong, J.Y., 2004. Granulomatous infectious diseases associated with tumor necrosis factor antagonists. *Clinical Infectious ….*

Walrath, J.R. & Silver, R.F., 2010. The {alpha}4{beta}1 Integrin in Localization of Mycobacterium Tuberculosis-specific Th1 Cells to the Human Lung. *Am J Respir Cell Mol Biol*.

Walzl, G. et al., 2011. Immunological biomarkers of tuberculosis. *Nat Rev Immunol*, 11(5), pp.343–354.

Wang, P. et al., 2008. A systematic assessment of MHC class II peptide binding predictions and evaluation of a consensus approach. *PLoS Comput Biol*, 4(4), p.e1000048.

Weng, N.P. et al., 1995. Human naive and memory T lymphocytes differ in telomeric length and replicative potential. *Proc Natl Acad Sci U S A*,

92(24), pp.11091–11094.

Wiker, H.G. & Harboe, M., 1992. The antigen 85 complex: a major secretion product of Mycobacterium tuberculosis. *Microbiological reviews*, 56(4), pp.648–661.

Wiker, H.G. et al., 2010. Evidence for waning of latency in a cohort study of tuberculosis. *BMC infectious diseases*, 10, pp.37–37.

Williams, M.A., Tyznik, A.J. & Bevan, M.J., 2006. Interleukin-2 signals during priming are required for secondary expansion of CD8+ memory T cells. *Nature*, 441(7095), pp.890–893.

Worku, S. & Hoft, D.F., 2003. Differential effects of control and antigen-specific T cells on intracellular mycobacterial growth. *Infect Immun*, 71(4), pp.1763–1773.

Wrammert, J. et al., 2009. Human immune memory to yellow fever and smallpox vaccination. *J Clin Immunol*, 29(2), pp.151–157.

Yang, J.J. et al., 2004. In vivo biotinylation of the major histocompatibility complex (MHC) class II/peptide complex by coexpression of BirA enzyme for the generation of MHC class II/tetramers. *Hum Immunol*, 65(7), pp.8–8.

Yang, X.O. et al., 2008. T helper 17 lineage differentiation is programmed by orphan nuclear receptors ROR alpha and ROR gamma. *Immunity*, 28(1), pp.29–39.

Zhang, H.H. et al., 2010. CCR2 identifies a stable population of human effector memory CD4+ T cells equipped for rapid recall response. *J Immunol*, 185(11), pp.6646–6663.

Zhang, X. et al., 2013. CD4(+)CD62L(+) central memory T cells can be converted to Foxp3(+) T cells. *PLoS One*, 8(10), p.e77322.

Zhang, Y. et al., 2005. Host-reactive CD8+ memory stem cells in graft-versus-host disease. *Nat Med*, 11(12), pp.1299–1305.

Zheng, W. & Flavell, R.A., 1997. The transcription factor GATA-3 is necessary and sufficient for Th2 cytokine gene expression in CD4 T cells. *Cell*, 89(4), pp.587–596.

Zhou, L. et al., 2007. IL-6 programs T(H)-17 cell differentiation by promoting sequential engagement of the IL-21 and IL-23 pathways. *Nat Immunol*, 8(9), pp.967–974.

Appendix:

Publications:

Heterologous vaccination against human tuberculosis modulates antigen-specific CD4$^+$ T-cell function.

[1]One B. Dintwe, [1,2,3]Cheryl L. Day, [1]Erica Smit, [1]Elisa Nemes, [4]Clive Gray, [1]Michele Tameris, [5]Helen McShane, [1]Hassan Mahomed, [1]Willem A. Hanekom and [1]Thomas J. Scriba

[1]South African Tuberculosis Vaccine Initiative and School of Child and Adolescent Health, Institute of Infectious Disease and Molecular Medicine, University of Cape Town, Cape Town, South Africa; [2]Department of Global Health, Rollins School of Public Health, Emory University, Atlanta, GA, USA; [3]Emory Vaccine Center, Emory University, Atlanta, GA, USA; [4]Division of Immunology, Institute of Infectious Disease and Molecular Medicine, University of Cape Town, Cape Town, South Africa; [5]Centre for Clinical Vaccinology and Tropical Medicine & The Jenner Institute Laboratories, Nuffield Department of Medicine, Oxford University, Oxford, UK.